

Analysis of Plant Secondary Metabolites from Specialized Organs, Tissue and Cells

Dissertation

zur Erlangung des akademischen Grades
doctor rerum naturalium (Dr. rer. nat.)

vorgelegt dem Rat der Biologisch-Pharmazeutischen Fakultät
der Friedrich-Schiller-Universität Jena

von Master of Natural Science in Medicinal Chemistry

Jingjing Fang

geboren am 18.10.1982 in Anhui, China

Gutachter

1. Prof. Dr. Jonathan Gershenzon (Max Planck Institute for Chemical Ecology)
2. PD Dr. Bernd Schneider (Max Planck Institute for Chemical Ecology)
3. Prof. Dr. Peter Spiteller (University of Bremen)

Tag der öffentlichen Verteidigung: 19.12.2012

Analysis of Plant Secondary Metabolites from Specialized Organs, Tissue and Cells



Max Planck Institute
for Chemical Ecology

Jingjing Fang, Biosynthesis / NMR Group

Contents

1. Introduction	1
2. Overview of manuscripts	9
3. Phytochemical study by HPLC-SPE-NMR	
3.1 C-methylated flavanones and dihydrochalcones from <i>Myrica gale</i> seeds	13
3.2 Phenylphenalenones and related natural products from <i>Wachendorfia thyrsiflora</i> L.	16
3.3 Phytochemical profile of aerial parts and roots of <i>Wachendorfia thyrsiflora</i> L. studied by LC-DAD-SPE-NMR.	22
3.4 Co-occurrence of phenylphenalenones and flavonoids in <i>Xiphidium caeruleum</i> Aubl. flowers.	31
4. Secondary metabolites profiling and their distribution in rapeseed	
4.1 Metabolic profiling of lignans and other secondary metabolites from rapeseed (<i>Brassica napus</i> L.).	38
4.2 Tissue-specific distribution of secondary metabolites in rapeseed (<i>Brassica napus</i> L.).	50
5. Saptio-temporal accumulation of secoisolariciresinol diglucoside in flaxseed	
5.1 Concentrations kinetics of secoisolariciresinol diglucoside and its biosynthetic precursor coniferin in developing flaxseed.	62
5.2 Laser microdissection-assisted quantitative cell layer-specific detection of secoisolariciresinol diglucoside in flaxseed coats.	68
6. Discussion	86
7. Summary	94
Zusammenfassung	96
References	98

Supplementary material	109
Acknowledgements	114
Curriculum Vitae	115

Chapter 1

Introduction

1.1 Plant secondary metabolites

In human history, use of plant secondary metabolites can be traced back to 2600 B. C. The first records were written on hundreds of clay tablets in cuneiform from Mesopotamia (Newman *et al.*, 2000). In next more than 4,000 years, plant secondary metabolites were used as mixtures or plant extracts mainly for food, medicine and poison purposes. Although plant secondary metabolites have been benefiting humans for thousands of years, their mysteries were disclosed in late two centuries. The isolation of the first pure natural product, morphine, from opium poppy (*Papaver somniferum*) by German pharmacist Friedrich Wilhelm Sertürner in 1806 opened a door to a new era of scientific plant secondary metabolites research (Croteau *et al.*, 2000). He demonstrated that the active principle of plant extract could be attributed to a single organic compound, which can be isolated. This finding initialized nature product chemistry, and speeded up developments of synthetic, analytical and pharmaceutical chemistry. To date, plant secondary metabolites are involved deeply in humans' life. For example, more than 30% of drugs are derived directly or indirectly from natural products (Cragg *et al.*, 1997; Newman *et al.*, 2003; Newman and Cragg, 2007; Newman and Cragg, 2012).

Primary metabolites have been widely studied in the past 200 years and have been proven to be involved in plant essential life cycles, such as growth, respiration, storage and reproduction. The concept of secondary metabolite was introduced by Albrecht Kossel in 1891 as plant "secondary product". Because of frequently low concentration of secondary metabolites in plants, their biological functions were largely neglected by plant physiologists, and they were recognized as metabolic waste or detoxification products, despite Ernst Stahl experimentally showed as early as 1888 that secondary metabolites play a defense role against herbivores. Following the increase in chemical and biochemical knowledge about plant secondary metabolism in recent four decades, currently, plant secondary metabolites are generally accepted as evolutionary products to adapt plants to their biotic and abiotic environments (Wink, 2003; Hartmann, 2007). During millions of years of evolution, plants actually acquired the capability to produce secondary metabolites on their own purposes to interact with other organisms.

Although secondary metabolites can be divided into three major groups based on the architecture of the skeleton and their biosynthetic pathways as the alkaloids, the terpenoids, the phenylpropanoids and allied phenolic compounds (Croteau *et al.*, 2000), they have vastly diverse structures, which play various ecological roles, and characterize plant taxa. By far, the structures of more than 200,000 secondary metabolites were elucidated (Hartmann, 2007). This number keeps increasing, and structure elucidation remains the primary step to comprehend and utilize secondary metabolites. In this thesis, some recently developed technologies that allow secondary metabolites research down to the cellular scale were applied. Several combined applications of high-performance liquid chromatography-solid phase extraction-nuclear magnetic resonance (HPLC-SPE-NMR), in natural products studies are presented. On the other hand, distribution studies of certain secondary metabolites in seed samples were performed by combined use of a recently developed sampling technology, laser microdissection (LMD), and chemical analysis by NMR and MS. These methods help researchers not only to study secondary metabolites faster, but also to better understand the functions of natural products.

1.2 Major methodologies used in the thesis

1.2.1 HPLC-SPE-NMR

In the early stage of natural product study, crystallization was the only method to obtain individual natural products from a plant extract, such cases as morphine, strychnine, caffeine and nicotine, in a pure form. In second half of 19th century, some pioneers performed “chromatographic” experiments to separate different mixtures (Touchstone, 1993). The Russian botanist Mikhail Semyonovich Tsvet used the word “chromatography” for the first time in his two papers published in 1906, in which, liquid column chromatography was applied to separate pigments from plant extract (Ettre and Sakodynskii, 1993a, b). The significance of chromatography was long ignored, until two Noble laureates, Archer John Porter Martin and Richard Laurence Millington Synge, elucidated the principles and established basic techniques of partition chromatography in 1941 (Martin and Synge, 1941), which truly speeded up the development of this technology. Afterwards, several chromatographic methods were developed, such as paper chromatography (PC), gas chromatography (GC), thin layer chromatography (TLC), liquid chromatography (LC) and supercritical fluid chromatography (SFC) (Touchstone, 1993). Motivated by Martin and Synge’s theory, to achieve a fast separation on liquid column chromatography, small particle size of sorbent and use of pressure on mobile phase were applied in 1963 (Halász and Horváth, 1963; Karr *et al.*, 1963). These are the initial applications of high performance liquid

chromatography (HPLC) as it is known today. Following numerous sorbents development and various detection methods applied, HPLC now represents the most powerful and versatile analytical method to separate complex mixtures.

On the other hand, the development of structure elucidation methods, the other key factor for natural products research, was also not smooth. At the early stage of natural products studies, structural elucidation was extremely difficult, because spectroscopic methods were unknown at that time and structures were proposed solely based on chemical and some physical properties of isolated compounds and their derivatives. For example, almost 120 years after its isolation, the structure of morphine was determined in 1923 (Gulland and Robinson, 1923), which was confirmed by synthesis in 1952 (Gates and Tschudi, 1952, 1956). The introduction of modern analytical methods such as ultraviolet-visible (UV) spectroscopy (Cary and Beckman, 1941), infrared (IR) spectroscopy (Rabkin, 1987) and mass spectrometry (MS) (Griffiths, 2008) in 1940s offered natural product chemists more options for structure elucidation. The real breakthrough technology for structure elucidation was NMR spectroscopy. As other analytical methods, NMR was also discovered by physicists (Rabi *et al.*, 1938), and it was not attractive to chemists until phenomena of chemical shifts (Proctor and Yu, 1950) and spin-spin coupling (Gutowsky *et al.*, 1951) were observed in NMR spectra. The application of Fourier transform technology on NMR (Ernst and Anderson, 1966) promoted rapid spread of this method. NMR became the fundamental method for natural products along with spectrometer hardware development and various pulse sequence invention.

The application of high field NMR magnet significantly increases the sensitivity and makes it possible to elucidate compounds in small scale as accessible from an analytical HPLC eluate. Therefore, hyphenated systems were developed, which combine advantages of HPLC in separation and NMR in structure elucidation. The first HPLC-NMR coupling experiment (Watanabe and Niki, 1978) was carried in stop-flow mode (Figure 1.1), in which, when the analyte reaches the NMR flow cell probe, the elution is stopped, and various experiments could be recorded by NMR. In one HPLC run, only one analyte could be measured. Soon after, a HPLC-NMR system that can run both stop-flow and on-flow modes (Figure 1.1) was developed (Bayer *et al.*, 1979). In on-flow mode, the NMR spectrometer is acting as a chromatographic detector, continuously measuring the spectrum of the eluate without stopping the flow. The measuring time for each analyte is limited to the residence time within the active volume of the NMR probe. This mode allows rapid screening of a mixture by recording ^1H NMR spectra, but in most case only major components can be recorded. To solve the problems occurring in the stop-flow and on-flow modes, capillary

loops are used to store each peak (Tseng *et al.*, 2000), without interrupting the chromatographic run. Subsequently, the stored analytes can be arbitrarily transferred to the NMR flow cell probe one by one, and it is possible to record different experiments for each analyte if enough material is stored. This mode is referred to loop-storage mode (Figure 1.1).

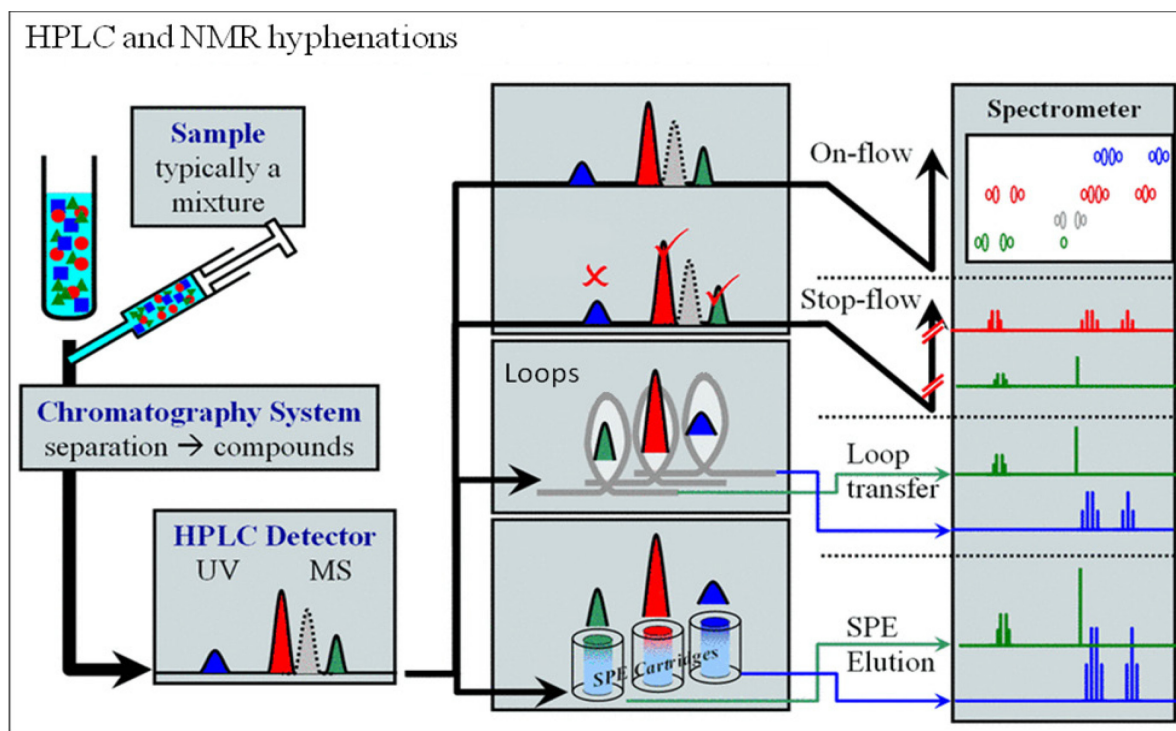


Figure 1.1 Different techniques of hyphenation between HPLC and NMR. (Picture modified from: http://www.bruker-biospin.com/hyphenation_lcnmr.html. Bruker Corporation is thanked for permission to use this picture. Copyright Bruker Corporation. Reproduced with permission.)

The above mentioned direct hyphenations between HPLC and NMR have two major inevitable drawbacks. The first one is use of costly deuterated solvent as eluent, the other is low sensitivity because analytes from only a single chromatographic run can be measured. Hence, these LC-NMR systems are not competitive to conventional measurement of isolated compounds (Jaroszewski, 2005a). The recent introduction of SPE into hyphenation of HPLC and NMR, namely HPLC-SPE-NMR, successfully overcame the two key disadvantages of the direct hyphenated LC-NMR systems. Figure 1.2 shows briefly how HPLC-SPE-NMR works. The SPE interface enables the use of normal solvents and multiple trappings to enrich each analyte. After trapping, undeuterated solvent can be removed by a stream of nitrogen gas flowing through the cartridge, and then the dried analyte is eluted from the SPE cartridge into the NMR flow cell for measurements. Since the first application of on-line automated HPLC-SPE-NMR in 2002 (Corcoran *et al.*, 2002), this system was successfully applied to elucidate structures of natural products from various sources (Exarchou *et al.*, 2005; Jaroszewski, 2005b; Brkljaca and Urban, 2011), as well as in other applications, such as drug metabolism studies (Godejohann *et al.*, 2004; Kammerer *et al.*, 2007; Ceccarelli *et al.*, 2008; De Tullio *et*

al., 2008; Gillotin *et al.*, 2010), drug degradation studies (Pan *et al.*, 2006; Larsen *et al.*, 2009; Mazumder *et al.*, 2010), reaction kinetics study (Seger *et al.*, 2006) and environmental study (Godejohann *et al.*, 2009). HPLC-SPE-NMR was proven as a versatile tool for structural elucidation of components from a complex mixture.

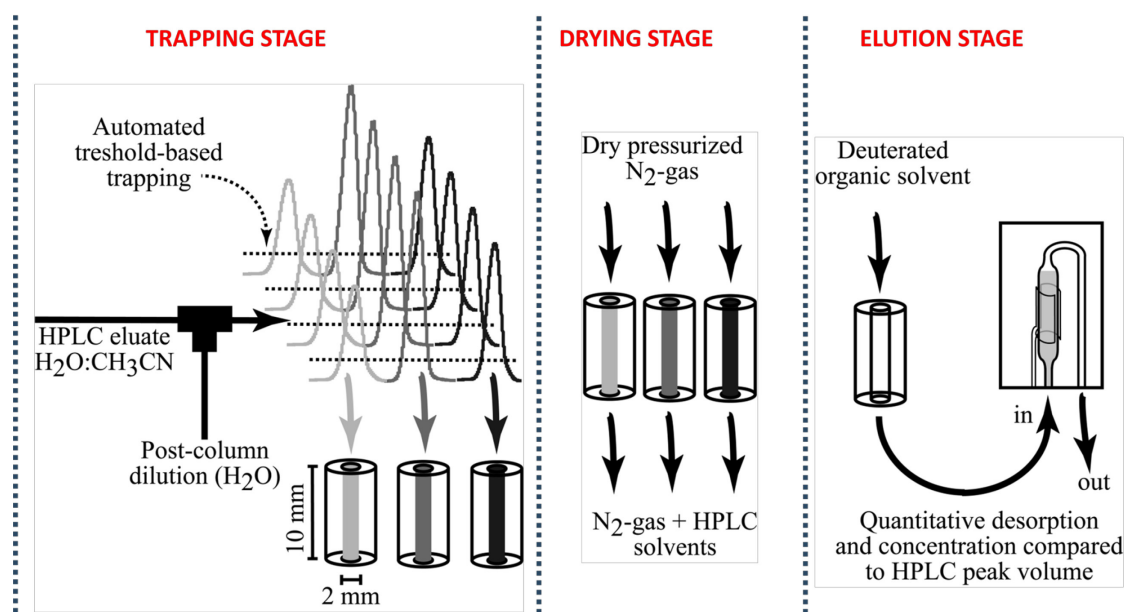


Figure 1.2 Schema of HPLC-SPE-NMR work flow. Staerk, D., Lambert, M., Jaroszewski, J. W., 2006. HPLC-NMR techniques for plant extract analysis. In “Medicinal Plant Biotechnology”, edited by Kayser, O. and Quax, W. Wiley-VCH: Weinheim, page 38. Copyright Wiley-VCH Verlag GmbH & Co. KGaA. Reproduced with permission.

1.2.2 Laser microdissection

Unlike medical and pharmaceutical chemists, who are fascinated by structure diversity and bioactivities for human use of natural products, phytologists and chemical ecologists are curious with the benefits of secondary metabolites’ biological functions for plants themselves and their interactions with other organisms. Therefore, the knowledge of distribution pattern can promote understanding of certain secondary metabolites’ biosynthesis and ecological functions in plants. Conventionally, histological methods were used to study the spatial distribution of secondary metabolites in microscopic plant samples making use of in situ labeling and (or) staining techniques. Due to the structural analogy among secondary metabolites of many plants, the specificity of histological methods is relative low. Recent developments in mass spectrometry imaging (Svatoš, 2011) and Raman imaging (Freudiger *et al.*, 2008) are promising tools in spatial metabolic profiling. However, these techniques mostly focus on metabolites on sample surfaces and do not allow detection of three-dimensional distribution of metabolites within the tissue. NMR, though representing the most informative analytical method and being able to provide data on three-dimensional spatial distribution, is of limited suitability to identify metabolites directly from plant samples, due to its moderate sensitivity. In order to take advantage of its superior properties for metabolic

profiling, a sampling method, laser microdissection (LMD) was developed to harvest specific cells, tissue or organs from plant material prior to various chemical analyses.

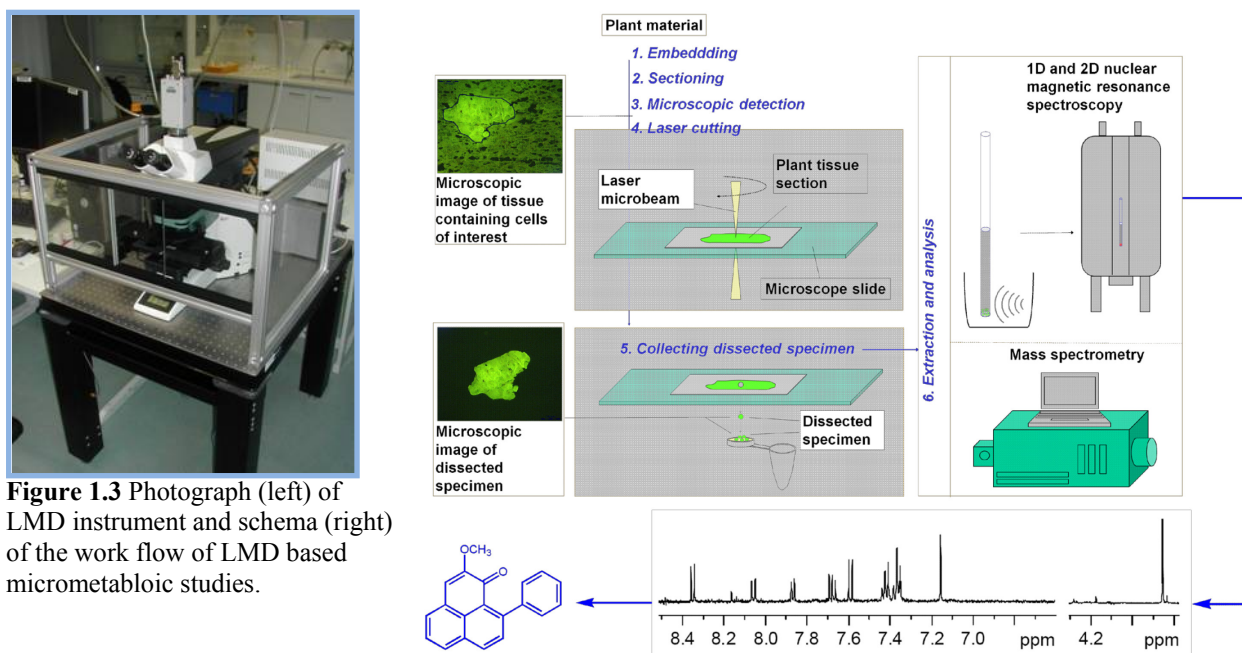


Figure 1.3 Photograph (left) of LMD instrument and schema (right) of the work flow of LMD based micrometabolic studies.

The LMD instrument, a microscope equipped with a laser-generating device (Figure 1.3), which was firstly applied to investigate animal samples around four decades ago (Berns and Floyd, 1971), was recently used for sampling plant material for DNA, RNA and protein analyses (Kehr, 2001, 2003; Day *et al.*, 2005b; Nelson *et al.*, 2006; Nelson *et al.*, 2008) and to dissect plant material for the analysis of both primary metabolites (Schad *et al.*, 2005; Angeles *et al.*, 2006; Obel *et al.*, 2009; Thiel *et al.*, 2009; Schiebold *et al.*, 2011) and secondary metabolites (Hölscher and Schneider, 2007; Li *et al.*, 2007; Hölscher *et al.*, 2009; Abbott *et al.*, 2010). As presented in the thesis, LMD combined with modern analytical methods, such as HPLC-DAD, HPLC-MS and NMR, allows for the quantitative analysis of secondary metabolites in plant tissue, even in specific cell populations, to obtain spatial distribution information of secondary metabolites.

1.3 Plants investigated in the thesis

1.3.1 *Myrica gale*

Diarylheptanoids were shown to be biosynthetic intermediates of phenylphenalenones (Hölscher and Schneider, 1995; Schmitt and Schneider, 1999; Munde *et al.*, 2011). However, details of the biosynthetic pathway remain to be studied. Moreover, it is still an open question, why diarylheptanoids in the Musaceae and Haemodoraceae undergo cyclization to form phenylphenalenones while diarylheptanoids in the Zingiberaceae and some dicotyledonous plants such as Betulaceae do not cyclize. *M. gale* (Myricaceae) plants are reported to contain

various diarylheptanoids and therefore the seeds were of special interest for the phytochemical study presented here. Confirming the occurrence of diarylheptanoids would make *M. gale* seeds suitable for future comparative biosynthetic studies, especially with respect to the question whether these compounds are of mono- or polyphyletic origin in various diarylheptanoid-producing families.

1.3.2 Haemodoraceae plants

Previous phytochemical studies on Haemodoraceae plants led to identification of various phenylphenalenone-type compounds (Cooke and Segal, 1955), which are biosynthesized from phenylpropanoid via diarylheptanoids. Except a few studies, which indicated that phenylphenalenones play a role as phytoalexins in *Musa* plants (Luis *et al.*, 1993; Kamo *et al.*, 1998), other biological functions of phenylphenalenons in plants are unexplored. As parts of our continuous efforts on structural and biosynthetic elucidation of phenylphenalenones, *Xiphidium caeruleum* Aubl. and *Wachendorfia thysiflora* L., two species of Haemodoraceae, which are native to the Neotropics (Maas and Maas-van de Kamer, 1993) and Capensis, respectively, were chosen. The phytochemical composition of *X. caeruleum* flowers and *W. thysiflora* aerial plant parts, roots and seeds were studied by HPLC-SPE-NMR.

1.3.3 Rapeseed (*Brassica napus* L.)

Rapeseed is a very important oilseed contributing up to 15 % of the global oilseed production (Wolfram *et al.*, 2010). Beside of the high content of fatty acids, it also contains various secondary metabolites. Among them, glucosinolates and sinapate esters are the predominant ones. Other minor compounds, flavonoids, spermidine conjugate and phenylpropanoids were also identified from rapeseed (Fenwick, 1982). Although glucosinolates and phenolics limit rapeseed nutritional value as food and feed, some of these secondary metabolites were indicated to play positive physiological roles in plant development. For example, glucosinolates are very important defense compounds for plants (Halkier and Gershenzon, 2006); sinapine, which is the dominant sinapate ester in rapeseed, was suggested to supply choline for phosphatidylcholine in young *Raphanus sativus* seedlings (Strack, 1981); phenolics generally protect plant from UV damage (Landry *et al.*, 1995).

In Chapter 4, a thorough phytochemical screening on rapeseed winter cultivar “Emerald” is described. Afterwards, LMD was used to sample four different parts from intact rapeseed. Major secondary metabolites, including glucosinolates and sinapine, as well as three minor secondary metabolites, a unique cyclic spermidine conjugate and two flavonoids, were identified and quantified in different dissected tissues. Cell- and tissue-specific distribution of

metabolites is one of the clues to understand their physiological and ecological importance of plants seeds.

1.3.4 Flaxseed (*Linum usitatissimum*)

Flaxseed is the richest source of lignans in the plant kingdom. Secoisolariciresinol diglucoside (SDG), a lignan with increasing interest in health functions, was reported as the predominant one in flaxseed. Previous studies (Madhusudhan *et al.*, 2000; Wiesenborn *et al.*, 2003; Hano *et al.*, 2006; Attoumbré *et al.*, 2010) showed that SDG is synthesized and accumulated in flaxseed coats. Chapter 5 described how a HPLC-DAD method was developed and validated to quantify SDG and its biosynthetic precursor coniferin in different developmental stages of flaxseed to obtain SDG accumulation kinetic information. On the other hand, LMD was employed to sample the materials from different layers of both developing and mature flaxseed coats. After SDG was released by alkaline hydrolysis, NMR and HPLC methods were applied to identify and quantify SDG in these samples to determine cellular distribution of SDG in flaxseed.

These studies are part of a project exploring possibilities for biotechnological production of lignans. So far existing cell cultures are much less productive in lignan formation compared to whole plants. Spatio-temporal information of SDG formation could be the basis to study the regulation of lignan biosynthesis in flaxseed and to identify biosynthetic bottlenecks in order to established genetically engineered cell lines with high potential for lignan production. On the other hand, information about cell-specific SDG accumulation probably makes possible establishing cell cultures from specific lignan-producing cells and using them to produce SDG *in vitro*.

Chapter 2

Overview of manuscripts

Phytochemical studies by HPLC-SPE-NMR (see Chapters 3.1 -3.4).

3.1 C-methylated flavanones and dihydrochalcones from *Myrica gale* seeds. Jingjing Fang, Christian Paetz, Bernd Schneider. *Biochem. Syst. Ecol.* 2011, (39): 68-70.

Twelve C-methylated flavanones and dihydrochalcones were elucidated were elucidated from 100.6 mg *Myrica gale* seeds by HPLC-SPE-NMR and LC-MS in the paper.

Dr. B. Schneider and J. Fang designed the experiments, J. Fang performed the experiments, Dr. C. Paetz performed the LC-MS experiments, J. Fang and Dr. B. Schneider wrote the manuscript.

3.2 Phenylphenalenones and related natural products from *Wachendorfia thyrsiflora* L. Jingjing Fang, Christian Paetz, Dirk Hölscher, Tobias Munde, Bernd Schneider. *Phytochem. Lett.* 2011, (4): 203-208.

Total 24 phenylphenalenon-type compounds including five new compounds were reported from *Wachendorfia thyrsiflora* plant material, including leaves, roots, root culture and seeds in the paper.

Dr. B. Schneider conceived the experiments, J. Fang designed and performed the experiments of phytochemical study on seeds by HPLC-SPE-NMR, and the other authors designed and performed experiments on the other plant parts, Dr. B. Schneider and J. Fang wrote the manuscript.

3.3 Phytochemical profile of aerial parts and roots of *Wachendorfia thyrsiflora* L. studied by LC-DAD-SPE-NMR. Jingjing Fang, Marco Kai, Bernd Schneider. *Phytochemistry* 2012, (81): 144-152.

Using HPLC-SPE-NMR, eleven phenylphenalenones and related compounds were identified in the aerial parts of the plant, ten compounds were found in the roots, and four additional compounds occurred in both plant parts. Twelve compounds are new compounds including five alkaloids (phenylbenzoisoquinolinones). Different chemical patterns of phenylphenalenones were found in roots and aerial parts, biosynthesis and translocation of phenylphenalenones in *W. thyrsiflora* were proposed.

Dr. B. Schneider and J. Fang designed the experiments, J. Fang performed the

experiments, Dr. M. Kai recorded the high-resolution MS data, J. Fang and Dr. B. Schneider wrote the manuscript.

3.4 Co-occurrence of phenylphenalenones and flavonoids in *Xiphidium caeruleum* Aubl. flowers. Jingjing Fang, Dirk Hölscher, Bernd Schneider. *Phytochemistry* 2012, (82): 143-148.

Seventeen phenylphenalenone-type compounds including five new ones, and three flavonoids were determined from fractions of a *Xiphidium caeruleum* flower extract by HPLC-SPE-NMR. Flavonoids were detected in Haemodoraceae plants for the first time.

Dr. B. Schneider, J. Fang and Dr. D. Hölscher designed the experiments, J. Fang performed the experiments, J. Fang and Dr. B. Schneider wrote the manuscript.

Secondary metabolites profiling and their distribution in rapeseed (see Chapters 4.1 and 4.2).

4.1 Metabolic profiling of lignans and other secondary metabolites from rapeseed (*Brassica napus* L.). Jingjing Fang, Michael Reichelt, Marco Kai, Bernd Schneider. *J. Agric. Food Chem.* 2012, under revision.

Eleven glucosinolates and eighteen phenolics including seven new lignans were determined from rapeseed (*Brassica napus*).

Dr. B. Schneider and J. Fang designed the experiments, J. Fang performed the experiments, Dr. M. Reichelt determined the glucosinolates, Dr. M. Kai recorded high-resolution MS data. J. Fang and Dr. B. Schneider wrote the manuscript.

4.2 Tissue-specific distribution of secondary metabolites in rapeseed (*Brassica napus* L.). Jingjing Fang, Michael Reichelt, William Hidalgo, Sara Agnolet, Bernd Schneider. *Plos One* 2012, under revision.

Major secondary metabolites, glucosinolates and sinapine, and minor secondary metabolites, two flavonoids and a cyclic spermidine conjugate were quantified in different mature rapeseed tissues dissected by laser microdissection (LMD). No qualitative and quantitative difference of glucosinolates and sinapine was detected in embryo tissues. The two flavonoids were predominantly detected in cotyledons, and the cyclic spermidine conjugate was exclusively found in hypocotyl and radicle.

Dr. B. Schneider and J. Fang designed the experiments, J. Fang performed the experiments, Dr. M. Reichelt performed quantification, W. Hidalgo synthesized one internal standard and analyzed partial data, Dr. S. Agnolet analyzed partial data, J. Fang and Dr. B. Schneider wrote the manuscript.

Spatio-temporal accumulation of secoisolariciresinol diglucoside in flaxseed (see Chapters 5.1 and 5.2).

5.1 Concentration kinetics of secoisolariciresinol diglucoside and its biosynthetic precursor coniferin in developing flaxseed. Jingjing Fang, Aina Ramsay, Christian Paetz, Evangelos C. Tatsis, Sullivan Renouard, Christophe Hano, Eric Grand, Ophélie Fliniaux, Albrecht Roscher, Francois Mesnard, Bernd Schneider. *Phytochem. Anal.* 2012, DOI: 10.1002/pca.2377.

Concentrations kinetics of secoisolariciresinol diglucoside and its biosynthetic precursor coniferin were established by quantifying the concentrations of the two compounds in developing flaxseed at different stages.

Dr. B. Schneider and J. Fang designed the experiments, J. Fang performed the experiments, J. Fang and Dr. B. Schneider wrote the manuscript, and the other authors contributed reagents, materials, and revised the manuscript.

5.2 Laser microdissection-assisted quantitative cell layer-specific detection of secoisolariciresinol diglucoside in flaxseed coats. Jingjing Fang, Aina Ramsay, Sullivan Renouard, Christophe Hano, Frédéric Lamblin, Brigitte Chabbert, François Mesnard, Bernd Schneider. In preparation.

SDG was identified and quantified by NMR and HPLC in different cell layers harvested from seed coats of mature and developing flaxseed. The result showed that SDG accumulated in the parenchymatous cell layer of the outer integument of flaxseed coats. The results were further confirmed by molecular methods. The promoter of one pinoresinol-lariciresinol reductase gene of *L. usitatissimum* (*LuPLR1*), a key gene involved in SDG biosynthesis, was fused to a β -glucuronidase (*GUS*) reporter gene, and the spatio-temporal regulation of *LuPLR1* gene expression in flaxseed was determined by histochemical and activity assays of *GUS*.

Dr. B. Schneider and J. Fang designed the experiments, J. Fang performed the chemical experiments including the LMD and quantification, and the other authors performed the molecular experiments, contributed reagents, material, J. Fang and Dr. B. Schneider wrote the manuscript, and the other authors critically revised the manuscript.

Chapter 3

Phytochemical study by HPLC-SPE-NMR

- 3.1 C-methylated flavanones and dihydrochalcones from
Myrica gale seeds. 13
- 3.2 Phenylphenalenones and related natural products from
Wachendorfia thyrsiflora L. 16
- 3.3 Phytochemical profile of aerial parts and roots of
Wachendorfia thyrsiflora L. studied by LC-DAD-SPE-NMR. 22
- 3.4 Co-occurrence of phenylphenalenones and flavonoids in
Xiphidium caeruleum Aubl. flowers. 31



C-methylated flavanones and dihydrochalcones from *Myrica gale* seeds

Jingjing Fang, Christian Paetz, Bernd Schneider*

Max Planck Institute for Chemical Ecology, Beutenberg Campus, Hans-Knöll-Straße 8, D-07745 Jena, Germany

ARTICLE INFO

Article history:

Received 10 September 2010

Accepted 16 January 2011

Available online 3 February 2011

Keywords:

Myrica gale

Myricaceae

Flavanones

Chalcones

HPLC-SPE-NMR

HPLC-MS

1. Subject and source

Myrica gale L. (Myricaceae), commonly known as sweet gale and bog myrtle, is a deciduous shrub widely distributed at high latitudes in the Northern hemisphere (Skene et al., 2000). It is known that the fruits of *M. gale* were used as a predominant beer additive before the utilization of hop (*Humulus lupulus* L.) (Behre, 1999). The essential oil from the aerial parts of *M. gale* is used as an effective insect repellent (Simpson et al., 1996). The seeds of *M. gale* used in this study were purchased from B&T World Seeds (Paguignan, France), reference number 26897.

2. Previous work

The essential oil from aerial parts of *M. gale* shows various activities, such as antimicrobial and anticancer properties, and the components of the oil were thoroughly investigated (Schantz and Kapetani, 1971; Popovici et al., 2008 and literature cited therein). Triterpenoids (Sakurai et al., 1997), diarylheptanoids and diarylheptanoid glucosides (Anthonsen et al., 1975; Malterud et al., 1976; Nagai et al., 1995; Morihara et al., 1997), flavonoids, flavonoid glucosides and tannins (Carlton et al., 1990; Nagai et al., 1995; Santos and Waterman, 2000), and phenolic acids (Perkin, 1900; Nagai et al., 1995; Kashina et al., 2008) were identified from the aerial parts of the plants. In addition, some unusual C-methylated plant polyketides, including a flavonol (Popovici et al., 2010), a chalcone (Mathiesen et al., 1996; Popovici et al., 2010), and nine dihydrochalcones (Anthonsen et al., 1971; Malterud et al., 1977, 1996; Malterud, 1992; Mathiesen et al., 1995, 1996; Sokolova et al., 2005; Popovici et al., 2010), were identified from the fruits or the fruit exudates of *M. gale*.

3. Present study

Seeds of *M. gale* (100.6 mg) were ground and extracted with 50% acetone solution in water (8 ml). The extract was filtered and dried by nitrogen gas to yield 10 mg residue, which was dissolved in DMSO (50 µl) for further analysis. The separation and

* Corresponding author. Tel.: +49 3641 571600; fax: +49 3641 571601.

E-mail address: schneider@ice.mpg.de (B. Schneider).

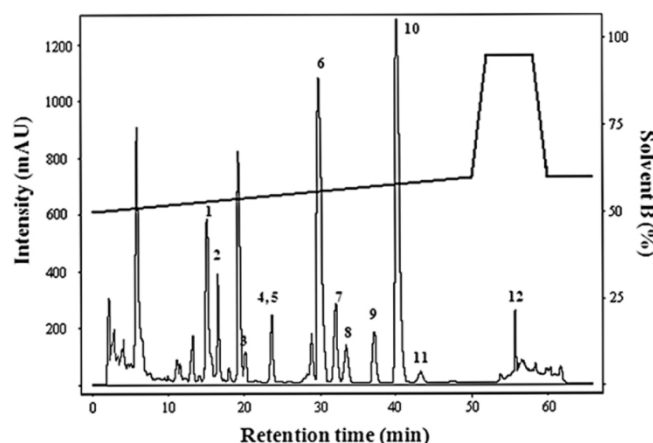


Fig. 1. HPLC profile of the seed extract of *M. gale* monitored at 280 nm. The identified metabolites are labeled 1–12 (for structures, see Fig. 2).

elucidation of the components of the extract were accomplished by HPLC-SPE-NMR and HPLC-MS. An Agilent 1100 chromatography system (quaternary solvent delivery pump G1311A, autosampler G1313A) and a J&M photodiode array detector (DAD; detection 200–700 nm) were connected to a Spark Prospekt 2 solid-phase extraction (SPE) device, containing HySphere resin GP cartridges (10 × 2 mm, 10 μm). The LC-SPE system was connected to a Bruker Avance 500 NMR spectrometer equipped with TCI CryoProbe™ (5 mm) and a CryoFIT™ flow conversion system (cell volume 30 μl). For LC-MS measurements, a Bruker Esquire 3000 ion trap mass spectrometer was connected to the Agilent 1100 chromatography system. HyStar™ 3.2 software was used to coordinate the LC-NMR and LC-MS experiments. Topspin™ 2.0 software was used to control the NMR spectrometer and to perform data processing. The chromatographic separation was conducted with a Purospher STAR RP-18e 5 μm (250 × 4.6 mm i.d.) column using a binary gradient of water (solvent A) and acetonitrile (solvent B), both containing 0.1% (v/v) formic acid, with a 1.0 ml/min flow rate at 25 °C. The following linear gradient was applied: 0 min: 50% B, 50 min: 60% B, 52 min: 95% B, 58 min: 95% B, and 60 min: 50% B, followed by a 5 min conditioning step. The injection volume was 6 μL. The HPLC eluate was monitored by DAD at wavelengths of 254, 280, and 320 nm with manually control SPE trappings. A total of six cumulative trappings were performed for each peak selected for analysis. After the cartridges were dried with nitrogen gas, the analytes were eluted with acetonitrile-*d*₃ and transferred through a capillary to the NMR CryoFIT™ flow cell for analysis. The same separation conditions were used for the ESI-MS measurement. Ions were detected in negative mode in the range of

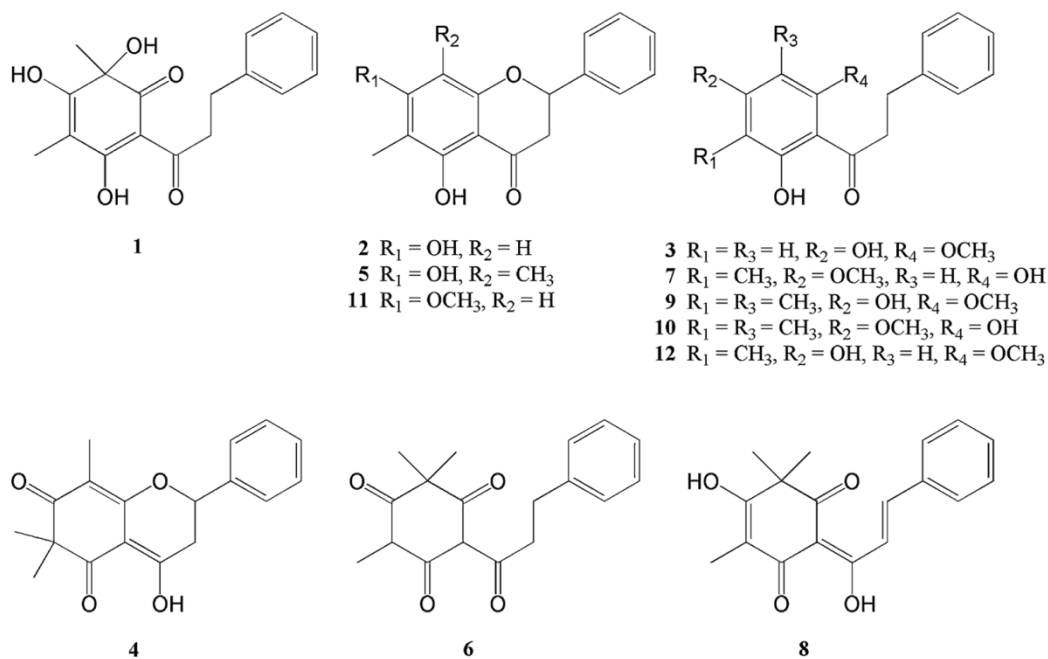


Fig. 2. Structures of the compounds isolated from *M. gale* seeds.

m/z 150–1000. The MS working conditions were as follows: the nebulizer pressure was 30 psi, the drying gas flow was kept at 7.0 l/min, the drying gas temperature was 300 °C, and the capillary spray voltage was 4.0 kV.

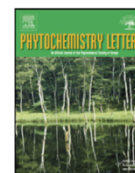
Twelve phenolic natural products were separated (Fig. 1) and identified by spectroscopic methods (MS, ^1H and 2D NMR) and comparison with literature data. Eventually, the compounds 1–6 were identified as ceratiolin (1) (Tanrisever et al., 1987), 5,7-dihydroxy-6-methylflavanone (2) (Pavan et al., 2009), uvangoletin (3) (Hufford and Oguntimein, 1980), hariganetin (4) (Wada et al., 1988), 5,7-dihydroxy-6,8-dimethylflavanone (5) (Pavan et al., 2009), and 3-(β -phenylpropionyl)-5-methyl filicinic acid (6) (Anthonsen et al., 1971). Compound 6 was also named 4,4,6-trimethyl-2-(3-phenylpropionyl)-cylohexane-1,3,5-trione (Uyar et al., 1978) and myrigalone A (Mathiesen et al., 1995). Furthermore, compounds 7–9 were identified as myrigalone G (7) (Mathiesen et al., 1995), champanone B (8) (Bonilla et al., 2005), and myrigalone D (9) (Mathiesen et al., 1996), which was also named angoletin (9) (Hufford and Oguntimein, 1980). Finally, compounds 10–12 were identified as 2',6'-dihydroxy-4'-methoxy-3',5'-dimethyldihydrochalcone (10) (Anthonsen et al., 1971; Uyar et al., 1978), also named myrigalone B (Mathiesen et al., 1995), 5-hydroxy-7-methoxy-6-methylflavanone (11) (Wollenweber et al., 1985a), and 2',4'-dihydroxy-6'-methoxy-3'-methyldihydrochalcone (12) (Malterud, 1992), also known as myrigalone H (Mathiesen et al., 1995) (Fig. 2). Compounds 1–5, 8 and 11 were detected from *M. gale* for the first time.

4. Chemotaxonomic and ecological significance

The genus *Myrica* contains about 60 species. Besides *M. gale*, C-methylflavonoids were only found in two other *Myrica* species, *Myrica pensylvanica* (Wollenweber et al., 1985b) and *Myrica serrata* (Gafner et al., 1996). The occurrence of unusual C-methylated dihydrochalcones and flavonoids may support the discussion (Verdcourt and Polhill, 1997; Skene et al., 2000) about segregating *M. gale* from the genus *Myrica* to a new genus named *Gale*. Some C-methylchalcones were also detected from *Comptonia peregrina* (Wollenweber et al., 1985b), which is the sole species of the genus *Comptonia* in the Myricaceae. Former studies showed that the C-methylchalcones, which are the dominant components in the exudates of *M. gale* fruits, have antifungal activity (Malterud and Faegri, 1982; Gafner et al., 1996). Recent research (Popovici et al., 2010) suggests that these compounds may act as signals in the establishment of mutualistic nitrogen-fixing symbioses by enhancing compatible fungi and inhibiting incompatible ones.

References

- Anthonsen, T., Falkenberg, I., Laake, M., Midelfart, A., Mortensen, T., 1971. *Acta Chem. Scand.* 25, 1929.
- Anthonsen, T., Lorentzen, G.B., Malterud, K.E., 1975. *Acta Chem. Scand.* B 29, 529.
- Bonilla, A., Duque, C., Garzon, C., Takaishi, Y., Yamaguchi, K., Hara, N., Fujimoto, Y., 2005. *Phytochemistry* 66, 1736.
- Behre, K.E., 1999. *Veg. Hist. Archaeobot.* 8, 35.
- Carlton, R.R., Gray, A.I., Lavaud, C., Massiot, G., Waterman, P.G., 1990. *Phytochemistry* 29, 2369.
- Gafner, S., Wolfender, J.L., Mavi, S., Hostettmann, K., 1996. *Planta Med.* 62, 67.
- Hufford, C.D., Oguntimein, B.O., 1980. *Phytochemistry* 19, 2036.
- Kashina, A.A., Tulaikin, A.I., Yakovlev, G.P., 2008. *Rastitel'nye Resursy* 44, 95.
- Malterud, K.E., 1992. *Acta Pharm. Nord.* 4, 65.
- Malterud, K.E., Anthonsen, T., Hjortas, J., 1976. *Tetrahedron Lett.* 35, 3069.
- Malterud, K.E., Anthonsen, T., Lorentzen, G.B., 1977. *Phytochemistry* 16, 1805.
- Malterud, K.E., Diep, O.H., Sund, R.B., 1996. *Pharmacol. Toxicol.* 78, 111.
- Malterud, K.E., Faegri, A., 1982. *Acta Pharm. Suecica* 19, 43.
- Mathiesen, L., Malterud, K.E., Sund, R.B., 1995. *Planta Med.* 61, 515.
- Mathiesen, L., Malterud, K.E., Sund, R.B., 1996. *Eur. J. Pharm. Sci.* 4, 373.
- Morihara, M., Sakurai, N., Inoue, T., Kawai, K., Nagai, M., 1997. *Chem. Pharm. Bull.* 45, 820.
- Nagai, M., Dohi, J., Morihara, M., Sakurai, N., 1995. *Chem. Pharm. Bull.* 43, 1674.
- Pavan, F.R., Leite, C.Q.F., Coelho, R.G., Coutinho, I.D., Honda, N.K., Cardoso, C.A.L., Vilegas, W., Leite, S.R.A., Sato, D.N., 2009. *Quim. Nova* 32, 1222.
- Perkin, A.G., 1900. *J. Chem. Soc.* 77, 423.
- Popovici, J., Bertrand, C., Bagnarol, E., Fernandez, M.P., Comte, G., 2008. *Nat. Prod. Res.* 22, 1024.
- Popovici, J., Comte, G., Bagnarol, E., Fournier, P., Bellvert, F., Bertrand, C., 2010. *Appl. Environ. Microbiol.* 76, 2451.
- Sakurai, N., Hosono, Y., Morihara, M., Ishida, J., Kawai, K., Inoue, T., Nagai, M., 1997. *Yakugaku Zasshi* 117, 211.
- Santos, S.C., Waterman, P.G., 2000. *Fitoterapia* 71, 610.
- Schantz, M.V., Kapetani, I., 1971. *Pharm. Acta Helv* 46, 649.
- Simpson, M.J.A., MacIntosh, D.F., Cloughley, J.B., Stuart, A.E., 1996. *Econ. Bot.* 50, 122.
- Skene, K.R., Sprent, J.I., Raven, J.A., Herdman, L., 2000. *J. Ecol.* 88, 1079.
- Sokolova, M., Orav, A., Koel, M., Kailas, T., Muurisepp, M., 2005. *J. Essent. Oil Res.* 17, 188.
- Tanrisever, N., Fronczek, F.R., Fischer, N., Williamson, G.B., 1987. *Phytochemistry* 26, 175.
- Uyar, T., Malterud, K.E., Anthonsen, T., 1978. *Phytochemistry* 17, 2011.
- Verdcourt, B., Polhill, R., 1997. *Taxon* 46, 347.
- Wada, H., Tanaka, N., Murakami, T., Uchida, T., Kozawa, K., Saiki, Y., Chen, C.M., 1988. *Yakugaku Zasshi* 108, 740.
- Wollenweber, E., Dietz, V.H., Schilling, G., Favre-Bonvin, J., Smith, D.M., 1985a. *Phytochemistry* 24, 965.
- Wollenweber, E., Kohorst, G., Mann, K., Bell, J.M., 1985b. *J. Plant Physiol.* 117, 423.



Phenylphenalenones and related natural products from *Wachendorfia thyrsiflora* L.

Jingjing Fang, Christian Paetz, Dirk Hölscher, Tobias Munde, Bernd Schneider*

Max Planck Institute for Chemical Ecology, Beutenberg Campus, Hans-Knöll Str. 8, 07745 Jena, Germany

ARTICLE INFO

Article history:

Received 13 January 2011
Received in revised form 25 March 2011
Accepted 26 March 2011
Available online 8 April 2011

Keywords:

Wachendorfia thyrsiflora
Haemodoraceae
LC-NMR
Oxabenzochrysenones
Phenylbenzoisochromenones
Phenylanthracene anhydrides
Phenylphenalenones

ABSTRACT

Phytochemical studies of different plant parts and root cultures of *Wachendorfia thyrsiflora* (Haemodoraceae) resulted in 24 phenylphenalenones and related compounds, which were elucidated by means of nuclear magnetic resonance (NMR) spectroscopy and mass spectrometry (MS). Among them, one new 9-phenylphenalenone, two new phenylphenalenone *O*-glycosides carrying the sugar moiety in position 4 of the 9-phenylphenalenone skeleton and two new 7-phenyl-benzoisochromenone-6-*O*-glucosides were identified.

© 2011 Phytochemical Society of Europe. Published by Elsevier B.V. All rights reserved.

1. Introduction

Previous phytochemical analyses of the flowers (Dora et al., 1991), roots (Edwards, 1974; Otálvaro et al., 2002), and root cultures (Opitz et al., 2002b; Opitz and Schneider, 2003; Otálvaro et al., 2010) of *Wachendorfia thyrsiflora*, a member of the family Haemodoraceae endemic to the South Africa's cape region, resulted in the isolation and identification of a variety of phenylphenalenones and related natural products. Root cultures of *W. thyrsiflora* have been used to study enzymes involved in the biosynthesis of phenylphenalenone precursors (Brand et al., 2006). Here we report the identification of five new and eighteen known natural products and one artifact (Fig. 1) of the phenylphenalenone type. To identify known compounds, we compared their spectroscopic data with those of authentic references or by full assignment of ^1H and ^{13}C NMR chemical shifts. 1D and 2D NMR data of compounds from seeds were recorded using liquid chromatography–diode array detection–solid phase extraction–NMR (LC–DAD–SPE–NMR) coupling. The isolated compounds possess chemotaxonomic significance for the family Haemodoraceae.

2. Results

2.1. Phenylphenalenones from leaves

Thyrsiflorin (**1**) from flowers of *W. thyrsiflora* is the only phenylphenalenone from aerial plant parts (Dora et al., 1991). In this study, separation of the EtOAc phase resulted in two metabolites. The low-field part of the ^1H NMR spectrum of compound **2** (Table 1) displayed the doublets of an AX spin system ($J = 7.5$ Hz) at δ 7.41 (H-8) and 8.15 (H-9), a singlet at δ 7.22, and AB doublets (δ 5.77 and 5.73, $J = 15.4$ Hz) of an oxygenated methylene group. Broadened signals of a monosubstituted phenyl ring appeared between δ 7.55 and 7.22, suggesting a 7-phenylbenzoisochromenone glucoside (Opitz et al., 2002a). This suggestion was confirmed by HSQC and HMBC cross-peaks, e.g. the signals δ 7.22, 8.15 and 5.77/5.73 with a quaternary carbon signal (δ 125.9), which therefore was assigned to the central C-9b of the phenalenone tricycle. The HMBC correlation between H-8 and C-1' indicated the position of the phenyl ring. Oxygen functionalities at C-5 (δ 148.9) and C-6 (δ 138.6) were established by means of their HMBC cross-peaks with the proton signal at δ 7.22. Signals in the carbohydrate region of the ^1H NMR spectrum suggested a glycosidic structure for compound **2**. The coupling constant $J = 7.7$ Hz of H-1'' (δ 4.66) indicated β -configuration at the anomeric centre of the carbohydrate unit and $^3J_{\text{H-2}''\text{-H-3}''}$, $^3J_{\text{H-3}''\text{-H-4}''}$, and $^3J_{\text{H-4}''\text{-H-5}''}$ of approximately 9 Hz showed that H-1'' to H-5'' are in axial geometry which is characteristic of glucose. The HMBC correlation between H-1'' and C-6 (δ 138.6) established that the glucose was attached to C-6 of the aglycon. From these data the

* Corresponding author. Tel.: +49 3641 571600; fax: +49 3641 571601.
E-mail address: schneider@ice.mpg.de (B. Schneider).

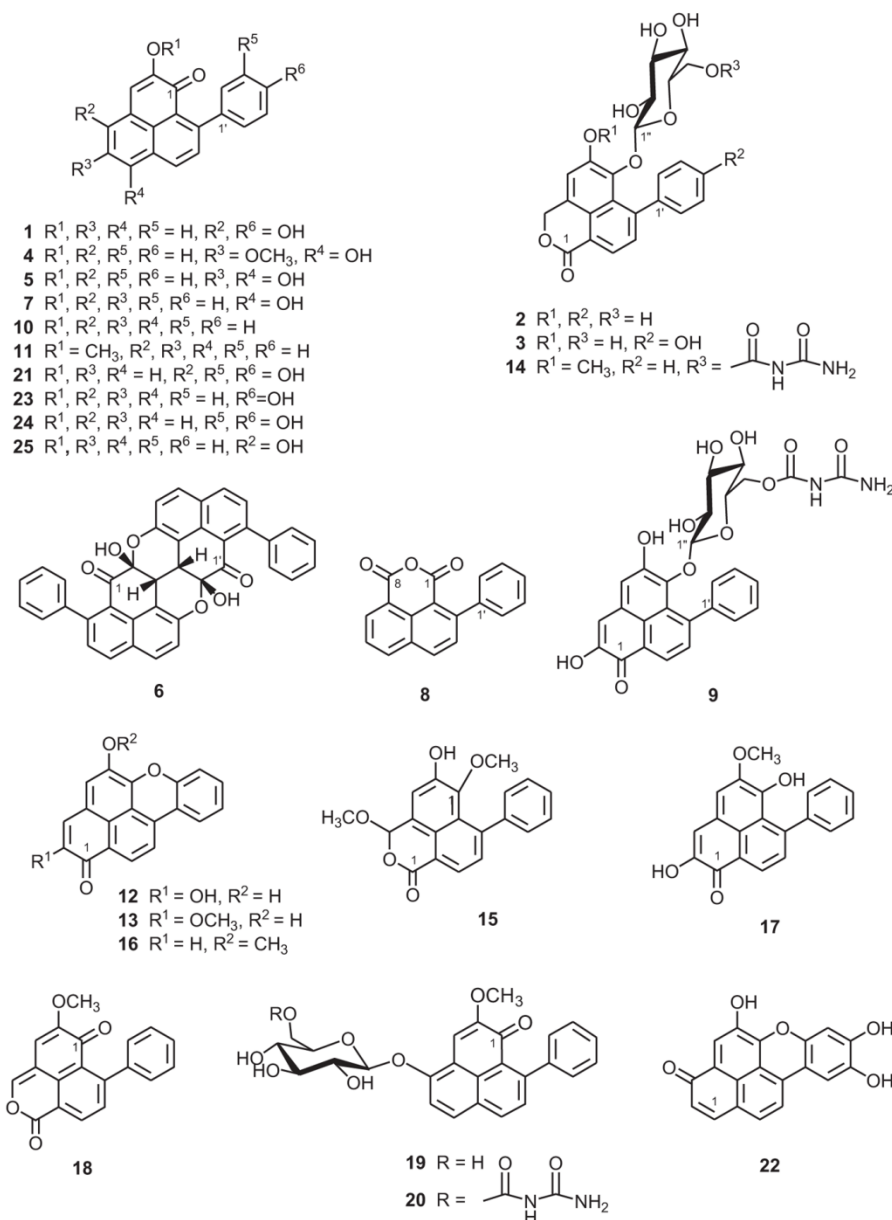


Fig. 1. Structures and numbering of phenylphenalenones and related compounds from *Wachendorfia thyrsoiflora*. Compounds **2**, **3**, and **19–21** are new natural products. Compound **7** was isolated from *W. paniculata* (Edwards, 1974).

structure of compound **2** was elucidated as 6-*O*-(β -D-glucopyranosyl)-5-hydroxy-7-phenyl-3*H*-benzo[de]isochromen-1-one. ESIMS and HRESIMS data confirmed the suggested structure (see Section 4).

The only striking difference between the NMR spectra (Table 1) of compounds **3** and **2** was detected in the signals of the lateral phenyl ring. Unlike **2**, the signals of the phenyl ring of **3** integrated for four instead of five protons. Although broadened due to the interaction between the aryl ring and the glucose unit, the signals of H-3'/5' appeared as the BB' part (d, J = 7.5 Hz) of an AA'BB' spin system, suggesting a substituent in the 4'-position of the aryl ring. ESIMS and HRESIMS (see Section 4) indicated a molecular mass of

m/z 470, which is consistent with an additional oxygen in the molecule of compound **3**. According to the NMR data, this oxygen must be situated at C-4' and compound **3** was therefore identified as 6-*O*-(β -D-glucopyranosyl)-5-hydroxy-7-(4'-hydroxyphenyl)-3*H*-benzo[de]isochromen-1-one.

2.2. Phenylphenalenones from roots

Compounds **4–6** have been previously reported from the roots of *W. thyrsoiflora* (Edwards, 1974; Otálvaro et al., 2002). Furthermore, lachnanthocarpone (**7**) was found in the roots of *Wachendorfia paniculata* (Edwards, 1974). Our investigation of root

Table 1
¹H NMR (500 MHz) and ¹³C NMR data (125 MHz) of compounds **2**, **3** (in acetone-*d*₆), **19** and **20** (in MeOH-*d*₄).

Position	2		3		19		20	
	δ_{H} (J, Hz)	δ_{C}	δ_{H} (J, Hz)	δ_{C}	δ_{H} (J, Hz)	δ_{C}	δ_{H} (J, Hz)	δ_{C}
1		166.9		167.0		181.4		181.3
2						154.3		154.0
3	5.77 (d, 15.4) 5.73 (d, 15.4)	70.6	5.75 (d, 15.8) 5.71 (d, 15.8)	70.6	7.69 (s)	108.1	7.68 (s)	107.9
3a		126.3		126.3		117.0		117.1
4	7.22 (s)	116.7	7.20 (s)	116.5		157.3		157.2
5		148.9		148.8	7.67 (d, 9.0)	119.2	7.62 (d, 9.0)	119.4
6		138.6		138.9	8.05 (d, 9.0)	133.3	8.09 (d, 9.0)	133.2
6a		120.0		119.7		129.5		129.5
7		146.0		146.1	8.25 (d, 8.2)	136.3	8.27 (d, 8.2)	136.1
8	7.41 (d, 7.5)	131.8	7.40 (d, 7.5)	131.8	7.47 (d, 8.2)	131.2	7.49 (d, 8.2)	131.2
9	8.15 (d, 7.5)	126.9	8.12 (d, 7.5)	127.1		150.9		150.8
9a		128.6		128.5		126.5		126.4
9b		125.9		126.0		127.6		127.5
OCH ₃					3.90 (s)	55.4	3.90 (s)	56.3
1'		145.0		136.2		145.0		144.8
2'	7.40–7.22 (br)	127.4 (br)	7.3 (br)	132.4 (br)	7.30 (m)	129.2	7.31 (m)	129.0
3'	7.55–7.45 (br)	130.8 (br)	6.80 (brd, 7.5)	114.7 (br)	7.40 (m)	129.4	7.42 (m)	129.2
4'	7.32 (br)	127.7		157.6	7.35 (m)	128.2	7.36 (m)	128.2
5'	7.35–7.40 (br)	131.7 (br)	6.80 (brd, 7.5)	114.7 (br)	7.40 (m)	129.4	7.42 (m)	129.0
6'	7.40–7.22 (br)	128.1 (br)	7.3 (br)	132.4 (br)	7.30 (m)	129.2	7.31 (m)	129.0
1''	4.66 (d, 7.7)	104.2	4.57 (d, 7.7)	104.8	5.21 (d, 7.8)	103.0	5.18 (d, 7.8)	102.9
2''	2.41 (dd, 7.7, 9.5)	74.7	2.69 (dd, 7.7, 9.5)	74.9	3.67 (dd, 7.8, 9.1)	75.3	3.66 (dd, 7.8, 9.1)	74.9
3''	3.17 (dd, 9.5, 9.2)	77.7	3.21 (dd, 9.5, 9.2)	77.7	3.55 (dd, 9.1, 8.6)	78.5	3.55 (dd, 9.1, 8.6)	77.9
4''	2.95 (dd, 9.2, 9.8)	71.4	3.03 (dd, 9.2, 9.8)	71.4	3.48 (dd, 8.6, 9.7)	71.5	3.45 (dd, 8.6, 9.7)	71.5
5''	2.90 (ddd, 9.8, 5.5, 2.3)	77.9	2.92 (ddd, 9.8, 5.5, 2.0)	78.0	3.57 (ddd, 9.7, 6.8, 2.0)	78.9	3.78 (ddd, 9.7, 6.8, 2.0)	75.7
6''a	3.58 (dd, 11.5, 5.5)	62.8	3.59 (dd, 11.5, 2.0)	62.7	3.94 (dd, 12.1, 2.0)	62.7	4.59 (dd, 12.1, 2.0)	65.6
6''b	3.45 (dd, 11.5, 2.3)		3.46 (dd, 11.5, 5.5)		3.76 (dd, 12.1, 6.8)		4.31 (dd, 12.1, 6.8)	
1'''								168.6
3'''								170.1

extracts identified, in addition to **4–6**, 2-phenylnaphthalic anhydride (**8**) (Cooke and Thomas, 1975), and the (6'-*O*-allophanil)-glucoside **9**, which was first found in *Xiphidium caeruleum* (Opitz et al., 2002a).

2.3. Phenylphenalenones from root cultures

Root cultures of *W. thyrsoflora* have proved to be a rich source of phenylphenalenones (Opitz et al., 2002b; Otálvaro et al., 2010). The occurrence of compounds **9–15** was reported by Opitz (2002). Compounds **16–18** also occurred in the root cultures (Opitz et al., 2002b; Brand et al., 2006).

Moreover, two new minor glucosides **19** and **20** are reported here for the first time, and their structure elucidation is described as follows: the ¹H NMR spectrum of compound **19** (Table 1) displayed four doublets of two AX spin systems, the signals of a monosubstituted phenyl ring and a methine singlet in the aromatic part of the spectrum. The chemical shifts and coupling constants of these signals resembled those of the ¹H NMR data of 4-hydroxyanigorufone (Hölscher and Schneider, 1999). In addition, a singlet of a phenolic *O*-methyl group and a set of carbohydrate signals occurred in the spectrum. Mutual ¹H–¹³C long-range heterocorrelation (HMBC) cross-signals between H-6/C-7 (δ 136.3) and H-7/C-6 (δ 133.3) assigned the two AX spin systems to H-5/H-6 and H-7/H-8. Strong HMBC correlations of the methine singlet at δ 7.69 (H-3) with the low-field quaternary carbon signals δ 181.4 and 157.3 established the presence of a carbonyl and a hydroxylated carbon at a distance of three bonds in positions 1 and 4. An HMBC cross-signal between H-6 and δ 157.3 indicated that C-4 was an oxygenated quaternary carbon. An HMBC cross-peak of the three-proton singlet (δ 3.90) indicated that the methoxyl group is attached to the remaining oxygenated aromatic carbon atom C-2 (δ 154.3). The position of the phenyl ring at C-9 was deduced from HMBC cross-peaks of H-8 and H-3'/5' with C-1', H-2'/4' and H-7 with C-9. The HSQC signals indicated a hexopyranose unit.

Coupling constants ³*J* = 6.8–9.7 Hz suggested that the methine protons H-1'' to H-5'' had an axial orientation, which is characteristic of glucose. The coupling constant ³*J*_{H-1''-H-2''} = 7.8 Hz indicated a β -configuration at the anomeric C-1'', and an HMBC correlation of H-1'' with δ 157.3 clearly confirmed that the β -glucose was linked to C-4. Based on these NMR data, compound **19** was identified as 4-*O*- β -D-glucopyranosyl-2-methoxy-9-phenyl-1*H*-phenalen-1-one. ESIMS and HRESIMS data further confirmed the structure (see Section 4).

The ¹H and ¹³C NMR chemical shifts of compound **20** (Table 1) closely resembled those of compound **19**; exceptions were those of H/C-6'', which are shifted to a low field, indicating substitution at the hydroxymethylene group of the glucose unit. Two additional carbonyl signals in the ¹³C NMR spectrum at δ 168.6 and 170.1 suggested an allophanil substituent in this position. From these data, compound **20** was identified as 6-*O*-[(6'-*O*-allophanil)- β -D-glucopyranosyl]-2-methoxy-9-phenyl-1*H*-phenalen-1-one. MS data further confirmed the structure of the aglycone (see Section 4).

2.4. Phenylphenalenones from seeds

Seeds of *W. thyrsoflora* vary in weight between 2 and 22 mg (the average is 14.7 mg; Bond et al., 1999) and possess an intensely corrugated dark brown surface. The seeds immediately release colored matter when immersed in organic solvents such as acetone or MeOH. The residue from methanolic extract from the seeds was subjected to LC–DAD–SPE–NMR and LC–MS analyses. Eight peaks were detected at *R*_t 13.3 min (**21**), 15.4 min (**22**), 15.8 min (**1**), 21.3 min (**24**), 27.4 min (**23**), 28.2 min (**25**), 35.8 min (**10**), 59.0 min (**6**), and trapped on HySphere resin GP cartridges for post-column solid-phase extraction (SPE). The long-wave absorption maxima of the isolated compounds suggested intact phenylphenalenones. The absorption around 525 nm and an intense autofluorescence of **22** was typical of an oxabenzochrysenone structure.

The ^1H NMR spectrum of compound **21** (Table 2) showed an aromatic singlet at δ 7.52 (H-3), four other broad singlets of hydroxyl groups at δ 6.72 (3'-OH), 6.80 (4'-OH), 7.27 (2-OH) and 8.40 (4-OH), respectively, two doublets of an AX spin system ($J = 8.1$ Hz) at δ 8.19 (H-7) and 7.44 (H-8), another AX spin system ($J = 8.9$ Hz) of the doublets at δ 7.29 (H-5) and 7.94 (H-6), three signals of an ABX spin system at δ 6.85 (H-2', d, $J = 2.0$ Hz), 6.89 (H-5', d, $J = 8.1$ Hz) and 6.75 (H-6', dd, $J = 8.1, 2.0$ Hz). The signal pattern suggested a phenylphenalenone. The substitution positions of the phenyl group and the hydroxyl groups were confirmed by HSQC and ^1H - ^{13}C long-range correlations in the HMBC spectrum, in which the correlations between signals δ 7.52 (H-3), 7.94 (H-6), 8.19 (H-7) and the carbon signal δ 127.3 assigned the carbon to C-9b, the central position of the phenalenone tricycle. The correlations between δ 7.94 (H-6) and δ 136.0 (C-7) and between δ 8.19 (H-7) and δ 133.1 (C-6), as well as a series of ^1H , ^1H COSY and long-range COSY signals between δ 7.29 (H-5) and 7.94 (H-6), and between δ 8.19 (H-7) and 7.44 (H-8), assigned the NMR data of protons to positions 5–8. The correlations between δ 8.19 (H-7), 6.85 (H-2'), 6.75 (H-6') and δ 150.0 (C-9), between δ 7.44 (H-8), 6.89 (H-5') and δ 136.4 (C-1') confirmed the phenyl substituent at C-9. Based on the above NMR data and combined with MS data (see Section 4), the structure of compound **21** was elucidated as 2,4-dihydroxy-9-(3,4-dihydroxyphenyl)-1H-phenalen-1-one.

The other seven known compounds were determined by ^1H NMR and/or 2D NMR spectroscopy, mass spectrometry, and comparison with reported data as thyriflorin (**1**) (Dora et al., 1991), haemofluorone B (**22**) (Cooke and Dagley, 1979), anigorufone (**10**), hydroxyanigorufone (**23**), dihydroxyanigorufone (**24**) (Cooke and Thomas, 1975), 4-hydroxyanigorufone (**25**), and anigorootin (**6**) (Hölscher and Schneider, 1999).

3. Discussion

In this work, phytochemical studies of the different plant parts and root cultures of *W. thyriflora* identified 14 phenylphenalenones, including a dimer and three glucosides, five phenylbenzochromenones including an artifact **15**, which received the *O*-methyl group at C-3 from methanol (Otálvaro et al., 2010), and three glucosides, four oxabenzochrysenones, and a phenyl-naphthalic anhydride. Tables 1 and 2 show the ^1H and ^{13}C NMR data of new natural products **2**, **3**, and **19–21**. In cases where only low-field ^1H NMR data are available from the original papers (compounds **1**, **4**, **5**, **17**, **22**), complete ^1H and ^{13}C NMR data from our isolates were assigned on the basis of 2D NMR experiments (Table 2). This investigation confirmed that roots and *in vitro* root cultures are rich sources of phenylphenalenones and their oxidative derivatives, while above-ground plant parts are rather poor sources of such compounds. In addition to accumulating in roots, the compounds occurred in seeds, suggesting phenylphenalenones protect against soil microflora and herbivores. Phenylphenalenones and related compounds are the dominant class of secondary metabolites found in the Haemodoraceae and therefore are considered to be chemotaxonomic markers of this family (Opitz et al., 2002a).

4. Experimental

4.1. General experimental procedures

^1H NMR, ^{13}C NMR, ^1H - ^1H COSY, HMBC, and HSQC spectra were measured on a Bruker AV 500 NMR spectrometer (Bruker Biospin, Karlsruhe, Germany), operating at 500.13 MHz for ^1H and 125.75 MHz for ^{13}C . A TCI cryoprobe (5 mm) was used to measure spectra at 300 K. Tetramethyl silane was used as an internal standard for referencing ^1H and ^{13}C NMR spectra. Spectra

measured in the LC-SPE-NMR coupling mode are referenced to the residual signal of MeCN- d_3 at $\delta_{^1\text{H}}$ 1.96 and $\delta_{^{13}\text{C}}$ 1.79.

Electron-impact mass spectra (EIMS) were recorded on a MasSpec sector field mass spectrometer (Micromass Ltd., Manchester, UK) with a direct insertion probe. Electrospray ionization mass spectra (ESIMS) and LC-ESIMS were recorded on a Bruker Esquire 3000 ion trap mass spectrometer (Bruker Daltonics, Bremen, Germany). HRESIMS was recorded on a UPLC-MS/MS system consisting of an Ultimate 3000 series RSLC (Dionex, Idstein, Germany) system, and an Orbitrap mass spectrometer (Thermo Fisher Scientific, Bremen, Germany). UPLC was performed using a Dionex Acclaim C18 Column (150 mm \times 2.1 mm, 2.2 μm) at a constant flow rate of 300 $\mu\text{l min}^{-1}$. A binary solvent system of H_2O (solvent A) and MeCN (solvent B), both containing 0.1% formic acid, was used as follows: 0 min: 20% B, 6 min: 95% B, 10 min: 95% B.

The LC-DAD-SPE-NMR system consisted of an Agilent 1100 chromatography system (quaternary solvent delivery pump G1311A, autosampler G1313A) and a J&M photodiode array detector (DAD, detection 200–700 nm) connected to a Spark Prospekt 2 solid-phase extraction (SPE) device (Spark Holland, Emmen, The Netherlands) containing HySphere resin GP cartridges (10 mm \times 2 mm, 10 μm). MeCN- d_3 was used to elute the analytes from the nitrogen-dried cartridges and transfer to the NMR spectrometer equipped with a CryoFITTM flow system (30 μl).

Preparative HPLC was performed on a Merck-Hitachi chromatography system (L-6200A gradient pump, L-4250 UV/Vis detector) using a LiChrospher RP18 column (5 μm , 250 mm \times 10 mm; flow rate 3.5 ml min^{-1} ; UV 254 nm). Analytical HPLC was performed on an Agilent series HP1100 as described above. The UV spectra were recorded by the DAD during analytical HPLC.

4.2. Plant material

Plants of *W. thyriflora* L. were obtained from the botanical garden of the University of Düsseldorf and vegetatively propagated and maintained in the greenhouse of the Max Planck Institute for Chemical Ecology. Sterile root cultures were maintained in liquid M3 (Murashige and Skoog, 1962) medium (100 ml) in conical flasks (volume 300 ml) on a gyratory shaker (90 rpm) at 23 $^\circ\text{C}$ under permanent diffuse light (4.4 $\mu\text{mol m}^{-2} \text{s}^{-1}$). Seeds obtained from B&T World Seeds (Paguignan, Aigues-Vives, France) were used for phytochemical analysis.

4.3. Extraction and isolation

Plant material of *W. thyriflora* (leaves, plant roots, cultured roots) was frozen in liquid N_2 , ground, and extracted with MeOH at room temperature. After evaporation (<40 $^\circ\text{C}$), the remainder was partitioned between *n*-hexane- H_2O (leaf extract only), CH_2Cl_2 - H_2O and EtOAc- H_2O . The *n*-hexane extract of the leaves was discarded. The CH_2Cl_2 and EtOAc fractions were purified by means of reversed-phase preparative HPLC (25 $^\circ\text{C}$; flow rate 3.5 ml min^{-1} ; DAD 200–600 nm) on a LiChrospher 100 RP18 column (10 μm ; 250 mm \times 10 mm). Linear binary gradients of H_2O containing 0.1% trifluoroacetic acid (TFA) (solvent A) and MeCN (solvent B) were applied. Gradient 1 – 0 min: 30% B, 30 min: 65% B, 35 min: 90% B, 45 min: 90% B – was used to separate the compounds from the CH_2Cl_2 fraction. Gradient 2 – 0 min: 5% B, 40 min: 50% B – was used for the EtOAc fraction.

Compounds **2** and **3** were obtained from the EtOAc fraction of the leaf extract. Compounds **4**, **5**, **6**, **8**, and **17** were isolated from the CH_2Cl_2 fraction and compound **9** from the EtOAc fraction of plant roots. Compounds **10–13** and **15–18** were isolated from the CH_2Cl_2 fraction, and **9**, **14**, **19** and **20** were purified from the EtOAc fraction of cultured roots. Final purification was performed on a LiChrospher 100 RP18 column (5 μm ; 250 mm \times 4 mm) using the same

Table 2¹H NMR (500 MHz) and ¹³C NMR data (125 MHz) of compounds **1**, **4**, **21** (in MeCN-d₃), **5** and **17** (in acetone-d₆), and **22** (¹H NMR in acetone-d₆; ¹³C NMR in benzene-d₆).

Position	1		4		5		17		21		Position	22	
	δ_{H} (J, Hz)	δ_{C}	δ_{H} (J, Hz)	δ_{C}	δ_{H} (J, Hz)	δ_{C}	δ_{H} (J, Hz)	δ_{C}	δ_{H} (J, Hz)	δ_{C}		δ_{H} (J, Hz)	δ_{C}
1		179.9		180.5		181.5		181.5		180.1	1	7.98 (d, 9.6)	139.1
2	7.26 (s, OH)	150.4		149.6		149.9		148.9	7.27 (s, OH)	150.1	2	6.80 (d, 9.6)	126.8
3	7.53 (s)	106.9	7.09 (s)	113.8	7.07 (s)	113.9	6.85 (s)	114.2	7.52 (s)	106.9	3		181.4
3a		112.7		121.7				121.1		112.7	3a		122.9
4	8.43 (s, OH)	157.4	7.66 (s)	119.7	7.40–7.51 (m)	123.4	7.02 (s)	117.2	8.40 (s, OH)	157.3	4	8.31 (s)	119.0
5	7.30 (d, 8.9)	119.1		143.9				147.6	7.29 (d, 8.9)	119.2	5		142.3
6	7.96 (d, 8.9)	133.1		143.9		139.7		144.5	7.94 (d, 8.9)	133.1	5a		141.4
6a		127.8		124.4		124.8		121.1		127.9	6a		149.8
7	8.21 (d, 8.1)	136.0	8.60 (d, 8.5)	129.7	8.58 (d, 8.8)	129.7		143.2	8.19 (d, 8.1)	136.0	7	7.10 (s)	103.5
8	7.44 (d, 8.1)	130.1	7.51 (d, 8.5)	131.3	7.52 (d, 8.8)	131.5	7.63 (d, 7.8)	130.3	7.44 (d, 8.1)	130.0	8		144.4
9		150.1		148.2		148.6	8.32 (d, 7.8)	129.9		150.0	9		144.4
9a		124.8		124.2		124.8		127.4		124.3	10	7.70 (s)	108.1
9b		127.6		120.9		122.4		121.0		127.3	10a		110.4
1'		135.3		144.0		144.8		143.8		136.4	10b		130.8
2'	7.25 (d, 8.7)	130.7	7.37 (m)	129.0	7.37 (m)	129.4	7.40–7.42 (m)	127.6	6.85 (d, 2.0)	116.6	11	7.88 (d, 7.6)	132.8
3'	6.89 (d, 8.7)	115.6	7.45 (m)	128.9	7.40–7.51 (m)	129.2	7.31 (dd, 7.7, 2.3)	129.2	6.72 (s, OH)	144.7	12	8.01 (d, 7.6)	112.9
4'	7.07 (s, OH)	157.2	7.43 (m)	127.9	7.40–7.51 (m)	128.7	7.40–7.42 (m)	127.4	6.80 (s, OH)	145.0	12a		122.9
5'	6.89 (d, 8.7)	115.6	7.45 (m)	128.9	7.40–7.51 (m)	129.2	7.31 (dd, 7.7, 2.3)	129.2	6.89 (d, 8.1)	115.9	12b		121.1
6'	7.25 (d, 8.7)	130.7	7.37 (m)	129.0	7.37 (m)	129.4	7.40–7.42 (m)	127.6	6.75 (dd, 8.1, 2.0)	121.1	12c		117.4
OCH ₃			4.05 (s)	57.5			3.95 (s)	56.3					

gradients as were used on the large column (flow rate 0.8 ml min⁻¹).

Seeds of *W. thyrsoflora* (10 seeds; 143 mg) were ground and extracted with acetone (10 ml). The extracts were filtered and dried using a stream of nitrogen gas to yield 7.2 mg residue, which was dissolved in MeOH (250 μ l) for further analysis. The separation and elucidation of the components of the extracts were accomplished by LC–DAD–SPE–NMR, resulting in the identification of compounds **1**, **6**, **10** and **21–25**. The chromatographic separation was conducted with a Diamonsil C-18 5 μ m (250 mm \times 4.6 mm) column using a linear binary gradient of H₂O (solvent A) and MeOH (solvent B), both containing 0.1% (v/v) formic acid, with a flow rate of 1.0 ml min⁻¹ at 25 °C as follows: 0 min: 50% B, 55 min: 95% B, 60 min: 95% B, 61 min: 50% B, and 65 min: 50% B. The injection volume was 10 μ l. The HPLC eluate was monitored by DAD at wavelengths of 254, 280, and 320 nm with manually controlled SPE trappings. A total of 10 cumulative trappings were performed for each peak selected for analysis.

4.4. 6-O- β -D-Glucopyranosyl-5-hydroxy-7-phenyl-3H-benzo[de]isochromen-1-one (2)

UV (MeCN–H₂O): λ_{max} 261, 334, 371 nm; ¹H NMR and ¹³C NMR data, see Table 1; ESIMS: *m/z* 455 [M+1]⁺; HRESIMS: *m/z* 455.13233 [M+1]⁺ (calcd for C₂₄H₂₃O₉, 455.13366).

4.5. 6-O- β -D-Glucopyranosyl-5-hydroxy-7-(4-hydroxyphenyl)-3H-benzo[de]isochromen-1-one (3)

UV (MeCN–H₂O): λ_{max} 259, 337, 369 nm; ¹H NMR and ¹³C NMR data, see Table 1; ESIMS: *m/z* 471 [M+1]⁺; HRESIMS: *m/z* 471.12737 (calcd for C₂₄H₂₃O₁₀, 471.12857).

4.6. 4-O- β -D-Glucopyranosyl-2-methoxy-9-phenyl-1H-phenalen-1-one (19)

UV (MeCN–H₂O): λ_{max} 206, 272, 328, 388 nm; ¹H NMR and ¹³C NMR data, see Table 1; EIMS: *m/z* 302 [aglycon]⁺ (rel. int. 100); ESIMS: *m/z* 465 (rel. int. 100), 303 [aglycon+H]⁺ (54), HRESIMS: *m/z* 465.15321 [M+H]⁺ (calcd for C₂₆H₂₅O₈, 465.15439).

4.7. 4-O-[(6'-O-Allophanyl)- β -D-glucopyranosyl]-2-methoxy-9-phenyl-1H-phenalen-1-one (20)

UV (MeCN–H₂O) λ_{max} 206, 269, 332, 386 nm; ¹H NMR and ¹³C NMR data, see Table 1; EIMS: *m/z* 302 [aglycon]⁺ (100).

4.8. 2,4-Dihydroxy-9-(3,4-dihydroxyphenyl)-1H-phenalen-1-one (21)

UV (MeOH–H₂O): λ_{max} 277, 329, 446 nm; ¹H NMR and ¹³C NMR data, see Table 2; ESIMS: *m/z* 321 [M+1]⁺, HRESIMS: *m/z* 321.07483 [M+1]⁺ (calcd for C₁₉H₁₃O₅, 321.07575).

Acknowledgments

We thank Sybille Lorenz and Dr. Ravi Kumar Maddula for recording mass spectra, Kati Gruner for technical assistance and Emily Wheeler for editorial help.

References

- Bond, W.J., Honig, M., Maze, K.E., 1999. Seed size and seedling emergence: an allometric relationship and some ecological implications. *Oecologia* 120, 132–136.
- Brand, S., Hölscher, D., Schierhorn, A., Svatoš, A., Schröder, J., Schneider, B., 2006. A type III polyketide synthase from *Wachendorfia thyrsoflora* and its role in diarylheptanoid and phenylphenalenone biosynthesis. *Planta* 224, 413–428.
- Cooke, R.G., Dagle, I.J., 1979. Colouring matters of Australian plants XXI. Naphtho-anthenones in the Haemodoraceae. *Aust. J. Chem.* 32, 1841–1847.
- Cooke, R.G., Thomas, R.L., 1975. Colouring matters of Australian plants V XIII. Constituents of *Anigozanthos rufus*. *Aust. J. Chem.* 28, 1053–1057.
- Dora, G., Edwards, J.M., Campbell, W., 1991. Thyrsoflorin: a novel phenalenone pigment from *Wachendorfia thyrsoflora*. *Planta Med.* 56, 569.
- Edwards, J.M., 1974. Phenylphenalenones from *Wachendorfia* species. *Phytochemistry* 13, 290–291.
- Hölscher, D., Schneider, B., 1999. HPLC–NMR analysis of phenylphenalenones and a stilbene from *Anigozanthos flavidus*. *Phytochemistry* 50, 155–161.
- Murashige, T., Skoog, F., 1962. A revised medium for rapid growth and bioassays with tobacco tissue cultures. *Physiol. Plant.* 15, 473–497.
- Opitz, S., 2002. Phenylphenalenones and related phenolic pigments of the Haemodoraceae: structure, biosynthesis and accumulation patterns in *Xiphidium caeruleum* and *Wachendorfia thyrsoflora*. PhD thesis. Friedrich Schiller University, Jena, Germany.
- Opitz, S., Schneider, B., 2003. Oxidative biosynthesis of phenylbenzoisochromenones from phenylphenalenones. *Phytochemistry* 62, 307–312.
- Opitz, S., Hölscher, D., Oldham, N.J., Bartram, B., Schmitt, B., Echeverri, F., Quiñones, W., Schneider, B., 2002. Phenylphenalenone-related compounds—chemotaxonomic markers of the Haemodoraceae from *Xiphidium caeruleum*. *J. Nat. Prod.* 65, 1122–1130.

208

J. Fang et al./Phytochemistry Letters 4 (2011) 203–208

- Opitz, S., Otálvaro, F., Echeverri, F., Quiñones, W., Schneider, B., 2002. Isomeric oxabenzochrysenones from *Musa acuminata* and *Wachendorfia thyrsiflora*. *Nat. Prod. Lett.* 16, 335–338.
- Otálvaro, F., Görls, H., Hölscher, D., Schmitt, B., Echeverri, F., Quiñones, W., Schneider, B., 2002. Dimeric phenylphenalenones from *Musa acuminata* and various Haemodoraceae species. Crystal structure of anigorootin. *Phytochemistry* 60, 61–66.
- Otálvaro, F., Jitsaeng, K., Munde, T., Echeverri, F., Quiñones, W., Schneider, B., 2010. O-Methylation of phenylphenalenone phytoalexins in *Musa acuminata* and *Wachendorfia thyrsiflora*. *Phytochemistry* 71, 206–213.



Phytochemical profile of aerial parts and roots of *Wachendorfia thyrsoflora* L. studied by LC-DAD-SPE-NMR

Jingjing Fang, Marco Kai, Bernd Schneider*

Max Planck Institute for Chemical Ecology, Beutenberg Campus, Hans-Knöll Str. 8, D-07745 Jena, Germany

ARTICLE INFO

Article history:

Received 10 February 2012
Received in revised form 10 May 2012
Available online 18 June 2012

Keywords:

Wachendorfia thyrsoflora
Haemodoraceae
LC-DAD-SPE-NMR
Phenylbenzoisochromenones
Phenylbenzoisoquinolinones
Phenylphthalic anhydride
Phenylphenalenones

ABSTRACT

Hyphenated liquid chromatography – diode array detection – solid phase extraction – nuclear magnetic resonance spectroscopy (LC-DAD-SPE-NMR) was used to investigate the phytochemical composition of aerial parts and roots of *Wachendorfia thyrsoflora* (Haemodoraceae). Eleven phenylphenalenones and related compounds were identified in the aerial parts of the plant, ten compounds were found in the roots, and four additional compounds occurred in both plant parts. Twelve compounds are previously unreported natural products including five alkaloids (phenylbenzoisoquinolinones) are described here for the first time. In the work presented here, phenylphenalenones with an intact C₁₉ core structure were found only in the roots. Oxa analogs with a C₁₈O scaffold occurred both in the roots and in the aerial plant parts, while most of the aza analogs with a C₁₈N scaffold were detected in the aerial plant parts. This distribution pattern suggests that phenylphenalenones form in the roots, then the intact C₁₉ skeleton is converted into oxa analogs in the roots, translocated into the leaves and further reacted with amines or amino acids to form aza analogs (phenylbenzoisoquinolin-1,6-dione alkaloids).

© 2012 Elsevier Ltd. All rights reserved.

1. Introduction

Phenylphenalenones and related compounds biosynthetically formed from phenylpropanoids via diarylheptanoids have been reported in the Haemodoraceae (Cooke and Segal, 1955; Opitz et al., 2002), Musaceae (Luis et al., 1993; Otálvaro et al., 2007), Strelitziaceae (Hölscher and Schneider, 2000), and Pontederiaceae (DellaGrecia et al., 2008; Hölscher and Schneider, 2005; Wang et al., 2011). The biological functions of this class of secondary metabolites in plants have yet to be explored in depth. Several studies have indicated that phenylphenalenones play a role as phytoalexins in banana and plantain (*Musa*) plants (Luis et al., 1993; Kamo et al., 2000). The compounds, inducible in *Musa* plants by burrowing nematodes (Binks et al., 1997) and fungi, show antifungal activity (Otálvaro et al., 2007). Leishmanicidal (Luque-Ortega et al., 2004) and antimicrobial (Dias et al., 2009) activity was also reported. The organ-specific and cell-type-specific accumulation of phenylphenalenones has been investigated (Opitz and Schneider, 2002; Opitz et al., 2003; Hölscher and Schneider, 2007). Although the roots of *Wachendorfia thyrsoflora* are considered the main accumulation site, and root cultures have been used in biosynthetic labeling experiments (Opitz and Schneider, 2003; Otálvaro et al., 2010) and as the source of the polyketide synthase catalyzing the initial step of diarylheptanoid biosynthesis (Brand et al., 2006), the

location in the intact plant where biosynthesis takes place needs to be established.

The structural elucidation of plant secondary metabolites is an essential task for natural product chemists, pharmacognosists and plant biologists. The structural diversity and occurrence of components with largely different abundance in one plant sample make the chromatographic separation and accumulation of individual components time-consuming and demanding, particularly for sensitive compounds. The application of high-field magnets and cryogenic probes significantly increases the sensitivity of nuclear magnetic resonance (NMR) spectroscopy and makes it possible to elucidate compounds in small amounts as obtained by analytical high-performance liquid chromatography (HPLC). Unlike direct liquid chromatography – NMR (LC-NMR) hyphenation (Hölscher and Schneider, 1999), in LC – diode array detection – solid phase extraction – NMR (LC-DAD-SPE-NMR) spectroscopy each compound separated by HPLC can be repeatedly trapped by post-column solid phase extraction (SPE). After the non-deuterated eluents are removed, the analytes enriched on SPE cartridges are eluted by deuterated solvents into an NMR flow cell probe to measure 1D and 2D NMR spectra. Since the first application of this system in 2002 (Corcoran et al., 2002), the method has been successfully applied to elucidate structures of natural products from various sources (Brkljaca and Urban, 2011; Exarchou et al., 2005; Jaroszewski, 2005; Daolio and Schneider, 2012).

Previous studies showed that *W. thyrsoflora*, a species of the family Haemodoraceae, native to Cape Province of South Africa

* Corresponding author. Tel.: +49 3641 571600; fax: +49 3641 571601.
E-mail address: schneider@ice.mpg.de (B. Schneider).

(Helme and Linder, 1992), is a rich source of phenylphenalenones and related compounds (Fang et al., 2011). As part of our effort to elucidate the structures, biosynthesis, localization, and function of all phenylphenalenones, we report the phytochemical screening of phenylphenalenones and related compounds from the aerial parts and the roots of a *W. thyrsoiflora* plant by LC-DAD-SPE-NMR.

2. Results

2.1. Different natural product profiles in aerial plant parts and roots

The accumulation of phenylphenalenones in underground plant parts is obvious, thanks to the impressive color of the roots (Fig. 1), and many structures of the phenylphenalenones-type are known from the roots, root cultures and seeds (Fang et al., 2011). In the green plant parts, the red pigmentation of phenylphenalenones is usually masked by chlorophyll and only three compounds of that type have been reported from the aerial parts (Dora et al., 1990; Fang et al., 2011). To study the occurrence of secondary metabolites in *W. thyrsoiflora*, a single plant was cut into two parts, the aerial parts and the roots. Since, in LC-DAD-SPE-NMR, well separated LC peaks are essential for post-column trapping on SPE cartridges and successful NMR analysis, optimized chromatographic procedures were used for each extract. Although the HPLC chromatograms (Fig. 2) of acetone extracts obtained from the two plant parts are not directly comparable, significant differences in the metabolite profiles were observed (see Section 3). The structures of the numbered peaks were elucidated and categorized into phenylphenalenones and their oxa- and aza-analogs, possessing C₁₉-, C₁₈O- and C₁₈N-scaffolds (Fig. 3). Multiple SPE trappings allowed us to collect material sufficient for *de novo* structure elucidation using hetero-nuclear 2D NMR experiments.

2.2. Compounds from the aerial parts

Fifteen phenylphenalenones and related compounds were identified from the aerial parts of *W. thyrsoiflora*, including four phenylbenzoisochromenone glucosides, two of which are known

compounds. Compounds **A2**, **A4**, **A6**, **A8**, **A9**, **A12**, and **A15** are new natural products. The structures of the two known compounds were determined by mass spectrometry (MS), 1D and 2D NMR spectroscopy as 6-O-(β -D-glucopyranosyl)-5-hydroxy-7-(4'-hydroxyphenyl)-3H-benzo[de]isochromen-1-one (**A1**) and 6-O-(β -D-glucopyranosyl)-5-hydroxy-7-phenyl-3H-benzo[de]isochromen-1-one (**A3**) (Fang et al., 2011). The ¹H NMR spectrum of compound **A2** is very similar to that of **A1**, except there is one more singlet at δ 3.21 representing two protons, and the signals of H-6'' protons in the glucose moiety are significantly shifted to a low field in **A2** compared to corresponding signals of **A1**. These data suggest that **A1** is a derivative of **A2**, in which the 6'' position of glucose is substituted. The molecular mass of **A2** appeared to be 86 units higher than **A1**, suggesting that the additional moiety is a malonyl. Thus, the structure of **A2** was putatively assigned to 6-O-[(6''-O-malonyl)- β -D-glucopyranosyl]-5-hydroxy-7-(4'-hydroxyphenyl)-3H-benzo[de]isochromen-1-one. The structure was further confirmed by high-resolution electrospray-ionisation mass spectrometry (HRESIMS) (see Section 5) and NMR assignments as follows. The ¹H NMR spectrum of **A2** (Table 1) showed a singlet at δ 5.74 representing two methylene protons (H₂-3), a doublet-like signal at δ 6.80 (J = 8.0 Hz, H-3'/5'), a broad signal at δ 7.19 (H-2'/6'), a singlet at δ 7.22 (H-4), two doublets at δ 7.43 (H-8) and 8.13 (H-9) with a coupling constant of 7.6 Hz, a singlet at δ 3.21 (H₂-2'' of the malonyl moiety), and a series of carbohydrate signals between δ 2.76 and 4.36. The doublet at δ 4.36 was assigned to the proton at the anomeric center (H-1'') of the carbohydrate unit. This signal displayed a coupling constant of 7.9 Hz, indicating β -configuration. The coupling constants ³J_{H-2''-H-3''}, ³J_{H-3''-H-4''} and ³J_{H-4''-H-5''} of approximately 9 Hz showed that H-1'' to H-5'' are in axial geometry and confirmed that the carbohydrate is glucose. Based on analyses of heteronuclear single quantum coherence (HSQC) and heteronuclear multiple-bond correlation (HMBC) spectra, the carbon signals were assigned as listed in Table 2 and the structure of **A2** was confirmed as suggested above.

The ¹H chemical shifts of compound **A4** (Table 1) closely resembled those of compound **A3**; the exceptions are the same differences as those between **A1** and **A2**: an additional methylene singlet at δ 3.19, and H-6'' protons shifted to a low field. The spectrum of **A4** is also very similar to that of **A2**, with differences indicating a monosubstituted lateral phenyl ring in **A4** signals instead of a 1,4-disubstituted 4'-hydroxyphenyl ring in **A2**. Broad signals indicated the hindered rotation of the phenyl ring due to the close proximity to the acyl sugar unit in *peri* position, as previously demonstrated for allophanlyl glucosides (Schneider et al., 2005). Based on the above evidence, compound **A4** is elucidated as 6-O-[(6''-O-malonyl)- β -D-glucopyranosyl]-5-hydroxy-7-phenyl-3H-benzo[de]isochromen-1-one. MS and HRESIMS data further confirmed the structure (see Section 5).

Seven compounds **A5**–**A9**, **A14** and **A15** share very similar ¹H NMR signal patterns in the aromatic range, consisting of two singlets at δ ~7.8 (H-3) and ~7.0 (H-4), two doublets at δ ~7.5 (H-8) and ~8.6 (H-9) with a coupling constant of 8.1, a doublet of doublets integrating for two protons at δ ~7.3 (H-2'/6'), and a series of signals distributed between δ 7.41 and 7.46 standing for three other aromatic protons (H-3', 4', 5'). All the compounds except **A7**, which has been identified as 5-hydroxy-7-phenylbenzo[de]isochromene-1,6-dione (lachnanthopyrone) by analyzing and comparing the MS and NMR data with those reported (Edwards and Weiss, 1972), have alkyl signals in their ¹H NMR spectra (Table 3) and possess uneven molecular masses (see Section 5). The evidence suggests a skeleton containing nitrogen instead of oxygen. Further inspection of the HSQC and HMBC spectra indicates that the nitrogen replaces the lactone-oxygen of phenylbenzoisochromenones such as lachnanthopyrone (**A7**), and an aliphatic



Fig. 1. Roots of a hydroponically grown plant of *Wachendorfia thyrsoiflora* (left) and a plant grown in soil under greenhouse conditions (right). Photo: Stefan Opitz.

146

J. Fang et al./Phytochemistry 81 (2012) 144–152

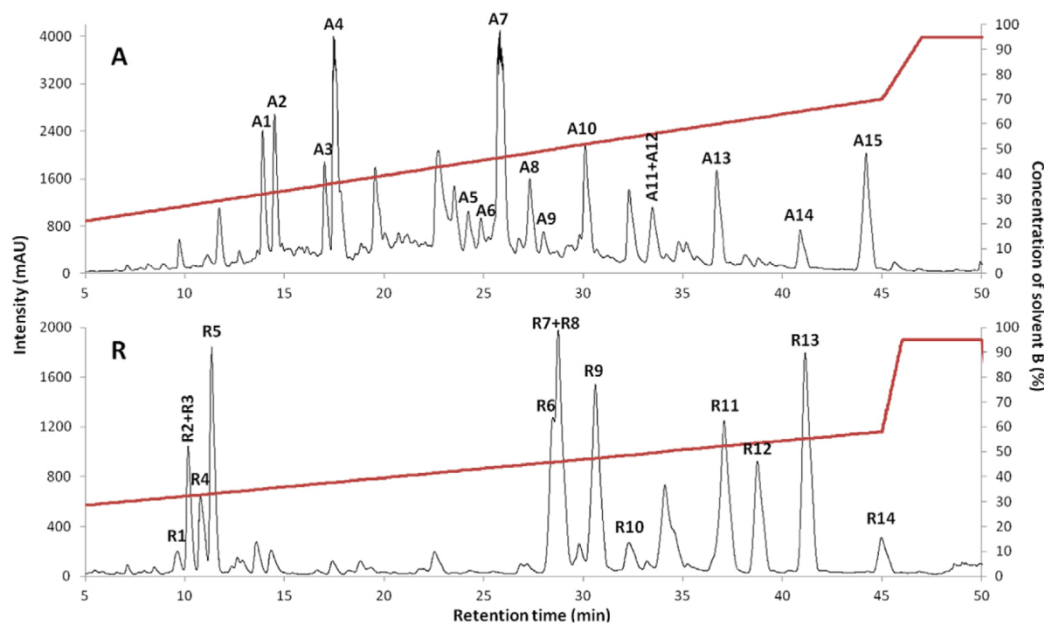


Fig. 2. HPLC chromatograms of extracts of aerial parts (A) and roots (R) of *Wachendorfia thyrsiflora*. The identified peaks are numbered according to the sequence of elution. HPLC gradient 1 was used for the analysis of extracts of aerial parts (A) and gradient 2 for root extracts (R).

moiety is attached to the nitrogen. Such lactam-type phenylphenalenone-related compounds have been reported from *Lachnantes tinctoria* (Edwards and Weiss, 1972) and *Xiphidium caeruleum* (Opitz et al., 2002). The ^1H NMR spectrum of compound **A5** displays, in addition to the aromatic signals, triplets of two methylene groups at δ 3.85 and 4.14. The triplet at δ 4.14 correlates with carbon signals at δ 139.9 (C-3) and 162.1 (C-1). Therefore, **A5** was determined as 2-(2-hydroxyethyl)-5-hydroxy-7-phenyl-2H-benzo[de]isoquinoline-1,6-dione, which was confirmed by MS and by comparing NMR data with those in literature (Edwards and Weiss, 1972).

The ^1H and ^{13}C data of **A6**, **A8**, **A9** and **A15** are listed in Tables 3 and 4, respectively. A singlet at δ 4.75 in the ^1H NMR spectrum of **A6** correlates through three bonds with carbons at δ 138.4 (C-3), 162.0 (C-1) and through two bonds with a carboxyl carbon atom at 169.4, which must be in the side chain (C-2''). From the NMR and HRESIMS data (see Section 5), the structure of **A6** was elucidated as 2-carboxymethyl-5-hydroxy-7-phenyl-2H-benzo[de]isoquinoline-1,6-dione. Compound **A8** shows three alkyl signals, each integrating for two protons, at δ 4.09, 2.06 and 2.40, representing H_2 -1'', 2'' and 3'', respectively. The HMBC correlations between H_2 -1'' (δ 4.09) and C-1 (δ 162.0) and C-3 (δ 138.7), between H_2 -2'' (δ 2.06) and the carboxyl carbon atom (δ 174.2, C-4''), suggest that the structure of **A8** is 2-(3-carboxy-*n*-propyl)-5-hydroxy-7-phenyl-2H-benzo[de]isoquinoline-1,6-dione. The structure was confirmed by HRESIMS (see Section 5) data. The ^1H NMR spectrum of **A9** displays a quartet at δ 5.40 (1H, H-1'') and a doublet of a methyl group at δ 1.73 (3H, H-3''). In the HMBC spectrum, H-1'' correlates with δ 161.7 (C-1), 136.0 (C-3) and 171.9 (C-2''), and the methyl signals correlate with the carboxyl carbon atom, resonating at 171.9 (C-2''). From the NMR and HRESIMS analysis (see Section 5), **A9** was determined to be 2-(1-carboxyethyl)-5-hydroxy-7-phenyl-2H-benzo[de]isoquinoline-1,6-dione. The spectrum of compound **A15** shows four proton signals in alkyl range at δ 4.05 (2H, H-1''), 1.78 (2H, H-2''), 1.40 (2H, H-3''), and 0.97 (3H, H-4''). Among them, H-1'' (δ 4.05) correlates with C-1 (161.9) and C-3 (138.8) in the HMBC spectrum. Therefore, **A15**

was elucidated as 2-(*n*-butyl)-5-hydroxy-7-phenyl-2H-benzo[de]isoquinoline-1,6-dione. The ^1H NMR spectrum of **A14** highly resembles that of **A15**, except for an additional methoxy signal at δ 3.78 in the spectrum of **A14**. Further analyses of MS and NMR data and comparisons to the data reported (Opitz et al., 2002) allowed us to elucidate the structure of **A14** as 2-(*n*-butyl)-5-methoxy-7-phenyl-2H-benzo[de]isoquinoline-1,6-dione. Due to its uneven molecular mass, **A12** was identified as another nitrogen-containing component. Compound **A12** was identified in a mixture with co-eluting **A11**. The signals of the two compounds were distinguished in the ^1H NMR spectrum of the mixture by the proportion of their integrals. The ^1H NMR signals assigned to **A12** (Table 3) are similar to those of **A15**. The difference was found in the signals of the lateral phenyl ring, which in the ^1H NMR spectrum of **A15** integrate for five protons. Unlike **A15**, the spectrum of **A12** shows an AA'BB' spin system of two doublet-like signals at δ 7.21 (2H, H-2'/6') and 6.86 (2H, H-3'/5'); these are typical of a 1,4-disubstitution. According to the molecular mass (see Section 5), the substituent at C-4' must be a hydroxyl group. Hence, **A12** was identified as 2-(*n*-butyl)-5-hydroxy-7-(4-hydroxyphenyl)-2H-benzo[de]isoquinoline-1,6-dione.

Three other known compounds were determined by MS and NMR analyses and by comparing the data with those in literature as 3,6-dihydroxy-5-methoxy-7-phenyl-3H-benzo[de]isochromene-1-one (**A10**) (Opitz et al., 2002), 5,6-dihydroxy-7-phenyl-3H-benzo[de]isochromene-1,3-dione (**A11**) (Bazan and Edwards, 1976), and 6-hydroxy-5-methoxy-7-phenyl-3H-benzo[de]isochromene-1-one (**A13**) (Edwards and Weiss, 1974).

2.3. Compounds from the roots

Fourteen phenylphenalenones and related compounds, including five glucosides, were identified from an acetone extract of *W. thyrsiflora* roots. The structures were elucidated by assigning the ^1H and 2D NMR data and further confirmed by HRESIMS. Compounds **R2**–**R5**, and **R13** are new natural products.

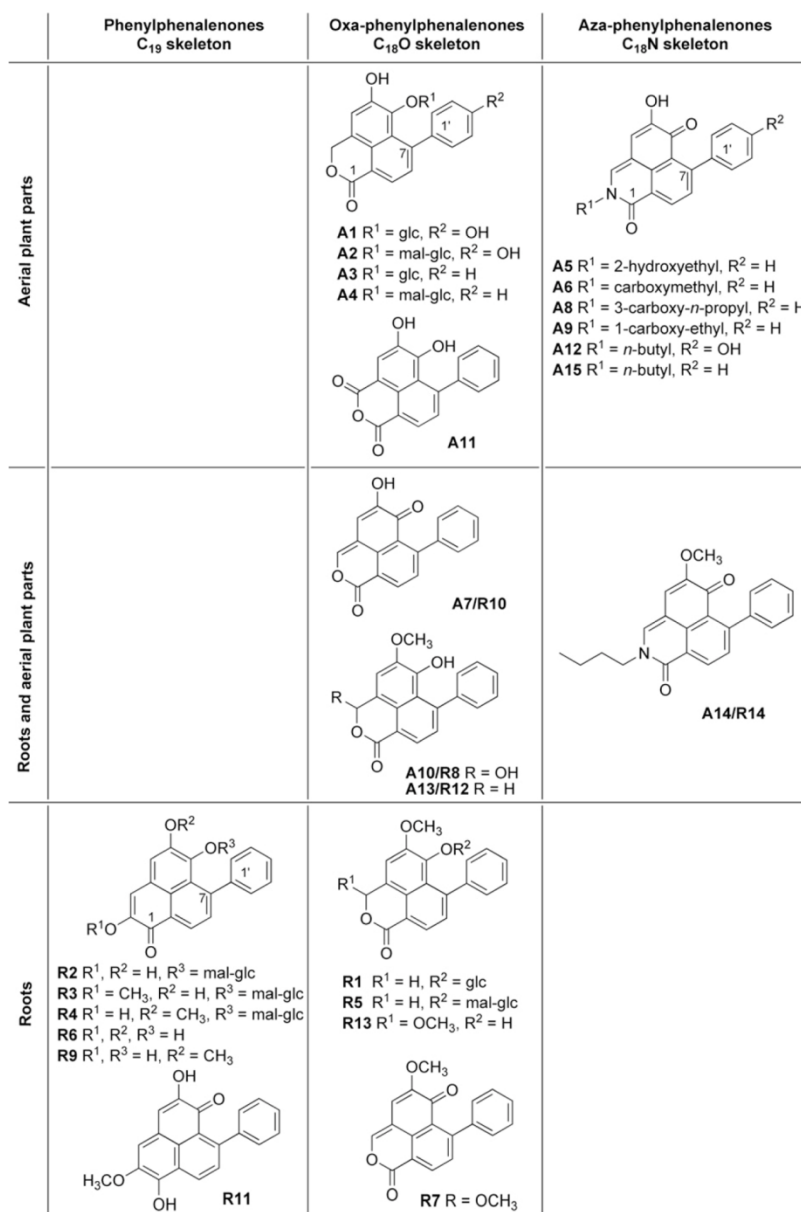


Fig. 3. Structures and skeleton types of compounds isolated from aerial parts and roots of *Wachendorfia thyrsoiflora*. Compounds **A2**, **A4**, **A6**, **A8**, **A9**, **A12**, **A15**, **R2–R5**, and **R13** are new natural products. glc, β -D-glucopyranosyl; mal-glc, 6-malonyl- β -D-glucopyranosyl.

The trapped LC peak eluting at 10 min (Fig. 2) was a mixture containing two glucosides, the major compound, **R2**, and the minor compound, **R3**. In the ¹H NMR spectrum (Table 1) the carbohydrate signals of the two compounds are overlapping, while the aromatic signals are separated from each other, except for the very broad signals of the phenyl groups. The major difference between the two very similar sets of signals is that the ¹H NMR spectrum of compound **R3** shows an additional methoxy signal at δ 3.89. The ¹H NMR spectrum of compound **R2** displays two singlets at δ 7.08 (H-3) and 7.51 (H-4), two doublets of an AX spin system at δ 7.59 (H-8) and 8.47 (H-9), and several broad signals, from δ 7.25 to 7.48, of the phenyl protons. This signal pattern suggests a

tetraoxygenated phenylphenalenone. The substitution positions of phenyl, hydroxyl and hexosyl groups were elucidated by analyzing the HSQC and HMBC spectra. In the HMBC spectrum, correlations between δ 7.59 (H-8) and 144.2 (C-1'), and between δ 8.47 (H-9) and δ 180.9 (C-1) as well as 147.8 (C-7) suggest the phenyl ring is attached to the 7 position. Correlations between δ 7.08 (H-3) and δ 180.9 (C-1), 150.2 (C-2), 123.6 (C-4), and 121.3 (C-9b); between δ 7.51 (H-4) and δ 114.4 (C-3), 140.9 (C-6) and 121.3 (C-9b); and between δ 4.45 (H-1'') and δ 140.9 (C-6) indicate the hexose in position 6, and one hydroxyl group in each of positions 2 and 5. Coupling constants ³J around 9 Hz for hexose signals suggest that the protons H-1'' to H-5'' have an axial orientation,

Table 1¹H NMR data (500 MHz, MeCN-*d*₃, δ values, *J* in Hz) of compounds **A2**, **A4** and **R2–R5** measured by LC-DAD-SPE-NMR.

	A2	A4	R2	R3	R4	R5
3	5.74 (s)	5.75 (s)	7.08 (s)	7.06 (s)	7.15 (s)	5.80 (s)
4	7.22 (s)	7.24 (s)	7.51 (s)	7.52 (s)	7.71 (s)	7.45 (s)
8	7.43 (d, 7.6)	7.45 (d, 7.4)	7.59 (d, 7.6)	7.56 (d, 7.6)	7.52 (d, 7.6)	7.35 (d, 7.4)
9	8.13 (d, 7.6)	8.15 (d, 7.4)	8.47 (d, 7.6)	8.39 (d, 7.6)	8.52 (d, 7.6)	8.16 (d, 7.4)
2'	7.19 (br)	7.34 (br)	7.36 (br)	7.36 (br)	7.34 (br)	7.35 (br)
3'	6.80 (d, 8.0)	7.43 (br)	7.48 (br)	7.48 (br)	7.44 (br)	7.42 (br)
4'		7.34 (br)	7.36 (br)	7.36 (br)	7.34 (br)	7.35 (br)
5'	6.80 (d, 8.0)	7.24 (br)	7.25 (br)	7.25 (br)	7.25 (br)	7.22 (br)
6'	7.19 (br)	7.43 (br)	7.40 (br)	7.40 (br)	7.46 (br)	7.44 (br)
1''	4.36 (d, 7.9)	4.39 (d, 7.9)	4.45 (d, 7.9)	4.45 (d, 8.0)	4.94 (d, 7.8)	4.87 (d, 7.8)
2''	2.76 (dd, 9.1, 7.9)	2.57 (dd, 9.2, 7.9)	2.55 (dd, 9.3, 7.9)	2.56 (dd, 9.4, 8.0)	1.89 (dd, 8.8, 7.8)	1.87 (dd, 9.3, 7.8)
3''	3.17 (dd, 9.1, 9.1)	3.15 (dd, 9.2, 9.0)	3.16 (dd, 9.3, 9.0)	3.16 (m)	3.11 (dd, 9.1, 8.8)	3.10 (dd, 9.3, 9.1)
4''	2.97 (dd, 9.6, 9.1)	2.90 (dd, 9.8, 9.0)	2.92 (dd, 9.7, 9.0)	2.93 (dd, 9.6, 8.9)	2.98 (dd, 9.3, 9.1)	2.95 (dd, 9.6, 9.1)
5''	3.15 (m)	3.13 (m)	3.14 (m)	3.14 (m)	3.11 (m)	3.09 (m)
6''a	4.05 (dd, 11.9, 6.8)	4.05 (dd, 11.9, 6.7)	4.07 (m)	4.07 (m)	3.88 (dd, 12.1, 2.3)	3.89 (dd, 11.9, 2.2)
6''b	4.12 (dd, 11.9, 1.9)	4.10 (dd, 11.8, 2.2)	4.08 (m)	4.08 (m)	4.12 (dd, 12.1, 6.1)	4.12 (dd, 11.9, 6.3)
2'''	3.21 (s)	3.19 (s)	3.16 (s)	3.16 (s)	3.00 (d, 13.2)	3.03 (d, 11.4)
OCH ₃				3.89 (s)	3.98 (s)	3.93 (s)

Table 2¹³C NMR data (125 MHz, MeCN-*d*₃, δ values) of compounds **A2**, **A4** and **R2–R5** measured by LC-DAD-SPE-NMR (125 MHz, MeCN-*d*₃, δ values).

	A2	A4	R2	R3	R4	R5
1	165.0	164.9	180.9	180.2	180.6	164.7
2			150.2	153.5	150.1	
3	70.0	70.0	114.4	113.8	114.8	70.4
3a	126.4	126.3	127.3	ND	126.6	125.5 ^a
4	116.0	116.1	123.6	123.4	120.4	112.8
5	148.3	148.3	148.5	148.4	150.6	150.3
6	138.6	138.2	140.9	140.6	142.1	139.1
6a	119.9	120.3	127.7 ^a	128.4 ^a	127.8 ^b	120.2
7	144.2	144.3	147.8	146.6	148.4	145.3
8	131.7	131.8	132.2	132.1	132.0	131.6
9	126.6	126.6	128.4	127.9	129.0	127.0
9a	127.4	127.3	127.7 ^a	128.4 ^a	128.3 ^b	128.2
9b	125.6	125.4	121.3	121.6	121.3	125.5 ^a
1'	135.3	143.9	144.2	144.2	145.1	144.9
2'	132.0	127.4	127.6	127.6	127.3	127.3
3'	114.4	130.6	130.6	130.6	129.9	130.4
4'	157.3	127.4	127.6	127.6	127.3	127.3
5'	114.4	130.7	131.1	131.1	130.9	131.0
6'	132.0	ND	128.1	128.1	128.1	128.1
1''	105.2	104.9	104.8	104.8	102.0	102.0
2''	74.2	74.1	74.1	74.1	73.9	74.0
3''	76.5	76.5	76.5	76.5	76.8	76.8
4''	70.5	70.5	70.6	70.6	70.6	70.7
5''	74.4	74.3	74.4	74.4	74.2	74.3
6''	65.1	65.1	65.0	65.0	64.6	64.9
1'''	167.6	167.6	167.6	167.6	167.5	167.5
2'''	41.3	41.3	41.2	41.2	41.0	41.1
3'''	167.9	167.8	167.8	167.8	167.8	167.6
OCH ₃				56.1	57.5	57.7

ND – Not detectable.

^a Values in the same column are overlapping.^b Values in the same column are exchangeable.

which is characteristic of glucose. The coupling constant 7.9 Hz of H-1'' indicated a β -configuration at the anomeric C-1''. A signal at $\delta_{\text{H}} 3.16/\delta_{\text{C}} 41.2$ (H/C-2''') was assigned to the methylene group of the malonyl unit. H₂-6 of the glucose correlates with one carbonyl carbon atoms appearing at $\delta 167.6$ (C-1'''). This evidence indicates that the malonyl group is attached to position 6'' of the glucose. Thus, **R2** was elucidated as 6-O-[(6''-O-malonyl)- β -D-glucopyranosyl]-2,5-dihydroxy-7-phenylphenalen-1-one, which is confirmed by HRESIMS (see Section 5). As mentioned above, compound **R3** has one methoxy group more than **R2**. HMBC correlations of the signals at $\delta 3.89$ (OCH₃) and 7.06 (H-3) with $\delta 153.5$ (C-2) allow us to assign the methoxy group to position 2. Based on these 1D

and 2D NMR data and HRESIMS (see Section 5), compound **R3** was identified as 6-O-[(6''-O-malonyl)- β -D-glucopyranosyl]-2-methoxy-5-hydroxy-7-phenylphenalen-1-one.

The HRESIMS data of **R3** and **R4** (see Section 5) suggest the same molecular formula for the two compounds. The ¹H NMR spectrum of **R4** (Table 1) shows close similarity with the spectra of **R2** and **R3**, although the signals of H-4 ($\delta 7.71$) and H-1'' ($\delta 4.94$) of **R4** were shifted significantly to a low field compared to those of **R2** and **R3**. Analyzing the HSQC and HMBC spectra of **R4**, we demonstrated that the methoxy group of **R4** is in position 5 instead of position 2 in the isomer, **R3**. Accordingly, **R4** is 6-O-[(6''-O-malonyl)- β -D-glucopyranosyl]-2-hydroxy-5-methoxy-7-phenylphenalen-1-one.

The ¹H NMR spectrum of **R5** resembles the spectra of **A3** and **A4** and shows two singlets at $\delta 5.80$ (2H, H-3) and 7.45 (1H, H-4), two doublets of an AX spin system at $\delta 7.35$ (H-8) and 8.16 (H-9) with a coupling constant of 7.4 Hz, a methoxy signal at $\delta 3.93$, one doublet at $\delta 3.03$ (H₂-2'''), and a set of signals of a hexose moiety. The aglycone of **R5** was identified as 6-hydroxy-5-methoxy-7-phenyl-3H-benzo[de]isochromene-1-one by comparing its ¹H- and ¹³C NMR data with those of **A13** and a reportedly related glycoside, 6-O-[(6''-O-allophanyl)- β -D-glucopyranosyl]-5-methoxy-7-phenyl-3H-benzo[de]isochromene-1-one (Opitz et al., 2002; Fang et al., 2011). Using the same assignment strategy as for elucidating glucosides **A1–A4**, the substituent at O-6 was deduced to be a glucopyranose, which carries a malonyl group in position 6''; the position of the malonyl group is proven by an HMBC correlation between H₂-6'' ($\delta 4.12/3.89$) and the carbonyl carbon atom at $\delta 167.5$. Thus, **R5** was determined to be 6-O-[(6''-O-malonyl)- β -D-glucopyranosyl]-5-methoxy-7-phenyl-3H-benzo[de]isochromene-1-one, and HRESIMS (see Section 5) confirmed the structure.

The ¹H NMR spectrum (Table 3) of **R13** displays a singlet at $\delta 6.45$ (1H), which is consistent with a hydroxymethine structure at C-3, another singlet at $\delta 7.62$ (H-4), two doublets of an AX spin system at $\delta 7.35$ (H-8) and 8.22 (H-9), a signal around $\delta 7.40$ representing five phenyl protons, and two methoxy signals at $\delta 3.64$ and 3.97, respectively. The low-field part of the ¹³C NMR spectrum (Table 4) shows 15 aromatic signals, two of them (C-2'/6' and C-3'/5') of double intensity, and one carbonyl signal. These data suggest that **R13** is another phenylbenzoisochromenone. Two methoxy groups at δ_{H} , 3.64/ δ_{C} 56.4 and 3.97/57.8, were assigned to positions 3 and 5, respectively, by HMBC correlations. The structure of **R13** therefore was deduced as 6-hydroxy-3,5-dimethoxy-7-phenyl-3H-benzo[de]isochromene-1-one. The HRESIMS data (see Section 5) are in agreement with the structure.

Table 3¹H NMR data (500 MHz, MeCN-*d*₃, δ values, *J* in Hz) of compounds **A6**, **A8**, **A9**, **A12**, **A15** and **R13** measured by LC-DAD-SPE-NMR.

	A6	A8	A9	A12	A15	R13
3	7.75 (s)	7.79 (s)	7.84 (s)	7.79 (s)	7.82 (s)	6.45 (s)
4	6.96 (s)	6.96 (s)	7.01 (s)	6.95 (s)	6.97 (s)	7.62 (s)
8	7.54 (d, 8.1)	7.52 (d, 8.1)	7.55 (d, 8.1)	7.52 (d, 8.1)	7.52 (d, 8.1)	7.35 (d, 7.4)
9	8.62 (d, 8.1)	8.62 (d, 8.1)	8.64 (d, 8.1)	8.59 (d, 8.1)	8.63 (d, 8.1)	8.22 (d, 7.4)
2', 6'	7.34 (dd, 7.8, 1.8)	7.33 (dd, 7.9, 2.0)	7.34 (dd, 7.9, 2.0)	7.21 (d, 8.6)	7.33 (dd, 7.5, 1.5)	7.37–7.40 (m)
3', 5'	7.41–7.45 (m)	7.41–7.44 (m)	7.42–7.46 (m)	6.86 (d, 8.6)	7.41–7.44 (m)	7.37–7.40 (m)
4'	7.41–7.45 (m)	7.41–7.44 (m)	7.42–7.46 (m)		7.41–7.44 (m)	7.37–7.40 (m)
1''	4.75 (s)	4.09 (t, 7.1)	5.40 (q, 7.4)	4.04 (t, 7.4)	4.05 (t, 7.3)	
2''		2.06 (m)		1.77 (m)	1.78 (m)	
3''		2.40 (t, 7.2)	1.73 (d, 7.4)	1.40 (m)	1.41 (m)	
4''				0.97 (m, 7.4)	0.97 (t, 7.4)	
3-OCH ₃						3.64 (s)
5-OCH ₃						3.97 (s)

Table 4¹³C NMR data (125 MHz, MeCN-*d*₃, δ values) of compounds **A6**, **A8**, **A9**, **A12**, **A15** and **R13** measured by LC-DAD-SPE-NMR.

	A6	A8	A9	A12	A15	R13
1	162.0	162.0	161.7	162.0	161.9	164.4
3	138.4	138.7	136.0	138.6	138.8	103.0
3a	ND	110.1	ND	ND	ND	119.9
4	110.6	110.9	110.7	110.6	110.9	114.9
5	149.0	148.9	149.2	148.9	149.0	144.4
6	179.2	179.2	179.2	179.1	179.3	143.6
6a	125.0 ^a	124.7 ^a	125.1 ^a	124.9 ^a	125.1 ^a	120.8
7	151.3	150.8	151.2	150.9	150.6	145.5
8	132.7	132.4	132.7	132.7	132.4	130.0
9	133.3	133.4	133.5	133.3	133.4	128.3
9a	125.3 ^a	125.4 ^a	125.3 ^a	125.5 ^a	125.7 ^a	119.5
9b	133.2	132.9	132.9	133.1	132.9	125.0
1'	142.8	143.0	142.8	134.3	143.0	143.8
2', 6'	128.9	129.1	128.9	130.8	129.0	130.0
3', 5'	128.5	128.7	128.5	115.4	128.5	128.0
4'	128.1	128.2	128.1	157.5	127.9	127.9
1''	50.9	49.3	56.1	49.7	49.8	
2''	169.4	31.1	171.9	31.8	31.7	
3''		24.9	16.0	20.5	20.4	
4''		174.2		13.9	13.9	
3-OCH ₃						56.4
5-OCH ₃						57.8

ND – Not detectable.

^a Values in the same column are exchangeable.

Nine known compounds were also identified from the root extract; four of them, **R8**, **R10**, **R12** and **R14**, are identical to **A10**, **A7**, **A13** and **A14**, respectively. The other known compounds were determined to be 6-*O*- β -D-glucopyranosyl-5-methoxy-7-phenyl-3*H*-benzo[*de*]isochromen-1-one (**R1**, haemodorose) (Dias et al., 2009), 2,5,6-trihydroxy-7-phenylphenalen-1-one (**R6**) (lachnanthoside aglycone; Munde et al., 2012), 5-methoxy-7-phenylbenzo[*de*]isochromene-1,6-dione (**R7**) (Opitz et al., 2002), 2,6-dihydroxy-5-methoxy-7-phenylphenalen-1-one (**R9**) (Bick and Blackman, 1973), 2,6-dihydroxy-5-methoxy-9-phenylphenalen-1-one (**R11**) (Cooke et al., 1958).

3. Discussion

In this study, eleven phenylphenalenones and related compounds were identified from an extract of aerial parts (24 mg), four compounds were found in the extracts of both the aerial plant parts and the roots, and ten compounds were detected exclusively in the root extract (14 mg) of *W. thyrsoiflora* by LC-DAD-SPE-NMR combined with MS. Twelve compounds are new natural products, including five 2-aza-7-phenylphenalenones (phenylbenzoisochromen-1,6-dione alkaloids) bearing an aliphatic side chain at the

nitrogen atom in position 2. The occurrence of such alkaloids in *W. thyrsoiflora* is reported here for the first time. Together with structures recently reported from different plant parts and root cultures (Fang et al., 2011), a total of 45 phenylphenalenones and related compounds have been identified from *W. thyrsoiflora*.

Considering the distribution of the compounds identified in this work, it is conspicuous that intact phenylphenalenones possessing a C₁₉ core structure were found in the roots but not in the aerial plant parts. The only exception from this finding is thyrsoiflorin, a phenylphenalenone previously isolated from the flowers of *W. thyrsoiflora* (Dora et al., 1990). Oxa analogs of phenylphenalenones (a C₁₈O scaffold), a group of compounds comprising phenyl-benzoisochromen-1-ones and phenylphthalic anhydrides, were found in both plant parts. With the exception of compound **A14/R14**, the aza analogs of phenylphenalenones (a C₁₈N scaffold) were isolated only from the aerial plant parts. Such alkaloids, which were reported in the flowers of *Lachnanthes tinctoria* (Edwards and Weiss, 1972; Bazan and Edwards, 1976) and in *Xiphidium caeruleum* (Opitz et al., 2002) are identified here for the first time in *W. thyrsoiflora*. The exclusive occurrence of phenylphenalenones in the roots and the distribution of oxa analogs to roots and aerial plant parts are in full agreement with the organ-specific analysis of such compounds in *Xiphidium caeruleum* (Opitz and Schneider, 2002) but not in secretory cavities in the leaf tissue of *Dilatris* species (Hölscher and Schneider, 2007).

The distribution pattern and the previously reported oxidative formation of phenylbenzoisochromenones from phenylphenalenones (Opitz and Schneider, 2002) have led to the suggestion that the C₁₉ core structure of phenylphenalenones is biosynthesized mainly in the roots without being translocated to the aerial parts of the plant. Translocation may occur after the hypothetical dioxygenase-catalyzed formation of 2-oxa analogs (Opitz and Schneider, 2003) and glucosylation in position 6. The independence of phenylphenalenone biosynthesis, including glycosidation and oxygen insertion into the phenalenone ring system, from green plant parts has been confirmed by the metabolite pattern of *W. thyrsoiflora* root cultures (Fang et al., 2011) and their biosynthetic potential (Opitz and Schneider, 2003; Brand et al., 2006). Unlike the site of phenylphenalenone biosynthesis and their glycosylated and oxygenated derivatives, the major site of phenylbenzoisochromen-1,6-dione alkaloid biosynthesis, i.e. the conversion of 2-oxa- to 2-aza- analogs, seems to be the aerial plant parts because no compound of the latter type has been identified from roots.

4. Conclusions

In conclusion, the results of the present work, together with previously reported data, not only confirm that the roots of *W. thyrsoiflora* (Haemodoraceae) are the site of the biosynthesis of phenyl-

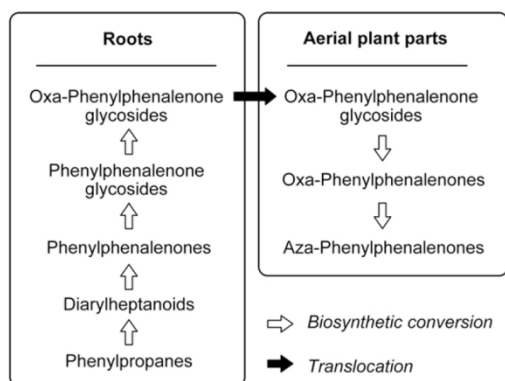


Fig. 4. Accumulation sites, hypothetical biosynthetic conversions, and translocation in the phenylphenalenone pathway in *Wachendorfia thyrsiflora*.

phenalenones but also suggest that glycosidation and the formation of oxa-phenylphenalenones takes place in the roots. The model shown in Fig. 4 further suggests the translocation of oxa-phenylphenalenone glycosides to the aerial plant parts, where they may be converted to aza-phenylphenalenones, probably after hydrolysis. However, the precise biosynthetic route downstream of lachnanthoside aglycone (R6) and its glycosides, the first tetraoxygenated phenylphenalenones in the pathway (Munde et al., 2012), remains to be elaborated.

This work also shows that LC-DAD-SPE-NMR is suitable for elucidating the structures of components from complex mixtures. Profiling the extracts of a single plant suggests that the method is useful for investigating the variability between individuals of a species or within a population, including the *de novo* structure elucidation of unknown metabolites.

5. Experimental

5.1. General experimental procedures

The LC-SPE-NMR system consisted of an Agilent 1100 chromatography system (quaternary solvent delivery pump G1311A, auto-sampler G1313A) and a J&M photodiode array detector (DAD, detection 200–700 nm) connected to a Spark Prospekt 2 solid-phase extraction (SPE) device (Spark Holland, Emmen, The Netherlands) containing HySphere resin GP cartridges (10 × 2 mm, 10 μm). UV spectra were recorded by DAD detector of the LC-SPE-NMR system during analytical HPLC in MeCN-H₂O containing 0.1% formic acid (FA) eluent. A make-up pump (Knauer, Berlin, Germany) was used to add water (2.5 ml min⁻¹) to the eluent after HPLC in order to reduce the elutropic capacity of the LC eluent. The system is controlled by Bruker software HyStar 3.2 (Bruker Biospin, Rheinstetten, Germany). ¹H NMR, ¹H-¹H COSY, HMBC, and HSQC spectra were measured on a Bruker AV 500 NMR spectrometer (Bruker Biospin, Karlsruhe, Germany), operating at a resonance frequency of 500.13 MHz for ¹H and 125.75 MHz for ¹³C. The NMR spectrometer was equipped with a TCI cryoprobe (5 mm) and a CryoFIT™ flow system (30 μl). Electrospray ionization mass spectra (ESIMS) were recorded on a Bruker Esquire 3000 ion trap mass spectrometer (Bruker Daltonics, Bremen, Germany). The spectrometer was fitted to the Agilent 1100 chromatography system described above. Eluents were directly transferred to the mass spectrometer after DAD detection without trapping on post-column SPE cartridges. LC-ESIMS was controlled by HyStar 3.2 software (Bruker Biospin, Rheinstetten, Germany) and MS data were analyzed using Esquire 5.3 (Bruker Daltonics,

Bremen, Germany). HRESIMS was recorded on a LC-MS/MS system consisting of an Ultimate 3000 series RSLC (Dionex, Sunnyvale, CA, USA) system, and an Orbitrap mass spectrometer (Thermo Fisher Scientific, Bremen, Germany). HRESIMS data were analyzed using XCALIBUR (Thermo Fisher Scientific, Waltham, MA, USA) software.

5.2. Plant material

Plants of *W. thyrsiflora* were raised from seeds obtained from B&T World Seeds (Paguignan, Aigues-Vives, France) in soil in the greenhouse of Max Planck Institute for chemical Ecology under the following conditions: day 22–24 °C, night 20–22 °C; relative air humidity 60–70%. The natural daily photoperiod was supported by 16 h illumination from Phillips Sun-T Agro 400 Na lights.

5.3. Extraction, isolation, and sample preparation

A single *W. thyrsiflora* plant, raised from seed and grown in the greenhouse for about 6 months, was separated into aerial parts and roots. Aerial parts were ground in liquid N₂ and freeze-dried. Lyophilized material (9 g) was extracted with acetone (50 ml). The extract was dried in vacuum at 40 °C to afford 600 mg residue, which was dissolved in DMSO (3 ml) and filtered for LC-SPE-NMR and LC-MS analysis. Roots (4.9 g) were ground in liquid N₂ and extracted with acetone (50 ml). The extract was filtered and dried in a vacuum at below 40 °C to yield 22 mg residue, which was dissolved in DMSO (200 μl) and filtered for LC-SPE-NMR and LC-MS analysis.

5.4. LC-SPE-NMR

The chromatographic separation of the extract from aerial plant parts was performed on a Purospher RP18e column (5 μm; 250 × 4.6 mm; Merck KGaA, Darmstadt, Germany) with a guard column (4 × 4 mm) at 25 °C with a flow rate of 1.0 ml min⁻¹. A linear binary gradient of H₂O (solvent A) and MeCN (solvent B), both containing 0.1% FA, was applied. Gradient 1 (0 min: 15% B, 45 min: 70% B, 47 min: 95% B, 52 min: 95% B, 54 min: 15% B, 59 min: 15% B) was used for aerial plant material. The injection volume was 20 μl, and the eluate was monitored at 254 nm. Six cumulative trappings on HySphere resin GP cartridges SPE were performed for each peak selected for NMR analysis. The chromatographic separation of the root extract was conducted on the same column and using the same conditions as for aerial part extract with linear binary gradient 2 as follows: 0 min: 25% B, 45 min: 58% B, 46 min: 95% B, 50 min: 95% B, 51 min: 25% and 55 min: 25% B. Five cumulative trappings were performed for each peak selected for NMR analysis.

SPE cartridges loaded with metabolites were dried in a stream of nitrogen. Then the analytes were eluted from the cartridges and transferred through the connecting capillary into the NMR spectrometer using MeCN-*d*₃. NMR spectra were measured at 300 K in MeCN-*d*₃. Standard Bruker pulse sequences were applied at a ¹H NMR resonance frequency of 500.13 MHz and a ¹³C NMR resonance frequency of 125.75 MHz. The residual signals of MeCN-*d*₃ at δ_{1H} 1.94 and δ_{13C} 1.32 were used as chemical shift references (Gottlieb et al., 1997).

5.5. LC-MS

Extracts of aerial plant parts and roots were used. Instruments and LC conditions for LC-MS were identical to those used for LC-NMR, except that samples were not trapped on the cartridge but directly transferred through the connecting capillary to the Esquire 3000 mass spectrometer. The eluate was split off in a ratio 3:1 before reaching the mass spectrometer. Samples were measured in positive and negative modes in the range *m/z* 150–1200 with

skimmer voltage ± 33.9 V. Capillary exit voltage was ± 106.7 V, capillary voltage ± 4000 V, nebulizer pressure 30 psi, drying gas 12.0 l min^{-1} , and gas temperature 350°C .

5.6. LC-HRMS

After NMR measurements, samples were flushed from the NMR flow cell, and evaporated to dryness. HRMS data of new compounds were recorded by LC-HRESIMS. LC was performed using a Dionex Acclaim C18 Column ($150 \times 2.1 \text{ mm}$, $2.2 \mu\text{m}$) at a constant flow rate of $300 \mu\text{l min}^{-1}$. A binary solvent system of H_2O (solvent A) and MeCN (solvent B), both containing 0.1% FA, was used as follows: 0–10 min: 0.5%–10% B, 10–14 min: 10%–80% B, 14–19 min: 80% B, 19–19.1 min 80%–0.5%, 19.1–25 min: 0.5% B. Capillary voltage and capillary temperature of the ESI source were set to 35 V resp. 275°C . Samples were measured in positive mode using the Orbitrap analyzer. Data were acquired in full scan mode using $30,000 \text{ m/}\Delta\text{m}$ resolving power.

5.7. 6-O-[(6'-O-Malonyl)- β -D-glucopyranosyl]-5-hydroxy-7-(4'-hydroxyphenyl)-3H-benzo[de]isochromen-1-one (A2)

UV (MeCN- H_2O): λ_{max} 258, 337, 368 nm; ^1H NMR data, see Table 1, and ^{13}C NMR data, see Table 2; ESIMS: m/z 511 $[\text{M}-45]^-$, 555 $[\text{M}-1]^-$, 1111 $[\text{M}-1]^-$, HRESIMS: m/z 557.12796 $[\text{M}+1]^+$ (calcd for $\text{C}_{27}\text{H}_{25}\text{O}_{13}$, 557.12952).

5.8. 6-O-[(6'-O-Malonyl)- β -D-glucopyranosyl]-5-hydroxy-7-phenyl-3H-benzo[de]isochromen-1-one (A4)

UV (MeCN- H_2O): λ_{max} 259, 333, 363 nm; ^1H NMR see Table 1, and ^{13}C NMR data, see Table 2; ESIMS: m/z 495 $[\text{M}-45]^-$, 539 $[\text{M}-1]^-$, 1079 $[\text{M}-1]^-$, HRESIMS: m/z 541.13310 $[\text{M}+1]^+$ (calcd for $\text{C}_{27}\text{H}_{25}\text{O}_{12}$, 541.13460).

5.9. 2-Carboxymethyl-5-hydroxy-7-phenyl-2H-benzo[de]isoquinoline-1,6-dione (A6)

UV (MeCN- H_2O): λ_{max} 236, 322, 432 nm; ^1H NMR, see Table 3, and ^{13}C NMR data, see Table 4; ESIMS: m/z 370 $[\text{M}+\text{Na}]^+$, HRESIMS: m/z 348.08595 $[\text{M}+1]^+$ (calcd for $\text{C}_{20}\text{H}_{14}\text{O}_5\text{N}$, 348.08720).

5.10. 2-(3-Carboxy-n-propyl)-5-hydroxy-7-phenyl-2H-benzo[de]isoquinoline-1,6-dione (A8)

UV (MeCN- H_2O): λ_{max} 236, 322, 439 nm; ^1H NMR, see Table 3, and ^{13}C NMR data, see Table 4; ESIMS: m/z 398 $[\text{M}+\text{Na}]^+$, 773 $[\text{M}+\text{Na}]^+$, HRESIMS: m/z 376.11765 $[\text{M}+1]^+$ (calcd for $\text{C}_{22}\text{H}_{18}\text{O}_5\text{N}$, 376.11850).

5.11. 2-(1-Carboxyethyl)-5-hydroxy-7-phenyl-2H-benzo[de]isoquinoline-1,6-dione (A9)

UV (MeCN- H_2O): λ_{max} 236, 322, 433 nm; ^1H NMR, see Table 3, and ^{13}C NMR data, see Table 4; ESIMS: m/z 384 $[\text{M}+\text{Na}]^+$, 745 $[\text{M}+\text{Na}]^+$, HRESIMS: m/z 362.10162 $[\text{M}+1]^+$ (calcd for $\text{C}_{21}\text{H}_{16}\text{O}_5\text{N}$, 362.10285).

5.12. 2-(n-Butyl)-5-hydroxy-7-(4-hydroxyphenyl)-2H-benzo[de]isoquinoline-1,6-dione (A12)

UV (MeCN- H_2O): λ_{max} 236, 263, 327, 425 nm; ^1H NMR, see Table 3, and ^{13}C NMR data, see Table 4; ESIMS: m/z 384 $[\text{M}+\text{Na}]^+$, 745 $[\text{M}+\text{Na}]^+$, HRESIMS: m/z 362.13826 $[\text{M}+1]^+$ (calcd for $\text{C}_{22}\text{H}_{20}\text{O}_4\text{N}$, 362.13923).

5.13. 2-(n-Butyl)-5-hydroxy-7-phenyl-2H-benzo[de]isoquinoline-1,6-dione (A15)

UV (MeCN- H_2O): λ_{max} 237, 266, 323, 442 nm; ^1H NMR, see Table 3, and ^{13}C NMR data, see Table 4; ESIMS: m/z 368 $[\text{M}+\text{Na}]^+$, 713 $[\text{M}+\text{Na}]^+$, HRESIMS: m/z 346.14343 $[\text{M}+1]^+$ (calcd for $\text{C}_{22}\text{H}_{20}\text{O}_3\text{N}$, 346.14432).

5.14. 6-O-[(6'-O-Malonyl)- β -D-glucopyranosyl]-2,5-dihydroxy-7-phenylphenalen-1-one (R2)

UV (MeCN- H_2O): λ_{max} 277, 374, 474 nm; ^1H NMR, see Table 1, and ^{13}C NMR data, see Table 2; ESIMS: m/z 507 $[\text{M}-45]^-$, 551 $[\text{M}-1]^-$, 1103 $[\text{M}-1]^-$, HRESIMS: m/z 553.13344 $[\text{M}+1]^+$ (calcd for $\text{C}_{28}\text{H}_{25}\text{O}_{12}$, 553.13460).

5.15. 6-O-[(6'-O-Malonyl)- β -D-glucopyranosyl]-2-methoxy-5-hydroxy-7-phenylphenalen-1-one (R3)

UV (MeCN- H_2O): λ_{max} 277, 374, 474 nm; ^1H NMR, see Table 1, and ^{13}C NMR data, see Table 2; ESIMS: m/z 521 $[\text{M}-45]^-$, 565 $[\text{M}-1]^-$, 1117 $[\text{M}-1]^-$, 1131 $[\text{M}-1]^-$, HRESIMS: m/z 567.14861 $[\text{M}+1]^+$ (calcd for $\text{C}_{29}\text{H}_{27}\text{O}_{12}$, 567.15025).

5.16. 6-O-[(6'-O-Malonyl)- β -D-glucopyranosyl]-2-hydroxy-5-methoxy-7-phenylphenalen-1-one (R4)

UV (MeCN- H_2O): λ_{max} 278, 374, 478 nm; ^1H NMR see Table 1 and ^{13}C NMR data, see Table 2; ESIMS: m/z 521 $[\text{M}-45]^-$, 565 $[\text{M}-1]^-$, 1131 $[\text{M}-1]^-$, HRESIMS: m/z 567.14927 $[\text{M}+1]^+$ (calcd for $\text{C}_{29}\text{H}_{27}\text{O}_{12}$, 567.15025).

5.17. 6-O-[(6'-O-Malonyl)- β -D-glucopyranosyl]-5-methoxy-7-phenyl-3H-benzo[de]isochromen-1-one (R5)

UV (MeCN- H_2O): λ_{max} 259, 333, 364 nm; ^1H NMR, see Table 1, and ^{13}C NMR data, see Table 2; ESIMS: m/z 509 $[\text{M}-45]^-$, 553 $[\text{M}-1]^-$, 1107 $[\text{M}-1]^-$, HRESIMS: m/z 555.14909 $[\text{M}+1]^+$ (calcd for $\text{C}_{28}\text{H}_{27}\text{O}_{12}$, 555.15025).

5.18. 6-Hydroxy-3,5-dimethoxy-7-phenyl-3H-benzo[de]isochromen-1-one (R13)

UV (MeCN- H_2O): λ_{max} 265, 323, 338, 384 nm; ^1H NMR, see Table 3, and ^{13}C NMR data, see Table 4; ESIMS: m/z 335 $[\text{M}-1]^-$, HRESIMS: m/z 337.10642 $[\text{M}+1]^+$ (calcd for $\text{C}_{20}\text{H}_{17}\text{O}_5$, 337.10760).

Acknowledgment

The authors thank Dr. Renate Ellinger for technical assistance with LC-DAD-SPE-NMR and Emily Wheeler for editorial help in preparation of the manuscript. J. Fang acknowledges the International Max Planck Research School (IMPRS) for a PhD scholarship. We are also grateful for financial support from the Max Planck Society (MPG).

References

- Bazan, A.C., Edwards, J.M., 1976. Phenalenone pigments of flowers of *Lachnanthes tinctoria*. *Phytochemistry* 15, 1413–1415.
- Bick, I.R.C., Blackman, A.J., 1973. Haemodorrin - A phenalenone pigment. *Aust. J. Chem.* 26, 1377–1380.
- Binks, R.H., Greenham, J.R., Luis, J.G., Gowen, S.R., 1997. A phytoalexin from roots of *Musa acuminata* var *Pisang sipulu*. *Phytochemistry* 45, 47–49.
- Brand, S., Höltscher, D., Schierhorn, A., Svatoš, A., Schröder, J., Schneider, B., 2006. A type III polyketide synthase from *Wachendorfia thyrsiflora* and its role in diarylheptanoid and phenylphenalenone biosynthesis. *Planta* 224, 413–428.

- Brkljaca, R., Urban, S., 2011. Recent advancements in HPLC-NMR and applications for natural product profiling and identification. *J. Liq. Chromatogr. Relat. Technol.* 34, 1063–1076.
- Cooke, R.G., Johnson, B.L., Segal, W., 1958. Colouring matters of Australian plants 6. Haemocerin: The structure of the aglycone. *Aust. J. Chem.* 11, 230–235.
- Cooke, R.G., Segal, W., 1955. Colouring matters of Australian plants 4. Haemocerin - a unique glycoside from *Haemodorum corymbosum* Vahl. *Aust. J. Chem.* 8, 107–113.
- Corcoran, O., Wilkinson, P.S., Godejohann, M., Braumann, U., Hofmann, M., Spraul, M., 2002. Advancing sensitivity for flow NMR spectroscopy: LC-SPE-NMR and capillary-scale LC-NMR. *American Lab.* 34, 18–21.
- Daolio, C., Schneider, B., 2012. Coupling liquid chromatography and other separation techniques to nuclear magnetic resonance spectroscopy. In: Shalliker, R.A. (Ed.), *Hyphenated and Alternative Methods of Detection in Chromatography*. Taylor & Francis - CRC Press, London, pp. 61–98.
- DellaGreca, M., Previtera, L., Zarrelli, A., 2008. Revised structures of phenylphenalene derivatives from *Eichhornia crassipes*. *Tetrahedron Lett.* 49, 3268–3272.
- Dias, D.A., Goble, D.J., Silva, C.A., Urban, S., 2009. Phenylphenalenones from the Australian plant *Haemodorum simplex*. *J. Nat. Prod.* 72, 1075–1080.
- Dora, G., Edwards, J.M., Campbell, W., 1990. Thyriflorin: A novel phenalenone pigment from *Wachendorfia thyriflora*. *Planta Med.* 56, 569.
- Edwards, J.M., Weiss, U., 1972. Quinone methides derived from 5-oxa and 5-aza-9-phenyl-1-phenalenone in flowers of *Lachnanthes tinctoria* (Haemodoraceae). *Tetrahedron Lett.* 17, 1631–1634.
- Edwards, J.M., Weiss, U., 1974. Phenalenone pigments of root system of *Lachnanthes tinctoria*. *Phytochemistry* 13, 1597–1602.
- Exarchou, V., Krucker, M., van Beek, T.A., Vervoort, J., Gerotheranassis, I.P., Albert, K., 2005. LC-NMR coupling technology: recent advancements and applications in natural products analysis. *Magn. Reson. Chem.* 43, 681–687.
- Fang, J.J., Paetz, C., Hölscher, D., Munde, T., Schneider, B., 2011. Phenylphenalenones and related natural products from *Wachendorfia thyriflora* L. *Phytochem. Lett.* 4, 203–208.
- Gottlieb, H.E., Kotlyar, V., Nudelman, A., 1997. NMR chemical shifts of common laboratory solvents as trace impurities. *J. Org. Chem.* 62, 7512–7515.
- Hölscher, D., Schneider, B., 1999. HPLC-NMR analysis of phenylphenalenones and a stilbene from *Anigozanthos flavidus*. *Phytochemistry* 50, 155–161.
- Hölscher, D., Schneider, B., 2000. Phenalenones from *Strelitzia reginae*. *J. Nat. Prod.* 63, 1027–1028.
- Hölscher, D., Schneider, B., 2005. The biosynthesis of 8-phenylphenalenones from *Eichhornia crassipes* involves a putative aryl migration step. *Phytochemistry* 66, 59–64.
- Hölscher, D., Schneider, B., 2007. Laser microdissection and cryogenic nuclear magnetic resonance spectroscopy: An alliance for cell type-specific metabolite profiling. *Planta* 225, 763–770.
- Helme, N., Linder, H.P., 1992. Morphology, evolution and taxonomy of *Wachendorfia* (Haemodoraceae). *Bothalia* 22, 59–75.
- Jaroszewski, J.W., 2005. Hyphenated NMR methods in natural products research, Part 2: HPLC-SPE-NMR and other new trends in NMR hyphenation. *Planta Med.* 71, 795–802.
- Kamo, T., Hirai, N., Tsuda, M., Fujioka, D., Ohigashi, H., 2000. Changes in the content and biosynthesis of phytoalexins in banana fruit. *Biosci. Biotechnol. Biochem.* 64, 2089–2098.
- Luis, J.G., Echeverri, F., Quiñones, W., Brito, I., López, M., Torres, F., Cardona, G., Aguiar, Z., Pelaez, C., Rojas, M., 1993. Irenolone and emenolone - Two new types of phytoalexin from *Musa paradisiaca*. *J. Org. Chem.* 58, 4306–4308.
- Luque-Ortega, J.R., Martínez, S., Saugar, J.M., Izquierdo, L.R., Abad, T., Luis, J.G., Pinero, J., Valladares, B., Rivas, L., 2004. Fungus-elicited metabolites from plants as an enriched source for new leishmanicidal agents: Antifungal phenylphenalenone phytoalexins from the banana plant (*Musa acuminata*) target mitochondria of *Leishmania donovani* promastigotes. *Antimicrob. Agents Chemother.* 48, 1534–1540.
- Munde, T., Brand, S., Hidalgo, W., Maddula, R.K., Svatoš, A., Schneider, B., 2012. Biosynthesis of tetraoxygenated phenylphenalenones in *Wachendorfia thyriflora*. *Phytochemistry*. <http://dx.doi.org/10.1016/j.phytochem.2012.02.020>.
- Opitz, S., Hölscher, D., Oldham, N.J., Bartram, S., Schneider, B., 2002. Phenylphenalenone-related compounds: chemotaxonomic markers of the Haemodoraceae from *Xiphidium caeruleum*. *J. Nat. Prod.* 65, 1122–1130.
- Opitz, S., Schneider, B., 2002. Organ-specific analysis of phenylphenalenone-related compounds in *Xiphidium caeruleum*. *Phytochemistry* 61, 819–825.
- Opitz, S., Schneider, B., 2003. Oxidative biosynthesis of phenylbenzoisochromenones from phenylphenalenones. *Phytochemistry* 62, 307–312.
- Opitz, S., Schnitzler, J.P., Hause, B., Schneider, B., 2003. Histochemical analysis of phenylphenalenone-related compounds in *Xiphidium caeruleum* (Haemodoraceae). *Planta* 216, 881–889.
- Otálvaro, F., Nanclores, J., Vásquez, L.E., Quiñones, W., Echeverri, F., Arango, R., Schneider, B., 2007. Phenalenone-type compounds from *Musa acuminata* var. “Yangambi km 5” (AAA) and their activity against *Mycosphaerella fijiensis*. *J. Nat. Prod.* 70, 887–890.
- Otálvaro, F., Jitsaeng, K., Munde, T., Echeverri, F., Quiñones, W., Schneider, B., 2010. O-Methylation of phenylphenalenone phytoalexins in *Musa acuminata* and *Wachendorfia thyriflora*. *Phytochemistry* 71, 206–213.
- Schneider, B., Paetz, C., Hölscher, D., Opitz, S., 2005. HPLC-NMR for tissue-specific analysis of phenylphenalenone-related compounds in *Xiphidium caeruleum* (Haemodoraceae). *Phytochemistry* 43, 724–728.
- Wang, M.Z., Cai, X.H., Luo, X.D., 2011. New phenylphenalene derivatives from water hyacinth (*Eichhornia crassipes*). *Helv. Chim. Acta* 94, 61–66.



Co-occurrence of phenylphenalenones and flavonoids in *Xiphidium caeruleum* Aubl. flowers

Jingjing Fang, Dirk Hölscher, Bernd Schneider*

Max Planck Institute for Chemical Ecology, Beutenberg Campus, Hans-Knöll Str. 8, D-07745 Jena, Germany

ARTICLE INFO

Article history:
Received 23 May 2012
Received in revised form 9 July 2012
Available online 4 August 2012

Keywords:
Xiphidium caeruleum
Haemodoraceae
LC–DAD–SPE–NMR
Flavonoids
Phenylbenzoisochromenones
Phenylbenzoisoquinolinones
Phenylanthracic anhydrides
Phenylphenalenones

ABSTRACT

A *Xiphidium caeruleum* flower extract was separated by semi-preparative HPLC into five fractions, from which three flavonoids, two phenylphenalenones and 17 phenylphenalenone-related compounds including five unknown compounds, were isolated and their structures elucidated by Liquid Chromatography–Diode Array Detection–Solid Phase Extraction–Nuclear Magnetic Resonance spectroscopy (LC–DAD–SPE–NMR) and mass spectrometry (MS). This is the first report of the co-occurrence of phenylphenalenones and flavonoids in the Haemodoraceae family. The ecological implications of flavonoids and various phenylphenalenone-type compounds and their putative biosynthesis sites in *X. caeruleum* are subject to discussion.

© 2012 Elsevier Ltd. All rights reserved.

1. Introduction

Xiphidium caeruleum Aubl. (Haemodoraceae) is native to the Neotropics (Maas and Maas-Van de Kamer, 1993). Previous studies have shown that this plant is a rich source of phenylphenalenones and related compounds (Cremona and Edwards, 1974; Opitz et al., 2002; Opitz and Schneider, 2002). As a part of our continuing efforts on the structure elucidation, tissue-specific distribution (Opitz et al., 2003; Hölscher and Schneider, 2007) and the biosynthesis (Brand et al., 2006; Otálvaro et al., 2010; Munde et al., 2012) of phenylphenalenones, Liquid Chromatography–Diode Array Detection–Solid Phase Extraction–Nuclear Magnetic Resonance spectroscopy (LC–DAD–SPE–NMR) and mass spectrometry (MS) were implemented to identify the compounds present in five semi-preparative high-performance liquid chromatography (HPLC) fractions obtained from the *X. caeruleum* flower extract. Twenty-two phenolic compounds (three flavonoids, two phenylphenalenones and 17 phenylphenalenone-related compounds) were identified, including five new natural products. Here we report the structure elucidation of the new compounds, four phenylbenzoisoquinolinones and a phenylisobenzochromenone. The specific metabolite pattern of *X. caeruleum* flowers, including various types of phenylphenalenones and the first reported occurrence of flavonoids in the Haemodoraceae, is discussed.

2. Results

The extract of fresh *X. caeruleum* flowers was fractionated by semi-preparative reversed phase HPLC and identified by LC–DAD–SPE–NMR and MS. For compound **6** (Fig. 1), the aromatic area of the ^1H NMR spectrum (Table 1) displays two singlets at δ 7.86 (H-3) and 6.99 (H-4), two doublets of an AB spin system at δ 7.54 (H-8) and 8.62 (H-9) with a coupling constant of 8.1 Hz, a doublet of doublets integrating for two protons at δ 7.34 (H-2'/6'), and signals of H-3'/5' and H-4' distributed between δ 7.41 and 7.44. The tricyclic partial structure was elucidated by means of heteronuclear multiple-bond correlation (HMBC) and heteronuclear multiple quantum coherence (HMQC) spectra. In the HMBC spectrum (Table S1, Supplementary data), H-9 correlates with a carbonyl signal at δ 161.7 (C-1) and signals of two other carbon atoms at δ 151.1 (C-7) and 132.9 (C-9b). The latter carbon (C-9b), which also correlates with H-3 and H-4, was confirmed as the central carbon of the tricyclic phenalenone. The *peri* position of H-3 and H-4 was deduced by mutual HMBC correlations with the corresponding C-4 (δ 110.6) and C-3 carbons (δ 138.4), respectively. H-4 correlates with another oxygenated carbon atom at δ 149.1 (C-5) and the carbonyl carbon atom at δ 179.1 (C-6). Additional HMBC correlations of H-8 with C-1' (δ 142.8) and of H-2'/6' with C-7 (δ 151.1) established that the phenyl group is attached to position 7. The NMR data suggested the presence of a 1,5,6-trioxygenated 7-phenylphenalenone-like structure which, similar to lachnanthopyrone (**8**) (Edwards and Weiss, 1972), has an oxygen or other heteroatom in position 2. In addition to the signals in the aromatic part of the ^1H NMR spectrum,

* Corresponding author. Tel.: +49 3641 571600; fax: +49 3641 571601.
E-mail address: schneider@ice.mpg.de (B. Schneider).

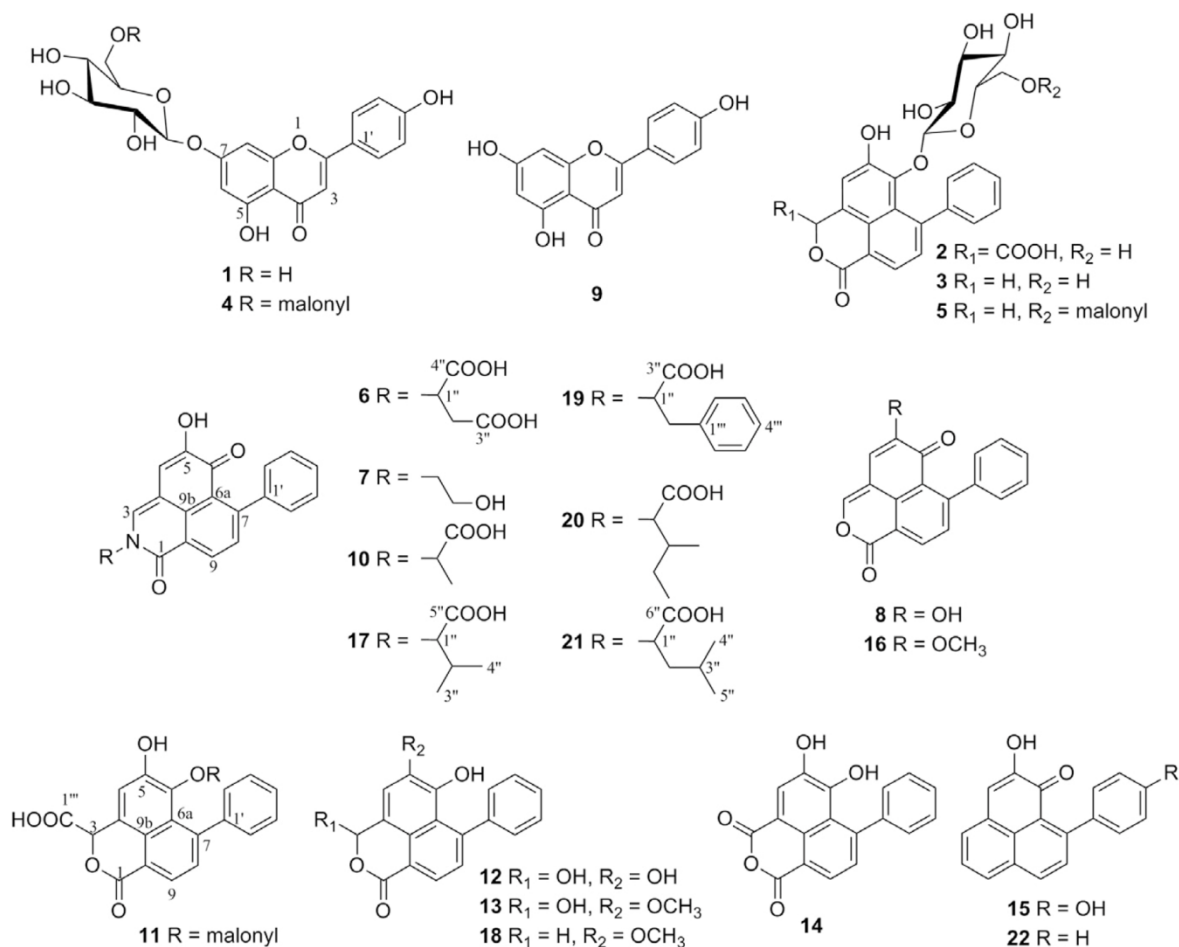


Fig. 1. Structures of compounds isolated from flowers of *Xiphidium caeruleum*. Compounds **6**, **11**, **17**, **19**, and **21** are new natural products.

Table 1

¹H NMR data of compounds **6**, **11**, **17**, **19** and **21** obtained by LC-DAD-SPE-NMR (500 MHz, MeCN-d₃, δ values, J in Hz).

Position	6	11	17	19	21
3	7.86 (s)	6.31 (s)	7.90 (s)	7.60 (s)	7.81 (s)
4	6.99 (s)	7.53 (s)	7.03 (s)	6.84 (s)	7.01 (s)
8	7.54 (d, 8.1)	7.45 (d, 7.4)	7.55 (d, 8.1)	7.49 (d, 8.1)	7.55 (d, 8.1)
9	8.62 (d, 8.1)	8.22 (d, 7.4)	8.64 (d, 8.1)	8.54 (d, 8.1)	8.64 (d, 8.1)
2'/6'	7.34 (dd, 7.8, 2.0)	7.31 (dd, 7.6, 1.9)	7.34 (dd, 7.8, 2.1)	7.30 (dd, 7.8, 2.0)	7.34 (dd, 7.9, 2.0)
3'/4'/5'	7.41–7.44 (m)	7.46 (m)	7.41–7.44 (m)	7.38–7.42 (m)	7.41–7.44 (m)
1''	5.43 (t-like, 7.1)		5.25 (d, 9.9)	5.58 (dd, 11.4, 4.9)	5.60 (dd, 11.1, 4.8)
2''a	3.30 (dd, 16.7, 5.7)	2.64 (s)	2.57 (m)	3.63 (dd, 14.6, 4.9)	2.16 (m)
2''b	3.07 (dd, 16.7, 7.8)			3.45 (dd, 14.6, 11.4)	2.04 (m)
3''			1.18 (d, 6.6)		1.50 (m)
4''			0.88 (d, 6.8)		0.96 (d, 6.6)
5''					0.94 (d, 6.7)
2'''/6'''				7.18 (m)	
3'''/5'''				7.18 (m)	
4'''				7.15 (m)	

a methine proton signal appears at δ 5.43 (H-1''), and signals of a diastereotopic methylene group are displayed at δ 3.30 (H-2''a) and 3.07 (H-2''b) (Table 1). The methine proton H-1'' correlates with C-1 and C-3 in the HMBC spectrum, indicating that a side-chain is attached to position 2, which therefore cannot be an oxygen atom but must be a nitrogen atom. The odd molecular mass of compound **6**

(m/z 405) confirmed the existence of a nitrogen atom in the molecule. Additional HMBC cross-peaks between H-1'' and H-2'' and the carbon signals at δ 170.4 and 172.2 disclosed two other carbonyl groups in the structure. Based on the above evidence, the structure of compound **6** was elucidated as 2-(1'',2''-dicarboxyethyl)-5-hydroxy-7-phenyl-2H-benzo[de]isoquinoline-1,6-dione. The

structure was further confirmed by high resolution ESIMS (HRESIMS).

The signal pattern in the aromatic region of the ^1H NMR spectra of three other compounds, **17**, **19** and **21** (Fig. 1), purified from fraction 4 closely resembled that of compound **6** (Table 1). The odd masses also confirmed **17**, **19** and **21** to be of a similar nature to alkaloid **6**. Inspection of the HSQC and HMBC spectra suggested that compounds **17**, **19** and **21** were lachnanthopyrone derivatives, each containing an amino acid-derived side-chain. Cross-signals of H-1'' with C-1 and C-3 indicate that the side-chain is attached to position 2.

The ^1H NMR spectrum of **17** (Table 1), in addition to the signals of the tricycle, showed the presence of two methine protons at δ 5.25 (H-1'') and 2.57 (H-2''), and two methyl groups at δ 1.18 and 0.88. HMBC cross-signals (Table S1, Supplementary data) between H-1'' and the two methyl carbon atoms and the C-2'' methine carbon indicated an isopropyl group as part of the amino acid moiety. Another HMBC correlation between H-1'' and the signal at δ 171.2 suggested the existence of a carbonyl group attached to C-1''. Thus, the amino acid moiety was deduced to be valine and the structure of **17** elucidated as 2-(1''-carboxy-2''-methyl-propyl)-5-hydroxy-7-phenyl-2H-benzo[de]isoquinoline-1,6-dione, for which HRESIMS confirmed the structure.

In addition to the aromatic signals indicating a phenylbenzoisoquinolinedione skeleton (Table 1), the ^1H NMR spectrum of **19** displayed signals of another phenyl group resonating between δ 7.15 and 7.18, one methine proton at δ 5.58 (H-1''), and two protons of a diastereotopic methylene group at δ 3.63 (H-2''a) and 3.45 (H-2''b). HMBC correlations (Table S1, Supplementary data) of H-1'' and H-2'' with the carbonyl signal at δ 170.7, and of H-2'' with C-1''' (δ 137.6) and C-2'''/6''' (δ 129.6) of the phenyl group suggested a phenylalanine moiety. Therefore, **19** was determined as 2-(1''-carboxy-2''-phenyl-ethyl)-5-hydroxy-7-phenyl-2H-benzo[de]isoquinoline-1,6-dione, which was confirmed by HRESIMS.

The alkyl signals in the ^1H NMR spectrum of **21** (Table 1) indicated the presence of two methines at δ 5.60 (H-1'') and 1.50 (H-3''), a diastereotopic methylene group at δ 2.16 (H-2''a) and 2.04 (H-2''b), and two methyl groups at δ 0.96 (H-4'') and 0.94 (H-5''). Correlations in the HMBC spectrum established the presence of a carbonyl (δ 171.4) attached to C-1'' and an isopropyl moiety at C-2''. Thus, the amino acid side-chain was identified as a leucine moiety. The structure of compound **21** was determined as 2-(1''-carboxy-3''-methyl-*n*-butyl)-5-hydroxy-7-phenyl-2H-benzo[de]isoquinoline-1,6-dione and further confirmed by HRESIMS.

Compound **11** (Fig. 1) was purified from fraction 3. Its ^1H NMR spectrum (Table 1) showed presence of two singlets at δ 6.31 (H-3) and 7.53 (H-4), two doublets of an AB spin system at δ 7.45 (H-8) and 8.22 (H-9), and signals of a phenyl group at δ 7.31 and 7.46, together representing five protons. In addition, a singlet at δ 2.64 (H-2'') integrating for two protons was also present in the ^1H NMR spectrum. The structure was elucidated on the basis of the HSQC and HMBC (Table S1, Supplementary data) spectra, in which H-9 links to a carbonyl carbon atom at δ 163.6 (C-1), a quaternary carbon signal at δ 142.8 (C-7) and a signal at δ 124.5 (C-9b). The latter carbon, which is assigned as the central carbon of the tricyclic system, also correlates with H-3 and H-4. Mutual HMBC correlations of H-3 with C-4 (δ 118.5) and of H-4 with C-3 (δ 78.2) established the *peri* relationship of H-3 and H-4. Another HMBC correlation of H-3 was observed with a carboxyl carbon atom (δ 170.5), which therefore must be attached to C-3. The ^1H NMR signal of H-4 showed correlations with carbon signals at δ 148.3 (C-5) and 132.1 (C-6) in the HMBC spectrum. Finally, HMBC cross-peaks of H-9 and H-2''/6'' (δ 7.31) with C-7, and of H-8 and H-3''/5'' (δ 7.46) with C-1'' (142.3), enabled the phenyl group to be placed at position 7. From these NMR data, the core structure of compound **11** was identified as 3-car-

boxy-5,6-dihydroxy-7-phenyl-3H-benzo[de]isochromen-1-one, previously reported as the aglycone of the corresponding 6-O-glucoside from *X. caeruleum* (Opitz et al., 2002). The additional methylene signal of H-2'' (δ_{H} 2.64; δ_{C} 40.0) correlated with two carbonyl signals at δ 165.7 and 170.3, suggesting a malonyl unit. HRESIMS confirmed the structure of a malonylated 3-carboxy-5,6-dihydroxy-7-phenyl-3H-benzo [de]isochromen-1-one. The malonyl moiety may be attached to one of the hydroxyl groups at C-5 or C-6. The chemical shifts of these two carbon atoms suggest acylation at position 6 (δ 132.1) and a non-acetylated OH at C-5 (δ 148.3). Moreover, the malonyl methylene group appears to be shielded by intramolecular interaction with the phenyl substituent in *peri* position at C-7, supporting the assumption of acylation at 6-OH. Therefore, the structure of compound **11** is proposed as 3-carboxy-5-hydroxy-6-O-malonyl-7-phenyl-3H-benzo[de]isochromen-1-one. Several malonyl glucosides of the phenylphenalenone-type have been reported from *Wachendorfia thyriflora* (Fang et al., 2011, 2012). However, compound **11** is the first phenylphenalenone-derived natural product bearing an O-malonyl unit directly attached to the tricycle.

The known compounds (Fig. 1) were determined by comparing their MS and NMR data with those in the literature as 7-O- β -D-glucopyranosylapigenin (**1**) (Oyama and Kondo, 2004), 3-carboxy-5-hydroxy-6-O- β -D-glucopyranosyl-7-phenyl-3H-benzo[de]isochromen-1-one (**2**) (Opitz et al., 2002), 6-O- β -D-glucopyranosyl-5-hydroxy-7-phenyl-3H-benzo[de]isochromen-1-one (**3**) (Fang et al., 2011), 7-O-(6''-O-malonyl- β -D-glucopyranosyl)-apigenin (**4**) (Švehlíkova et al., 2004) and 6-O-(6''-O-malonyl- β -D-glucopyranosyl)-5-hydroxy-7-phenyl-3H-benzo[de]isochromen-1-one (Fang et al., 2012) (**5**) from fraction 1; 2-(2''-hydroxyethyl)-5-hydroxy-7-phenyl-2H-benzo[de]isoquinoline-1,6-dione (**7**) (Edwards and Weiss, 1972), 5-hydroxy-7-phenylbenzo[de]isochromene-1,6-dione (lachnanthopyrone) (**8**) (Edwards and Weiss, 1972), apigenin (**9**) (Van Loo et al., 1986) and 2-(1''-carboxyethyl)-5-hydroxy-7-phenyl-2H-benzo[de]isoquinoline-1,6-dione (Fang et al., 2012) (**10**) from fraction 2; 3,5,6-trihydroxy-7-phenyl-3H-benzo[de]isochromen-1-one (**12**) (Opitz et al., 2002), 3,6-dihydroxy-5-methoxy-7-phenyl-3H-benzo[de]isochromen-1-one (**13**) (Opitz et al., 2002), 5,6-dihydroxy-7-phenyl-3H-benzo[de]isochromene-1,3-dione (**14**) (Bazan and Edwards, 1976) and hydroxyanigorufone (**15**) (Cooke and Thomas, 1975) from fraction 3; 5-methoxy-7-phenylbenzo[de]isochromene-1,6-dione (**16**) (Opitz et al., 2002), 6-hydroxy-5-methoxy-7-phenyl-3H-benzo[de]isochromen-1-one (**18**) (Edwards and Weiss, 1974), and 2-(1''-carboxy-2''-methyl-*n*-butyl)-5-hydroxy-7-phenyl-2H-benzo[de]isoquinoline-1,6-dione (**20**) (Bazan and Edwards, 1976) from fraction 4; anigorufone (**22**) (Cooke and Thomas, 1975) from fraction 5.

3. Discussion

Phenylphenalenones and related compounds occur in the Haemodoraceae family (Cooke and Edwards, 1981; Hölscher and Schneider, 1997; Opitz et al., 2002; Dias et al., 2009; Fang et al., 2011), Pontederiaceae (DellaGreca et al., 2008; Hölscher and Schneider, 2005; Hölscher et al., 2006; Wang et al., 2011), Musaceae (Luis et al., 1993; Kamo et al., 2001; Otálvaro et al., 2007) and Strelitziaceae (Hölscher and Schneider, 2000). Within these phenalenone-producing plants, the occurrence of flavonoids has been reported from the Musaceae (Lewis et al., 1999; Someya et al., 2002; Pascual-Villalobos and Rodríguez, 2007), Strelitziaceae (Harborne, 1967; Merh et al., 1986) and Pontederiaceae families (Toki et al., 1994). Phytochemical studies of various Haemodoraceae family plants, mostly carried out using root or leaf material, have detected phenylphenalenones but not flavonoids. In *Strelitzia reginae* (Strelitziaceae) and in *Eichhornia crassipes* (Pontederia-

caea), two plants that accumulate phenalenone-type compounds in their roots and leaves, respectively, flavonoids were detected in flower petals (Harborne, 1967). Notably (delphinidin 3-gentio-biosyl) (apigenin 7-glucosyl) malonate was isolated from the ornamental blue flower petals of *E. crassipes* (Toki et al., 1994). In the present study, apigenin (9) and its glycosides 1 and 4 (Fig. 1) are reported from the white flowers of *X. caeruleum* together with various phenylphenalenone-type compounds. The specific natural product pattern of the flower parts is considered to be adapted to the interaction of the plant with pollinators. The pollinator-attracting function is clearly different from the role of phenylphenalenones in pathogen defense (Otalvaro et al., 2007; Jitsaeng and Schneider, 2010). In contrast to colored delphinidin derivatives occurring in flowers of *S. reginae* and *E. crassipes*, apigenin and its glycosides provide white pigmentation to the flowers of *X. caeruleum*. Together with phenylphenalenones (Lazzaro et al., 2004), phenylisobenzochromenones, and phenylbenzoisquinolinones, apigenin derivatives appear to be responsible for the UV-reflecting properties of the *X. caeruleum* petals (Buchmann, 1980) and for guiding visiting insects to the pollen.

According to their closely related phenylphenalenone profile and metabolite distribution, *X. caeruleum* (Opitz et al., 2002, 2003; Opitz and Schneider, 2002; Schneider et al., 2005) and *W. thyrsoiflora* (Fang et al., 2011, 2012) are sister species within the Haemodoraceae family. Phenylphenalenones with an intact C₁₉ core structure (“C₁₉-phenylphenalenones”) accumulate in the roots, while phenylisobenzochromenones (“oxa-phenylphenalenones”) occur both in the roots and in aerial plant parts, and phenylbenzoisquinolinones (“aza-phenylphenalenones”) are mainly found in the aerial parts. Therefore, the roots have been suggested to be the site of the biosynthesis of C₁₉-phenylphenalenones and their oxidation to oxa-phenylphenalenones. Presumably, oxidation is followed by translocation to the aerial plant parts where they are converted to aza-phenylphenalenones (Fang et al., 2012).

Unlike the phytochemical profile of vegetative tissue, the flowers of *W. thyrsoiflora* contain thyrsoiflorin, a C₁₉-phenylphenalenone (Dora et al., 1990). Here we report the co-occurrence of C₁₉-phenylphenalenones, oxa-phenylphenalenones, and aza-phenylphenalenones in the flowers of *X. caeruleum*. Hence, the flowers of *X. caeruleum* and *W. thyrsoiflora* are a location of C₁₉-phenylphenalenones, and the flowers of the former are also known to contain oxa- and aza-phenylphenalenones. Therefore, it may be speculated that the entire biosynthetic machinery of the phenylphenalenone biosynthetic pathway, including the formation of the C₁₉ skeleton and processing to oxa- and aza-phenylphenalenones, is expressed in flowers.

4. Conclusions

Flowers of *X. caeruleum*, and possibly flowers of other phenylphenalenone-producing plants, display a metabolite pattern which is different from other plant parts such as the roots and leaves. The flowers contain flavonoids, which have not been detected in other plant parts, and they also contain C₁₉-phenylphenalenones, which do not occur in vegetative above-ground tissue. The tissue-specific distribution may suggest that phenylphenalenone-type metabolites play a dual role in the attraction of pollinators and in plant defense.

5. Experimental

5.1. General experimental procedures

Semi-preparative HPLC was performed on a Merck-Hitachi chromatography system (L-6200A gradient pump, L-4250 UV/Vis detector; Hitachi, Ltd. Tokyo, Japan) using an endcapped reversed

phase column (Purospher RP18e, 5 μm, 250 × 10 mm; Merck KGaA, Darmstadt, Germany) with a flow rate of 3.5 ml min⁻¹ and UV detection at 254 nm.

The LC-DAD-SPE-NMR system consisted of an Agilent 1100 chromatography system (quaternary solvent delivery pump G1311A, autosampler G1313A; Agilent Technologies, Waldbronn, Germany) and a J&M photodiode array detector (DAD, detection 200–700 nm; J&M Analytik AG, Aalen, Germany) connected to a Spark Prospekt 2 solid phase extraction (SPE) device (Spark Holland, Emmen, The Netherlands) containing HySphere resin GP cartridges (10 × 2 mm, 10 μm). UV profiles were obtained via DAD detection during analytical HPLC in the eluent. A make-up pump (Knauer, Berlin, Germany) was used to add water (2.5 ml min⁻¹) to the eluent after HPLC in order to reduce the eluotropic capacity. The system is controlled by Bruker software HyStar 3.2 (Bruker Biospin, Rheinstetten, Germany). Standard Bruker pulse sequences were used for measuring ¹H NMR, ¹H–¹H COSY, HMBC, and HSQC spectra on a Bruker AV 500 NMR spectrometer (Bruker Biospin, Karlsruhe, Germany), operating at a resonance frequency of 500.13 MHz for ¹H and 125.75 MHz for ¹³C. The NMR spectrometer was equipped with a TCI cryoprobe (5 mm) and a CryoFIT™ flow system (30 μl).

Electrospray ionization mass spectra (ESIMS) and LC-ESIMS were recorded on a Bruker Esquire 3000 ion trap mass spectrometer (Bruker Daltonics, Bremen, Germany). The spectrometer was fitted to the Agilent 1100 chromatography system described above. LC-ESIMS was controlled by HyStar 3.2 software (Bruker Biospin, Rheinstetten, Germany) and MS data were analyzed using Esquire 5.3 (Bruker Daltonics, Bremen, Germany). HRESIMS was recorded on a LC-MS/MS system consisting of an Ultimate 3000 series RSLC (Dionex, Sunnyvale, CA, USA) system, and an Orbitrap mass spectrometer (Thermo Fisher Scientific, Bremen, Germany). HRESIMS data were analyzed using XCALIBUR (Thermo Fisher Scientific, Waltham, MA, USA) software.

5.2. Plant material

Plants of *X. caeruleum* were obtained from the Ruhr University of Bochum (Botanical Institute), and vegetatively propagated in soil in the greenhouse of the Max Planck Institute for Chemical Ecology under the following conditions: day 22–24 °C, night 20–22 °C; relative air humidity 60–70%. The natural daily photoperiod was supported by 16 h illumination from Phillips Sun-T Agro 400 Na lights.

5.3. Extraction and fractionation

Fresh flowers (3.4 g) were collected from *X. caeruleum* plants, ground in liquid N₂, and extracted with 50% aqueous acetone (150 ml) three times. The combined extracts were evaporated in a vacuum (<40 °C) to afford 212 mg residue, which was reconstituted in water (200 ml). The aqueous solution was then loaded onto a SPE cartridge Discovery DSC-18 (60 ml/10 g; Supelco, Bellefonte, PA, USA), which was conditioned with MeCN and equilibrated with water before use. The loaded cartridge was eluted with water (20 ml) and 80% aqueous MeCN sequentially. The 80% MeCN eluate was evaporated to yield 100 mg residue, which was used to isolate the natural products.

This material was dissolved in MeCN and subjected to semi-preparative HPLC. A linear binary gradient of H₂O (solvent A) and MeCN (solvent B), both containing 0.1% formic acid (FA) was applied: 0 min: 20% B, 60 min: 80% B, 62 min: 95% B, 67 min: 95% B, 69 min: 20% B, 74 min: 20% B. Five fractions were collected: fraction 1 (4–16 min, 29.9 mg), fraction 2 (16–36 min, 36.8 mg), fraction 3 (36–46 min, 6 mg), fraction 4 (46–56 min, 4.1 mg), and fraction 5 (58–64 min, 2 mg).

5.4. LC-DAD-SPE-NMR

LC-DAD-SPE-NMR of fractions 1–4 obtained from semi-preparative HPLC was performed on a Purospher RP18e column (5 μ m, 250 \times 4.6 mm; Merck KGaA, Darmstadt, Germany) with a flow rate of 1 ml min⁻¹. A binary solvent system of H₂O (solvent A) and MeOH (solvent B), both containing 0.1% FA, was used as follows: 0 min: 40% B, 35 min: 50% B, 47 min: 95% B, 52 min: 95% B, 55 min: 40% B, 60 min: 40% B for fraction 1 to yield compounds **1–5**; 0 min: 50% B, 45 min: 50% B, 47 min: 95% B, 52 min: 95% B, 55 min: 50% B, 60 min: 50% B for fraction 2 to give **6–10**. A binary solvent system of H₂O (solvent A) and MeCN (solvent B), both containing 0.1% FA, was used as follows: 0 min: 30% B, 36 min: 48% B, 38 min: 95% B, 43 min: 95% B, 45 min: 30% B, 50 min: 30% B for fraction 3 to give **11–15**; 0 min: 42% B, 40 min: 58% B, 43 min: 95% B, 48 min: 95% B, 50 min: 42% B, 55 min: 42% B for fraction 4 to afford **16–21**. Fraction 5 was separated on a Lichrospher RP18 column (5 μ m, 250 \times 4 mm; Merck KGaA, Darmstadt, Germany) with a flow rate of 0.8 ml min⁻¹. A binary solvent system of H₂O (solvent A) and MeOH (solvent B), both containing 0.1% FA, was used as follows: 0 min: 60% B, 30 min: 80% B, 35 min: 95% B, 40 min: 95% B, 43 min: 60% B, 48 min: 60% B to yield **22**. The eluate was monitored at 254 nm. SPE cartridges loaded with metabolites were dried in a stream of nitrogen. MeCN-d₃ was used to elute the analytes from the cartridges, transfer them through the connecting capillary into the CryoFIT™ flow system (30 μ l) of the NMR spectrometer, and measure ¹H and 2D NMR spectra at 300 K. The residual signals of MeCN-d₃ at δ_{1H} 1.94 and δ_{13C} 1.32 were used as chemical shift references.

5.5. LC-MS

Fractions obtained from semi-preparative HPLC were used. LC instruments and conditions for LC-MS were identical to those used for LC-DAD-SPE-NMR, except that samples were not trapped on the cartridge but directly transferred through the connecting capillary to the Esquire 3000 mass spectrometer. The eluate was split off in a ratio of 3:1 before reaching the mass spectrometer. Samples were measured in both positive and negative modes in the range m/z 150–1200 with skimmer voltage ± 33.9 V. Capillary exit voltage was ± 106.7 V, capillary voltage ∓ 4000 V, nebulizer pressure 30 psi, drying gas 12.0 l min⁻¹, and gas temperature 350 °C.

5.6. LC-HRMS

After NMR measurements, samples were flushed from the NMR flow cell and evaporated to dryness. HRMS data of compounds were recorded by LC-HRESIMS. HPLC was performed using a Dionex Acclaim C18 Column (150 \times 2.1 mm, 2.2 μ m) at a constant flow rate of 300 μ l min⁻¹. A binary solvent system of H₂O (solvent A) and MeCN (solvent B), both containing 0.1% FA, was used as follows: 0 min: 0.5% B, 10 min: 10% B, 14 min: 80% B, 19 min: 80% B, 19.1 min: 0.5% B, 25 min: 0.5% B. Capillary voltage was set to 35 V and capillary temperature of the ESI source was 275 °C. Samples were measured in positive mode using the Orbitrap analyzer. The data was acquired in full scan mode using 30,000 m/ Δ m resolving power.

5.7. 2-(1'',2''-Dicarboxyethyl)-5-hydroxy-7-phenyl-2H-benzo[de]isoquinoline-1,6-dione (**6**)

UV (measured by HPLC-DAD in MeOH-H₂O) λ_{max} 236.9, 321.2, 433.9 nm; ¹H NMR data, see Table 1, and ¹³C NMR data, see Table 2; ESIMS (negative mode): m/z 404 [M-H]⁻; ESIMS (positive mode):

m/z 428 [M+Na]⁺; HRESIMS: m/z 406.09127 [M+H]⁺ (calcd C₂₂H₁₆NO₇, 406.09268).

5.8. 3-Carboxy-5-hydroxy-6-O-malonyl-7-phenyl-3H-benzo[de]isochromen-1-one (**11**)

UV (measured by HPLC-DAD in MeCN-H₂O) λ_{max} 219.5, 252.9, 325.2, 357.1 nm; ¹H NMR data, see Table 1, and ¹³C NMR data, see Table 2; ESIMS (negative mode): m/z 421 [M-H]⁻, 843 [2 M-H]⁻; ESIMS (positive mode): m/z 445 [M+Na]⁺; HRESIMS: m/z 423.07043 [M+H]⁺ (calcd C₂₂H₁₅O₉, 423.07161).

5.9. 2-(1''-Carboxy-2''-methyl-propyl)-5-hydroxy-7-phenyl-2H-benzo[de]isoquinoline-1,6-dione (**17**)

UV (measured by HPLC-DAD in MeCN-H₂O) λ_{max} 235.9, 265.3, 322.7, 427.5 nm; ¹H NMR data, see Table 1, and ¹³C NMR data, see Table 2; ESIMS (negative mode): m/z 388 [M-H]⁻, 777 [2 M-H]⁻; ESIMS (positive mode): m/z 412 [M+Na]⁺, 801 [2 M+Na]⁺; HRESIMS: m/z 390.13339 [M+H]⁺ (calcd C₂₃H₂₀NO₅, 390.13415).

5.10. 2-(1''-Carboxy-2''-phenyl-ethyl)-5-hydroxy-7-phenyl-2H-benzo[de]isoquinoline-1,6-dione (**19**)

UV (measured by HPLC-DAD in MeCN-H₂O) λ_{max} 236.9, 322.2, 432.9 nm; ¹H NMR data, see Table 1, and ¹³C NMR data, see Table 2; ESIMS (negative mode): m/z 436 [M-H]⁻, 873 [2 M-H]⁻; ESIMS (positive mode): m/z 460 [M+Na]⁺, 897 [2 M+Na]⁺; HRESIMS: m/z 438.13301 [M+H]⁺ (calcd C₂₇H₂₀NO₅, 438.13415).

Table 2

¹³C NMR data of compounds **6**, **11**, **17**, **19** and **21** obtained by LC-DAD-SPE-NMR (125 MHz, MeCN-d₃, δ values).

Position	6	11	17	19	21
1	161.7	163.6	162.0	161.8	161.8
3	138.4	78.2	136.0	136.7	136.1
3a	ND	125.9	ND	109.4	ND
4	110.6	118.5	110.7	110.5	110.8
5	149.1	148.3	149.0	148.9	149.1
6	179.1	132.1	179.2	179.0	179.2
6a	125.2 ^a	125.9 ^a	125.0 ^a	124.8 ^b	124.8 ^b
7	151.1	142.8	151.2	151.1	151.1
8	132.6	131.7	132.6	132.7	132.8
9	133.3	127.0	133.6	133.4	133.6
9a	124.9 ^a	121.2 ^a	124.7 ^a	124.8 ^b	124.8 ^b
9b	132.9	124.5	132.8	132.7	132.8
1'	142.8	142.3	142.9	143.2	142.3
2'/6'	128.9	129.9	129.1	128.9	129.0
3'/5'	128.6	128.6	128.5	128.4	128.6
4'	128.0	128.5	128.1	128.1	128.1
1''	59.8	170.3	63.9	61.9	57.4
2''	35.7	40.0	30.4	35.8	39.2
3''	170.4	165.7	20.1	170.7	25.5
4''	172.2		19.0		21.4
5''			171.2		23.1
6''					171.4
1'''		170.5		137.6	
2'''/6'''				129.6 ^c	
3'''/5'''				129.6 ^c	
4'''				127.7	

ND, not detected.

^a Signals in the same column are exchangeable.

^b Signals with the same mark in the same column are overlapping.

^c Signals with the same mark in the same column are overlapping.

5.11. 2-(1''-Carboxy-3''-methyl-n-butyl)-5-hydroxy-7-phenyl-2H-benzof[de]isoquinoline-1,6-dione (21)

UV (measured by HPLC–DAD in MeCN–H₂O) λ_{\max} 236.4, 321.7, 433.4 nm; ¹H NMR data, see Table 1, and ¹³C NMR data, see Table 2; ESIMS (negative mode): *m/z* 402 [M–H][–], 805 [2 M–H][–]; ESIMS (positive mode): *m/z* 426 [M + Na]⁺, 829 [2 M + Na]⁺; HRESIMS: *m/z* 404.14901 [M + H]⁺ (calcd C₂₄H₂₂NO₅, 404.14980).

Acknowledgments

We thank Dr. Macro Kai for recording HRMS spectra, Dr. Renate Ellinger for technical assistance with LC–DAD–SPE–NMR and Emily Wheeler for editorial assistance. J. Fang acknowledges the International Max Planck Research School (IMPRS) for a PhD scholarship. We are also grateful for financial support from the Max Planck Society (MPG).

Appendix A. Supplementary data

Supplementary data associated with this article can be found, in the online version, at <http://dx.doi.org/10.1016/j.phytochem.2012.07.005>.

References

- Bazan, A.C., Edwards, J.M., 1976. Phenalenone pigments of flowers of *Lachnanthes tinctoria*. *Phytochemistry* 15, 1413–1415.
- Brand, S., Hölscher, D., Schierhorn, A., Svatoš, A., Schröder, J., Schneider, B., 2006. A type III polyketide synthase from *Wachendorfia thyrsiflora* and its role in diarylheptanoid and phenylphenalenone biosynthesis. *Planta* 224, 413–428.
- Buchmann, S.L., 1980. Preliminary anthecological observations on *Xiphidium caeruleum* Aubl. (Monocotyledoneae: Haemodoraceae) in Panama. *J. Kansas Entomol. Soc.* 53, 685–699.
- Cooke, R.G., Edwards, J.M., 1981. Naturally occurring phenalenones and related compounds. *Prog. Chem. Org. Nat. Prod.* 40, 153–190.
- Cooke, R.G., Thomas, R.L., 1975. Colouring matters of Australian plants. XVIII. Constituents of *Anigozanthos rufus*. *Aust. J. Chem.* 28, 1053–1057.
- Cremona, T.L., Edwards, J.M., 1974. Xiphidone, major phenalenone pigment of *Xiphidium caeruleum*. *Lloydia* 37, 112–113.
- DellaGreca, M., Previtera, L., Zarrelli, A., 2008. Revised structures of phenylphenalene derivatives from *Eichhornia crassipes*. *Tetrahedron Lett.* 49, 3268–3272.
- Dias, D.A., Goble, D.J., Silva, C.A., Urban, S.J., 2009. Phenylphenalenones from the Australian plant *Haemodorum simplex*. *J. Nat. Prod.* 72, 1075–1080.
- Dora, G., Edwards, J.M., Campbell, W., 1990. Thyrsiflorin: A novel phenalenone pigment from *Wachendorfia thyrsiflora*. *Planta Med.* 56, 569.
- Edwards, J.M., Weiss, U., 1972. Quinone methides derived from 5-oxa and 5-aza-9-phenyl-1-phenalenone in flowers of *Lachnanthes tinctoria* (Haemodoraceae). *Tetrahedron Lett.* 13, 1631–1634.
- Edwards, J.M., Weiss, U., 1974. Phenalenone pigments of the root system of *Lachnanthes tinctoria*. *Phytochemistry* 13, 1597–1602.
- Fang, J.J., Paetz, C., Hölscher, D., Munde, T., Schneider, B., 2011. Phenylphenalenones and related natural products from *Wachendorfia thyrsiflora* L. *Phytochem.* Lett. 4, 203–208.
- Fang, J.J., Kai, M., Schneider, B., 2012. Phytochemical profile of aerial parts and roots of *Wachendorfia thyrsiflora* L. studied by LC–DAD–SPE–NMR. *Phytochemistry* 81, 144–152.
- Harborne, J.B., 1967. *Comparative Biochemistry of the Flavonoids*. Academic Press, New York, NY.
- Hölscher, D., Reichert, M., Görts, H., Ohlenschläger, O., Bringmann, G., Schneider, B., 2006. Monolaterol, the first configurationally assigned phenylphenalenone derivative with a stereogenic center at C-9, from *Monochoria elata*. *J. Nat. Prod.* 69, 1614–1617.
- Hölscher, D., Schneider, B., 1997. Phenylphenalenones from root cultures of *Anigozanthos preissii*. *Phytochemistry* 45, 87–91.
- Hölscher, D., Schneider, B., 2000. Phenalenones from *Strelitzia reginae*. *J. Nat. Prod.* 63, 1027–1028.
- Hölscher, D., Schneider, B., 2005. The biosynthesis of 8-phenylphenalenones from *Eichhornia crassipes* involves a putative aryl migration step. *Phytochemistry* 66, 59–64.
- Hölscher, D., Schneider, B., 2007. Laser microdissection and cryogenic nuclear magnetic resonance spectroscopy: An alliance for cell type-specific metabolite profiling. *Planta* 225, 763–770.
- Jitsaeng, K., Schneider, B., 2010. Metabolic profiling of *Musa acuminata* challenged with *Sporobolomyces salmonicolor*. *Phytochem. Lett.* 3, 84–87.
- Kamo, T., Hirai, N., Iwami, K., Fujioka, D., Ohigashi, H., 2001. New phenylphenalenones from banana fruit. *Tetrahedron* 57, 7649–7656.
- Lazzaro, A., Corominas, M., Martí, C., Flors, C., Izquierdo, L.R., Grillo, T.A., Luis, J.G., Nonell, S., 2004. Light- and singlet oxygen-mediated antifungal activity of phenylphenalenone phytoalexins. *Photochem. Photobiol. Sci.* 3, 706–710.
- Lewis, D.A., Fields, W.N., Shaw, G.P., 1999. A natural flavonoid present in unripe plantain banana pulp (*Musa sapientum* L. var. *paradisica*) protects the gastric mucosa from aspirin-induced erosions. *J. Ethnopharmacol.* 65, 283–288.
- Luis, J.G., Echeverri, F., Quiñones, W., Brito, I., López, M., Torres, F., Cardona, G., Aguiar, Z., Pelaez, C., Rojas, M.J., 1993. Irenolone and emenolone: Two new types of phytoalexin from *Musa paradisica*. *J. Org. Chem.* 58, 4306–4308.
- Maas, P.J.M., Maas-Van de Kamer, H., 1993. *Haemodoraceae*. *Fl. Neotrop. Monogr.* 61, 1–44.
- Merh, P.S., Daniel, M., Sabnis, S.D., 1986. Chemistry and taxonomy of some members of the Zingiberales. *Curr. Sci.* 55, 835–839.
- Munde, T., Brand, S., Hidalgo, W., Maddula, R.K., Svatoš, A., Schneider, B., 2012. Biosynthesis of tetraoxygenated phenylphenalenones in *Wachendorfia thyrsiflora*. *Phytochemistry*. <http://dx.doi.org/10.1016/j.phytochem.2012.02.020>.
- Opitz, S., Hölscher, D., Oldham, N.J., Bartram, S., Schneider, B., 2002. Phenylphenalenone-related compounds: Chemotaxonomic markers of the Haemodoraceae from *Xiphidium caeruleum*. *J. Nat. Prod.* 65, 1122–1130.
- Opitz, S., Schneider, B., 2002. Organ-specific analysis of phenylphenalenone-related compounds in *Xiphidium caeruleum*. *Phytochemistry* 61, 819–825.
- Opitz, S., Schnitzler, J.-P., Hause, B., Schneider, B., 2003. Histochemical analysis of phenylphenalenone-related compounds in *Xiphidium caeruleum* (Haemodoraceae). *Planta* 216, 881–889.
- Otálvaro, F., Nanclares, J., Vázquez, L.E., Quiñones, W., Echeverri, F., Arango, R., Schneider, B., 2007. Phenalenone-type compounds from *Musa acuminata* var. “Yangambi km 5” (AAA) and their activity against *Mycosphaerella fijiensis*. *J. Nat. Prod.* 70, 887–890.
- Otálvaro, F., Jitsaeng, K., Munde, T., Echeverri, F., Quiñones, W., Schneider, B., 2010. O-Methylation of phenylphenalenone phytoalexins in *Musa acuminata* and *Wachendorfia thyrsiflora*. *Phytochemistry* 71, 206–213.
- Oyama, K.-I., Kondo, T., 2004. Total synthesis of apigenin 7,4'-di-O- β -glucopyranoside, a component of blue flower pigment of *Salvia patens*, and seven chiral analogues. *Tetrahedron* 60, 2025–2034.
- Pascual-Villalobos, M.J., Rodríguez, B., 2007. Constituents of *Musa balbisiana* seeds and their activity against *Cryptolestes pusillus*. *Biochem. Syst. Ecol.* 35, 11–16.
- Schneider, B., Paetz, C., Hölscher, D., Opitz, S., 2005. HPLC–NMR for tissue-specific analysis of phenylphenalenone-related compounds in *Xiphidium caeruleum* (Haemodoraceae). *Magn. Reson. Chem.* 43, 724–728.
- Someya, S., Yoshiki, Y., Okubo, K., 2002. Antioxidant compounds from bananas (*Musa cavendish*). *Food Chem.* 79, 351–354.
- Švehlíková, V., Bennett, R.N., Mellon, F.A., Needs, P.W., Piacente, S., Kroon, P.A., Bao, Y.P., 2004. Isolation, identification and stability of acylated derivatives of apigenin 7-O-glucoside from chamomile (*Chamomilla recutita* [L.] Rauschert). *Phytochemistry* 65, 2323–2332.
- Toki, K., Saito, N., Imura, K., Suzuki, T., Honda, T., 1994. (Delphinidin 3-gentiobiosyl) (apigenin 7-glucosyl) malonate from the flowers of *Eichhornia crassipes*. *Phytochemistry* 36, 1181–1183.
- Van Loo, P., De Bruyn, A., Buděšínský, M., 1986. Reinvestigation of the structural assignment of signals in the ¹H and ¹³C NMR-spectra of the flavone apigenin. *Magn. Reson. Chem.* 24, 879–882.
- Wang, M.-Z., Cai, X.-H., Luo, X.-D., 2011. New phenylphenalene derivatives from water hyacinth (*Eichhornia crassipes*). *Helv. Chim. Acta.* 94, 61–66.

Chapter 4

Secondary metabolites profiling and their distribution in rapeseed

- 4.1 Metabolic profiling of lignans and other secondary metabolites from rapeseed (*Brassica napus* L.). 38
- 4.2 Tissue-specific distribution of secondary metabolites in rapeseed (*Brassica napus* L.). 50

Metabolic profiling of lignans and other secondary metabolites from rapeseed (*Brassica napus* L.)

Jingjing Fang, Michael Reichelt, Marco Kai, Bernd Schneider*

Max Planck Institute for Chemical Ecology, Beutenberg Campus, Hans-Knöll Str. 8,
D-07745 Jena, Germany

ABSTRACT: A metabolic profiling study was carried out on rapeseed (*Brassica napus* L.). Eleven glucosinolates were identified by high-performance liquid chromatography coupling with diode array detection (DAD) and mass spectrometry (MS). Phenolic compounds were profiled from an ethanol extract of rapeseed. Beside two major phenols, sinapine and sinapate methyl ester, 16 minor phenolic compounds were isolated and identified, seven of which are new lignans including three (\pm)-thomasidioic acid derivatives and four (*E,E*)-dienolignan derivatives. The structures of novel phenolic compounds were elucidated by 1D and 2D nuclear magnetic resonance (NMR) spectroscopy and MS.

KEYWORDS: *Brassica napus*, *dienolignan derivatives*, *glucosinolates*, *lignans*, *rapeseed*, *sinapates*, *thomasidioic acid derivatives*

INTRODUCTION

Rapeseed (*Brassica napus* L.) is a very important oilseed in temperate regions worldwide and contributes up to 15 % of the global oleiferous production (Wolfram *et al.*, 2010). Although mainly used as an oil crop, rapeseed has a high protein and essential amino acid content which makes it both animal feed and potential human food additive. However, high levels of glucosinolates in rapeseed meal of conventional cultivars limit its nutritional value, because the decomposition products of glucosinolates are goitrogenic and hepatotoxic. Therefore, low-glucosinolate cultivars have been bred and commercially introduced, containing only 0.5-1.0 % glucosinolates. Phenolic choline esters, mainly sinapate esters, are the other major class of anti-nutritional compounds in rapeseed. The predominant one is sinapine, which is present in 1-2 % (w/w) of the rapeseed meal (Fenwick, 1982). Due to the economic importance of rapeseed and in order to investigate the consequences of genetic modifications, several studies were performed on profiling phenolic choline esters in rapeseed (Naczka *et al.*, 1998; Baumert *et al.*, 2005; Böttcher *et al.*, 2009; Wolfram *et al.*, 2010; Clauß *et al.*, 2011).

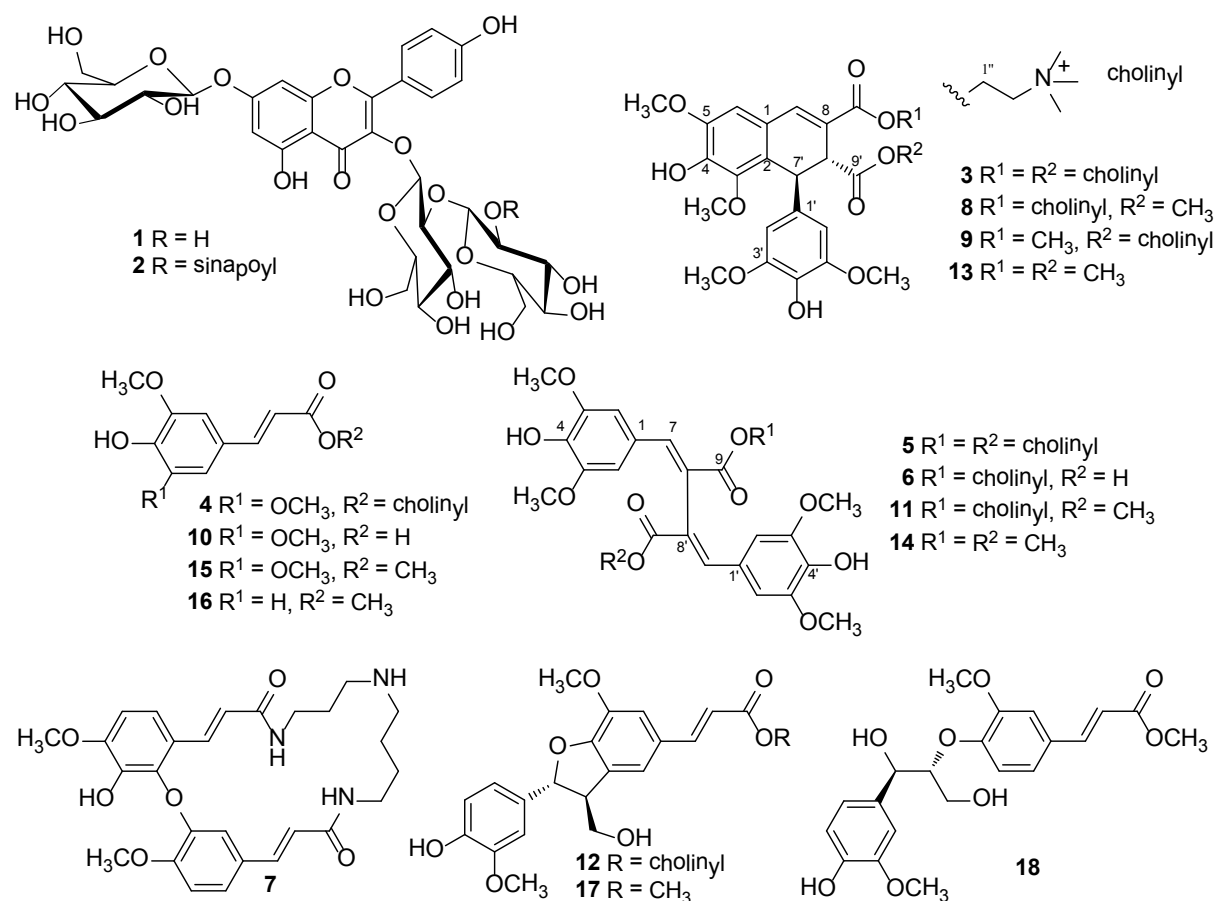


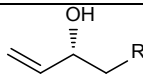
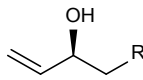
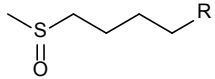
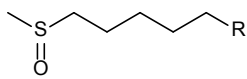
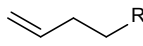
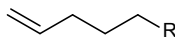
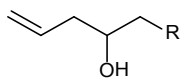
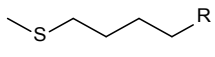
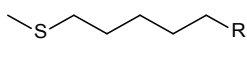
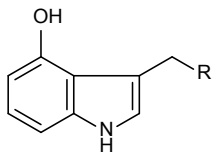
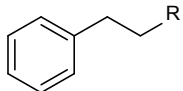
Figure 1. Structures of phenolic compounds isolated from rapeseed in this study.

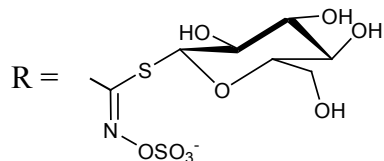
High levels of glucosinolates and sinapates, although unwanted in rapeseed-derived food and feed, may have positive physiological effects on plant development and on the protection of seeds against pathogens and the deterrence of herbivores. For example, glucosinolates, which are very important for plants as defense compounds, have been thoroughly explored during the last decade, and more than 120 glucosinolates have been identified (Halkier and Gershenzon, 2006). Sinapine, which is the choline ester of sinapic acid, was suggested to be involved in supplying choline for phosphatidylcholine in young *Raphanus sativus* seedlings (Strack, 1981). Sinapate esters, especially with phenylpropanoids, play an important role in UV protection (Landry *et al.*, 1995). Although the ecological effects of secondary metabolites of cruciferous plants have been extensively studied, information about their specific role in rapeseed is limited. The cell- and tissue-specific distribution of metabolites is one of the clues to understand their physiological and ecological importance of plants seeds. Hence, a thorough phytochemical screening of the seeds of *B. napus* (winter cultivar “Emerald”) was undertaken to assemble analytical data for subsequent localization studies of secondary metabolites in rapeseed.

Here we report the identification of eleven glucosinolates (Table 1) by high-performance liquid chromatography - diode array detection/mass spectrometry (HPLC-

DAD/MS), and purification and structure elucidation of 18 phenolic compounds (Figure 1) from rapeseed, including three new (\pm)-thomasidioic acid derivatives and four new (*E,E*)-dienolignan derivatives by means of nuclear magnetic resonance (NMR) spectroscopy and MS. The phytochemical profile and the analytical data presented here form the basis for tissue-specific localization studies, which are in progress

Table 1 Glucosinolate Structures Identified from Rapeseed in This Study

Common name	Systematic name	Structure
progoitrin	(2 <i>R</i>)-2-hydroxy-3-butenyl glucosinolate	
epiprogoitrin	(2 <i>S</i>)-2-hydroxy-3-butenyl glucosinolate	
glucoraphanin	4-methylsulfinylbutyl glucosinolate	
glucoalyssin	5-methylsulfinylpentyl glucosinolate	
gluconapin	3-butenyl glucosinolate	
glucobrassicinapin	4-pentenyl glucosinolate	
gluconapoleiferin	2-hydroxy-4-pentenyl glucosinolate	
glucoerucin	4-methylthiobutyl glucosinolate	
glucoberteroin	5-methylthiopentyl glucosinolate	
4-hydroxyglucobrassicin	4-hydroxyindol-3-ylmethyl glucosinolate	
gluconasturtiin	2-phenethyl glucosinolate	



MATERIALS AND METHODS

General experimental procedures. Glucosinolates were identified in their desulfated form with HPLC-DAD/MS by comparing the retention times and the mass data with those of references. HPLC was conducted on an Agilent series HP1100 (binary pump G1312A, autosampler G1367A, diode array detector G1315A; Agilent Technologies, Waldbronn, Germany). The chromatographic separation was performed on a LiChrospher RP18 column (5 μ m, 250 \times 4.6 mm; Merck KGaA, Darmstadt, Germany) with a guard column (5 μ m, 4 \times 4

mm) using a linear binary gradient of H₂O (solvent A) containing 0.2% (v/v) formic acid (FA) and MeCN (solvent B), with a flow rate of 1.0 ml min⁻¹ at 25 °C as follows: 0 min: 1.5% B, 1 min: 1.5% B, 6 min: 5% B, 8 min: 7% B, 18 min: 21% B, 23 min: 29% B, 23.1 min: 100% B, 24 min: 100% B, 24.1 min: 1.5% B, and 28 min: 1.5% B. The injection volume was 50 µl. The HPLC eluate was monitored by DAD at 229 nm. An Esquire 6000 ion trap mass spectrometer (Bruker Daltonics, Bremen, Germany) was coupled to the same HPLC system for recording electrospray ionization mass spectra (ESIMS). Positive ionization mode was used in the range *m/z* 60-1000.

Semi-preparative HPLC was performed on a Promonice system (LC-20AT gradient pump, SPD-20A UV/Vis detector; Shimadzu Corporation, Tokyo, Japan) using a Nucleosil 100 C₁₈ column (7 µm, 250 × 21 mm; Macherey-Nagel GmbH & Co. KG, Düren, Germany) in the first chromatographic step and a Purospher RP18e column (5 µm, 250 × 10 mm; Merck KGaA, Darmstadt, Germany) in the second step.

NMR spectra of isolated compounds were recorded on a Bruker AV 500 NMR spectrometer (Bruker Biospin, Karlsruhe, Germany), operating at 500.13 MHz for ¹H and 125.75 MHz for ¹³C. The NMR spectrometer was equipped with a TCI cryoprobe (5 mm). Standard Bruker pulse sequences were used for measuring ¹H, ¹³C, ¹H-¹H COSY, HMBC, and HSQC spectra at 298 K. Tetramethylsilane (TMS) was used as internal chemical shift reference.

LC-ESIMS of isolated phenolic compounds were recorded in positive ionization mode on a LC-ESIMS/MS system, which consists of an Agilent 1100 chromatography (quaternary solvent delivery pump G1311A, autosampler G1313A; Agilent Technologies, Waldbronn, Germany) and a Bruker Esquire 3000 ion trap mass spectrometer (Bruker Daltonics, Bremen, Germany). LC was performed on a Purospher RP18e column (5 µm, 250 × 4.6 mm; Merck KGaA, Darmstadt, Germany) at a constant flow rate of 1.0 ml min⁻¹. A binary gradient of H₂O (solvent A) and MeOH (solvent B), both containing 0.1% (v/v) formic acid (FA), was used as follows: 0 min: 20% B, 15 min: 100 % B, 20 min: 100% B, 21 min: 20% B, 25 min: 20%. UV spectra were recorded during the LC-ESIMS runs by a DAD detector (detection 200-700 nm; J&M Analytik AG, Aalen, Germany), which was integrated in the LC-ESIMS system.

LC-HRESIMS of new compounds were recorded on a LC-MS/MS system consisting of an Ultimate 3000 series RSLC system (Dionex, Sunnyvale, CA, USA), and an Orbitrap mass spectrometer (Thermo Fisher Scientific, Bremen, Germany). A Dionex Acclaim C18 column (2.2 µm, 150 × 2.1 mm; Dionex, Sunnyvale, CA, USA) was used for LC with a binary solvent system of H₂O (solvent A) and MeCN (solvent B), both containing 0.1% (v/v) FA: 0

min: 0.5 % B, 10 min: 10 % B, 14 min: 80% B, 19 min: 80% B, 19.1 min: 0.5% B, 25 min: 0.5% B; flow rate 300 $\mu\text{l min}^{-1}$. HRESIMS spectra were measured in positive ionization mode on the Orbitrap mass analyzer.

Optical rotation was recorded on a P-1030 automatic digital polarimeter (Jasco, Tokyo, Japan) at 25 °C.

Plant material. Rapeseed winter cultivar “Emerald” used in this experiment was purchased from Raps GbR (Langballig, Germany).

Metabolic profiling of glucosinolates. Methods for extracting and desulfating glucosinolates were modified from the literature (Burow *et al.*, 2006). One rapeseed (4.9 mg) was put into a 2 ml Eppendorf tube. MeOH (1 ml, 80%, v/v) and 4 metal balls (3 mm) were added to the tube; the tube was then put into a paint-shaker (Skandex SO-10m; Fluid Management, Sassenheim, The Netherlands) for 10 min. After centrifuging at 13,000 rpm for 10 min (Centrifuge 5415R; Eppendorf, Hamburg, Germany), 800 μl supernatant was added to a weak anion exchange DEAE-sephadex cartridge A25 (Sigma, Steinheim, Germany), which was conditioned with 800 μl H₂O and equilibrated with 500 μl 80% (v/v) MeOH before use. The cartridge was eluted with 500 μl 80% (v/v) MeOH, 1 ml H₂O twice and 500 μl 0.02 M MES buffer (pH 5.2), successively, after which 30 μl sulfatase (Sigma, Steinheim, Germany) solution prepared as described was added (Graser *et al.*, 2001). The cartridge was capped and incubated at ambient temperature overnight. Afterwards the cartridge was eluted with 500 μl H₂O for desulfated glucosinolate analysis.

Extraction and purification of phenolic compounds. Rapeseed (25 g) was ground in liquid N₂ and extracted with 100 ml 80 % ethanol (24 h \times 3). The combined extract was filtered and evaporated in a vacuum (<40 °C) to yield 3.24 g residue, which was dissolved in 20 ml H₂O. The aqueous solution was loaded on a Discovery DSC-18 SPE cartridge (10 g, 60 ml; Supelco, Bellefonte, PA, USA), which was conditioned with 20 ml MeCN and then equilibrated with 20 ml H₂O before being used. After the eluate of 60 ml H₂O was discarded, the eluate of 60 ml 80% MeCN aqueous solution was collected and dried <40°C in a vacuum to give 760 mg residue. The residue was fractionated on a Nucleosil 100 C₁₈ column (7 μm , 250 \times 21 mm; Macherey-Nagel GmbH & Co. KG, Düren, Germany). Flow rate was 10 ml min^{-1} ; UV detection was at 240 and 330 nm. The following linear gradient of H₂O (solvent A) containing 0.1 % (v/v) trifluoroacetic acid (TFA) and MeOH (solvent B) was applied: 0 min: 35% B, 30 min: 80% B, 32 min: 100% B, 42 min: 100% B, 45 min: 30% B, 50 min: 30%. Two fractions were collected as F1 (18.5-28.1 min) and F2 (28.1-38.0 min). Further separation of fractions F1 and F2 was performed on a Purospher RP18e column (5 μm , 250 \times 10 mm; Merck KGaA, Darmstadt, Germany) with a flow rate of 4 ml min^{-1} . H₂O (A)

containing 0.1 % (v/v) TFA and MeCN (B) was used to elute compounds **1-12** from fraction F1 as follows: 0 min: 15% B, 30 min: 25% B, 32 min: 100% B, 37 min: 100% B, 39 min: 15% B, 42 min: 15% B. H₂O (A) containing 0.1% (v/v) TFA and MeOH (B) was used to elute compounds **13-18** from F2 as follows: 0 min: 55 % B, 15 min: 65% B, 16 min: 100% B, 21 min: 100% B, 22 min: 55% B, 25 min: 55% B.

(±)-*Dicholinylnyl thomasidioate* [*dicholinylnyl* (±)-4,4'-*dihydroxy-3,3',5,5'-tetramethoxy-2,7'-cyclo lign-7-en-9,9'-dioate*] (**3**). 2.3 mg; UV (MeOH-H₂O): λ_{\max} 247.9, 340.2 nm; $[\alpha]_{\text{D}}^{25}$ 0.0 (*c* 0.1, MeOH); ¹H and ¹³C NMR data, see Table 2; ESIMS: *m/z* 309.1 [M]²⁺, HRESIMS: *m/z* 309.1568 [M]²⁺ (calcd for C₁₆H₂₃O₅N, 309.1576).

Dicholinylnyl (E,E)-4,4'-dihydroxy-3,3',5,5'-tetramethoxylign-7,7'-dien-9,9'-dioate (**5**). 0.5 mg; UV (MeOH-H₂O): λ_{\max} 243.4, 338.7 nm; ¹H and ¹³C NMR data, see Table 3; ESIMS: *m/z* 309.1 [M]²⁺, HRESIMS: *m/z* 309.1566 [M]²⁺ (calcd for C₁₆H₂₃O₅N, 309.1576).

Cholinylnyl hydrogen (E,E)-4,4'-dihydroxy-3,3',5,5'-tetramethoxylign-7,7'-dien-9,9'-dioate (**6**). 3.5 mg; UV (MeOH-H₂O): λ_{\max} 240.9, 330.7 nm; ¹H and ¹³C NMR data, see Table 3; ESIMS: *m/z* 532.4 [M]⁺, HRESIMS: *m/z* 532.2169 [M]⁺ (calcd for C₂₇H₃₄O₁₀N, 532.2183).

9-Cholinylnyl-9'-methyl (±)-*thomasidioate* [*9-cholinylnyl-9'-methyl* (±)-4,4'-*dihydroxy-3,3',5,5'-tetramethoxy-2,7'-cyclo lign-7-en-9,9'-dioate*] (**8**). 0.32 mg (calculated from integrals of ¹H NMR signals in the isolated mixture of **8** and **9**); UV (MeOH-H₂O): λ_{\max} 248.4, 337.7 nm; $[\alpha]_{\text{D}}^{25}$ 0.0 (*c* 0.05, MeOH); ¹H and ¹³C NMR data, see Table 2; ESIMS: *m/z* 546.5 [M]⁺, HRESIMS: *m/z* 546.2314 [M]⁺ (calcd for C₂₈H₃₆O₁₀N, 546.2339).

9-methyl-9'-cholinylnyl (±)-*thomasidioate* [*9-methyl-9'-cholinylnyl* (±)-4,4'-*dihydroxy-3,3',5,5'-tetramethoxy-2,7'-cyclo lign-7-en-9,9'-dioate*] (**9**). 0.28 mg (calculated from integrals of ¹H NMR signals in the isolated mixture of **8** and **9**); UV (MeOH-H₂O): λ_{\max} 248.4, 337.7 nm; $[\alpha]_{\text{D}}^{25}$ 0.0 (*c* 0.05, MeOH); ¹H and ¹³C NMR data, see Table 2; ESIMS: *m/z* 546.5 [M]⁺, HRESIMS: *m/z* 546.2314 [M]⁺ (calcd for C₂₈H₃₆O₁₀N, 546.2339).

Cholinylnyl methyl (E,E)-4,4'-dihydroxy-3,3',5,5'-tetramethoxylign-7,7'-dien-9,9'-dioate (**11**). 3.5 mg; UV (MeOH-H₂O): λ_{\max} 241.9, 337.7 nm; ¹H and ¹³C NMR data, see Table 3; ESIMS: *m/z* 546.5 [M]⁺, HRESIMS: *m/z* 546.2333 [M]⁺ (calcd for C₂₈H₃₆O₁₀N, 546.2339).

Dimethyl (E,E)-4,4'-dihydroxy-3,3',5,5'-tetramethoxylign-7,7'-dien-9,9'-dioate (**14**). 1.7 mg; UV (MeOH-H₂O): λ_{\max} 240.4, 329.7 nm; ¹H and ¹³C NMR data, see Table 3; ESIMS: *m/z* 497.2 [M+23]⁺, 475.1 [M+1]⁺, HRESIMS: *m/z* 475.1600 [M+1]⁺ (calcd for C₂₄H₂₇O₁₀, 475.1604).

Table 2. ^1H NMR (500 MHz) and ^{13}C NMR (125 MHz) Data of Compounds **3**, **8**, **9** and **13** (CD_3OD)

Position	3		8		9		13	
	δ_{H} (J, Hz)	δ_{C}	δ_{H} (J, Hz)	δ_{C}	δ_{H} (J, Hz)	δ_{C}	δ_{H} (J, Hz)	δ_{C}
1		123.93		124.01		124.04		124.24
2		125.00		125.05		125.10		124.92
3		146.74		146.92		146.82		146.85
4		144.31		144.14		143.91		143.61
5		149.71		149.59		149.56		149.42
6	6.98 (s)	109.60	6.94 (s)	109.56	6.92 (s)	109.42	6.89 (s)	109.38
7	7.81 (s)	141.05	7.78 (s)	140.89	7.73 (s)	139.86	7.70 (s)	139.62
8		133.91		134.39		134.17		134.64
9		167.20		167.28		168.85		168.93
3-OCH ₃	3.52 (s)	60.83	3.58 (s)	60.81	3.55 (s)	60.79	3.58 (s)	60.80
5-OCH ₃	3.93 (s)	56.83	3.924 (s)	56.80	3.919 (s)	56.82	3.91 (s)	56.78
9-COOCH ₃					3.75 (s)	52.56	3.73 (s)	52.44
1''	4.62 (br t)	59.37	4.62 (br s)	59.24				123.16
2''	3.74 (t, 4.8)	66.08	3.73 (t, 4.7)	66.14				105.77
N''-CH ₃	3.18 (s)	54.34	3.18 (s)	54.34				149.06
1'		121.81		122.22		122.61		135.37
2'/6'	6.23 (s)	105.96	6.26 (s)	105.87	6.29 (s)	105.87	6.28 (s)	105.77
3'/5'		149.20		149.16		149.12		149.06
4'		135.76		135.55		135.63		135.37
7'	5.06 (br s)	40.47	5.01 (br s)	40.78	5.02 (br s)	40.66	4.97 (br s)	40.88
8'	4.07 (d, 1.3)	48.39	3.99 (d, 1.4)	48.33	4.05 (d, 1.4)	48.08	3.97 (d, 1.4)	48.11
9'		172.55		174.02		172.67		174.19
3'/5'-OCH ₃	3.69 (s)	56.76	3.69 (s)	56.69	3.70 (s)	56.71	3.69 (s)	56.64
9'-COOCH ₃			3.64 (s)	53.01			3.62 (s)	52.92
1'''	4.52 (br m)	59.95			4.51 (br m)	59.80		
2'''	3.67 (m)	65.96			3.64 (t, 4.6)	65.99		
N'''-CH ₃	3.12 (s)	54.34			3.11 (s)	54.34		

Table 3. ^1H NMR (500 MHz) and ^{13}C NMR (125 MHz) Data of Compounds **5**, **6**, **11** and **14** (CD_3OD)

Position	5		6		11		14	
	δ_{H} (J, Hz)	δ_{C}	δ_{H} (J, Hz)	δ_{C}	δ_{H} (J, Hz)	δ_{C}	δ_{H} (J, Hz)	δ_{C}
1		126.2		126.6		126.3 ^a		126.7
2/6	6.99 (s)	109.1	6.97 (s)	109.1	6.94 (s)	109.0	6.88 (s)	108.7
3/5		149.4		149.3		149.3		149.1
4		140.2		139.6		139.6		139.1
7	8.00 (s)	145.9	7.95 (s)	145.8	7.95 (s)	146.0	7.85 (s)	144.2
8		124.0		124.7		124.2		125.6
9		167.9		168.2		168.0		169.5
3/5'-OCH ₃	3.76 (s)	56.8	3.75 (s)	56.7	3.75 (s)	56.7	3.74 (s)	56.6
9'-COOCH ₃							3.69 (s)	52.9
1''	4.57 (m)	59.8	4.57 (m)	59.7	4.56 (m)	59.7		
2''a	3.63 (m)	66.0	3.64 (m)	66.0	3.62 (dd, 6.7, 3.2)	66.0		
2''b	3.54 (m)		3.58 (m)		3.56 (dd, 6.2, 3.2)			
N''-CH ₃	3.04 (s)	54.3	3.08 (s)	54.3	3.06 (s)	54.3		
1'		126.2		126.5		126.4 ^a		126.7
2'/6'	6.99 (s)	109.1	6.92 (s)	108.8	6.93 (s)	108.9	6.88 (s)	108.7
3'/5'		149.4		149.2		149.2		149.1
4'		140.2		139.4		139.8		139.1
7'	8.00 (s)	145.9	7.90 (s)	143.9	7.89 (s)	144.2	7.85 (s)	144.2
8'		124.0		125.8		125.2		125.6
9'		167.9		170.5		169.4		169.5
3'/5'-OCH ₃	3.76 (s)	56.8	3.76 (s)	56.7	3.75 (s)	56.7	3.74 (s)	56.6
9'-COOCH ₃					3.71 (s)	53.0	3.69 (s)	52.9
1'''	4.57 (m)	59.8						
2'''a	3.63 (m)	66.0						
2'''b	3.54 (m)							
N'''-CH ₃	3.04 (s)	54.3						

^a Values in the same column may be interchanged.

RESULTS AND DISCUSSION

Glucosinolate profiling. Glucosinolates were determined in the desulfated form by comparing their MS data and retention times with those of references. A total of eleven glucosinolates were identified. The majority of them, except 4-hydroxyglucobrassicin and gluconasturtiin, are aliphatic glucosinolates (progoitrin, epiprogoitrin, glucoraphanin, gluconapoleiferin, glucoalyssin, gluconapin, glucobrassicinapin, glucoerucin, glucoberteroin) (Table 1).

Isolation of phenolic compounds. From the ethanol extract of 25 g rapeseed, 18 phenolic compounds were isolated and identified, including three new (\pm)-thomasidioic acid derivatives **3**, **8** and **9**, and four new (*E,E*)-dienolignan derivatives **5**, **6**, **11** and **14**. In addition, for the first time compound **18** was isolated as a natural product.

(\pm)-Thomasidioic acid derivatives. Four (\pm)-thomasidioic acid derivatives, namely compounds **3**, **8**, **9**, and **13**, were isolated from rapeseed extract and identified by NMR, MS, and optical rotation data. Compound **13** (NMR data in Table 2 for comparison with data of **3**, **8**, and **9**) was elucidated as (\pm)-thomasidioic acid dimethyl ester by comparing the analytical data with those reported for the synthetic product (Ahmed *et al.*, 1973).

The singlets at δ 7.81 (H-7), 6.98 (H-6) and 6.23 (2H, H-2'/6') in the aromatic range of the ^1H NMR spectrum of compound **3** (Table 2), two doublets at δ 5.06 (H-7') and 4.07 (H-8') with a coupling constant of $J = 1.3$ Hz, and four *O*-methyl signals at δ 3.93 (8-OCH₃), 3.69 (3'/5'-OCH₃) and 3.52 (3-OCH₃) resemble the ^1H NMR spectrum of **13** and therefore were attributed to the lignan part of the molecule. In addition, the spectrum displays two broad signals at δ 4.62 (H₂-1'') and 4.52 (H₂-1'''), a triplet at δ 3.74 (H₂-2''), a multiplet at δ 3.67 (H₂-2'''), and two singlets, each integrating for nine protons at δ 3.18 and 3.12 assignable to N-CH₃ groups. These ^1H NMR data suggest two choline moieties in compound **3**. The ^{13}C NMR spectrum displays signals of two choline ester moieties with identical (N''/N'''-CH₃, δ 54.34) or slightly different (C-1'' and C-1''', C-2'' and C-2''') chemical shifts (Table 2), signals of two phenylpropanoids (two C₉ units), as well as four phenolic *O*-methyl groups (two of them, C-3'/5', δ 56.76, are equivalent). Heteronuclear single-quantum correlation (HSQC) and heteronuclear multiple-bond correlation (HMBC) data were used to assign all proton and carbon signals (Table 2). The connection positions of two phenylpropanoid moieties were determined by the key correlations of H-7 (δ 7.81) with C-2 (δ 125.00) and C-8' (δ 48.39); H-8' (δ 4.07) with C-9 (δ 167.20), C-7 (δ 141.05), C-2 (δ 125.00) and C-1' (δ 121.81); H-7' (δ 5.06) with C-8 (δ 133.91), C-1 (δ 123.93), C-3 (δ 146.74), C-9' (δ 172.55), C-2'/6' (δ 105.96) in the HMBC spectrum (Figure 2A), confirming the constitution of compound **3** as an arylnaphthalene lignan derivative. The small coupling constant of $J_{\text{H-7'-H-8'}} = 1.3$ Hz was

consistent with a *trans* (diaxial) configuration of the syringyl ring at C-7' and the choline ester substituent at C-8' as proposed by Wallis (Wallis, 1968). No optical activity was observed, indicating that compound **3** is racemic. Hence, the structure was elucidated as dicholinylnyl (\pm)-thomasidioate [dicholinylnyl (\pm)-4,4'-dihydroxy-3,3',5,5'-tetramethoxy-2,7'-cyclo lign-7-en-9,9'-dioate] (Figure 1), which is further confirmed by LC-ESIMS and LC-HRESIMS.

Despite many efforts, compounds **8** and **9** could not be separated by HPLC. Therefore, the structures of the two compounds were elucidated from the NMR spectra of the mixture. The signals in the ^1H NMR spectrum showed two sets of signals (Table 2), which were readily distinguished by means of their integral values (ratio **8** : **9** = 8 : 7). Furthermore, NMR spectra of the two compounds are highly similar to those of compounds **3** and **13**. 2D NMR data (^1H , ^1H COSY, HSQC, HMBC) suggest the two compounds are also (\pm)-thomasidioate derivatives (Figure 2A). In addition to the thomasidioate signals, ^1H and ^{13}C NMR spectra from each of the two compounds display signals of one *O*-methyl group and one cholinylnyl moiety. The HMBC correlations of H₂-1'' (δ 4.62) with C-9 (δ 167.28) and COOCH₃ (δ 3.64) with C-9' (δ 174.02) assign the choline ester to position 9 and methyl ester to position 9' in **8**. In contrast, in compound **9**, the choline ester moiety is attached to C-9' (δ 172.67) and the methyl ester to position 9 (δ 168.85), as inferred from their HMBC correlations with H₂-1''' (δ 4.51) and COOCH₃ (δ 3.75), respectively. Thus, compounds **8** and **9** are isomers, a fact which was confirmed by their ESIMS and HRESIMS data, and their structures were elucidated as 9-cholinylnyl-9'-methyl (\pm)-thomasidioate [9-cholinylnyl-9'-methyl (\pm)-4,4'-dihydroxy-3,3',5,5'-tetramethoxy-2,7'-cyclo lign-7-en-9,9'-dioate] (**8**) and 9-methyl-9'-cholinylnyl (\pm)-thomasidioate [9-methyl-9'-cholinylnyl (\pm)-4,4'-dihydroxy-3,3',5,5'-tetramethoxy-2,7'-cyclo lign-7-en-9,9'-dioate] (**9**).

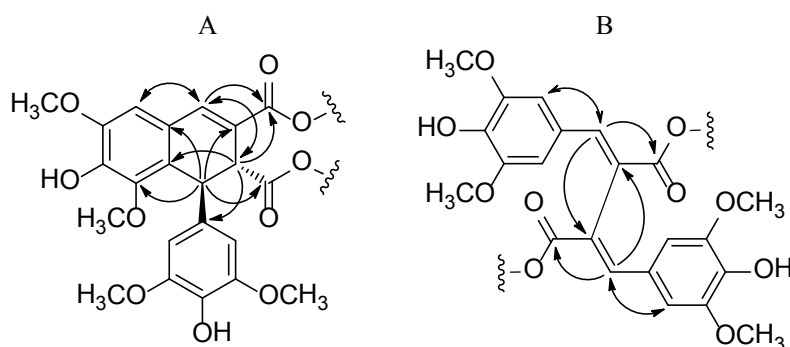


Figure 2. Selected HMBC correlations of (\pm)-thomasidioic acid derivatives **3**, **8**, **9**, **13** (A) and (*E,E*)-dienolignan derivatives **5**, **6**, **11**, **14** (B).

(*E,E*)-dienolignan derivatives. The ^1H NMR spectrum of compound **5** (Table 3) shows an *O*-methyl singlet at δ 3.76 (12H), and singlets at δ 8.00 (2H, H-7/7') and δ 6.99 (4H, H-2/6/2'/6'), assignable to the protons attached to the double bond and in the aromatic ring, respectively. Another series of signals, representing choline moieties, appears at δ 4.57 (4H,

H-1''/1'''), 3.63 (2H, H-2''a/2''a), 3.54 (2H, H-2''b/2''b) and 3.04 (18H, N''/N''-CH₃). The signals in the ¹H NMR spectrum of **5** resemble those of sinapine, except the missing signal of the olefinic H-8 and decoupling of the other olefinic proton, H-7. The lack of H-8, together with ESIMS and HRESIMS data, suggested a dimer, consisting of two sinapine units connected through a C-8/8' carbon-carbon bond. The downfield shift of C-8 from δ 114.7 in the ¹³C NMR spectrum of sinapine to δ 124.0 in the spectrum of compound **5** also supported the connection through C-8/8'. The *E* configuration of the two double bonds was established by comparing the chemical shifts of the olefinic protons with those of reported compounds (Heller and Swinney, 1967; Zhang *et al.*, 1998). Finally, **5** was elucidated as dicholinylnyl (*E,E*)-4,4'-dihydroxy-3,3',5,5'-tetramethoxylign-7,7'-dien-9,9'-dioate.

The ¹H NMR spectrum of compound **6** (Table 3) displays four singlets at δ 7.95 (H-7), 7.90 (H-7'), 6.97 (H-2/6) and 6.92 (H-2'/6'), two *O*-methyl group signals at δ 3.75 (3/5-OCH₃) and 3.76 (3'/5'-OCH₃), a series of choline moiety signals at δ 4.57 (H₂-1''), 3.64 (H-2''a), 3.58 (H-2''b) and 3.08 (N''-CH₃). The proton and carbon signals (Table 3) were assigned by analyzing connections in the HSQC and HMBC spectra, from which a sinapine moiety and a sinapic acid moiety were deduced. Mutual correlations between H-7 and C-8' and H-7' and C-8 in the HMBC spectrum (Figure 2B) indicated a connection between the two sinapoyl units through a carbon-carbon bond between C-8 and C-8'. Therefore, the structure of compound **6** was elucidated as cholinylnyl hydrogen (*E,E*)-4,4'-dihydroxy-3,3',5,5'-tetramethoxylign-7,7'-dien-9,9'-dioate, which was confirmed by ESIMS and HRESIMS.

The ¹H NMR spectrum of compound **11** (Table 3) highly resembles that of **6**, except there is an additional *O*-methyl signal at δ 3.71 in the spectrum of **11**. Compound **11** was deduced as a dimer of sinapine and sinapate methyl ester, compounds which are connected through a carbon-carbon bond between C-8 and C-8'. The ¹H and ¹³C NMR signals (Table 3) and the ESIMS and HRESIMS data confirmed the structure of **11** as cholinylnyl methyl (*E,E*)-4,4'-dihydroxy-3,3',5,5'-tetramethoxylign-7,7'-dien-9,9'-dioate.

The ¹H NMR spectrum of the symmetric compound **14** displays only four singlets, which were assigned to H-7/7' (2H, δ 7.85), H-2/6/2'/6' (4H, δ 6.88), the *O*-methyl signals at δ 3.74 (12H) and δ 3.69 (6H). The ¹³C NMR spectrum shows nine signals, all of which were readily assigned by the analyses of HSQC and HMBC (Figure 2B) spectra. The HRESIMS data suggest a formula C₂₄H₂₆O₁₀. Thus, the structure was determined as a dimer of two sinapate methyl ester units, which are connected to each other through positions 8/8', and named dimethyl (*E,E*)-4,4'-dihydroxy-3,3',5,5'-tetramethoxylign-7,7'-dien-9,9'-dioate.

Known phenolic compounds. Known compounds were determined by comparing their 1D and 2D NMR spectra and MS data with those of corresponding compounds in the

literature as kaempferol-3-*O*- β -D-glucopyranosyl-(1 \rightarrow 2)- β -D-glucopyranoside-7-*O*- β -D-glucopyranoside (**1**) (Kim *et al.*, 2002), kaempferol-3-*O*-(2-*O*-sinapoyl)- β -D-glucopyranosyl-(1 \rightarrow 2)- β -D-glucopyranoside-7-*O*- β -D-glucopyranoside (**2**) (Jung *et al.*, 2009), sinapine (**4**) (Sakushima *et al.*, 1995), a cyclic spermidine conjugate (**7**) (Baumert *et al.*, 2005), sinapic acid (**10**) (Salum *et al.*, 2010), 3-[2,3-dihydro-2-(4-hydroxy-3-methoxyphenyl)-3-(hydroxymethyl)-7-methoxy-5-benzofuranyl]-(2*Z*)-acrylic acid choline ester (**12**) (Böttcher *et al.*, 2008; Böttcher *et al.*, 2009), (\pm)-thomasidioic acid dimethyl ester (**13**) (Ahmed *et al.*, 1973), sinapate methyl ester (**15**) and ferulic acid methyl ester (**16**) (Yao *et al.*, 2006), 3-[2,3-dihydro-2-(4-hydroxy-3-methoxyphenyl)-3-(hydroxymethyl)-7-methoxy-5-benzofuranyl]-(2*Z*)-acrylic acid methyl ester (**17**) (Fukuyama *et al.*, 1986) and 4-[2-hydroxy-2-(4-hydroxy-3-methoxyphenyl)-1-(hydroxymethyl)ethyl]-ferulic acid methyl ester (**18**) (Helm and Ralph, 1992), a synthetic model compound.

Conclusion. In total, 11 glucosinolates and 18 phenolic compounds were identified from rapeseed. All the glucosinolates detected in this study had previously been found from rapeseed. In addition to eight new natural products (**3**, **5**, **6**, **8**, **9**, **11**, **14** and **18**), compounds **13** and **17** were reported from rapeseed for the first time. The acquired information about purification and structures of secondary metabolites in rapeseed is useful for further tissue-specific detection of these compounds.

AUTHOR INFORMATION

Corresponding author

* Tel: +49 3641 571600. Fax: +49 3641 571601. E-mail: schneider@ice.mpg.de (B. Schneider)

Funding

This work was supported by the Max Planck Society (MPG). J. Fang was financed a PhD scholarship by the International Max Planck Research School (IMPRS).

ACKNOWLEDGMENTS

The authors acknowledge Stefan Bartram for the help with the polarimeter and Emily Wheeler for editorial assistance.

Tissue-specific distribution of secondary metabolites in rapeseed (*Brassica napus* L.)

Jingjing Fang, Michael Reichelt, William Hidalgo, Sara Agnolet, Bernd Schneider*

Max Planck Institute for Chemical Ecology, Beutenberg Campus, Hans-Knöll Str. 8,
D-07745 Jena, Germany

*Corresponding author. Tel.: +49 3641 571600; fax: +49 3641 571601.

E-mail address: schneider@ice.mpg.de (B. Schneider)

ABSTRACT

Four different parts, hypocotyl and radicle (HR), inner cotyledon (IC), outer cotyledon (OC), seed coat and endosperm (SE), were sampled from mature rapeseed (*Brassica napus*) by laser microdissection. Subsequently, major secondary metabolites, glucosinolates and sinapine, as well as three minor ones, a cyclic spermidine conjugate and two flavonoids, representing different compound categories, were qualified and quantified in dissected samples by high-performance liquid chromatography with diode array detection and mass spectrometry. No qualitative and quantitative difference of glucosinolates and sinapine was detected in embryo tissues (HR, IC and OC). On the other hand, the three minor compounds were observed to be distributed unevenly in different rapeseed tissues. The hypothetical biological functions of the distribution patterns of different secondary metabolites in rapeseed are discussed.

INTRODUCTION

Seeds, the reproductive organs of plants, generally consist of seed coat, endosperm and embryo. Seed coats protect seeds during dormancy; endosperms normally provide nutrients during germination and, in the initial growth phase of the developing seedling; while embryos, which consist of cotyledons, hypocotyl and radicle, develop into different organs of the seedlings. According to the requirements of different physiological processes, nutrients and other metabolites are distributed and deposited in various seed organs. The embryo -- which in the case of rapeseed (*Brassica napus* L.) refers especially to the cotyledons -- is a storage site for lipids. In rapeseed, the oil contents reach approximately 40% (w/w), making rape a major oil crop; worldwide it contributes up to 15 % of global oil production (Wolfram *et al.*, 2010). Glucosinolates, which account for 3-8 % of the rapeseed meal of conventional cultivars and 0.5-1.0 % of low-glucosinolate cultivars, may have a depot function for nitrogen, as cyanogenic glucosides do (Bones and Rossiter, 1996). Phenolic choline esters, mainly sinapate choline esters, are the other major class of secondary metabolites in rapeseed. Sinapine, the choline ester of sinapic acid, is the predominant compound of that type,

constituting 1-2 % (w/w) of the rapeseed meal (Fenwick, 1982). Although the sinapine biosynthesis pathway has been well investigated in Brassicaceae plants (Milkowski and Strack, 2010), the biological functions of sinapate choline esters are barely known. Sinapine was thought to be stored in *Raphanus sativus* seeds as a supply of choline, a compound that aids phosphatidylcholine biosynthesis in young seedlings (Strack, 1981). From a nutritional point of view, the presence of the major secondary metabolites, glucosinolates and sinapates, are unwanted because of their antinutritive properties (Nesi *et al.*, 2008). However, these compounds are very important for helping plants adapt to their biotic and abiotic environments (Wink, 2003; Hartmann, 2007), and in plants different classes of secondary metabolites play specific ecological functions.

The glucosinolate-myrosinase system found in rape and other Brassicales is one of the best-explored plant chemical defense systems against herbivores (Winde and Wittstock, 2011). Glucosinolate-derived indolics are also involved in antifungal defense (Bednarek *et al.*, 2009). Flavonoids, sinapates and other phenolics have been found in rapeseed and protect plants from ultraviolet-B (UV-B) stress (Li *et al.*, 1993; Landry *et al.*, 1995; Li *et al.*, 2010). Because different classes of secondary metabolites possess individual biological functions, it is reasonable to speculate that diverse secondary metabolites in rapeseed accumulate separately in specific tissues and play different roles in physiological processes or ecological interactions.

A recent study, in which laser microdissection (LMD) was successfully used to harvest specific tissues from developing rapeseed (Schiebold *et al.*, 2011), encouraged us to apply LMD to sample different tissues of mature rapeseed and map the distribution of diverse secondary metabolites in the seed tissues. Insights gained from understanding how secondary metabolites are distributed in rapeseed can help us to conceive the biosynthesis and function of these metabolites in the plant.

LMD has been successfully used to harvest specific tissues or cells from plant material for transcript and protein analyses (Hölscher and Schneider, 2008; Nelson *et al.*, 2008), and micro-spatial metabolic profiling studies (Hölscher and Schneider, 2007; Li *et al.*, 2007; Nakashima *et al.*, 2008; Obel *et al.*, 2009; Abbott *et al.*, 2010). In this study, LMD was used to sample four different parts, namely, hypocotyl and radicle (HR), inner cotyledon (IC), outer cotyledon (OC), seed coat and endosperm (SE) (Figure 1) from mature rapeseed. Secondary metabolites of different classes found in rapeseed cv. “Emerald,” namely glucosinolates, sinapine, a cyclic spermidine conjugate and flavonoids (manuscript 4.1), were quantified in the extracts of dissected tissues by high-performance liquid chromatography - diode array detection and mass spectrometry (HPLC-DAD/MS). Here we report the distribution patterns

of the above secondary metabolites in different rapeseed tissues and discuss their potential physiological and ecological relevance.

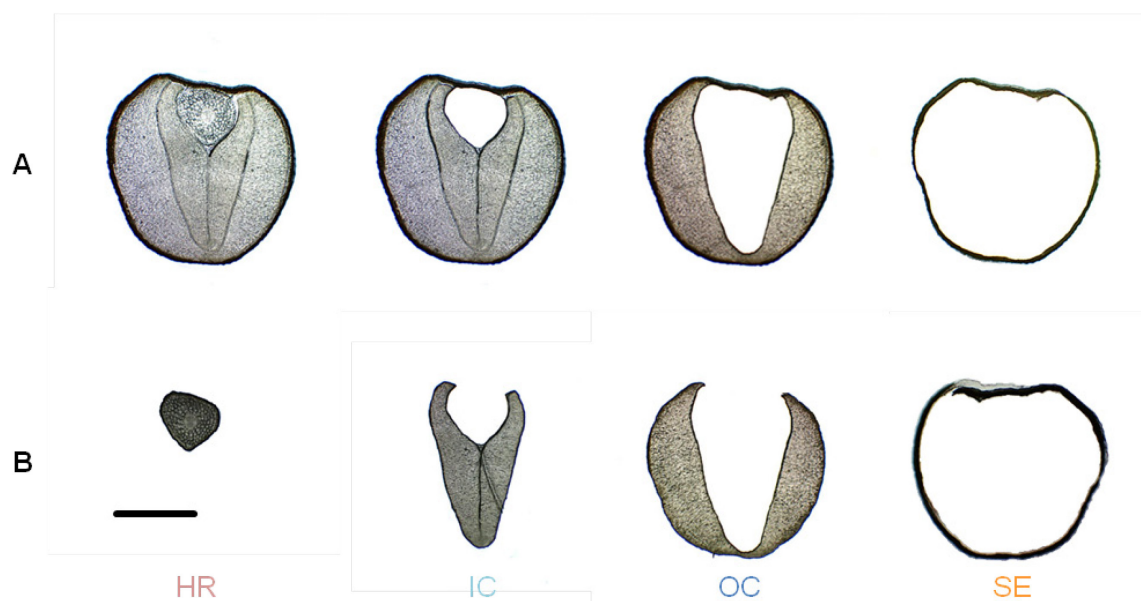


Figure 1. Work flow of laser microdissection of rapeseed. (A) Progress of laser microdissection workflow applied to rapeseed. Hypocotyl and radicle (HR), inner cotyledon (IC), outer cotyledon (OC), seed coat and endosperm (SE) were successively dissected from rapeseed. (B) Micrographs of dissected tissues. Bar represents 1 mm.

RESULTS AND DISCUSSION

Laser microdissection of rapeseed

The progress of LMD workflow applied to rapeseed is shown in Figure 1A. Four tissue parts, hypocotyl and radicle (HR), inner cotyledon (IC), outer cotyledon (OC), seed coat and endosperm (SE) (Figure 1B), were successively dissected from rapeseed cryosections and collected for analysis. HR, IC, and OC constitute the rapeseed embryo, and SE is material from the seed hull. The sampling was performed on four individual seeds. The weights of the four parts from each seed are listed in Table 1. The weights include the supporting polyethylene terephthalate (PET) membrane of the frame slide, which was unavoidably cut along with the seed tissues. The dissected materials were prepared for further analysis according to procedures described in the Materials and methods section.

Table 1. Weights (mg) of laser microdissected samples¹ obtained from four individual seeds. HR: hypocotyl and radicle; IC, inner cotyledon; OC, outer cotyledon; SE, seed coat and endosperm.

Seed	HR	IC	OC	SE
1	0.50	1.19	2.05	0.69
2	0.46	1.11	1.59	0.57
3	0.64	1.00	1.43	0.57
4	0.58	0.98	1.39	0.47

¹ The samples include the supporting polyethylene terephthalate (PET) membrane of frame slides, which was cut together with the seed material.

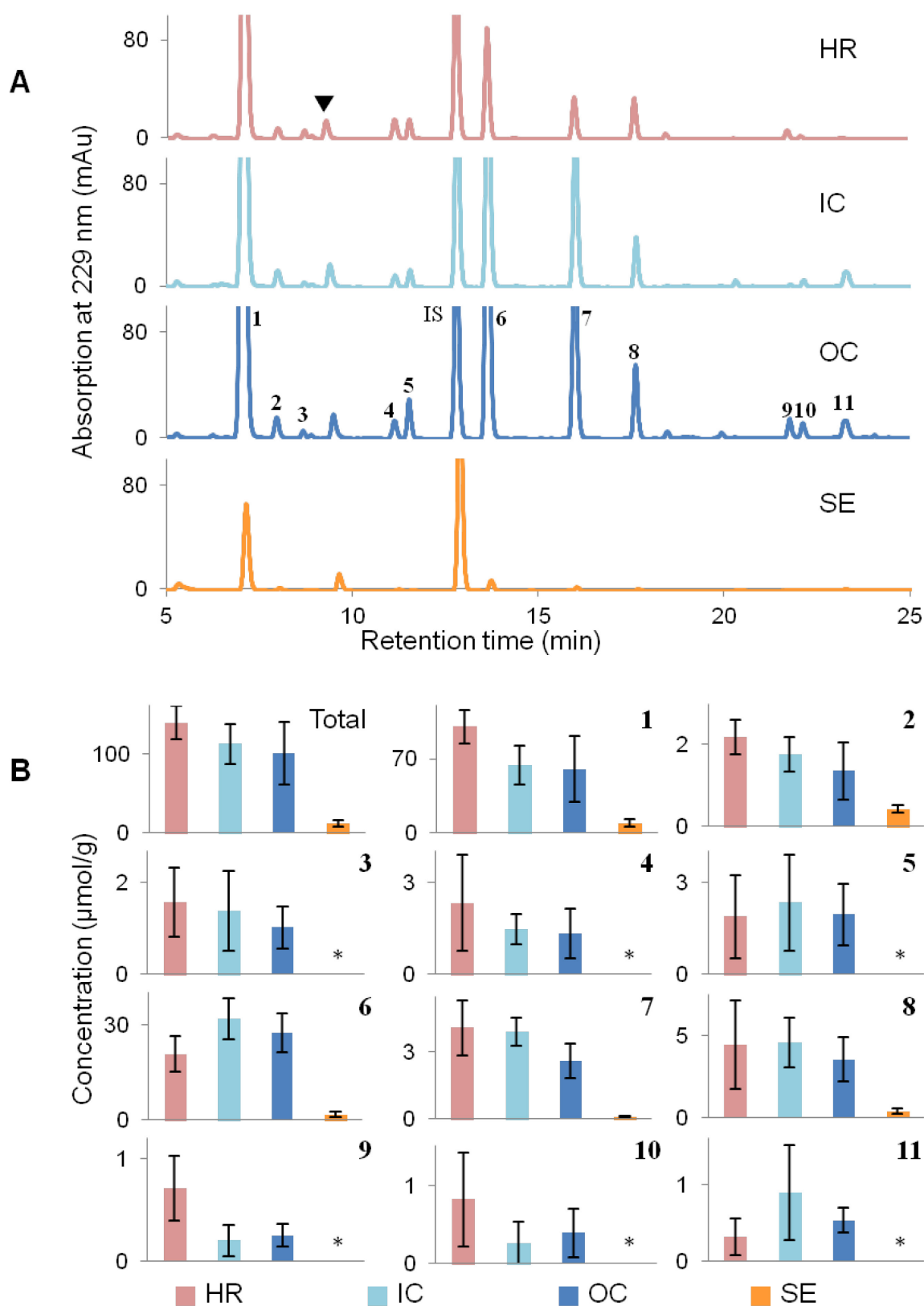


Figure 2. glucosinolate profiles and distribution in different rapeseed tissues. (A) HPLC chromatograms of glucosinolate profiling in laser-microdissected samples from rapeseed detected at 229 nm. \blacktriangledown contamination peaks. (B) Total glucosinolate concentration and concentrations of individual glucosinolates 1 – 11 in four dissected samples. HR, hypocotyl and radicle; IC, inner cotyledon; OC, outer cotyledon; and SE, seed coat and endosperm. Each column shows the mean of four replicates with standard error. * means not detectable. Peaks: 1, progoitrin; 2, epiprogoitrin; 3, glucoraphanin; 4, gluconapoleiferin; 5, glucoalyssin; 6, gluconapin; 7, 4-hydroxyglucobrassicin; 8, glucobrassicinapin; 9, glucoerucin; 10, glucoberteroin; and 11, gluconasturtiin.

Glucosinolates in rapeseed

Glucosinolates were determined in their desulfated form by HPLC-DAD/MS at 229 nm. Figure 2A shows chromatograms of the extracts of four seed tissues, HR, IC, OC and SE, dissected from rapeseed. Altogether, 11 desulfated glucosinolates, which have been recently identified in the “Emerald” cultivar of rapeseed (manuscript 4.1), were determined by comparing MS data and retention times with those of references. The concentrations of identified glucosinolates (Figure 2B) from different seed tissues were calculated relative to the internal standard sinalbin. The concentration of glucosinolates in this cultivar is relatively high. Total glucosinolate concentrations in embryo tissues (HR, IC and OC) are higher than 100 $\mu\text{mol/g DW}$, and they are not statistically different between embryo tissues. Progoitrin (**1**) and gluconapin (**6**) are the predominant glucosinolates in this cultivar as they are in other rapeseed cultivars (El-Din Saad El-Beltagi and Amin Mohamed, 2010). In the three embryo parts (HR, IC and OC), glucosinolate profiles are the same, and the individual glucosinolate concentrations are not significantly different. The concentrations of detected glucosinolates in SE samples are significantly lower than those in embryo tissues. Glucosinolates, glucoraphanin (**3**), gluconapoleiferin (**4**), glucoalyssin (**5**), glucoerucin (**9**), glucoberteroin (**10**) and gluconasturtiin (**11**) could not be detected in SE tissues, probably because of the very small amounts of dissected material available for analysis (Table 1), and the SE tissue is dominated by a hard seed coat. Glucosinolates of brassicaceous plants are well-known defense compounds, effective against herbivores and pathogens (Bednarek *et al.*, 2009; Winde and Wittstock, 2011). The evenly distributed glucosinolates in HR, IC and OC seem to provide protection for the entire embryo and, during germination, may help defend the emerging seedling.

Sinapine in rapeseed

Sinapine (**12**), the choline ester of sinapic acid, represents the dominant phenolic compound in rapeseed (Figure 3A). The concentration of sinapine in four tested seeds of the “Emerald” cultivar averaged 20.36 $\mu\text{mol/g}$. Average sinapine concentrations (Figure 3B) found in three embryo tissues (HR, IC and OC) are close to each other, and all of them are higher than 22 $\mu\text{mol/g}$. The concentration detected in SE (0.72 $\mu\text{mol/g}$) is significantly lower than that in the embryo tissues. This finding is in accordance with the reported occurrence of sinapine mainly in rapeseed embryo (Liu *et al.*, 2012).

Much experimental evidence suggests that the sinapine stored in rapeseed provides a supply of sinapic acid and choline, both of which serve as important precursors for essential plant components. Sinapine (**12**) degrades into sinapic acid and choline during early stages of seed germination (Tzagoloff, 1963; Bopp and Ludicke, 1975; Strack, 1981), and the two

components are used in later biosynthetic processes (Tzagoloff, 1963). In *Raphanus sativus* seedlings, choline released from sinapine was proven to be processed biosynthetically to phosphatidylcholine (Strack, 1981), and the sinapic acid moiety was hypothesized as the precursor for the biosynthesis of further phenolic compounds, such as flavonoids (Tzagoloff, 1963). The even distribution of sinapine in rapeseed embryo tissue supports its hypothetical depot function.

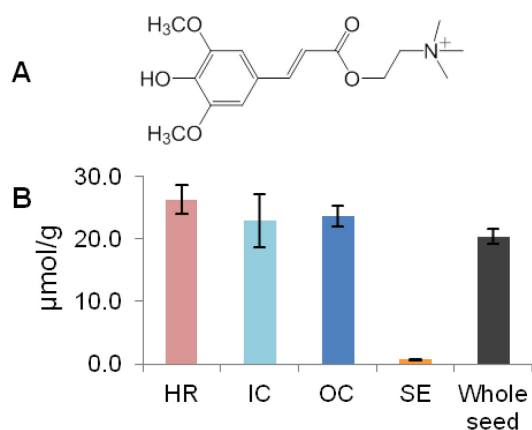


Figure 3. Distribution of sinapine in rapeseed. (A) Structure of sinapine (**12**). (B) Sinapine concentrations in different rapeseed tissues and whole rapeseed. HR, hypocotyl and radicle; IC, inner cotyledon; OC, outer cotyledon; and SE, seed coat and endosperm. Each column shows the mean of four replicates with standard error.

Cyclic spermidine conjugates in rapeseed

Cyclic spermidine conjugates in non-glucosinolate (NG) fractions of laser-microdissected rapeseed tissues were detected by HPLC-ESIMS in positive ionization mode (see Materials and methods). The major peak in extracted ion chromatogram (EIC) for ions at m/z 496.4 ($[M+1]^+$) (Figure S1) was identified as the major cyclic spermidine conjugate (**13**) (Figure 4A), based on its molecular mass of 495 Da and comparing the retention time with the compound recently isolated from rapeseed (manuscript 4.1). Based on the same molecular mass in the EIC and the same fragmentation patterns in MS/MS analysis compared to those of the major peak, several minor peaks (Figure S1) were suggested to be isomeric cyclic spermidine conjugates. However, structural details remained unassigned because nuclear magnetic resonance (NMR) data are lacking. The average concentration of compound **13** in the whole rapeseed is 1.94 µmol/g, as calculated from a calibration curve. Interestingly, the cyclic spermidine conjugates were found only in HR, where the average concentration of **13** is as high as 13.48 µmol/g. Compound **13** and minor cyclic spermidines are absent in SE, IC and OC tissues (Figures 4B, S1). No free spermidine was detected in any sample.

Polyamines (PAs) and phenylpropanoid-polyamine conjugates (PPCs) are widely distributed in plants (Bienz *et al.*, 2005), including seeds (Luo *et al.*, 2009), and play important roles in plant growth, abiotic stress tolerance and defense against insect herbivores (Kusano *et al.*, 2008; Alcázar *et al.*, 2010; Kaur *et al.*, 2010). Compound **13** (Figure 4A) was previously identified as the sole PPC from the same plant material, rapeseed (Baumert *et al.*,

2005; Clauß *et al.*, 2011). Nevertheless, this is the first time that the distribution of PPCs in seeds has been directly demonstrated. Our results showed that PPCs in rapeseed accumulate only in HR. This is consistent with the expression of PPC biosynthetic genes in *Arabidopsis* seeds (Luo *et al.*, 2009). The same authors also demonstrated that PPCs degrade at an early stage of seed germination (Luo *et al.*, 2009). Based on this evidence, PPCs that have accumulated in rapeseed are proposed to be sources of PAs and involved in diverse processes of plant growth and development (Kusano *et al.*, 2008; Alcázar *et al.*, 2010). Further experiments will establish the precise roles of PPCs distributed in hypocotyl and/or radicle in rapeseed. Degradation products derived from PPCs also contain phenylpropanoids, which are universal precursors for condensed phenolics in plants.

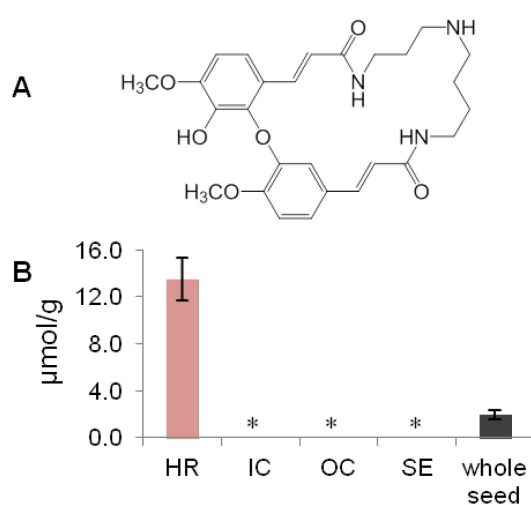


Figure 4. Distribution of the major cyclic spermidine in rapeseed. (A) Structure of the major cyclic spermidine conjugate (**13**) identified from rapeseed. (B) The concentration of **13** in different tissues and whole rapeseed. HR, hypocotyl and radicle; IC, inner cotyledon; OC, outer cotyledon; and SE, seed coat and endosperm. Each column shows the mean of four replicates with standard error, and * means not detectable.

Flavonoids in rapeseed

Two major flavonoids, kaempferol-3-*O*- β -D-glucopyranosyl-(1 \rightarrow 2)- β -D-glucopyranoside-7-*O*- β -D-glucopyranoside (**14**) and kaempferol-3-*O*-(2-*O*-sinapoyl)- β -D-glucopyranosyl-(1 \rightarrow 2)- β -D-glucopyranoside-7-*O*- β -D-glucopyranoside (**15**) (Figure 5A), are known from the rape cultivar “Emerald” (manuscript 4.1). Using calibration curves, the two flavonoids in dissected rapeseed samples were quantified by HPLC-ESIMS in negative mode. The average concentrations of flavonoids **14** and **15** in the whole seed are 0.23 and 0.42 μ mol/g, respectively (Figure 5B). The distribution pattern of flavonoids in different rapeseed tissues is contrary to that of PPCs. Compounds **14** and **15** were mainly detected in cotyledon parts (IC and OC) (Figure S2), where their concentrations are similar. Meanwhile, the two flavonoids are not detectable in SE and almost undetectable in HR (Figure 5B). In fact, a trace of flavonoid **15** was detected in only one of the four HR samples. No kaempferol derivative was detectable in the other three HR samples.

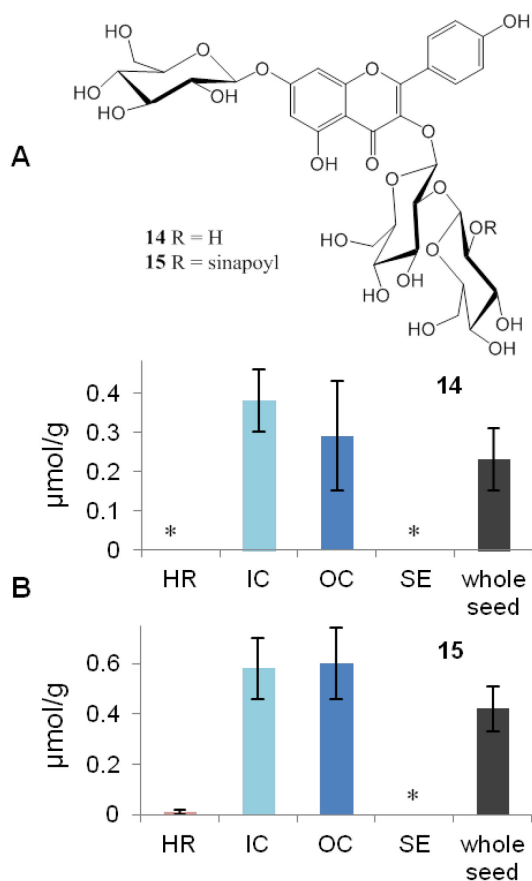


Figure 5. Distribution of the two major flavonoids in rapeseed. (A) Structures of two major flavonoids found in rapeseed: **14**, kaempferol-3-*O*- β -D-glucopyranosyl-(1 \rightarrow 2)- β -D-glucopyranoside-7-*O*- β -D-glucopyranoside; and **15**, kaempferol-3-*O*-(2-*O*-sinapoyl)- β -D-glucopyranosyl-(1 \rightarrow 2)- β -D-glucopyranoside-7-*O*- β -D-glucopyranoside. (B) Concentrations of **14** and **15** in different rapeseed tissues and whole rapeseed. HR, hypocotyl and radicle; IC, inner cotyledon; OC, outer cotyledon; and SE, seed coat and endosperm. Each column shows the mean of four replicates with standard error, and * means not detectable.

Flavonoids, which constitute an enormously diverse class of phenolic secondary metabolites, are involved in various physiological and ecological processes in plants (Croteau *et al.*, 2000). A common function of flavonoids is protecting plants from UV-B irradiation (Harborne and Williams, 2000), which was also demonstrated in rape (Wilson and Greenberg, 1993; Wilson *et al.*, 1998). Here, the finding of flavonoid accumulation in the primordial tissue of the cotyledons (IC and OC) of mature rapeseed leads to the hypothesis that these compounds are preformed for protecting the chlorophyll and other light-sensitive components from UV-B irradiation in cotyledons emerging during germination. Flavonoids also accumulate in seed coats to protect seeds against diverse biotic and abiotic stresses (Lepiniec *et al.*, 2006). As in other seeds, proanthocyanidins accumulate in rapeseed coats. Responsible for the seed color, they are normally insoluble (Auger *et al.*, 2010). Oligomers and polymers are the probable reason why monomeric flavonoids were not detected in rapeseed hull tissue, specifically in SE.

CONCLUSION

Recent studies on the tissue-specific distribution of soluble primary metabolites such as lipids, amino acids, carbohydrates and polymers (starch) demonstrated the feasibility of the LMD-based chemical analysis of rapeseed organs (Schiebold *et al.*, 2011). The major primary

metabolites in rapeseed embryo tissues are quantitatively but not qualitatively different, because these components are storage products and are involved in essential life cycles of plant growth and development. Unlike primary components, secondary metabolites help plants adapt to their biotic and abiotic environments (Wink, 2003; Hartmann, 2007). Seed tissues play different roles before and during germination, and develop into individual plant organs after germination. Therefore, secondary metabolites are speculated to accumulate unevenly in different seed tissues. The finding that some of the secondary metabolites detected in this work have different tissue-specific distribution patterns not only solidly supports this hypothesis but also offers the first clue to the biological functions of the secondary metabolites in the mature seed and probably during germination. The knowledge about the specific localization may be used to study the regulation of the biosynthesis and metabolic modification of secondary metabolites. On the other hand, the described sampling methodology, LMD, can be adjusted to facilitate the tissue-specific detection of metabolites, proteins and RNA in other plant materials.

MATERIAL AND METHODS

Plant material

Rapeseed (winter cultivar “Emerald”) used in this study was purchased from Raps GbR (Langballig, Germany). Entire seeds were used for analysis.

Laser microdissection

The basic work flow of LMD and its application to plant tissue has been reported (Hölscher and Schneider, 2008; Moco *et al.*, 2009). Mature rapeseed was fixed vertically in Jung tissue freezing medium (Leica Microsystems GmbH, Nussloch, Germany), and immediately frozen in liquid nitrogen. Serial cryosections (60 µm thickness) were prepared at -24°C using a cryostat microtome (Leica CM1850, Bensheim, Germany) and directly mounted on PET-Membrane FrameSlides (MicroDissect GmbH, Herborn, Germany). LMD was performed on the Leica LMD 6000 laser microdissection system (Leica Microsystems GmbH, Wetzlar, Germany) equipped with a nitrogen solid state diode laser of a short pulse duration (355 nm). The cutting settings were as follows: 20 × magnification, laser intensity of 128 (the strongest), laser moving speed of 1 (the slowest). The cut materials were collected in the cap of 0.5 ml centrifuge tubes by gravity and then transferred to an HPLC vial. The pictures were taken by a microscope-integrated camera HV-D20P (Hitachi, Tokyo, Japan). Rapeseed was dissected into four parts, HR, IC, OC, and SE (Figure1), and weights, including

the supporting PET membrane of the frame slide, which was unavoidably cut along with the plant tissue, are listed in Table 1.

Sample preparation

Generally, each sample was separated into glucosinolate fraction and non-glucosinolate (NG) fraction for further analysis through the procedure adapted from the literature (Burow *et al.*, 2006). The four dissected tissue groups (HR, IC, OC, and SE) were extracted separately in an ultrasonic bath for 10 min with 1 ml 80% (v/v) MeOH, which contains 10 μ M sinalbin as an internal standard for glucosinolates and 10 μ M cinnamic acid choline ester synthesized according to (Böttcher *et al.*, 2009) as an internal standard for sinapine. The weak anion exchange DEAE Sephadex cartridges (Sigma, Steinheim, Germany), which were conditioned with 800 μ l H₂O and equilibrated with 500 μ l 80% (v/v) MeOH before use, were used to separate glucosinolates from the other compounds. Each sample (800 μ l extract) was loaded to the cartridge and eluted with 500 μ l 80% (v/v) MeOH. Eluate (1300 μ l) was collected as an NG fraction and dried in a vacuum centrifuge evaporator Genevac HT-4X (Genevac Ltd, Suffolk, UK). Samples were reconstituted in 200 μ l 20% (v/v) MeCN for NG analysis. The DEAE Sephadex cartridges were further eluted by 1 ml H₂O twice and 500 μ l 0.02 M 2-(*N*-morpholino)ethanesulfonic acid buffer (pH 5.2). Sulfatase (30 μ l solution) (Sigma, Steinheim, Germany) was prepared as described in (Graser *et al.*, 2001) and loaded onto the cartridge. The cartridges were capped, incubated at ambient temperature overnight, and eluted with 500 μ l H₂O for desulfated glucosinolate analysis.

Identification and quantification of glucosinolates

Desulfated glucosinolates were identified with HPLC-DAD/MS by comparing their mass spectrometric data and retention times with those of references. The compounds were quantified based on an internal standard with DAD. HPLC was conducted on an Agilent series HP1100 (binary pump G1312A, autosampler G1367A, diode array detector G1315A; Agilent Technologies, Waldbronn, Germany). Chromatographic separation was performed on a LiChrospher RP18 column (5 μ m, 250 \times 4.6 mm, Merck, Darmstadt, Germany) with a guard column (5 μ m, 4 \times 4 mm) using a linear binary gradient of H₂O (solvent A) containing 0.2% (v/v) formic acid (FA) and MeCN (solvent B), with a flow rate of 1.0 ml min⁻¹ at 25 °C as follows: 0 min: 1.5% B, 1 min: 1.5% B, 6 min: 5% B, 8 min: 7% B, 18 min: 21% B, 23 min: 29% B, 23.1 min: 100% B, 24 min: 100% B, 24.1 min: 1.5% B, and 28 min: 1.5% B. The injection volume was 50 μ l. The absorption of HPLC eluate was monitored by DAD at 229 nm.

Identification and quantification of phenolics in the NG fractions

HPLC-ESIMS was applied to quantify phenolics in laser-microdissected samples in NG fractions. The chromatographic separation was performed on a Nucleodur Sphinx RP column (5 μm , 250 \times 4.6 mm; Macherey-Nagel GmbH, Düren, Germany) using the above-mentioned separation conditions (HPLC system, flow rate, temperature, and eluent) except a linear gradient, which was as follows: 0 min: 10% B, 20 min: 30% B, 25 min: 70% B, 25.1 min: 100% B, 28 min: 100% B, 28.1 min: 10% and 32 min: 10% B. The injection volume was 10 μl . Electrospray ionization mass spectra of HPLC eluate were monitored on an Esquire 6000 ion trap mass spectrometer (Bruker Daltonics, Bremen, Germany). Both positive and negative modes were used in the range m/z 150-1200 with skimmer voltage ± 40 V, capillary exit voltage ± 150 V, capillary voltage ± 4000 V, nebulizer pressure 35 psi, drying gas 10 L min^{-1} , and gas temperature 350 $^{\circ}\text{C}$. Phenolics were identified based on their MS data and comparing the chromatographic retention times to those of compounds reported for rapeseed of cv. “Emerald” (manuscript 4.1). The concentration of sinapine was calculated relative to the internal standard cinnamic acid choline ester in positive mode. The cyclic spermidine conjugate and two flavonoids were quantified using calibration curves in positive and negative modes, respectively.

Data analysis

The experiments were performed in four replicates. Data are reported as means \pm standard deviation (SD). Analyses of variance and significant differences among means were tested by one-way ANOVA using SPSS Statistics 17.0. The least significant difference at $P = 0.05$ level was calculated.

ACKNOWLEDGEMENT

We thank Emily Wheeler for editorial help.

FUNDING

This work was supported by the Max Planck Society (MPG). J. Fang was financed a PhD scholarship by the International Max Planck Research School (IMPRS).

Chapter 5

Spatio-temporal accumulation of secoisolariciresinol diglucoside in flaxseed

- 5.1 Concentration kinetics of secoisolariciresinol diglucoside and its biosynthetic precursor coniferin in developing flaxseed. 62
- 5.2 Laser microdissection-assisted quantitative cell layer-specific detection of secoisolariciresinol diglucoside in flaxseed coats (Preliminary version). 68

Concentration Kinetics of Secoisolariciresinol Diglucoside and its Biosynthetic Precursor Coniferin in Developing Flaxseed

Jingjing Fang,^a Aina Ramsay,^b Christian Paetz,^a Evangelos C. Tatsis,^a Sullivan Renouard,^c Christophe Hano,^c Eric Grand,^d Ophélie Fliniaux,^b Albrecht Roscher,^e Francois Mesnard^b and Bernd Schneider^{a*}

ABSTRACT:

Introduction – In the plant kingdom, flaxseed (*Linum usitatissimum* L.) is the richest source of secoisolariciresinol diglucoside (SDG), which is of great interest because of its potential health benefits for human beings. The information about the kinetics of SDG formation during flaxseed development is rare and incomplete.

Objective – In this study, a reversed-phase high-performance liquid chromatography–diode array detection (HPLC-DAD) method was developed to quantify SDG and coniferin, a key biosynthetic precursor of SDG in flaxseed.

Methodology – Seeds from different developmental stages, which were scaled by days after flowering (DAF), were harvested. After alkaline hydrolysis, the validated HPLC method was applied to determine SDG and coniferin concentrations of flaxseed from different developing stages.

Results – Coniferin was found in the entire capsule as soon as flowering started and became undetectable 20 DAF. SDG was detected 6 DAF, and the concentration increased until maturity. On the other hand, the SDG amount in a single flaxseed approached the maximum around 25 DAF, before desiccation started. Concentration increase between 25 DAF and 35 DAF can be attributed to corresponding seed weight decrease.

Conclusion – The biosynthesis of coniferin is not synchronous with that of SDG. Hence, the concentrations of SDG and coniferin change during flaxseed development. Copyright © 2012 John Wiley & Sons, Ltd.

Keywords: HPLC-DAD; coniferin; flaxseed; secoisolariciresinol diglucoside; *Linum usitatissimum*

Introduction

Flax is an economically important fibre and oil plant. The seeds are used for food and feed purposes in many parts of the world. They contain high concentrations of digestible proteins, soluble fibre, soluble polysaccharides and oil; the oil is rich in omega-3 fatty acids (e.g. α -linolenic acid, 45–52% of total fatty acids). Additionally, flaxseed is the richest source of nutritional lignans in plants. Altogether, these components contribute to the nutritional and health functions of flaxseed diets (Oomah, 2001).

Lignans are phenolic compounds that are formed from two phenylpropanoid moieties, which are C–C coupled through the 8 and 8' positions (Moss, 2000). The biological functions of these compounds for flaxseed are still unknown. The strong anti-oxidant activity of lignans (Hu *et al.*, 2007) has led to the hypothesis that they protect abundant polyunsaturated fatty acids in the embryo from oxidation (Hano *et al.*, 2006). Additionally, lignans may be involved in flaxseed defence against pathogens, predators and other biotic stresses (Dixon *et al.*, 2002). In the past few decades, flaxseed lignans have become of great interest because of their wide spectrum of biological activity and potentially beneficial health functions, such as anti-oxidant, anti-cancer and diabetes prevention. Most of the biological effects of flaxseed lignans are attributed to the predominant compound, secoisolariciresinol diglucoside (SDG; **6**, Fig. 1), and its mammalian lignan derivatives, enterolactone and enterodiol,

which are formed from SDG by the action of intestinal bacteria in the human colon (Westcott and Muir, 2003; Eeckhaut *et al.*, 2008; Adolphe *et al.*, 2010). However, free SDG has rarely been detected in flaxseed at any developmental stage (Ford *et al.*, 2001; Hano *et al.*, 2006). Directly after its formation, SDG is assembled into lignan macromolecules (**7**, Fig. 1). From one to seven SDG units are connected by 3-hydroxy-3-methylglutaric

* Correspondence to: B. Schneider, Max Planck Institute for Chemical Ecology, Hans-Knöll-Str. 8, Beutenberg Campus, 07745 Jena, Germany. E-mail: schneider@ice.mpg.de

^a Max Planck Institute for Chemical Ecology, Hans-Knöll-Str. 8, Beutenberg Campus, 07745 Jena, Germany

^b Université de Picardie Jules Verne, EA3900 – BioPI 'Biologie des Plantes et Contrôle des Insectes Ravageurs', Faculté de Pharmacie, 1 rue des Louvels, 80037 Amiens cedex, France

^c Laboratoire de Biologie des Ligneux et des Grandes Cultures, UPRES EA 1207, Antenne Scientifique Universitaire de Chartres, 21, rue de Loigny-la-Bataille, 28000 Chartres, France

^d Laboratoire des Glucides CNRS UMR 6219, Faculté des Sciences, Université de Picardie Jules Verne, 33 rue Saint-Leu, 80039 Amiens, France

^e Génie Enzymatique et Cellulaire, UMR CNRS 6022, Université de Picardie, 33, rue Saint-Leu, 80039 Amiens, France

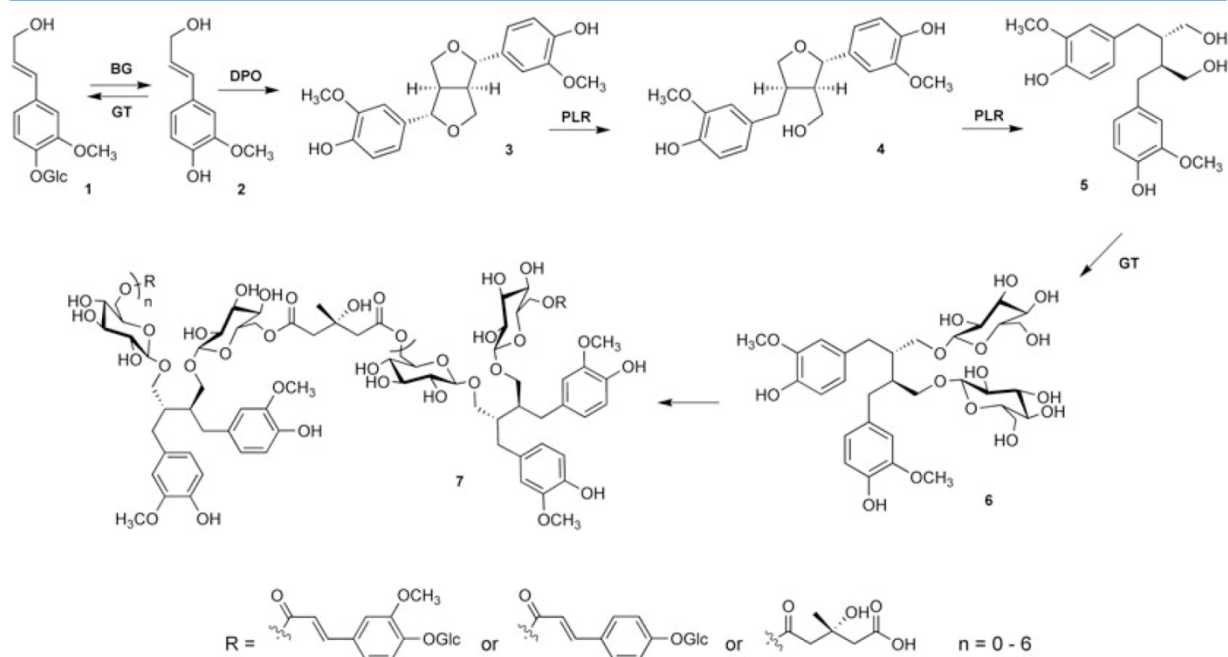


Figure 1. Biosynthesis pathway of the secoisolariciresinol diglucoside oligomer: BG, β -glucosidase; GT, glucosyltransferase; DPO, dirigent-protein oxidase; PLR, pinoresinol-lariciresinol reductase; Glu, β -D-glucosyl.

acid (HMGA) through ester bonds (Kamal-Eldin *et al.*, 2001) to form the SDG-HMG oligomer complex. SDG concentration in whole flaxseed varies between 6.1 and 28.8 mg/g depending on several factors, such as cultivar, growing condition and cultivation season. Furthermore, the yield of SDG obtained from flaxseed is affected by the hydrolysis methods applied to the SDG-HMG oligomer (Johnsson *et al.*, 2000; Eliasson *et al.*, 2003; Beejmohun *et al.*, 2007; Renouard *et al.*, 2010). Two other major phenolics, ferulic acid glucoside and *p*-coumaric acid glucoside, as well as other minor components, such as pinoresinol, isolariciresinol, matairesinol and herbacetin diglucoside, are also constituents of the SDG-HMG oligomer complex (Ford *et al.*, 2001; Struijs *et al.*, 2009). Biosynthetic investigations of SDG in flaxseed suggest the following pathway (Fig. 1): the dirigent protein-assisted coupling of two *E*-coniferyl alcohol (2) units results in one (-)-pinosresinol (3) molecule, which is successively converted into (-)-lariciresinol (4) and (+)-secoisolariciresinol (SECO, 5) mediated by a bifunctional nicotinamide adenine dinucleotide phosphate hydrogen (NADPH)-dependent pinoresinol-lariciresinol reductase (PLR). Then the latter molecule is glycosylated to SDG (6) via the action of a glucosyl transferase (Umezawa *et al.*, 1991; Ford *et al.*, 2001; Hano *et al.*, 2006). The monolignol, *E*-coniferyl alcohol, is unstable and relatively toxic to plants and does not accumulate at high levels in living plant cells. Glycosylation can stabilise and detoxify the monolignols; therefore, in plants *E*-coniferyl alcohol is stored and transported as its glucoside, coniferin (1, Fig. 1; Whetten *et al.*, 1998).

Because of SDG's wide spectrum of bioactivities, both the releasing procedures (Beejmohun *et al.*, 2007; Yuan *et al.*, 2008; Renouard *et al.*, 2010) from the lignan oligomer of mature flaxseed or flaxseed products and the quantification methods (Muir, 2006; Coran *et al.*, 2008; Popova *et al.*, 2009; Mukker *et al.*, 2010) of SDG and its aglycon, SECO (5 in Fig. 1), have been investigated extensively. However, information about the

kinetics of SDG formation during flaxseed development is rare and incomplete. To study the biosynthesis of the SDG oligomer, Ford *et al.* (2001) measured the concentration of free and polymerised SDG in flaxseed at early developmental stages, which were classified by the diameters of capsules. Hano *et al.* (2006) reported that SDG concentrations increased during seed development. They also confirmed that the site of PLR expression in flaxseed coat matched the localisation of SDG. Attoumbré *et al.* (2011) determined SDG concentrations in developing flaxseed from flowering to mature seeds. In this work, we present the first validated method comprising sample preparation and quantification by reversed-phase high-performance liquid chromatography-diode array detection (HPLC-DAD); this method was applied to monitor concentrations of both SDG and its precursor, coniferin (1), in flaxseed during development.

Experimental

Plant materials

Seeds of *L. usitatissimum* cv. Barbara were obtained from Laboulet semences (Airaines, France). Flax plants were grown in soil in the greenhouse of Max Planck Institute for Chemical Ecology in Jena, Germany, under the following conditions: day 20–22°C, night 18–20°C; 30–55% relative humidity; the natural photoperiod was supplemented with 14 h illumination from Philips Sun-T Agro 400 Na lights. The flowering date was recorded by tagging individual flowers of flax plants.

Chemicals and standard solutions

Chemicals used in this study are HPLC grade. Secoisolariciresinol diglucoside (SDG, > 98%) was purified as follows: powder obtained by grinding mature seed coats was defatted with *n*-hexane (10 mL, 3 h \times 3). The residue was hydrolysed with 20 mL 20 mM NaOH (50% MeOH and

50% H₂O solution) overnight; then the solution was centrifuged at 13200 rpm (Centrifuge 5415R, Eppendorf, Hamburg, Germany), and the supernatant was evaporated in vacuum < 40°C to remove MeOH. The residual aqueous solution was neutralised with 1% (v/v) acetic acid to pH 7.0, and loaded on a Discovery DSC-18 SPE cartridge (10 g, 60 mL; Supelco, Bellefonte, PA, USA), which was conditioned with 20 mL MeOH and then equilibrated with 20 mL H₂O before use. After discarding the eluate of 40 mL H₂O, the eluate of 40 mL 75% MeOH aqueous solution was collected and dried < 40°C in vacuum. The extract was purified on a Merck-Hitachi preparative HPLC system (L-6200A gradient pump, L-4250 UV-vis detector; Hitachi, Ltd, Tokyo, Japan) using a Purospher RP18e column (5 µm, 250 × 10 mm; Merck KGaA, Darmstadt, Germany). The flow rate was kept at 3.5 mL/min and UV detection was at 280 nm. The following linear gradient of H₂O (solvent A) and MeOH (solvent B) was applied: 0 min: 25% B; 35 min: 40% B; 37 min: 95% B; 42 min: 95% B; and 44 min: 25% B; followed by a 5 min equilibration step. The retention time of SDG was around 19.6 min. The structure was determined by NMR and MS data analyses and by comparison with those in the literature (Chimichi *et al.*, 1999). Coniferin (> 99%) was synthesised (Beejmohun *et al.*, 2006). The stock standard solutions were prepared by dissolving SDG and coniferin in methanol (1000 µg/mL). These solutions were further diluted with methanol for two series of calibration standard solutions (1000, 500, 200, 40 and 8 µg/mL for SDG, and 1000, 200, 40, 8 and 1.6 µg/mL for coniferin).

Flaxseed sample preparation

Capsules of each stage (0, 5, 10, 15, 20, 25, 30, 35 and 40 days after flowering, DAF) were harvested from flax plants. Except the 0 DAF seeds, which were too small to be separated from the capsules, seeds were picked out from each capsule. The entire capsule (0 DAF) and immature seeds (5–25 DAF) from one capsule were weighed, transferred into a 25 mL glass vial and crushed by tweezers. The seeds older than 30 DAF from one capsule were cut into slices < 1 mm wide and transferred into a 25 mL glass vial for alkaline hydrolysis. The hydrolysis method was adapted from the literature (Li *et al.*, 2008) as follows: 4 mL 20 mM NaOH (in MeOH:H₂O 1:1) solution was added into a glass vial containing the seed material. After being magnetically stirred at ambient temperature for 3 h, the solution was neutralised with 1% (v/v) acetic acid, filtered and filled to 5 mL in a volumetric flask. Then about 1 mL solution was taken and filtered through a 0.45 µm membrane filter (Rotilabo-syringe filter, nylon; Carl Roth GmbH + Co. KG, Karlsruhe, Germany) into a HPLC vial for further analysis. The experiments were performed in triplicate for each developmental stage. Seeds from 6, 7, 8 and 9 DAF capsules were measured to see when SDG biosynthesis began.

High-performance liquid chromatography

The HPLC was conducted on an Agilent series HP1100 (binary pump G1312A, autosampler G1367A, diode array detector G1315A, 200–700 nm) (Agilent Technologies, Waldbronn, Germany). The chromatographic separation was performed on a LiChrospher RP18 column (5 µm, 250 × 4 mm; Merck KGaA, Darmstadt, Germany) with a guard column (5 µm, 4 × 4 mm) using a linear binary gradient of H₂O (solvent A) and MeCN (solvent B), both containing 0.1% (v/v) trifluoroacetic acid, with a flow rate of 0.8 mL/min at 25°C as follows: 0 min: 5% B; 35 min: 25% B; 37 min: 95% B; 47 min: 95% B; 50 min: 5% B; and 60 min: 5% B. The injection volume was 5 µL. The HPLC eluate was monitored by DAD at 280 nm for SDG and 260 nm for coniferin.

Method validation

Standard calibration curves were generated using five standard solutions of coniferin and five standard solutions of SDG. Every standard solution was injected in triplicate. Arithmetic means of each triplicate were calculated. The linear regression equations were carried out by plotting the peak areas (y) against the injected amounts (x) of standard compounds.

The linearity was demonstrated by coefficients of determination (R^2). The limits of detection (LOD) and the limits of quantification (LOQ) were determined based on the signal-to-noise ratios (S:N) of approximately 3:1 and 10:1, respectively.

Accuracy was evaluated by measuring recovery rates using flaxseed from three different developmental stages: 10, 25 and 40 DAF. Seeds from one capsule of each stage were homogenised and separated into two parts of equal mass, one of which was spiked with a known volume of stock solutions. The spiked and non-spiked parts were analysed by HPLC in triplicate following the procedures described. The recovery rates were calculated according to the following formula:

$$\text{Recovery rate (\%)} = \frac{\text{amount in spiked part} - \text{amount in non-spiked part}}{\text{spiked amount}} \times 100.$$

The method precision was evaluated by determining the intraday and interday variations, which were calculated from data obtained by the repeated injections of standard solutions. The intraday variation was obtained by five replicates in a day, and the interday variation was determined by three injections over three continuous days. Retention times and peak areas were evaluated. The precision was further checked by measuring the repeatability using five continuous injections of 10, 25 and 40 DAF samples. The precision was expressed as the relative standard deviation (RSD, %).

Results and discussion

HPLC method validation

The HPLC method was validated to ensure the precision and accuracy of the method used to quantify SDG and coniferin. The validation parameters are presented in Table 1. The calibration curves of the peak areas (y) against the injected amounts (x) of SDG at 280 nm and coniferin at 260 nm possessed linearity over wide ranges: from 40 to 5000 ng for SDG and from 8 to 5000 ng for coniferin. The LOD of SDG and coniferin were as low as 2.5 and 0.32 ng, respectively, and the LOQ of SDG and coniferin were 8.0 and 1.0 ng, respectively. The RSDs of intra- and interday variation were between 0.13 and 0.85%, and the RSDs of five repeats of three developmental stage samples were less than 1.34%. The small variation reflects the high precision of the HPLC method. The recovery rates between 100.2 and 102.7% of SDG and between 93.1 and 104.8 of coniferin indicate the accuracy of the method.

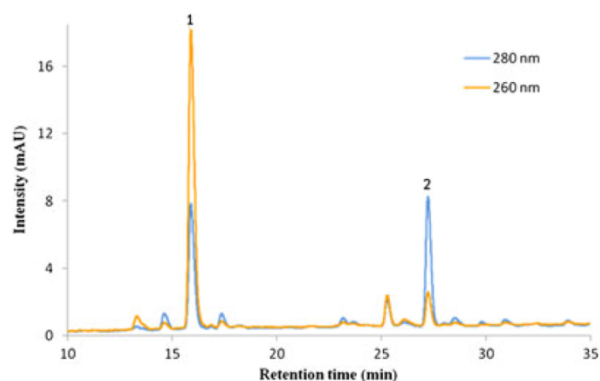
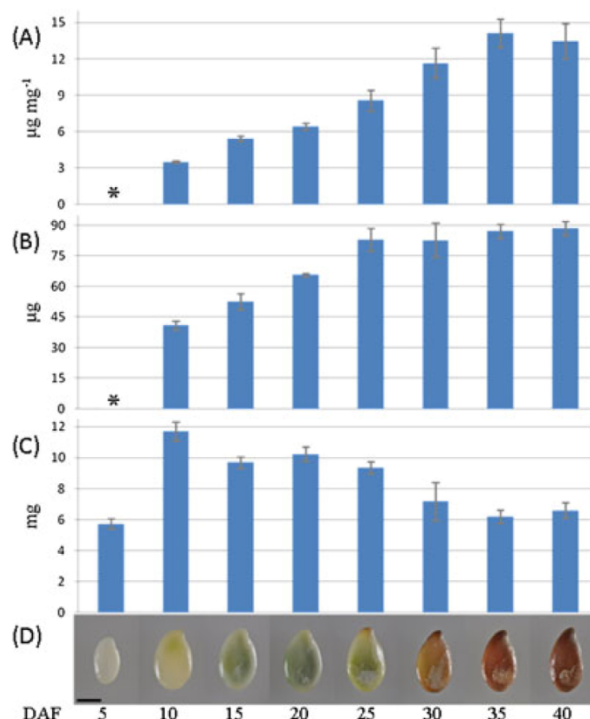
The concentrations of SDG and coniferin change during development of flaxseed

The HPLC-DAD method described above was applied to hydrolysed flaxseed in order to determine the concentrations of SDG and coniferin in seeds during development. The SDG concentration detected here includes the polymerised SDG and free SDG, if it exists. Chromatograms of one sample obtained after alkaline hydrolysis of 10 DAF seeds display peaks of both SDG and coniferin (Fig. 2). The SDG was detectable 6 DAF, when the concentration in fresh seeds was 0.32 µg/mg and the average amount was 2.46 µg/seed. The development of SDG content was determined from 0 to 40 DAF at regular 5-day intervals (Fig. 3). In seeds harvested 10 DAF, the SDG concentration was 3.50 µg/mg, an amount which then increased and reached a maximum of 14.11 µg/mg at 35 DAF (Fig. 3A) in mature seeds. On the other hand, the average amount of SDG per seed was 40.99 µg at 10 DAF, which rapidly increased to 83.09 µg at 25 DAF. After that, the SDG amount did not change significantly until seed maturity

Table 1. Validation parameters of the HPLC method developed for quantifying secoisolariciresinol diglucoside (SDG) and coniferin

	Regression equation	R^2	Linear range	LOD (ng)	LOQ (ng)	Precision (% RSD)		Repeatability (% RSD)			Recovery (%)		
						Intraday	Interday	10 DAF	25 DAF	40 DAF	10 DAF	25 DAF	40 DAF
SDG	$y = 0.4260x - 1.8551$	1.000	40–5000	2.5	8.0	0.70	0.85	1.34	0.17	0.41	101.5	100.2	102.7
Coniferin	$y = 3.5535x - 0.4654$	1.000	8–5000	0.32	1.0	0.13	0.44	0.23	ND	ND	104.8	93.1	95.7

The RSDs of intraday precision were measured by five replicates. Other measurements were performed in triplicate. ND: not detectable.

**Figure 2.** The HPLC chromatograms of a hydrolysate obtained from 10 DAF seeds. Ultraviolet detection under 260 and 280 nm. Peak 1: coniferin; peak 2: secoisolariciresinol diglucoside.**Figure 3.** Development of (A) secoisolariciresinol diglucoside (SDG) concentration in flaxseed ($\mu\text{g}/\text{mg}$ seed fresh weight), (B) SDG amount in a single flaxseed (μg per seed), (C) fresh weight of a single flaxseed, and (D) photographs of flaxseeds at different developmental stages. Data shown as mean \pm SD ($n=3$). Student's *t*-test was used for statistics ($p < 0.01$). The bar represents 2 mm. * means not calculable.

(Fig. 3B). Coniferin was detected in the whole capsule at 0 DAF at a concentration of $2.21 \mu\text{g}/\text{mg}$ (Table 2). Then the concentration of coniferin declined very quickly in the early developmental period. There was a trace of coniferin detected in only one of the three capsules investigated. No coniferin was observed at developmental stages later than 15 DAF (Table 2).

Seed development generally includes two stages, morphogenesis and maturation. The maturation stage can be divided

Concentration of SDG and Coniferin in Flaxseeds

Table 2. Development of coniferin concentration in flaxseed

DAF	$\mu\text{g}/\text{mg}$	μg per seed
0	2.21 ± 0.07	23.49 ± 0.59
5	1.73 ± 0.06	9.92 ± 0.80
10	0.86 ± 0.19	9.96 ± 1.63
15	Trace	Trace
20–40	ND	ND

Data shown as mean \pm SD ($n = 3$). ND: not detectable.

into three phases: transition, embryo growth and seed filling, and desiccation (Gutierrez *et al.*, 2007). Based on the experimental results, SDG biosynthesis starts at the beginning of maturation and stops when seeds start desiccating, around 25 DAF. The significant increase in SDG concentration between 25 and 35 DAF was a result of the decrease of seed weight during desiccation (Fig. 3C), which leads to seed dormancy and simultaneous browning (Fig. 3D).

The biosynthesis of coniferin is not synchronous with that of SDG. Coniferin is synthesized and pooled in flaxseed at a high concentration immediately at 0 DAF, then the concentration decreases dramatically and coniferin becomes undetectable 20 DAF, when embryos in flaxseed stop growing (Fig. 3D). Coniferin is the precursor not only for lignan SDG but also for the guaiacyl (G) type of lignin, which is the second most abundant biopolymer after cellulose in plants (Boerjan *et al.*, 2003). From flowering (0 DAF) to 15 DAF, flaxseed enlarges very quickly and the embryo grows almost to its final size (Fig. 3D). It is reasonable to speculate that a significant part of coniferin is used during this period to synthesise the lignin in order to shape and stabilise the seed coat and make secondary cell walls for new cells. The accumulation of SDG during embryo growth and seed filling requires coniferin to be used for lignan biosynthesis instead of lignin formation. Recently, guaiacyl lignin was found in the seeds of the 'Barbara' cultivar, supporting the above assumption (B. Chabbert, personal communication, 2012).

It is difficult to compare our data on the development of SDG concentrations with published results because information by Ford *et al.* (2001) is restricted to early developmental stages. Hano *et al.* (2006) observed that both the weight of flaxseed and the accumulation of SDG in flaxseed increased until 'nearly mature seed'. In another study, Renouard *et al.* (2012) reported that the concentration of SDG reached a maximum when the seed was brown. Their results probably differed from ours because of different sampling time.

Conclusions

In conclusion, a HPLC-DAD method was established and validated in order to quantify SDG and its biosynthetic precursor, coniferin, in flaxseed. Using this method, we found SDG started to be detectable at 6 DAF, and its concentration increased constantly up to maturity. On the other hand, SDG accumulation stops around 25 DAF, when seed desiccation starts; no significant increase of SDG amount per seed occurs during desiccation. Coniferin was found in the entire capsule once flowering began and became undetectable 20 DAF. These data provide in-depth understanding of temporal concentration changes of both SDG and coniferin during flaxseed development.

Acknowledgements

J. Fang acknowledges the International Max Planck Research School (IMPRS) for a PhD scholarship. A. Ramsay wishes to thank the Conseil Régional de Picardie for financial support. Sullivan Renouard and Christophe Hano kindly acknowledge the "Ligue Contre le Cancer, Comité d'Eure et Loir" for its support. We are also grateful for financial support from Max Planck Society (MPG) and the European Regional Development Fund (ERDF). We thank Emily Wheeler for editorial help in the preparation of this manuscript.

References

- Adolphe JL, Whiting SJ, Juurlink BHJ, Thorpe LU, Alcorn J. 2010. Health effects with consumption of the flax lignan secoisolariciresinol diglucoside. *Brit J Nutr* **103**: 929–938.
- Attoubré J, Laoualy ABM, Bienaimé C, Dubois F, Baltora-Rosset S. 2011. Investigation of lignan accumulation in developing *Linum usitatissimum* seeds by immunolocalization and HPLC. *Phytochem Lett* **4**: 194–198.
- Beejmohun V, Grand E, Lesur D, Mesnard F, Fliniaux MA, Kovensky J. 2006. Synthesis and purification of [1,2- $^{13}\text{C}_2$]coniferin. *J Labelled Compd Rad* **49**: 463–470.
- Beejmohun V, Fliniaux O, Grand É, Lamblin F, Bensaddek L, Christen P, Kovensky J, Fliniaux MA, Mesnard F. 2007. Microwave-assisted extraction of the main phenolic compounds in flaxseed. *Phytochem Anal* **18**: 275–282.
- Boerjan W, Ralph J, Baucher M. 2003. Lignin biosynthesis. *Ann Rev Plant Biol* **54**: 519–546.
- Chimichi S, Bambagiotti-Alberti M, Coran SA, Giannellini V, Biddau B. 1999. Complete assignment of the ^1H and ^{13}C NMR spectra of secoisolariciresinol diglucoside, a mammalian lignan precursor isolated from *Linum usitatissimum*. *Magn Reson Chem* **37**: 860–863.
- Coran SA, Bartolucci G, Bambagiotti-Alberti M. 2008. Validation of a reversed phase high performance thin layer chromatographic-densitometric method for secoisolariciresinol diglucoside determination in flaxseed. *J Chromatogr A* **1207**: 155–159.
- Dixon RA, Achnine L, Kota P, Liu CJ, Reddy MSS, Wang LJ. 2002. The phenylpropanoid pathway and plant defence – a genomics perspective. *Mol Plant Pathol* **3**: 371–390.
- Eeckhaut E, Struijs K, Possemiers S, Vincken JP, De Keukeleire D, Verstraete W. 2008. Metabolism of the lignan macromolecule into enterolignans in the gastrointestinal lumen as determined in the simulator of the human intestinal microbial ecosystem. *J Agric Food Chem* **56**: 4806–4812.
- Eliasson C, Kamal-Eldin A, Andersson R, Åman P. 2003. High-performance liquid chromatographic analysis of secoisolariciresinol diglucoside and hydroxycinnamic acid glucosides in flaxseed by alkaline extraction. *J Chromatogr A* **1012**: 151–159.
- Ford JD, Huang KS, Wang HB, Davin LB, Lewis NG. 2001. Biosynthetic pathway to the cancer chemopreventive secoisolariciresinol diglucoside-hydroxymethyl glutaryl ester-linked lignan oligomers in flax (*Linum usitatissimum*) seed. *J Nat Prod* **64**: 1388–1397.
- Gutierrez L, Van Wuytswinkel O, Castelain M, Bellini C. 2007. Combined networks regulating seed maturation. *Trends Plant Sci* **12**: 294–300.
- Hano C, Martin I, Fliniaux O, Legrand B, Gutierrez L, Arroo RRJ, Mesnard F, Lamblin F, Lainé E. 2006. Pinorensin-lariciresinol reductase gene expression and secoisolariciresinol diglucoside accumulation in developing flax (*Linum usitatissimum*) seeds. *Planta* **224**: 1291–1301.
- Hu C, Yuan YV, Kitts DD. 2007. Antioxidant activities of the flaxseed lignan secoisolariciresinol diglucoside, its aglycone secoisolariciresinol and the mammalian lignans enterodiol and enterolactone *in vitro*. *Food Chem Toxicol* **45**: 2219–2227.
- Johnsson P, Kamal-Eldin A, Lundgren LN, Åman P. 2000. HPLC method for analysis of secoisolariciresinol diglucoside in flaxseeds. *J Agric Food Chem* **48**: 5216–5219.
- Kamal-Eldin A, Peerlkamp N, Johnsson P, Andersson R, Andersson RE, Lundgren LN, Åman P. 2001. An oligomer from flaxseed composed of secoisolariciresinoldiglucoside and 3-hydroxy-3-methyl glutaric acid residues. *Phytochemistry* **58**: 587–590.
- Li X, Yuan JP, Xu SP, Wang JH, Liu X. 2008. Separation and determination of secoisolariciresinol diglucoside oligomers and their hydrolysates in

- the flaxseed extract by high-performance liquid chromatography. *J Chromatogr A* **1185**: 223–232.
- Moss GP. 2000. Nomenclature of lignans and neolignans (IUPAC Recommendations 2000). *Pure Appl Chem* **72**: 1493–1523.
- Muir AD. 2006. Flax Lignans – Analytical methods and how they influence our understanding of biological activity. *J AOAC Int* **89**: 1147–1157.
- Mukker JK, Kotlyarova V, Singh RSP, Alcorn J. 2010. HPLC method with fluorescence detection for the quantitative determination of flaxseed lignans. *J Chromatogr B* **878**: 3076–3082.
- Oomah BD. 2001. Flaxseed as a functional food source. *J Sci Food Agric* **81**: 889–894.
- Popova IE, Hall C, Kubátová A. 2009. Determination of lignans in flaxseed using liquid chromatography with time-of-flight mass spectrometry. *J Chromatogr A* **1216**: 217–229.
- Renouard S, Hano C, Corbin C, Fliniaux O, Lopez T, Montguillon J, Barakzoy E, Mesnard F, Lamblin F, Lainé E. 2010. Cellulase-assisted release of secoisolariciresinol from extracts of flax (*Linum usitatissimum*) hulls and whole seeds. *Food Chem* **122**: 679–687.
- Renouard S, Corbin C, Lopez T, Montguillon J, Gutierrez L, Lamblin F, Lainé E, Hano C. 2012. Abscisic acid regulates pinoresinol-lariciresinol reductase gene expression and secoisolariciresinol accumulation in developing flax (*Linum usitatissimum* L.) seeds. *Planta* **235**: 85–98.
- Struijs K, Vincken JP, Doeswijk TG, Vorgen AGJ, Gruppen H. 2009. The chain length of lignan macromolecule from flaxseed hulls is determined by the incorporation of coumaric acid glucosides and ferulic acid glucosides. *Phytochemistry* **70**: 262–269.
- Umezawa T, Davin LB, Lewis NG. 1991. Formation of lignans (–)-secoisolariciresinol and (–)-matairesinol with *Forsythia intermedia* cell-free extracts. *J Biol Chem* **266**: 10210–10217.
- Westcott ND, Muir AD. 2003. Flax seed lignan in disease prevention and health promotion. *Phytochem Rev* **2**: 401–417.
- Whetten RW, MacKay JJ, Sederoff RR. 1998. Recent advances in understanding lignin biosynthesis. *Ann Rev Plant Physiol Plant Mol Biol* **49**: 585–609.
- Yuan JP, Li X, Xu SP, Wang JH, Liu X. 2008. Hydrolysis kinetics of secoisolariciresinol diglucoside oligomers from flaxseed. *J Agric Food Chem* **56**: 10041–10047.

Laser microdissection-assisted quantitative cell layer-specific detection of secoisolariciresinol diglucoside in flaxseed coats

Jingjing Fang¹, Aina Ramsay², Sullivan Renouard³, Christophe Hano³, Frédéric Lamblin³, Brigitte Chabbert^{4,5}, François Mesnard² and Bernd Schneider^{1*}

¹ Max-Planck Institute for Chemical Ecology, Hans-Knöll-Str. 8, Beutenberg Campus, 07745 Jena, Germany

² Université de Picardie Jules Verne, EA3900 – BioPI “Biologie des Plantes et contrôle des Insectes ravageurs”, Faculté de Pharmacie, 1 rue des Louvels, 80037 Amiens cedex, France

³ Laboratoire de Biologie des Ligneux et des Grandes Cultures (LBLGC), UPRES EA 1207, Antenne Scientifique Universitaire de Chartres (ASUC), Université d’Orléans, 21 rue de Loigny la Bataille, 28000 Chartres, France

⁴ INRA, UMR614 Fractionnement des AgroRessources et Environnement, F-51100 Reims, France

⁵ Université de Reims Champagne-Ardenne, UMR614 Fractionnement des AgroRessources et Environnement, F-51100 Reims, France

Abstract

The concentration of secoisolariciresinol diglucoside (SDG) found in flaxseed (*Linum usitatissimum* L.) is higher than that found in any other plant. It exists in flaxseed coats as an SDG-3-hydroxy-3-methylglutaric acid (HMGA) oligomer complex. A laser microdissection (LMD) method was applied to harvest material from different cell layers of seed coats of mature and developing flaxseed to detect the cell-layer specific localization of SDG in flaxseed; NMR and HPLC were used to identify and quantify SDG in dissected cell layers after alkaline hydrolysis. The obtained results were further confirmed by a standard molecular method. The promoter of one pinoresinol-lariciresinol reductase gene of *L. usitatissimum* (*LuPLRI*), which is a key gene involved in SDG biosynthesis, was fused to a β -glucuronidase (*GUS*) reporter gene, and the spatio-temporal regulation of *LuPLRI* gene expression in flaxseed was determined by histochemical and activity assays of *GUS*. The result showed that SDG was synthesized and accumulated in the parenchymatous cell layer of the outer integument of flaxseed coats.

Keywords: flaxseed, gene expression, β -glucuronidase, laser microdissection, lignans, *Linum usitatissimum*, localization, parenchymatous cells, pinoresinol-lariciresinol reductase, secoisolariciresinol diglucoside.

Introduction

Linum usitatissimum, a plant with multiple uses, has traditionally been cultivated for fiber and oil production. Flaxseed is a rich source of polyunsaturated fatty acids and lignans. These components contribute beneficial nutritional and health-related functions to a flaxseed diet (Oomah, 2001; Adolphe *et al.*, 2010; Singh *et al.*, 2011).

Flaxseed is by far the richest source of lignans in the plant kingdom. Between 6.1 and 28.8 mg/g of secoisolariciresinol diglucoside (SDG) (**5** in Fig. S1), was reported as the predominant lignan in whole flaxseed. This SDG concentration is higher in flaxseed than in any other edible plant (Axelson *et al.*, 1982; Thompson *et al.*, 1991). SDG was almost undetectable in flaxseed in any developing stage (Ford *et al.*, 2001; Hano *et al.*, 2006). Directly after its formation, SDG is assembled into oligomeric lignan macromolecules (**6** in Fig. S1), in which from one to seven SDGs are linked by 3-hydroxy-3-methylglutaric acid (HMGA) through ester bonds (Klosterman and Smith, 1954; Kamal-Eldin *et al.*, 2001; Struijs *et al.*, 2009). Here, these macromolecules are collectively designated the SDG-HMG oligomer complex.

The following biosynthetic pathway (Fig. S1) of both SDG and SDG macromolecules in flaxseed, has been proposed: a dirigent protein-assisted coupling of two *E*-coniferyl alcohol (**1** in Fig. S1) units results in one molecule of (–)-pinoresinol (**2** Fig. S1). (–)-Pinoresinol is successively converted into (–)-lariciresinol and (+)-secoisolariciresinol (**3** and **4** in Fig. S1). Then the latter molecule is glycosylated to SDG. Finally, SDG condenses with HMG-CoA to form the SDG-HMG oligomer complex (Umezawa *et al.*, 1991; Ford *et al.*, 2001; Hano *et al.*, 2006; Hemmati *et al.*, 2010).

The *L. usitatissimum* pinoresinol-lariciresinol reductase (*LuPLR1*) gene encoding the enzyme responsible for the synthesis of the major enantiomer (+)-secoisolariciresinol is strongly expressed in the seed coats of developing flaxseed, suggesting that SDG is synthesized and accumulated in this tissue (Hano *et al.*, 2006). This is in agreement with enhanced levels of SDG in mechanically obtained coat-enriched fractions of mature seeds (Madhusudhan *et al.*, 2000; Wiesenborn *et al.*, 2003). *LuPLR2*, another *PLR* gene, encoding a protein with an enantiospecificity opposite to *LuPLR1* exists in flaxseeds (Hemmati *et al.*, 2010). *LuPLR2* is responsible for the synthesis of the minor (–)-secoisolariciresinol enantiomer in flaxseeds. It is generally accepted knowledge that lignans accumulate in the seed coats and are absent in embryos.

Fig. 1 shows the anatomical structure of mature flaxseed coats. It consists of an outer integument with layers of mucilaginous cells (MCs), parenchymatous cells (PCs), and sclerified cells (SCs) and a flat layer of compressed cells (CCs), and the inner integument

comprising the brown cell (BC) and the endosperm cell (EC) layers. Immunolocalization data obtained by using antibodies against secoisolariciresinol, the aglycone of SDG, suggested accumulation of SDG mainly in the SCs of the outer integument of mature flaxseed (Attoumbré *et al.*, 2010). The same method was applied to detect SDG in immature flaxseed at different developmental stages (Attoumbré *et al.*, 2011).

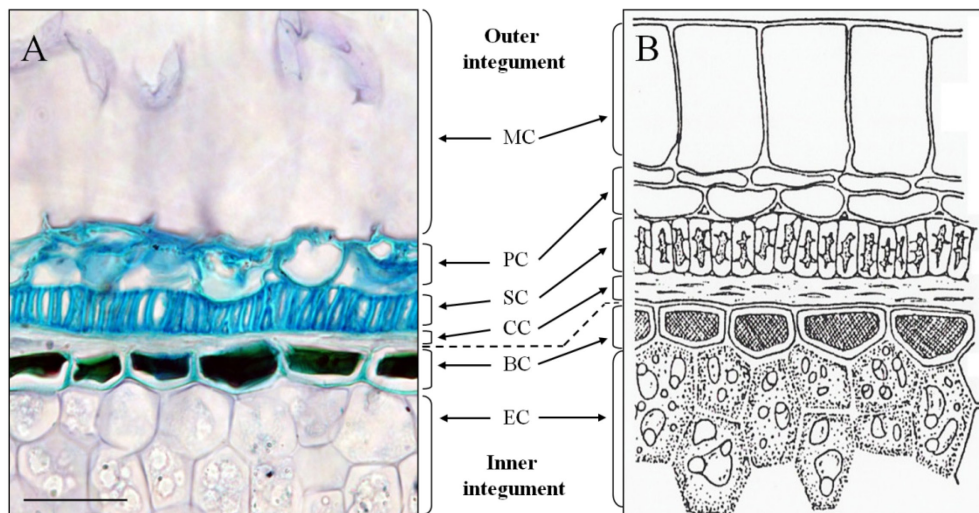


Fig. 1. Anatomy of a mature flaxseed coat. (A) Micrograph of a semi-thin section (5 μm) of mature flaxseed (cv. Barbara) coats stained with toluidine blue. Bar represents 50 μm . (B) Schematic organization of mature flaxseed coats (from P. Ozenda, *Les végétaux – organisation et diversité biologique*, Ed. Dunod, 2000 p 378, ISBN 2 10 004684 5), reproduced with kind permission of Dunod Éditeur (Paris, France). MC, mucilaginous cell; PC, parenchymatous cell; SC, sclerified cell; CC, compressed cell; BC, brown cell; EC, endosperm cell.

Further localization studies to better understand the site of synthesis and accumulation of SDG at a cellular level are presented here. Knowledge of cell-type specific localization of metabolites in seed coats would shed light on the putative ecological function of lignans, especially of the SDG oligomer complex, in defending the seeds against pathogens and/or their physiological role in seed development and germination. In addition, knowing the biosynthetic capacity of special cells in the seed coat would allow studying regulatory processes involved in individual steps of lignan biosynthesis in these cells. Understanding regulation of the lignan biosynthetic pathway would potentially open the chance to establish biotechnological production of lignans.

Laser microdissection (LMD) has been used to harvest specific tissues or cells from plant materials for transcript and protein analysis (Hölscher and Schneider, 2008; Nelson *et al.*, 2008) and enabled micro-spatial metabolic profiling studies (Hölscher and Schneider, 2007; Nakashima *et al.*, 2008; Hölscher *et al.*, 2009). In this work, LMD was employed to sample the materials from different layers of both developing and mature flaxseed coats. After SDG was released by alkaline hydrolysis, NMR and HPLC methods were applied to identify and quantify SDG in these samples by comparing data with those of the standard compound isolated from flaxseed coats.

The *LuPLR1* gene, which is involved in converting (–)-pinoresinol into (–)-lariciresinol and then into (+)-secoisolariciresinol, is expressed in flaxseed coats (Hano *et al.*, 2006). To confirm the results obtained by LMD, flax transgenic plants containing the *LuPLR1* gene promoter upstream from the β -glucuronidase (*GUS*) reporter gene (Jefferson *et al.*, 1987) were prepared. The histochemical staining of *GUS* was used to determine the location of *LuPLR1* gene expression in different developmental stage seeds, as well as *LuPLR1* gene expression was detected in different parts of wild type flaxseed by the semi-quantitative reverse transcription-polymerase chain reaction (RT-PCR). Moreover, fluorescence spectrophotometry was applied to quantify *GUS* activities in various parts of the flaxseed to obtain temporal information about *LuPLR1* gene expression.

In this article, we describe the cell layer-specific detection of secondary metabolites by using chemical and molecular methods in parallel to elucidate both the spatial distribution of SDG as well as the temporal production of SDG in flaxseed during maturation. Our results are different from those reported by immunolocalization studies of SDG in flaxseed (Attoumbré *et al.*, 2010, 2011).

Material and methods

Wild type and transgenic flaxseed

Seeds of *L. usitatissimum* cv. Barbara were obtained from the cooperative Terre de Lin (Fontaine le Dun, France) and Laboulet semences (Airaines, France). Flax plants used for LMD were raised in the greenhouse of the Max Planck Institute for Chemical Ecology in Jena, Germany. The plants were grown in soil under greenhouse conditions (day 22–24°C, night 18–20°C; 30–55% relative humidity; the natural photoperiod was supplemented with 14 h illumination from Phillips Sun-T Agro 400 Na lights). Bolls were harvested at 25 days after flowering (DAF) in order to obtain immature seeds.

Transgenic flax plants were obtained as described (Renouard *et al.*, 2012). In brief, the *Agrobacterium tumefaciens* strain GV3101 (pGV2260) was used for transformation. The construct contained an 895 bp fragment of the *LuPLR1* gene promoter (accession number AY654626) cloned upstream from the *GUSint* reporter gene (which contains an intron) into the *HindIII-XbaI* sites of pGIBin19 plasmid; a transcriptional fusion with the *GUSint* reporter gene was then created.

Transgenic flax plants and wild type plants were grown in the greenhouse of the Centre de Ressources Régionales en Biologie Moléculaire (CRRBM) of the University of Picardie Jules Verne under the conditions mentioned above. Seeds were harvested at different developmental stages for further gene expression studies: S0 (ca 4 DAF, embryo not visible);

S1 (ca 10 DAF, embryo 0.5-1 mm); S2 (ca 16 DAF, embryo 2-3 mm); S3 (ca 22 DAF, embryo 4-5 mm, green seed), S4 (ca 28 DAF, embryo 5 mm, seed coat turning brown), S5 (mature seed ca 40 DAF, embryo 5 mm, brown seed coat).

Manual separation of mature seeds

The work flow involved in separating mature seeds and 25 DAF seeds is shown in Fig. 2. Flaxseed was manually separated under a binocular microscope Stemi DV4 (Carl Zeiss MicroImaging GmbH, Jena, Germany). Mature seeds were cut longitudinally around the equator into two halves and embryos were removed from seeds by using a needle. The seed coats contain two parts, outer and inner integuments, which attach to each other loosely (Fig. S2A). It was easy to separate the outer and inner integuments by a very fine forceps and a needle under a microscope (Fig. S2B). Material of the mucilaginous cell layer can be picked by a needle under the microscope and separated from the rest of the seed coat (Fig. S2C).

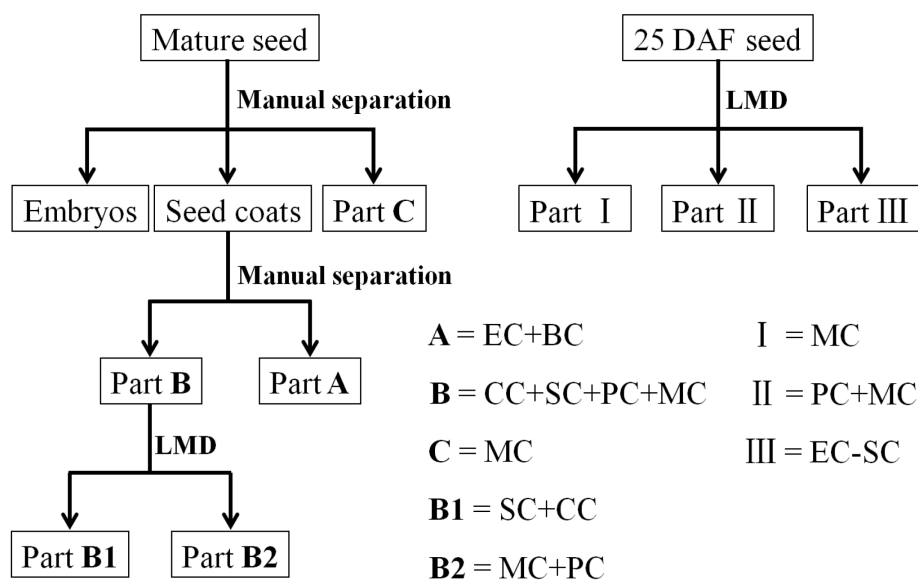


Fig. 2. Schematic representation of workflow involved in separating mature and 25 DAF flax seeds. Mature flaxseed was divided into embryos and seed coats; seed coats are further separated into two parts, **A** and **B**. **A** contains ECs and BCs, and **B** consists of CCs, SCs, PCs and MCs. LMD was applied to cut **B** into two subparts, **B1** and **B2**, which comprise SCs and CCs, PCs and MCs, respectively. Some material was isolated from MCs as part **C**. After sample preparation, 25 DAF seed coats were directly dissected into three parts, **I** (MCs), **II** (MCs + PCs) and **III** (ECs-SCs). DAF, days after flowering; LMD, laser microdissection; MC, mucilaginous cell; PC, parenchymatous cell; SC, sclerified cell; CC, compressed cell; BC, brown cell; EC, endosperm cell.

Laser microdissection

The basic work flow of LMD has been reported (Moco *et al.*, 2009). The materials (outer integument for a mature seed or a whole developing seed) were fixed vertically in Jung tissue freezing medium (Leica Microsystems GmbH, Nussloch, Germany), and immediately frozen in liquid nitrogen. Serial cryosections (25 µm thickness) were prepared at -24°C using a cryostat microtome (Leica CM1850, Bensheim, Germany) and directly mounted on PET-Membrane FrameSlides (MicroDissect GmbH, Herborn, Germany).

The laser dissections were performed on the Leica LMD 6000 microdissection system (Leica Microsystems GmbH, Wetzlar, Germany) equipped with a nitrogen solid state diode laser of a short pulse duration (355 nm). The settings were as follows: 20× magnification, laser intensity of 90, laser moving speed of 1 (the slowest). The cut materials were collected in the cap of a 0.5 ml centrifuge tube by gravity. The pictures were taken by an integrated camera HV-D20P (Hitachi, Tokyo, Japan).

Alkaline hydrolysis of separated samples

Manually separated samples were transferred into 20 ml glass vials. Then 4 ml 20 mM NaOH (in MeOH / H₂O 1:1) was added. After magnetic stirring at ambient temperature for 3 h, the solutions were neutralized with 1% (V/V) acetic acid. Laser-microdissected samples were transferred into HPLC vials (1.5 ml), 1 ml 20 mM NaOH (in MeOH / H₂O 1:1) was added and the samples were hydrolyzed correspondingly. The hydrolysis solutions were dried in vacuum <40 °C.

NMR analysis of alkaline hydrolyzed samples

The manually separated samples were extracted with 600 µl MeOH-*d*₄ (99.96%, Deutero GmbH, Kastellaun, Germany) in an ultrasonic bath for 2 min and filtered into 5 mm diameter NMR tubes. The LMD samples were prepared in the same way but with 90 µl solvent and 2 mm NMR tubes. ¹H NMR and 2D spectra (¹H, ¹H COSY and HSQC) were recorded at 300 K in a Bruker Avance 500 NMR spectrometer equipped with a 5 mm cryogenic TCI probe (Bruker-Biospin, Rheinstetten, Germany). ¹H NMR spectra were recorded with 1024 scans. The residual HDO signal was suppressed using the PURGE sequence (Simpson and Brown, 2005). The residual signals of methanol-*d*₄ at δ_{1H} 3.31 and δ_{13C} 49.00 were used as chemical shift references (Gottlieb *et al.*, 1997).

HPLC analysis of alkaline hydrolyzed samples

Analytical HPLC (paper 5.1) was performed on an Agilent series HP1100 (binary pump G1312A, autosampler G1367A, diode array detector (DAD) G1315A, 200–700 nm) (Agilent Technologies, Waldbronn, Germany). A LiChrospher RP18 column (5 µm, 250 × 4 mm, Merck KGaA, Darmstadt, Germany) was used with a linear binary gradient of H₂O (solvent A) and MeCN (solvent B), both containing 0.1% (V/V) trifluoroacetic acid, with a flow rate of 0.8 ml min⁻¹ at 25 °C as follows: 0 min: 5% B, 35 min: 25% B, 37 min: 95% B, 47 min: 95% B, 50 min: 5% B, and 60 min: 5% B. The injection volume was 5 µl. The HPLC eluate was monitored by DAD at 280 nm.

Manual dissection of developing seeds for gene expression studies

For *GUS* activity assays, immature seeds of stages S2, S3 and S4 were cut longitudinally with a scalpel and the embryos were removed with a needle. S0 and S1 early stages (embryo too small) and S5 (mature seeds) were used as a whole. For semi-quantitative RT-PCR, S3 developing seeds (wild type) were cut longitudinally on one side with a scalpel; the embryos were removed with a needle, and inner and outer integuments were separated under binocular microscope using fine forceps.

Quantitative GUS activity assay

β -Glucuronidase activity of immature seeds (whole seeds, manually separated seed coats and embryos) was estimated as described by Renouard *et al.* (2012) using 4-methylumbelliferyl- β -D-glucuronide (4-MUG, Sigma) as substrate. Immature seeds of stages S2, S3 and S4 were cut longitudinally with a scalpel and the embryos were removed with a needle, *GUS* activities of seed coats and embryo were measured separately. Seeds of early stages, S0 and S1 (embryo too small), and S5 (mature seeds) were used as a whole.

Histochemical GUS assays

Seeds (harvested from transgenic plants grown in the greenhouse) at different stages of development (S1, S2, S3, and S5) were cut transversally and subjected to histochemical staining for *GUS* activity as described by Jefferson *et al.* (1987) and modified (Kosugi *et al.*, 1990) to avoid background that could be due to non-specific endogenous *GUS* activity (i.e. with 20% methanol in 5-bromo-4-chloro-3-indolyl- β -D-glucuronic acid (X-Gluc) solution). A K^+ ferricyanide/ferrocyanide mixture (2 mM of each) was also added to the incubation buffer to prevent the diffusion of the indoxyl derivative before its oxidative dimerization.

Semi-thin sections were then obtained as described by Hawkins *et al.* (2002). Briefly, *GUS*-stained samples were fixed in formalin acetic alcohol (FAA) (10% formalin (37% formaldehyde stabilized with methanol), 5% glacial acetic acid, 60% ethanol) for 24 h, dehydrated and embedded in paraffin. Semi-thin sections (5 μ m) were made on a RM 2145 rotary microtome (Leica, Wetzlar, Germany), then deparaffined and counter-stained with periodic acid Schiff to visualize the cell walls in each tissue before permanent mounting and microscopic observation. Pictures were taken with a Nikon Coolpix 5400 digital camera (Nikon, Tokyo, Japan). The same experiments were conducted on different stage wild type seeds as negative control.

RNA extraction and semi-quantitative RT-PCR

RNA was isolated from the embryo, inner integument and outer integument of S3 (ca 22 DAF) immature seeds (separated using scalpel and forceps under binocular microscope) using the protocol described (Gutierrez *et al.*, 2006). S3 developing seeds (wild type) were cut

longitudinally on one side with a scalpel; the embryos were removed with a needle, and inner and outer integuments were separated under binocular microscope using fine forceps.

Reverse transcription and PCR amplification were performed as described by Renouard *et al.* (2012). A 939 bp fragment of the *LuPLR1* cDNA was amplified using *PLRF1* forward primer (5'-ATGGGGCGGTGCAGAGTTCT-3') and *PLR-R1* reverse primer (5'-TCAAAGGTAGATCATCAG A-3') designed from the flax *LuPLR1* cDNA sequence (accession number AX191955). A PCR product (632 bp) corresponding to the exon 2 of the *ACTIN* gene was amplified with ACT-F2 forward primer (5'-TCTGGAGATGGTGTGAGCCACAC-3') and ACT-R2 reverse primer (5'-GGAAGGTACTGAGGGAGGCCAAG-3') designed from the tobacco sequence. cDNA fragments were amplified during 25, 27 and 30 cycles.

Lignin analysis

Entire integuments of mature flaxseed were ground (grinder MM301, Retsch, Germany) and ultrasonicated for 10 min in EtOH / H₂O 1:1 to extract the lignan macromolecule. The residue was then submitted to thioacidolysis. Another sample was submitted to thioacidolysis without prior extraction. The monomer composition of the labile ether lignin fraction was determined by thioacidolysis, which specifically disrupts the non-condensed intermonomer linkages (alkyl-aryl ether). The reaction was performed using 10 mg teguments and ethanethiol/BF₃ etherate/dioxane reagent as detailed previously (Lapierre *et al.*, 1986). Tetracosane was added as an internal standard. After 4 h, the mixture was extracted with CH₂Cl₂ (3×25 ml). Guaiacyl (G) and syringyl (S) thioethylated monomers were determined as their trimethylsilyl derivatives using a gas chromatograph equipped with a fused silica capillary DB1 column (30 m×0.3 mm) (J&W Scientific, Folsom, CA, USA) and flame ionization detector. The temperature gradient was 160–280°C at 2°C min⁻¹.

Results

Manual separation and laser microdissection of the seed coat cell layers

First, the embryo was removed from the mature seed and embryo extracts were analyzed by HPLC and NMR, demonstrating the absence of SDG (data not shown). Then the seed coats were manually separated into two parts (Fig. S2B), **A** (inner integument, 10.5 mg) and **B** (outer integument, 13.0 mg). Part **A** contains layers of endosperm cells (ECs) and brown cells (BCs), and part **B** comprises four layers, from inner to outer: compressed cells (CCs), sclerified cells (SCs), parenchymatous cells (PCs) and mucilaginous cells (MCs) (Figs. 1, 2 and 3A). Material from MCs (1.8 mg) was manually collected from seed coats as part **C** (Fig. S2C). Part **B** obtained by manual separation was cryosectioned. LMD was used to

dissect cell layers of part **B** into two subparts **B1** (CCs + SCs, 380 µg) and **B2** (PCs + MCs, 440 µg) (Fig. 3E-H). The material includes the supporting polyethylene terephthalate (PET) membrane of the frame slide, which was unavoidably cut together with the cells. LMD turned out to be excellent for dissecting seed coats because of the rigid architecture of their cell walls and relatively low water content. The characteristic cell shape and the autofluorescence of seed coat cells were used to identify the target material without staining.

Table 1. SDG contents of seed coat cell layers determined by HPLC after alkaline hydrolysis. SDG concentrations were calculated as the percent of SDG amounts in separated material amounts. ND means no detectable peak in chromatogram.

	Part	Cell layer	Separated material amount (mg)	Peak area (mAU)	SDG amount (µg)	SDG concentration (%)
Mature seeds	Manual separation	A EC + BC	10.50	3.64	1.6	<<0.1
		B CC + SC + PC + MC	13.00	1418.22	400.0	3.1
	LMD	C MC	1.80	1.69	1.0	<0.1
		B1 CC + SC	0.38	ND		
		B2 PC + MC	0.44	46.11	13.5	3.1
25 DAF seed	LMD	I MC	0.20	0.74	0.7	0.4
		II PC + MC	0.25	24.00	7.3	2.9
		III EC-SC	0.57	2.98	1.4	0.2

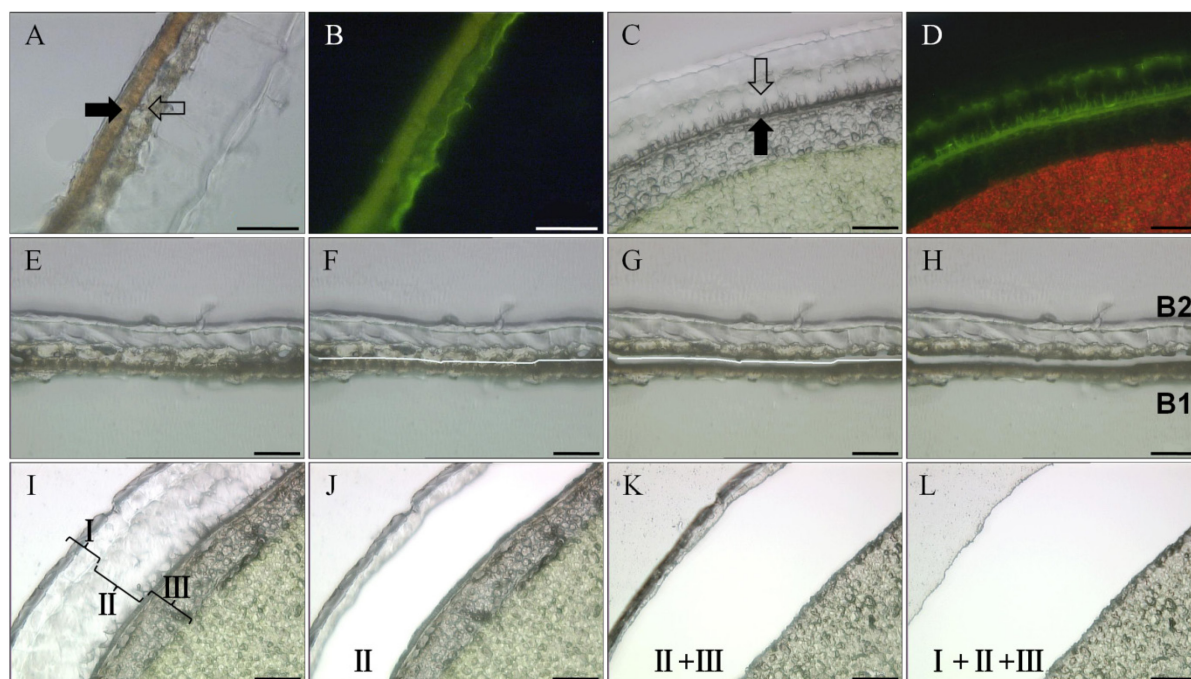


Fig. 3. Anatomical pictures and workflow of laser microdissection (LMD) taken with a HV-D20P camera integrated in the LMD 6000 micro dissection system. (A, B) Micrographs of part **B** of mature flaxseed coats under light and fluorescence, respectively. The full arrow shows SCs, and the empty arrow shows PCs. Bars represent 100 µm. (C, D) Anatomical structures of 25 DAF seed coats under light and fluorescence. Developing SCs and PCs are marked by full and empty arrows, respectively. Bars represent 50 µm. The fluorescence optic settings are as follows: excitation = 450-490 nm, dichroic mirror = 510 nm, and emission = 515 nm. (E-H) The LMD work flow of dividing part **B** is as follows: (E) Tissue of part **B** before laser cutting, (F) drawing a cutting line using the software of the laser microscope, (G) laser cutting alongside the software-drawn line, and (H) separated subparts **B1** and **B2** after cutting. Bars represent 100 µm. (I-L) Work flow of separating 25 DAF seed coats into three parts **I** to **III**. (I) Tissue of immature seed coats before laser cutting, (J) tissue after cutting part **II**, (K) tissue after successively cutting parts **II** and **I**, (L) tissue after successively cutting parts **II**, **I** and **III**. Bars represent 50 µm. DAF, days after flowering; PC, parenchymatous cell; SC, sclerified cell.

Immature seeds were harvested at 25 DAF. At that developmental stage, the ultrastructure of seed coats (Figs. 3C and D) is not yet fully developed and manually separating cell layers is very difficult. Hence, the entire seed was subjected to cryosectioning. LMD was used to dissect seed coats into three different parts: **I** (MCs, 200 μ g), **II** (PCs + MCs, 250 μ g) and **III** (from SCs to ECs, 570 μ g) (Figs. 3I-L). Again, the collected masses contain a portion of the PET slide membrane. The material sampled by LMD was subjected to HPLC and NMR analyses. Some blank membrane pieces with fixation medium was collected and analyzed as control. No clear signal in NMR spectrum and no clear peak in HPLC chromatogram were observed.

NMR analysis results of alkaline hydrolyzed samples

SDG was released from the separated samples by alkaline hydrolysis. In the ^1H NMR spectra (Fig. 4), SDG is readily determined by the diagnostic SDG signals of the trisubstituted phenyl ring (H-5/5': δ 6.64; H-2/2': 6.58; H-6/6': 6.56) and the doublet of the proton at the anomeric center of glucose (H-1''/1''': δ 4.23). Intense signals of SDG appeared in the NMR spectra obtained from extracts of the outer integument (**B**) of the mature seed coats. However, SDG can hardly be observed in part **A** (ECs + BCs) and **C** (MCs). In LMD samples, SDG was the major component of **B2** (MCs + PCs), and SDG was not found in **B1** (CCs + SCs). In the immature seeds (25 DAF), SDG was detected mostly in part **II**, which corresponds to MCs + PCs. A trace of SDG was found in part **III** (from SCs to ECs), and no SDG was observed in part **I** (MCs).

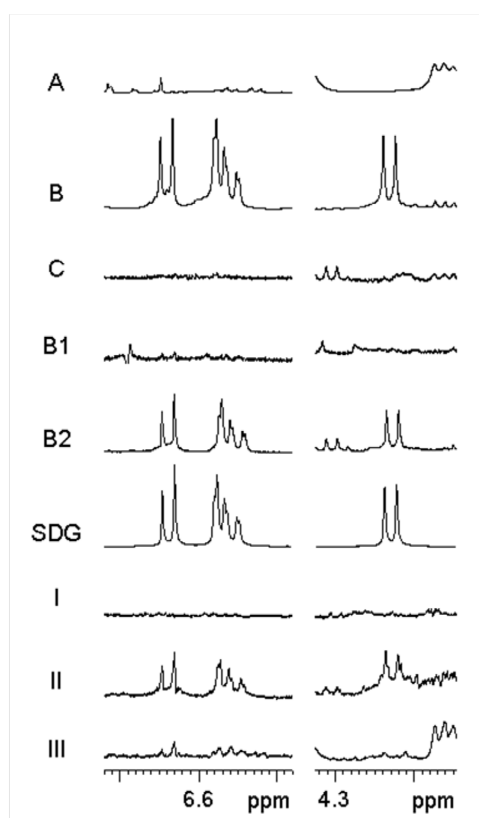


Fig. 4. ^1H NMR spectra (500 MHz, methanol- d_4) of hydrolyzed material from different cell types of flaxseed coats. ^1H NMR spectra **A**, **B**, **C**, **B1**, and **B2** were obtained from mature seed samples. **SDG**: ^1H NMR spectrum of secoisolariciresinol diglucoside. ^1H NMR spectra **I**, **II**, and **III** were obtained from 25 DAF seed samples. For details of sample preparation, see Figs. 1 and 2. Partial ^1H NMR spectra show characteristic SDG signals of the aromatic protons (H-5/5': δ 6.64; H-2/2': 6.58; H-6/6': 6.56) and the doublet of the proton at the anomeric center of glucose (H-1''/1''': δ 4.23). DAF, days after flowering.

HPLC analysis results of alkaline hydrolyzed samples

SDG concentrations in seed coat samples were quantified using HPLC-DAD. The chromatograms (280 nm) of extracts from cells of mature seeds and 25 DAF seeds are shown in Fig. S3, and the concentration values, which were calculated by using an SDG linearity equation, are listed in Table 1. The HPLC and NMR data are consistent. In mature seed coats, part **B** contains 3.1% (w/w) SDG, and the concentrations of SDG in parts **A** and **C** were clearly below 0.1 % (calculated as 0.01% in **A** and 0.06% in **C**). SDG was detected only in **B2** in a concentration of 3.1%. In 25 DAF seed coats, SDG was mostly found in part **II**, most of whose material was from developing PCs.

Quantification of LuPLR1 gene expression by β -glucuronidase (GUS) activity assay

LuPLR1 promoter transcriptional activity was estimated by measuring *GUS* activity in seeds of transgenic plants (*LuPLR1* promoter-*GUS* reporter gene construct) (Fig. 5). Enzyme activity was detectable as early as S0, then increased during phases of seed development to reach a maximum at S3 and finally decreased during the seed maturation phase (S4, S5). Manual separation at stages S2, S3 and S4 revealed that activity was mainly localized in seed coats. Indeed, *GUS* activity in embryos was very low and did not exceed the non-specific “*GUS*-like” activity of wild type S3 whole seeds.

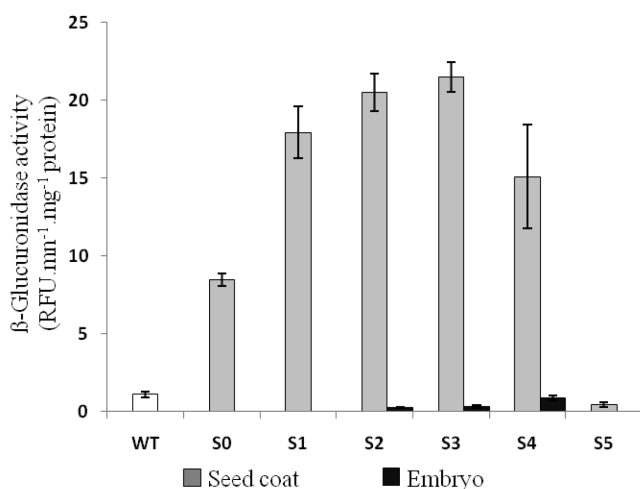


Fig. 5. *GUS* activities from embryo and seed coats in the developing seeds of flax plants stably transformed with an 895-bp *LuPLR1* promoter-*GUS* reporter gene construct are shown. S0, S1, S2, S3, S4 and S5 correspond to ca 4, 10, 16, 22, 28 and 40 days after flowering, respectively, and WT represents the activity measured in an S3 wild type whole seed.

Cell-specific LuPLR1 gene expression by histochemical GUS assay

Histochemical *GUS* assay performed on developing seeds at stages S1, S2, S3 and S5 revealed strong *GUS* activities localized in the outer integument (Part **B**) of S1, S2 and S3 but not S5, whereas no enzyme activity could be detected in the inner integument (Part **A**) and the embryo regardless of the developmental stage (Figs. 6A-D).

Semi-thin sections of seeds preliminary assayed for *GUS* activity allowed more precise localization of *LuPLR1* promoter transcriptional activity. *GUS* activity was mainly localized in the PCs, no matter what developmental stage was studied (S1, data not shown; S2

and S3) except for the mature seeds, in which no staining could be detected (Figs. 6B-F). Weak *GUS* activity could be detected in the MCs of S2 developing seeds. Staining was also observable in SCs and in CCs from S3 seed coats. No *GUS* activity was observed in BCs and ECs regardless of the development stage considered. In the seeds of wild type plants, no *GUS* staining could be observed in any cell layer and at any developmental stage studied (data not shown).

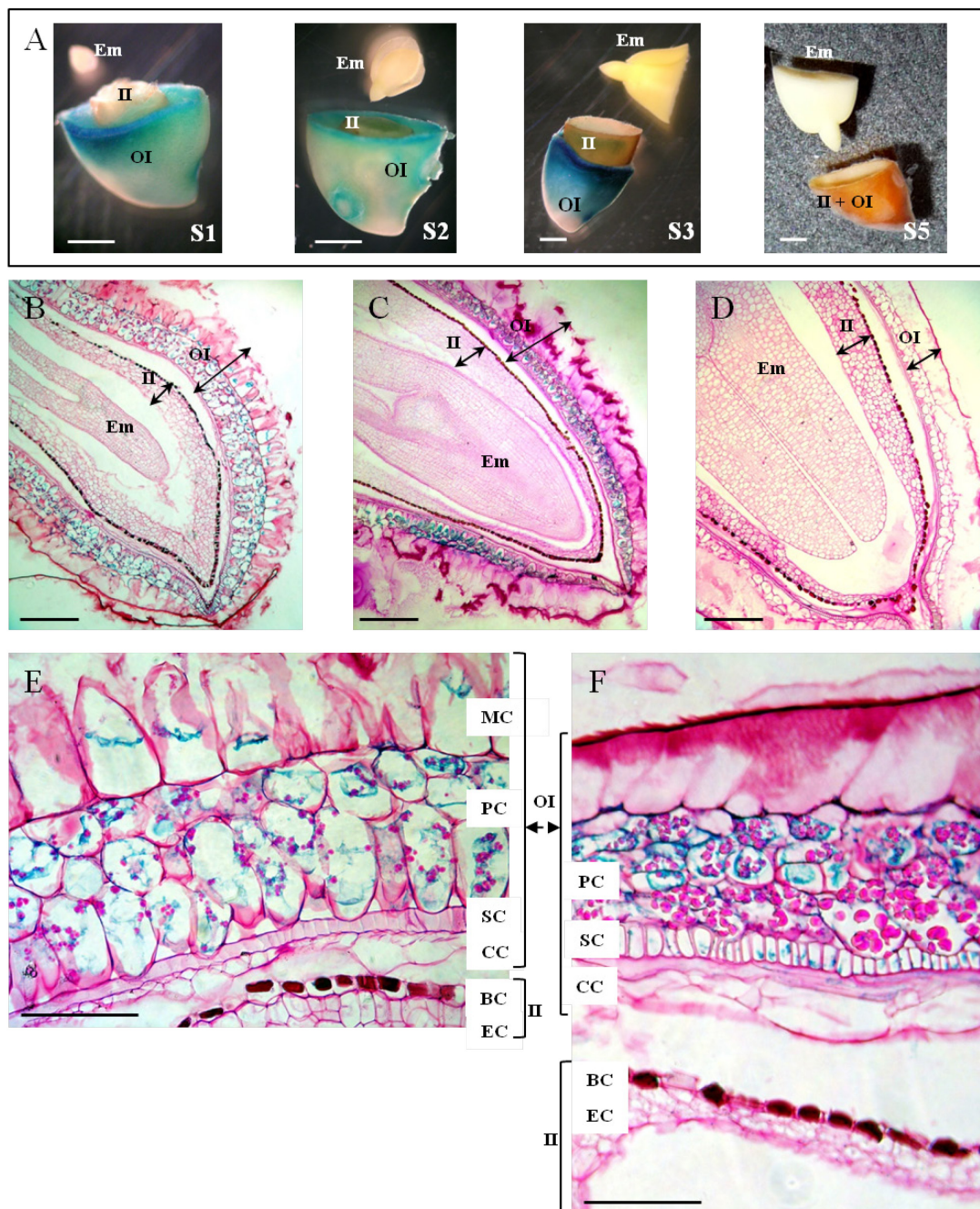


Fig. 6. Histochemical studies of the localization of *LuPLR1* promoter-driven *GUS* gene expression in transgenic flaxseed at different developing stages. (A) *GUS* assays performed on transversely cut seeds at S1, S2, S3 and S5 (mature seed). Bars represent 1 mm. (B-D) Semi-thin sections (5 μ m) of S2 (B, longitudinal), S3 (C, longitudinal) and S5 (D, transverse) seeds assayed by *GUS* activities. Bars represent 250 μ m. (E, F) *GUS* staining in semi-thin sections (5 μ m) of S2 (E) and S3 (F) seed coats. Bars represent 50 μ m. OI, outer integument (Part B); II, inner integument (Part A); Em, embryo. MC, mucilaginous cell; PC, parenchymatous cell; SC, sclerified cell; CC, compressed cell; BC, brown cell; EC, endosperm cell.

RT-PCR detection of LuPLR1 gene expression in wild type plants

Since gene expression was highest in S3 of transgenic seeds and then dropped, this developmental stage was used to detect *LuPLR1* by RT-PCR in manually separated outer integument (Part **B**), inner integument (Part **A**) and embryo. S3 stage developing seeds (ca 22 DAF) of wild type plants were chosen for manual dissection. *LuPLR1* gene expression was by far the highest in the outer integument of transgenic seeds. The results shown in Fig. 7 indicate that *LuPLR1* is expressed strongly in the outer integument. Only a weak *LuPLR1* signal was visible in the inner integument, while no transcripts could be detected in the embryo, confirming the results of quantitative *GUS* assays.

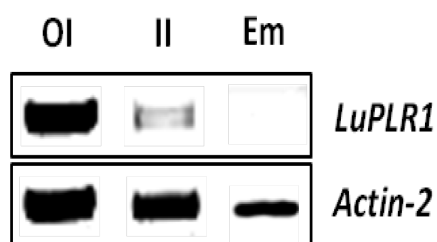


Fig. 7. *LuPLR1* gene expression in the outer integument (OI), inner integument (II) and embryo (Em) of S3 (ca 22 days after flowering) wide type developing seeds analyzed by RT-PCR. Total RNA isolated from manually separated tissues was subjected to RT-PCR semi-quantitative analysis using an *ACTIN* gene as internal control. 27-cycle PCR products (10 μ m) were loaded on 1 % (w/v) agarose gel. OI, outer integument (Part **B**); II, inner integument (Part **A**); Em, embryo.

Lignin analysis

Chemical characterization and quantification of lignin were performed on material from mature seed coats. Thioacidolysis was used as previously described for flax stem material (Day *et al.*, 2005a). Before and after methanol extraction, no syringyl lignin was found; only guaiacyl was quantified (non-extracted sample: 22.8 \pm 4 μ mol g⁻¹ sample; ethanol-extracted sample 15.3 \pm 1 μ mol g⁻¹ sample). Although these values are low, they indicate the occurrence of lignin or lignin-like structures in the flax seed coat. The tri-substituted aromatic rings of the guaiacyl lignin are identical with those of the SDG.

Discussion*SDG localization in mature and immature flaxseed*

The cell layer-specific localization of SDG in flaxseed coats and the temporal progression of SDG production during maturation have been investigated by chemically analyzing microdissected samples and gene expression. As previously reported (Hano *et al.*, 2006; Attoumbré *et al.*, 2010, 2011), and also indicated by our NMR and HPLC analyses, SDG accumulates in seed coats, not in embryos.

Based on the NMR and HPLC analyses of samples from mature seed coats collected by manual separation, a high concentration of SDG (3.1%) was located in the outer integument (part **B**) but only a trace concentration (0.06%) was found in the layer of mucilaginous cells (MCs, part **C**). Because the constituents of MCs are pectins (Naran *et al.*, 2008), and no

phenolics have been found there before, it seems reasonable to assume that the trace of SDG detected in MCs resulted from contamination by material from the adjacent parenchymatous cell (PC) layer displaced during manual separation. In the two subparts divided from **B** by LMD, SDG was detected only in **B2**, which contains MCs and PCs, but not in **B1**, which contains compressed cells (CCs) and sclerified cells (SCs) (Figs. 4 and S3, Table 1). The concentration of SDG in the inner integument (part **A**), which was as low as 0.01%, was probably due to contamination, again originating from PCs during manual separation. Therefore, according to chemical analysis, all SDG in mature seeds was thought to locate in the PC layer of the outer integument.

The NMR and HPLC results (Figs. 4 and S3, Table 1) obtained from 25 DAF seeds indicated that the highest level of SDG was found in part **II** of the seed coats and minor levels were found in parts **III** and **I** of the seed coats. Thus, the PC layer is the major location of SDG in developing seeds already; around 78% of the total amount of SDG in 25 DAF seeds was detected in this cell layer. Unlike mature seeds, seeds in the early developing stage do not contain a complete PC layer. The PC layer, which is around 80 µm wide measured in the middle of 25 DAF seeds, is filled with liquid-like material. This could explain how a small amount of SDG is found in part **I**, because the material in PCs may easily delocalize during cryosectioning or the preparation of the slides, and LMD. Material diffusion may also cause the boundary between SCs and PCs to become indistinct, another reason may be SDG detected in part **III** of 25 DAF seeds.

The detection of high levels of SDG in PCs contradicts recently reported immunolocalization data (Attoumbré *et al.*, 2010, 2011), arguing for the accumulation of lignans in the secondary cell walls of SCs. Attoumbré *et al.* (2011) immuno-detected lignans in the SCs of developing flaxseeds. However, they failed to detect SDG in future SCs at an early developmental stage, while at the same time SDG was measured by HPLC in extracts of whole seeds. If these data are correct, it must be concluded that SDG is compartmentalized to tissue different from the SCs. Furthermore, lignans were not detected by immunolocalization in the endosperm of the developing seeds at any stage. Using HPLC instead of immunolocalization to analyze separated endosperm and inner integument cells layers, however, SDG was detected at 16 DAF. Again, contradictory results were obtained using two different methods, immunolocalization and HPLC. Therefore, it seems problematic to conclude from such data that lignans are located in SCs. It is likely that the reported immunoreaction is not specific to lignans including the SDG-HMG oligomer complex. In fact, Attoumbré *et al.* (2010, 2011) used antibodies which were developed using secoisolariciresinol (which occurs in flaxseed coats in very low levels only), not SDG nor the

SDG-HMG complex, as a hapten for immunization. Moreover, considering that cross-reactivity for SDG was 22.1% and for other lignans up to 32.8 %, the specificity of the antibodies to SDG used was relatively low. It was also pointed out in Attoumbré *et al.* (2010, 2011) that the specificity of the antibodies is relative to the substituent at the aromatic ring and at C-8 /C-8' of the lignan side chains. It is unclear, therefore, whether the ester-type bond, which connects SDG through HMGA to SDG-HMG oligomer complexes (Ford *et al.*, 2001), affects the interaction with the antibodies. Although monolignols (coniferyl alcohol, *p*-coumaryl alcohol) may cross-react with the antibodies used no such data were reported (Attoumbré *et al.*, 2010).

Flax lignin has been reported as highly condensed and rich in guaiacyl moieties (G lignin) (Day *et al.*, 2005a) and our data indicate the occurrence of G lignin or lignin-like structures in the flax seed coat. Recent attempts to localize lignin using the Wiesner reaction in the outer integument resulted in light red coloration of sclerified cells but failed when polyclonal antibodies against guaiacyl lignin homopolymer were applied (Attoumbré *et al.* (2010). The failure of immunodetection was used in a chain of arguments to suggest that anti-lignan antibodies do not recognize lignin epitopes and are specific of lignans (Attoumbré *et al.* (2010). However, to be conclusive, the data obtained with polyclonal antibodies against guaiacyl lignin homopolymer would have to be supplemented by using antibodies directed against the other lignin types. Moreover, the reactivity of lignan antibodies should have been tested against different types of lignin. Our finding that flax seed coats contain guaiacyl units but no syringyl units in the lignin supports the suggestion that structures other than SDGs are responsible for the positive reaction of antibodies raised against SDG reported (Attoumbré *et al.*, 2010). Another explanation for the positive immunolabelling in SCs (Attoumbré *et al.*, 2010) could be that the *PLR* product (aglycone SECO) might have been synthesized but not converted to a diglucosylated and complex form (SDG-HMG); from this form, it is incorporated in the cell wall in a post-lignification “infusion” process.

Another point to be mentioned is the poor solubility of SDG and SDG oligomers in water (Zhang *et al.*, 2009) which may result in leakage from PCs to their neighbor cells, i.e. SCs during the ethanol dehydration steps applied by Attoumbré *et al.* (2010); meanwhile, SDG may stick to the lignified SC walls as these are more hydrophobic than the walls of PCs. Attoumbré *et al.* (2011) manually separated flaxseed of different developmental stages after they had been immersed in water for 1 h. In our experience, such separation methods are inadequate, again because of the weak solubility of SDG and SDG oligomers in water (Zhang *et al.*, 2009). Also the physical stability of the PC layer at the early developmental stages is insufficient to allow it to keep its integrity during the separation procedure.

Location of SDG biosynthesis

Two enzymatic assays (quantitative and histochemical) combined with semi-quantitative RT-PCR measurements confirmed that *LuPLR1* is expressed mainly in the seed coats. *LuPLR1* is responsible for the synthesis of the major (+)-secoisolariciresinol enantiomer (87%) while a minor quantity of the (–)-secoisolariciresinol enantiomer (13%) is synthesized by *LuPLR2* (Hemmati *et al.*, 2010). The very weak β -glucuronidase (*GUS*) activity detected in embryos has to be attributed to non-specific *GUS* that has already been reported in seeds of a number of plants (Hu *et al.*, 1990; Hänsch *et al.*, 1995). *GUS* activities measured at different developmental stages in the coats and embryos of transgenic flax seeds containing the *LuPLR1* gene promoter were in accordance with those of previously published semi-quantitative RT-PCR experiments (Hano *et al.*, 2006), confirming that the SDG biosynthetic pathway is active already at S0 and reaches a maximum during S1, S2 and S3 (Fig. 5). RT-PCR analyses of three separated parts (embryos, inner and outer integuments) of S3 seeds from wild type plants indicated that *LuPLR1* is expressed in the outer integument, which also has been observed in transgenic plants. The weak amplification signal in the inner integument could be attributed to tissue contamination during manual dissection, confirming data of NMR and HPLC analyses. Co-localization of SDG and *LuPLR1* expression suggests that glucosylation of (+)-secoisolariciresinol (**4** in Fig. S1) also occurs in the PCs, which both synthesize (+)-secoisolariciresinol and accumulate SDG.

Generally, data on histolocalization of *LuPLR1* promoter-driven *GUS* expression at development stages S1 – S3 show that PCs are the major location of SDG synthesis, which LMD / HPLC and NMR data on SDG accumulation in mature and 25 DAF flaxseed also show. Histochemical assay did not detect *GUS* at S5. This is consistent with data showing that *GUS* activity is very weak in S5 flaxseed, suggesting that SDG synthesis is completed before maturity.

GUS activity observed in some MCs at S2, and in some SCs and CCs at S3, suggesting that SDG in layers of non-PCs is due to the delocalization of PC material during cryosectioning and mounting. Otherwise, *GUS* would be detected in all MCs, SCs or CCs. The literature offers several other possible explanations of visible *GUS* staining in partial SCs and CCs at S3 of seed development as the result of *LuPLR1* promoter transcriptional activity. Expression of *LuPLR1* in SCs could be related to the fact that these cells are undergoing lignification. It has been proven using immunolocalization and in situ hybridization techniques in *Forsythia intermedia*, that lignan biosynthetic genes such as dirigent proteins and *PLR* genes are expressed in xylem and other lignifying tissues (Burlat *et al.*, 2001; Kwon *et al.*, 2001). More recently, it has been demonstrated that overexpression of two *Pinus taeda*

MYB transcription factors (PtMYB1 and PtMYB8) in *Picea glauca* resulted in up-regulation of phenylpropanoid and monolignol biosynthetic genes as well as two *PLR* encoding genes (Bomal *et al.*, 2008). Lignans such as pinoresinol can also be found in a methanol-soluble oligolignol fraction of lignifying xylem (Morreel *et al.*, 2004) or in differentiating tracheary elements (Tokunaga *et al.*, 2005) and are therefore able to be incorporated into the lignin polymer. In some Pinaceae species, lignans (8-8' linked) and neo-lignans (8-5' linked) are known to be infused in the heartwood after lignification, increasing its resistance and durability (Gang *et al.*, 1999). The hydrophilic knotwood extracts of different coniferous species have been also shown to contain mainly lignans, among which lariciresinol, secoisolariciresinol or matairesinol can be found in variable amounts according to the species (Willför *et al.*, 2003).

Applications of LMD in plant metabolite studies

The conventional histological methods to study the spatial distribution of metabolites in microscopic plant samples make use of in situ labeling and (or) staining techniques. Due to the structural analogy among metabolites of many plants, the specificity of histological method is relative low. Recent developments in mass spectrometry (Svatoš, 2011) and Raman imaging (Freudiger *et al.*, 2008) are promising tool in metabolic profiling. However, these techniques mostly focus on metabolites on sample surfaces and do not allow detection of three-dimensional distribution of metabolites within the tissue. NMR, though representing the most informative analytical method and being able to provide data on three-dimensional spatial distribution, is of limited suitability to identify metabolites directly from plant samples, due to its moderate sensitivity. In order to take advantage of its superior properties for metabolic profiling, NMR has to be combined with appropriate sampling methods. LMD was used for sampling plant material for DNA, RNA and protein analyses (Kehr, 2001, 2003; Day *et al.*, 2005b; Nelson *et al.*, 2006; Nelson *et al.*, 2008) and to dissect plant material for the analysis of both primary metabolites (Angeles *et al.*, 2006; Obel *et al.*, 2009; Thiel *et al.*, 2009; Schiebold *et al.*, 2011) and secondary metabolites (Hölscher and Schneider, 2007; Li *et al.*, 2007; Hölscher *et al.*, 2009; Abbott *et al.*, 2010). As presented here, LMD combined to NMR and HPLC, allows for the quantitative spatio-temporal analysis of metabolites in plant cells. Future advances in LMD, such as improvement in target cell-recognizing software, multi-target sampling, hyphenation with sensitive detectors, together with NMR sensitivity enhancement, will enable more efficient cell-specific identification and quantification of metabolites in plant tissue.

As a conclusion, LMD was applied for the first time in combination with chemical treatment, and two analytical methods, NMR and HPLC, to elaborate the spatio-temporal

location of metabolites in plants on the cellular level. This work also shows that laser microdissection is able to provide material sufficient for multiple analytical manipulations. The study constitutes a technical advance for the better understanding of the regulation of SDG biosynthetic pathway in flaxseed. Not only it allowed cell layer-specific location and time course analysis of SDG synthesis but also could be a powerful tool for future transcriptomic studies (Hölscher and Schneider, 2008; Nelson *et al.*, 2008; Matas *et al.*, 2011; Rajhi *et al.*, 2011; Olofsson *et al.*, 2012), the isolation of transcription factors controlling SDG synthesis in the parenchymatous cell layer being a great challenge.

The ecological role of flax lignans in the developing and mature seed still awaits to be identified. However, the location of the SDG polymer complex in the parenchymatous cells just below the external mucilaginous cell layer suggests chemical defense against insects and microorganisms. An additional physiological function of lignans in seed development or germination is possible. It is also plausible that the SCs, supplementary to their role in providing the flaxseed scaffold, represent a mechanical defense barrier against invading organisms. Further studies are required in order to reveal the benefit to the flax plant of producing and accumulating lignans in the seed coat.

Acknowledgement

Jingjing Fang acknowledges the International Max Planck Research School for a PhD scholarship. Aïna Ramsay thanks the Conseil Régional de Picardie for a PhD grant. Sullivan Renouard obtained a grant from the French Ministry of Research and Technology. Part of the work was supported by the “Conseil Général d’Eure et Loir” and the “Ligue Contre le Cancer, Comité d’Eure et Loir”. The authors are grateful for financial support from the European Regional Development Fund (ERDF) and the Max Planck Society (MPG). We thank Dr. Dirk Hölscher, Jena, for support with the laser microdissection and Emily Wheeler for editorial help in the preparation of this manuscript.

Chapter 6

Discussion

6.1 General discussion

Examples from different plants showed prominent merits of HPLC-SPE-NMR in structure elucidation of mass-limited natural products extracted from a small amount of tissue (Chapter 3). Results also demonstrated inhomogeneous secondary metabolites distribution in plants. Taking the two Haemodoraceae plants, *Wachendorfia thysiflora* and *Xiphidium caeruleum*, as an example, the metabolic profiling is different between the vegetative part and reproductive part. Even within the vegetative part, secondary metabolites patterns are not the same in different organs, such as in roots and aerial parts. These findings motivated us to investigate secondary metabolites and their distribution in a smaller scale of single organ. Rapeseed was chosen, not only because of the economic importance of this crop, but also because seeds are reproductive organs, in which different tissues play individual role and develop into different plant parts of seedling. It was reasonable to speculate that each tissue in rapeseed possesses individual secondary metabolite patterns. To explore this hypothesis, secondary metabolites in rapeseed were profiled (manuscript 4.1); subsequently, these compounds of different structural types were determined in four laser-microdissected tissues (manuscript 4.2). The experimental results confirmed that some secondary metabolites are distributed unevenly in seed tissues. The distribution pattern offers a first clue to understand the biological functions of these compounds, which could be unveiled by further studies. The tissue-specific distribution pattern found in rapeseed encouraged us to study flax seeds for the cell-specific accumulation of secoisolariciresinol diglucoside (SDG), a lignan with increasing interest for human's health. Previous studies proved SDG accumulation in seed coats, and a recent immunological report (Attoumbré *et al.*, 2010) proposed SDG localizes mainly in one layer constituted by sclerified cells of seed coats. Chapter 5 not only elucidated temporal information of SDG biosynthesis, but also determined the accumulation site of SDG in flaxseed. SDG was detected in parenchymatous cells, a finding which is different from a previous immunolocalization study (Attoumbré *et al.*, 2010).

This thesis combines eight papers and manuscripts dedicated to elucidation and spatial distribution studies of plant secondary metabolites using state-of-the-art analytical techniques.

The results provided solid evidences of uneven distribution of secondary metabolites among plant organs, tissues, and even cell populations, which create the basis for future biosynthesis and biological function studies of the secondary metabolites investigated here. As different methodologies were applied, and plants belonging to diverse families were explored, findings in this thesis are discussed in detail from different aspects.

6.2 Analytical methods and sampling

6.2.1 HPLC-SPE-NMR

In Chapter 3, twelve *C*-methylated flavonoids from *Myrica gale* seeds, 33 phenylphenalenone-type compounds from seed and plant material of *W. thyrsiflora*, and three flavonoids and 19 phenylphenalenone-type compounds from *X. caeruleum* flowers, totally including 18 new phenylphenalenone-type compounds, were elucidated by hyphenated HPLC-SPE-NMR combined with MS. These applications demonstrated several advantages of HPLC-SPE-NMR analysis of a complex matrix over conventional identification of secondary metabolites. The first advantage is the possibility for full automation. HPLC-SPE-NMR enables chromatographic separation, peak collection and sample desiccation to be controlled automatically by software. By HPLC-SPE-NMR, multiple components of a mixture can be prepared for NMR measurements in several additive HPLC runs, which are fully automatically controlled and can be done during a single day, thus greatly accelerating the analysis. The other major advantage is high sensitivity. In addition to multiple SPE trapping, the special designed flow-cell probe typically with a volume of 30 or 60 μl , resp.) in HPLC-SPE-NMR significantly increases NMR sensitivity. In paper 3.3, the directly detected ^{13}C NMR spectrum of one major compound (**R13**) was measured in HPLC-SPE-NMR mode at 125 MHz with high signal-to-noise ratios (4-20) after about 10,000 scans corresponding to approximate 9 h. In a recent publication (Wubshet *et al.*, 2012), authors were also successful to measure ^{13}C NMR spectra at 150 MHz of two triterpenoids from an approximate 600 μg prefractionated mixture by HPLC-SPE-NMR in 13 h for each compound. Although the sensitivity highly depends on the NMR system used, in most applications, milligram scale extract were sufficient for structures elucidation.

Although HPLC-SPE-NMR is very efficient in structural elucidation, the complexity of plant natural product mixtures is a still big challenge. For example, in most cases, compounds in a mixture have a wide-spread polarity, which makes SPE cartridge trapping capacity for each compound different. While separation in the reported HPLC-SPE-NMR applications was readily performed on reversed phase stationary material, trapping very polar analytes is problematic regardless of SPE cartridges with different sorbents (Clarkson *et al.*,

2007). Another challenge for the analysis of plant extracts is the large variation in compound concentration. Comparing with major compounds in a mixture, many more HPLC run replicates and trappings are needed to accumulate enough amounts of minor metabolites for NMR measurements; meanwhile, the major compounds could partially elute from the SPE cartridge because of limited sorbent capacity. Nevertheless HPLC-SPE-NMR is useful as a rapid tool for metabolic profiling of mixtures.

6.2.2 Laser microdissection

The application of a laser beam to dissect small plant samples for studying RNA and proteins in specific tissues and cells is getting common (Nelson *et al.*, 2006). Although, secondary metabolites generally exist in plants at low concentrations, they may accumulate to high levels in specialized cells or tissue and, after microdissection, can be successfully determined in specific plant cells and tissues (Li *et al.*, 2007; Hölscher and Schneider, 2007; Hölscher *et al.*, 2009; Abbott *et al.*, 2010). In Chapter 4, LMD was shown to be a precise tool to dissect different tissues from mature rapeseed for further tissue-specific secondary metabolites distribution study. Chapter 5 describes the capability of LMD to dissect specific cells from flaxseed coat. The two applications demonstrated the advantages of LMD to study secondary metabolites distribution over the conventional histological methods, which occasionally are lowly specific in distinguishing structures of related plant secondary metabolites. LMD-based chemical analyses of plant cells and tissue have to be distinguished from modern imaging technologies, such as infrared, Raman and mass spectrometry imaging methods, which mostly determine metabolites on sample surfaces. Currently, a limiting factor in using LMD in secondary metabolite studies is laborious preparation of cryosections and microscopic detection of target tissue. Future advances in LMD, such as improvement in target cell-recognizing software, multi-target sampling, hyphenation with sensitive detectors, will enable more efficient cell-/ tissue-specific identification and quantification of metabolites in plant tissue.

6.3 Secondary metabolites distribution and biological significances

6.3.1 C-methylated flavonoids from *Myrica gale* seeds

Unexpectedly, diaryheptanoids, which have been reported in the vegetative part of *M. gale* plant as described in introduction, were not detected in the seeds. Instead, twelve C-methylflavonoids were identified. This finding indicated the secondary metabolites profiles are different between the vegetative organs and the reproductive organs of *M. gale* plant.

Besides *M. gale*, C-methylflavonoids were only found in two other *Myrica* species, *M. pennsylvanica* (Wollenweber *et al.*, 1985b) and *M. serrata* (Gafner *et al.*, 1996). The unusual

C-methylated chalcones and flavonoids found in *M. gale* may support the discussion (Verdcourt and Polhill, 1997; Skene et al., 2000) about segregating *M. gale* from the genus *Myrica* to a new genus named *Gale*. Some *C*-methylchalcones were also detected from *Comptonia peregrine* (Wollenweber et al., 1985b), which is the sole species of the genus *Comptonia* in the Myricaceae.

Recent research (Popovici et al., 2010) suggests *C*-methylchalcones, which are the dominant components from the exudates of *M. gale* fruits, may act as signals in the establishment of mutualistic nitrogen-fixing symbioses by enhancing compatible fungi and inhibiting incompatible ones. One major *C*-methylchalcone, myrigalone A was shown to be an allelochemical, which has in vitro phytotoxicity to some classic plant species (Popovici et al., 2011), and inhibits *Lepidium sativum* seed germination (Oracz et al., 2012).

6.3.2 Phenylphenalenones and flavonoids in Haemodoraceae

Chemical structures of identified phenylphenalenones and flavonoids

In Chapter 3, eight, fifteen and fourteen phenylphenalenone-type compounds were identified from seeds, aerial parts and roots of *Wachendorfia thyrsiflora*, respectively; nineteen phenylphenalenone related compound and three flavonoids were elucidated from *Xiphidium caeruleum* flowers. The characterized phenylphenalenones can be categorized into three groups based on their skeletons as phenylphenalenone (C_{19}), oxa-phenylphenalenone ($C_{18}O$) and aza-phenylphenalenone ($C_{18}N$). Each group can be further divided into several subgroups (Figure 6.1). The distribution of phenylphenalenones according to different categories is listed in Table 6.1. The flavonoids detected in *X. caeruleum* flowers are apiginin and two of its glucosides.

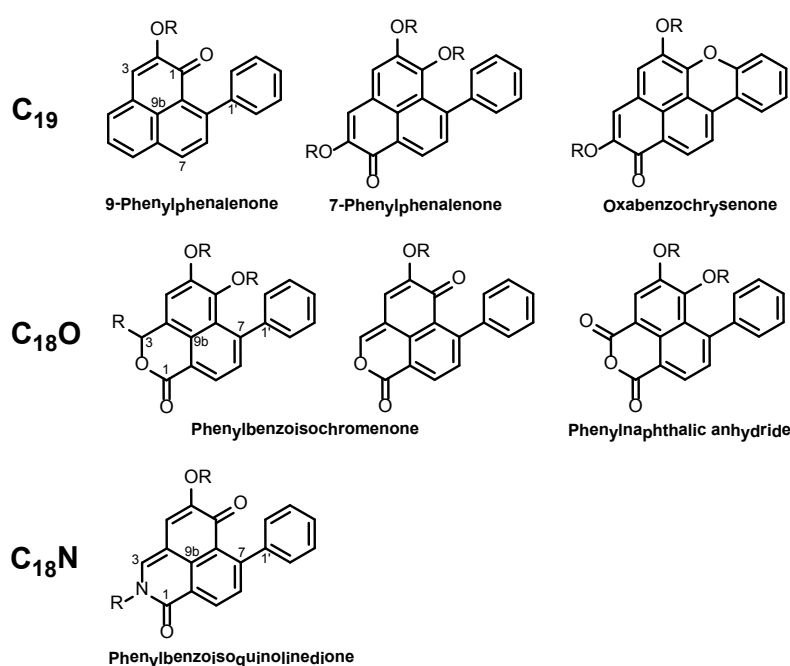


Figure 6.1 Skeletons of different phenylphenalenone-type secondary metabolites found in Haemodoraceae.

Table 6.1 Distribution of different types of phenylphenalenone-related secondary metabolites in different organs of Haemodoraceae plants.

	<i>Wachendorfia thyrsiflora</i>			<i>Xiphidium caeruleum</i>
	Roots	Aerial parts	Seeds	Flowers
C ₁₈ N	1	7	0	7
C ₁₈ O	7	8	0	10
C ₁₉	6	0	8	2

Biosynthesis and putative translocation of phenylphenalenones

In vegetative parts of *W. thyrsiflora* plants, intact phenylphenalenones (C₁₉) were only detected in roots. Oxa analogues phenylphenalenones (C₁₈O) were found in roots and aerial plant parts. Except one compound (A14/R14 in paper 3.3) isolated from both parts, aza analogues of phenylphenalenones were mostly found in the plant aerial parts. The phenylphenalenone distribution pattern in *W. thyrsiflora* vegetative parts is highly similar to that in *X. caeruleum* (Opitz and Schneider, 2002), in which, C₁₉ phenylphenalenones occurred exclusively in roots and C₁₈O analogues distributed in both roots and aerial parts. The distribution pattern suggests the C₁₉ phenylphenalenones were biosynthesized in the roots. C₁₉ phenylphenalenones can be oxidized to C₁₈O analogues (Opitz and Schneider, 2003) and glucosylated. The occurrence of C₁₉ and C₁₈O phenylphenalenones, and their glucosides (Fang et al., 2011), and direct evidence of formation of phenylbenzochromenones from phenylphenalenones (Opitz and Schneider, 2003) in *W. thyrsiflora* root cultures indicated the oxidation and glucosylation are independent of the aerial part. Afterwards, C₁₈O phenylphenalenones could be translocated from roots to aerial parts, where C₁₈O phenylphenalenones were hypothetically converted to C₁₈N analogues.

Formation in the roots and transportation to the leaves and reproductive organs of tropane alkaloids has been demonstrated in the Solanaceae. The enzymes of the tropane biosynthetic pathway have been localized in root tissue (Nakajama and Hashimoto, 1999; Kaiser et al., 2006). To confirm transport from underground plant parts to leaves in *W. thyrsiflora* and *X. caeruleum*, identification of biosynthetic enzymes would be required, followed by molecular studies to compare gene expression in the roots and the leaves.

Different from the results found in *W. thyrsiflora* and *X. caeruleum*, *Dilatris* species (Hölscher and Schneider, 2007) accumulate C₁₉ phenylphenalenones in secretory cavities of leaf tissues. Moreover, unlike the phytochemical profile of vegetative tissue, the flowers of *W. thyrsiflora* contain thyrsiflorin, a C₁₉-phenylphenalenone (Dora et al., 1990). The co-occurrence of C₁₉-phenylphenalenones, oxa-phenylphenalenones, and aza-phenylphenalenones was found in the flowers of *X. caeruleum* (Table 6.1). Hence, the flowers of *X. caeruleum* and *W. thyrsiflora* are a location of C₁₉-phenylphenalenones, and the flowers

of the former are also known to contain oxa- and aza-phenylphenalenones. Therefore, it may be speculated that the entire biosynthetic machinery of the phenylphenalenone biosynthetic pathway, including the formation of the C₁₉ skeleton and processing to oxa- and aza-phenylphenalenones, is expressed in flowers of *X. caeruleum* and *W. thyrsiflora* and probably other Haemodoraceae species as well.

A previous phytochemical study of *L. tinctoria* seeds identified two 9-phenylphenalenones and one dimer derived from them (Edwards *et al.*, 1979). Eight 9-phenylphenalenones and one dimer were determined from *W. thyrsiflora* seeds (Table 6.1). Above evidences indicated only intact phenylphenalenones (C₁₉) were synthesized and accumulated in seeds but oxa-phenylphenalenone (C₁₈O) and aza-phenylphenalenone (C₁₈N) were not.

Co-occurrence of phenylphenalenones and flavonoids in Haemodoraceae flowers

Previous phytochemical studies of Haemodoraceae plants identified various phenylphenalenones and related compounds (Cooke and Edwards, 1981; Hölscher and Schneider, 1997; Opitz *et al.*, 2002; Dias *et al.*, 2009). Apigenin and its two glucosides found in *X. caeruleum* flowers are the first flavonoids detected in this family (paper 3.4). Secondary metabolites, especially pigments and volatiles, of flowers are considered to attract pollinators. Natural compounds absorbing in the visible or UV range of the spectrum, accumulate in flower petals and serve as nectar guides (Chittka and Raine, 2006). Flavonoids and carotenoids are among the most common flower pigments and are responsible for various flower colors (Tanaka *et al.*, 2008). Since in the Haemodoraceae no flavonoids were detected before the present investigation, phenylphenalenones were considered to have replaced the flavonoids in this family, similar to betalaines, which replaced flavonoids as the flower pigments in plants of most families of the Caryophyllales (Strack *et al.*, 2003; Brockington *et al.*, 2011). However, colored delphinidin derivatives occur in flower petals of other phenylphenalenone-producing plants (Hölscher and Schneider, 2000; Wang *et al.*, 2011) such as *Strelitzia reginae* (Strelitziaceae) (Harborne, 1967) and *Eichhornia crassipes* (Pontederiaceae) (Toki *et al.*, 1994). In our study (paper 3.4) phenylphenalenones (Lazzaro *et al.*, 2004), phenylbenzochromenones, and phenylbenzisoquinolinones, apigenin and its glycosides providing the white color to the flowers of *X. caeruleum*, seem to be responsible for the UV-reflecting properties of the *X. caeruleum* petals (Buchmann, 1980) and for guiding visiting insects to the pollen. Hence, general replacement of flavonoids by phenylphenalenones in the Haemodoraceae is no longer sustainable. Nevertheless, phenylphenalenones, but not flavonoids, are chemotaxonomic markers of the family Haemodoraceae.

6.3.3 Secondary metabolites in rapeseed and their tissue-specific distribution

Although phytochemistry of rapeseed was explored many times, metabolic profile of each batch should be treated differently, because secondary metabolites in plants could be affected by several factors, such as cultivar, growth condition, and harvesting time. Therefore secondary metabolites in rapeseed winter cultivar “Emerald” were thoroughly explored prior to distribution studies. The secondary metabolites found in rapeseed “Emerald” can be categorized into five groups, phenolic choline esters, glucosinolates, phenylpropanoids, flavonoids and conjugated polyamines. Among them, major components, glucosinolates and sinapine, the dominant phenolic choline ester in rapeseed, were found evenly distributed in embryo tissues. Two flavonoids were mainly detected in cotyledons, and cyclic spermidine conjugates were found exclusively in hypocotyl and radicle parts in rapeseed embryo. One phenylpropanoid, sinapate methyl ester was isolated from rapeseed as a major component (manuscript 4.1); however it failed to be detected in LMD samples. The sinapate methyl ester probably is a methylation product of sinapic acid degraded from sinapine during separation.

The different distribution patterns of these secondary metabolites indicate each class of compounds may play individual roles for rapeseed. The glucosinolate-myrosinase system is a well explored plant chemical defense system in Brassicales order (Winde and Wittstock, 2011). The even distribution of glucosinolates in rapeseed embryo tissues suggests that they protect seeds and future seedlings from herbivore attacks. Sinapine also accumulates uniformly in rapeseed embryos since sinapine is the source of choline to synthesize phosphatidylcholines (Strack, 1981), which are major components of biological membranes. Polyamines play diverse biological roles in plants (Kusano *et al.*, 2008; Alcázar *et al.*, 2010). The conjugated polyamines, cyclic spermidine conjugates, were exclusively detected in hypocotyl and/or radicle in rapeseed, which infers that they are probably involved in root and shoot formation and growth (Nag *et al.*, 2001; Couée *et al.*, 2004). Flavonoids are well known antioxidant compounds and radical scavengers in plants and protect them from UV-B irradiation. Therefore the predominant occurrence of two major rapeseed flavonoids in cotyledons, which develop to the first leaves of young seedling primarily exposed to light, is reasonable.

6.3.4 Secoisolariciresinol diglucoside (SDG) in flaxseed (*Linum usitatissimum*)

Although a lot of research was carried out on flaxseed to elucidate the pharmacological and chemical properties of SDG and few studies approached understanding of SDG biosynthesis (Ford *et al.*, 2001; Hano *et al.*, 2006), nothing has been reported about the biological function of SDG for flaxseed.

Chapter 5 in the thesis was dedicated to establish the formation kinetics of SDG and its biosynthetic precursor, coniferin, and to elucidate the cell-layer specific accumulation of SDG in flaxseed. As a result, SDG biosynthesis was found to start around 6 days after flowering and cease before the seeds browned and desiccated. On the other hand, SDG accumulates predominantly in parenchymatous cells in mature flaxseed. SDG was proposed to protect abundant polyunsaturated fatty acids in embryo from oxidation (Hano *et al.*, 2006). The brown cell layer probably contains further metabolites, which may function as antioxidants, because the browning process in plants suggests the existence of proanthocyanidins (Pourcel *et al.*, 2007), and showed significant antioxidative activity in plant seeds (Takahata *et al.*, 2001). Therefore, it is plausible that the location of the SDG polymer complex in the parenchymatous cells just below the external mucilaginous cell layer suggests chemical defense against insects and microorganisms. Further studies are required in order to reveal the benefit to the flax plant of producing and accumulating lignans in the seed coat.

Chapter 7

Summary

In Chapter 3, it is described how HPLC-SPE-NMR was successfully applied to elucidate structures of secondary metabolites from different plant materials. Twelve C-methylated chalcones and flavonoids were identified from *Myrica gale* seeds. Recent investigations have shown that these compounds are involved in establishing nitrogen-fixing symbioses with compatible fungi. A phytochemical study on vegetative part of *Wachendorfia thyrsiflora* plant led to identification of eleven and ten phenylphenalenone-type compounds from aerial parts and roots, respectively, and four others from both parts. Twelve of them are new natural compounds. Among the 25 phenylphenalenone-type compounds from *W. thyrsiflora*, the phenylphenalenones (C₁₉ skeleton) occurred exclusively in roots, oxa-phenylphenalenones (C₁₈O skeleton) were found in both aerial part and roots, and most aza-phenylphenalenones (C₁₈N skeleton) were detected in aerial parts. This distribution pattern suggests that the phenylphenalenones were biosynthesized and oxidized to oxa-phenylphenalenones in roots, then translocated to aerial parts and partially converted to aza-phenylphenalenones. Eight phenylphenalenones with a C₁₉ skeleton and a corresponding dimer were elucidated from *W. thyrsiflora* seeds. This finding indicates that phenylphenalenones accumulated in the seeds without further oxidation, glucosylation or other conversion. Seventeen phenylphenalenones, oxa-phenylphenalenones and aza-phenylphenalenones, including five new ones, and three flavonoids were identified from *Xiphidium caeruleum* flowers. This is the first report on the isolation of flavonoids from the Haemodoraceae family. Current results of investigations on *Xiphidium caeruleum* flower components indicate that phenylphenalenone-type compounds are characteristic flower pigments of this species and have in part replaced the flavonoids. The most common flower pigments, anthocyanins and carotenoids, were not reported from flowers of the Haemodoraceae so far.

In Chapter 4, it is described how eleven glucosinolates and eighteen phenolics including seven new lignans were characterized from rapeseed (*Brassica napus*) winter cultivar “Emerald”. Further study on the organ-specific distribution of these compounds in rapeseed was conducted. As a result, glucosinolates and sinapine, the predominant sinapate in rapeseed, were proven to be accumulated evenly in embryo of rapeseed, while a cyclic

spermidine conjugate was exclusively found in hypocotyl and/or radicle, and the major amount of flavonoids was detected in cotyledons of rapeseed embryos. The different distribution patterns of these secondary metabolites indicate that each class of compounds may play individual roles for rapeseed dormancy and germination, which needs further experiments to elucidate.

Chapter 5 was dedicated to explore spatio-temporal formation and accumulation of the predominant lignan, secoisolariciresinol diglucoside (SDG), in flaxseed (*Linum usitatissimum*). SDG was detectable in developing flaxseed around six days after flowering, and its biosynthesis ceased before the seeds browned and desiccated. SDG accumulates predominantly in parenchymatous cells in mature flaxseed coat. This finding is different from previous reports of SDG accumulation in lignified sclerified cells of the seeds coat.

Zusammenfassung

In Kapitel 3 wird beschrieben, wie die HPLC-SPE-NMR Kopplung erfolgreich zur Strukturaufklärung von Sekundärstoffen aus verschiedenen Pflanzenmaterialien eingesetzt wurde. Zwölf C-methylierte Chalcone und Flavonoide wurden aus Samen von *Myrica gale* isoliert und identifiziert. Wie kürzlich nachgewiesen wurde, sind diese Verbindungen an der Etablierung von Symbiosen der Pflanze mit Stickstoff-fixierenden kompatiblen Pilzen beteiligt. Phytochemische Untersuchungen vegetativer Teile von *Wachendorfia thyrsiflora* führten zur Identifizierung von elf Verbindungen des Phenylphenalenon-Typ in oberirdischen Pflanzenteilen und zehn Verbindungen in den Wurzeln sowie vier weiteren Verbindungen in beiden Pflanzenteilen. Zwölf dieser Verbindungen sind neue Naturstoffe. Von den insgesamt 25 Verbindungen des Phenylphenalenon-Typs aus *W. thyrsiflora* kommen die eigentlichen Phenylphenalene (C_{19} Gerüst) ausschließlich in Wurzeln vor. Oxa-Phenylphenalene ($C_{18}O$ Gerüst) wurden sowohl in oberirdischen Pflanzenteilen als auch in Wurzeln gefunden während die meisten Aza-Phenylphenalene ($C_{18}N$ Gerüst) oberirdisch vorkommen. Dieses Verteilungsmuster lässt vermuten, dass Phenylphenalene zunächst in den Wurzeln gebildet und auch dort in Oxa-Phenylphenalene überführt werden. Anschließend werden sie vermutlich in die grünen Pflanzenteile transportiert und dort zum Teil in Aza-Phenylphenalene umgewandelt. Acht Phenylphenalene mit C_{19} Gerüst und ein entsprechendes Dimer wurden in *W. thyrsiflora* Samen nachgewiesen. Dieses Ergebnis zeigt, dass Phenylphenalene in Samen ohne weitere Oxidation, Glucosylierung oder andere Metabolisierungsschritte akkumulieren. Siebzehn Phenylphenalene, Oxa-Phenylphenalene und Aza-Phenylphenalene einschließlich fünf neuen Verbindungen und drei Flavonoiden wurden in Blüten von *Xiphidium caeruleum* gefunden. Dieses ist der erste Bericht über die Isolierung von Flavonoiden in der Familie Haemodoraceae. Die Ergebnisse der Untersuchungen an Blütenbestandteilen von *Xiphidium caeruleum* zeigen, dass Verbindungen des Phenylphenalenon-Typs charakteristische Blütenfarbstoffe dieser Art sind, wo sie zum Teil die sonst in Pflanzen verbreiteten Flavonoide ersetzen. Über das Vorkommen von Anthocyaninen und Carotenoiden, den allgemein häufigsten Blütenfarbstoffe, in den Haemodoraceae ist bisher nichts bekannt.

In Kapitel 4 werden elf Glucosinolate und 18 phenolische Verbindungen einschließlich sieben neuen Lignanen aus Raps (*Brassica napus*) "Emerald" beschrieben. Es

wurden weitere Arbeiten zur organ-spezifischen Verteilung dieser Verbindungen in Raps durchgeführt. Die Ergebnisse zeigen, dass Glucosinolate und Sinapin, das vorherrschende Sinapinsäure-Derivat in Raps, gleichmäßig im Rapssamen verteilt sind, während cyclische Spermidinkonjugate ausschließlich im Hypocotyl und/oder Radikel vorkommen und Flavonoide hauptsächlich in Kotyledonen der Rapssamen-Embryos gefunden wurden. Die unterschiedliche Verteilung der Sekundärmetabolite in verschiedenen Organen der Rapssamen lässt individuelle Funktionen jeder dieser Verbindungsklassen während der Samenruhe und Keimung vermuten. Dafür sind jedoch weitere Untersuchungen erforderlich.

Kapitel 5 ist der Untersuchung des räumlichen und zeitlichen Verlaufs der Bildung und Akkumulation von Secoisolariciresinol-Diglucosid (SDG), dem dominierenden Lignan in Leinsamen (*Linum usitatissimum*), gewidmet. Als Ergebnis wurde SDG in sich entwickelndem Leinsamen etwa sechs Tage nach der Blüte nachgewiesen und es wurde gezeigt, dass die Biosynthese vor der Bräunung und Trocknung der Samen abgeschlossen ist. SDG wurde hauptsächlich in parenchymatischen Zellen der Schale reifer Leinsamen nachgewiesen. Dieses Ergebnis unterscheidet sich von früheren Berichten, wonach lignifizierte Skleritzellen als Ort der SDG-Akkumulation beschrieben sind.

References

- Abbott E, Hall D, Hamberger B, Bohlmann J.** 2010. Laser microdissection of conifer stem tissues: isolation and analysis of high quality RNA, terpene synthase enzyme activity and terpenoid metabolites from resin ducts and cambial zone tissue of white spruce (*Picea glauca*). *BMC Plant Biology* **10**, 106.
- Adolphe JL, Whiting SJ, Juurlink BHJ, Thorpe LU, Alcorn J.** 2010. Health effects with consumption of the flax lignan secoisolariciresinol diglucoside. *British Journal of Nutrition* **103**, 929-938.
- Ahmed R, Lehrer M, Stevenso.R.** 1973. Synthesis of thomasidioic acid. *Tetrahedron Letters* **14**, 747-750.
- Alcázar R, Altabella T, Marco F, Bortolotti C, Reymond M, Koncz C, Carrasco P, Tiburcio AF.** 2010. Polyamines: molecules with regulatory functions in plant abiotic stress tolerance. *Planta* **231**, 1237-1249.
- Angeles G, Berrio-Sierra J, Joseleau JP, Lorimier P, Lefèbvre A, Ruel K.** 2006. Preparative laser capture microdissection and single-pot cell wall material preparation: a novel method for tissue-specific analysis. *Planta* **224**, 228-232.
- Anthonse T, Falkenbe I, Laake M, Midelfar A, Mortense T.** 1971. Some unusual flavonoids from *Myrica gale* L. *Acta Chemica Scandinavica* **25**, 1929-1930.
- Anthonsen T, Lorentzen GB, Malterud KE.** 1975. Porson, a new [7,0]-metacyclopheane from *Myrica gale* L. *Acta Chemica Scandinavica Series B-Organic Chemistry and Biochemistry* **29**, 529-530.
- Attoumbré J, Bienaimé C, Dubois F, Fliniaux MA, Chabbert B, Baltora-Rosset S.** 2010. Development of antibodies against secoisolariciresinol - Application to the immunolocalization of lignans in *Linum usitatissimum* seeds. *Phytochemistry* **71**, 1979-1987.
- Attoumbré J, Laoualy ABM, Bienaimé C, Dubois F, Baltora-Rosset S.** 2011. Investigation of lignan accumulation in developing *Linum usitatissimum* seeds by immunolocalization and HPLC. *Phytochemistry Letters* **4**, 194-198.
- Auger B, Marnet N, Gautier V, Maia-Grondard A, Leprince F, Renard M, Guyot S, Nesi N, Routaboul JM.** 2010. A detailed survey of seed coat flavonoids in developing seeds of *Brassica napus* L. *Journal of Agricultural and Food Chemistry* **58**, 6246-6256.
- Axelson M, Sjövall J, Gustafsson BE, Setchell KDR.** 1982. Origin of lignans in mammals and identification of a precursor from plants. *Nature* **298**, 659-660.
- Böttcher C, von Roepenack-Lahaye E, Schmidt J, Clemens S, Scheel D.** 2009. Analysis of phenolic choline esters from seeds of *Arabidopsis thaliana* and *Brassica napus* by capillary liquid chromatography/electrospray-tandem mass spectrometry. *Journal of Mass Spectrometry* **44**, 466-476.
- Böttcher C, von Roepenack-Lahaye E, Schmidt J, Schmotz C, Neumann S, Scheel D, Clemens S.** 2008. Metabolome analysis of biosynthetic mutants reveals a diversity of metabolic changes and allows identification of a large number of new compounds in *Arabidopsis*. *Plant Physiology* **147**, 2107-2120.
- Baumert A, Milkowski C, Schmidt J, Nimtz M, Wray V, Strack D.** 2005. Formation of a complex pattern of sinapate esters in *Brassica napus* seeds, catalyzed by enzymes of a serine carboxypeptidase-like acyltransferase family? *Phytochemistry* **66**, 1334-1345.
- Bayer E, Albert K, Nieder M, Grom E.** 1979. On-line coupling of high-performance liquid chromatography and nuclear magnetic resonance. *Journal of Chromatography* **186**, 497-507.
- Bazan AC, Edwards JM.** 1973. Lachnantonin, a novel 5-aza-9-phenylphenalenone from flowers of *Lachnanthes tinctoria*. *Lloydia-the Journal of Natural Products* **36**, 442-442.
- Bazan AC, Edwards JM.** 1976. Phenalenone pigments of flowers of *Lachnanthes tinctoria*. *Phytochemistry* **15**, 1413-1415.
- Bednarek P, Piślewska-Bednarek M, Svatoš A, Schneider B, Doubský J, Mansurova M, Humphry M, Consonni C, Panstruga R, Sanchez-Vallet A, Molina A, Schulze-Lefert P.** 2009. A glucosinolate metabolism pathway in living plant cells mediates broad-spectrum antifungal defense. *Science* **323**, 101-106.
- Beejmohun V, Fliniaux O, Grand É, Lamblin F, Bensaddek L, Christen P, Kovensky J, Fliniaux MA, Mesnard F.** 2007. Microwave-assisted extraction of the main phenolic compounds in flaxseed. *Phytochemical Analysis* **18**, 275-282.
- Beejmohun V, Grand E, Lesur D, Mesnard F, Fliniaux MA, Kovensky J.** 2006. Synthesis and purification of [1,2-¹³C₂]coniferin. *Journal of Labelled Compounds & Radiopharmaceuticals* **49**, 463-470.
- Behre KE.** 1999. The history of beer additives in Europe - a review. *Vegetation History and Archaeobotany* **8**, 35-48.
- Berns MW, Floyd AD.** 1971. Chromosomal microdissection by laser - A cytochemical and functional analysis. *Experimental Cell Research* **67**, 305-310.
- Bick IRC, Blackman AJ.** 1973. Haemodorin - A phenalenone pigment. *Australian Journal of Chemistry* **26**, 1377-1380.

- Bienz S, Bisegger P, Guggisberg A, Hesse M.** 2005. Polyamine alkaloids. *Natural product reports* **22**, 647-658.
- Binks RH, Greenham JR, Luis JG, Gowen SR.** 1997. A phytoalexin from roots of *Musa acuminata* var Pisang sipulu. *Phytochemistry* **45**, 47-49.
- Boerjan W, Ralph J, Baucher M.** 2003. Lignin biosynthesis. *Annual Review of Plant Biology* **54**, 519-546.
- Bomal C, Bedon F, Caron S, Mansfield SD, Levasseur C, Cooke JEK, Blais S, Tremblay L, Morency MJ, Pavy N, Grima-Pettenati J, Séguin A, MacKay J.** 2008. Involvement of *Pinus taeda* MYB1 and MYB8 in phenylpropanoid metabolism and secondary cell wall biogenesis: a comparative *in planta* analysis. *Journal of Experimental Botany* **59**, 3925-3939.
- Bond WJ, Honig M, Maze KE.** 1999. Seed size and seedling emergence: an allometric relationship and some ecological implications. *Oecologia* **120**, 132-136.
- Bones AM, Rossiter JT.** 1996. The myrosinase-glucosinolate system, its organisation and biochemistry. *Physiologia Plantarum* **97**, 194-208.
- Bonilla A, Duque C, Garzón C, Takaishi Y, Yamaguchi K, Hara N, Fujimoto Y.** 2005. Champanones, yellow pigments from the seeds of champa (*Campomanesia lineatifolia*). *Phytochemistry* **66**, 1736-1740.
- Bopp M, Ludicke W.** 1975. Degradation of sinapine during early development of *Sinapis alba* L. *Zeitschrift Fur Naturforschung C-a Journal of Biosciences* **30**, 663-667.
- Brand S, Hölscher D, Schierhorn A, Svatoš A, Schröder J, Schneider B.** 2006. A type III polyketide synthase from *Wachendorfia thyrsiflora* and its role in diarylheptanoid and phenylphenalenone biosynthesis. *Planta* **224**, 413-428.
- Brkljaca R, Urban S.** 2011. Recent advancements in HPLC-NMR and applications for natural product profiling and identification. *Journal of Liquid Chromatography & Related Technologies* **34**, 1063-1076.
- Brockington SF, Walker RH, Glover BJ, Soltis PS, Soltis DE.** 2011. Complex pigment evolution in the Caryophyllales. *New Phytologist* **190**, 854-864.
- Buchmann SL.** 1980. Preliminary anthecological observation on *Xiphidium caeruleum* Aubl. (Monocotyledoneae: Haemodoraceae) in Panama. *Journal of the Kansas Entomological Society* **53**, 685-699.
- Burlat V, Kwon M, Davin LB, Lewis NG.** 2001. Dirigent proteins and dirigent sites in lignifying tissues. *Phytochemistry* **57**, 883-897.
- Burow M, Müller R, Gershenzon J, Wittstock U.** 2006. Altered glucosinolate hydrolysis in genetically engineered *Arabidopsis thaliana* and its influence on the larval development of *Spodoptera littoralis*. *Journal of Chemical Ecology* **32**, 2333-2349.
- Carlton RR, Gray AI, Lavaud C, Massiot G, Waterman PG.** 1990. Kaempferol-3-(2,3-diacetoxy-4-*p*-coumaroyl)rhamnoside from leaves of *Myrica gale*. *Phytochemistry* **29**, 2369-2371.
- Cary HH, Beckman AO.** 1941. A quartz photoelectric spectrophotometer. *Journal of the Optical Society of America* **31**, 682-689.
- Ceccarelli SM, Schlotterbeck G, Boissin P, Binder M, Buettelmann B, Hanlon S, Jaeschke G, Kolczewski S, Kupfer E, Peters J-U, Porter RHP, Prinssen EP, Rueher M, Ruf I, Spooren W, Staempfli A, Vieira E.** 2008. Metabolite identification via LC-SPE-NMR-MS of the *in vitro* biooxidation products of a lead mGlu5 allosteric antagonist and impact on the improvement of metabolic stability in the series. *Chemmedchem* **3**, 136-144.
- Chimichi S, Bambagiotti-Alberti M, Coran SA, Giannellini V, Biddau B.** 1999. Complete assignment of the ¹H and ¹³C NMR spectra of secoisolariciresinol diglucoside, a mammalian lignan precursor isolated from *Linum usitatissimum*. *Magnetic Resonance in Chemistry* **37**, 860-863.
- Chittka L, Raine NE.** 2006. Recognition of flowers by pollinators. *Current Opinion in Plant Biology* **9**, 428-435.
- Clarkson C, Sibum M, Mensen R, Jaroszewski JW.** 2007. Evaluation of on-line solid-phase extraction parameters for hyphenated, high-performance liquid chromatography-solid-phase extraction-nuclear magnetic resonance applications. *Journal of Chromatography A* **1165**, 1-9.
- Clauß K, von Roepenack-Lahaye E, Böttcher C, Roth MR, Welti R, Erban A, Kopka J, Scheel D, Milkowski C, Strack D.** 2011. Overexpression of sinapine esterase *BnSCE3* in oilseed rape seeds triggers global changes in seed metabolism. *Plant Physiology* **155**, 1127-1145.
- Cooke RG, Dagley IJ.** 1979. Coloring matters of Australian plants .XXI Naphthoxanthones in the Haemodoraceae. *Australian Journal of Chemistry* **32**, 1841-1847.
- Cooke RG, Edwards JM.** 1981. Naturally occurring phenalenones and related compounds. *Progress in the Chemistry of Organic Natural Products* **40**, 153-190.
- Cooke RG, Johnson BL, Segal W.** 1958. Colouring matters of Australian plants VI . Haemocorin: the structure of the aglycone. *Australian Journal of Chemistry* **11**, 230-235.
- Cooke RG, Segal W.** 1955. Colouring matters of Australian plants IV. Haemocorin - a unique glycoside from *Haemodorum corymbosum* Vahl. *Australian Journal of Chemistry* **8**, 107-113.
- Cooke RG, Thomas RL.** 1975. Coloring matters of Australian plants .XVIII Constituents of *Anigozanthos rufus*. *Australian Journal of Chemistry* **28**, 1053-1057.
- Coran SA, Bartolucci G, Bambagiotti-Alberti M.** 2008. Validation of a reversed phase high performance thin layer chromatographic-densitometric method for secoisolariciresinol diglucoside determination in flaxseed. *Journal of Chromatography A* **1207**, 155-159.

- Corcoran O, Wilkinson PS, Godejohann M, Braumann U, Hofmann M, Spraul M.** 2002. Advancing sensitivity for flow NMR spectroscopy: LC-SPE-NMR and capillary-scale LC-NMR. *American Laboratory* **34**, 18-21.
- Couée I, Hummel I, Sulmon C, Gouesbet G, El Amrani A.** 2004. Involvement of polyamines in root development. *Plant Cell Tissue and Organ Culture* **76**, 1-10.
- Cragg GM, Newman DJ, Snader KM.** 1997. Natural products in drug discovery and development. *Journal of Natural Products* **60**, 52-60.
- Cremona TL, Edwards JM.** 1974. Xiphidone, major phenalenone pigment of *Xiphidium caeruleum*. *Lloydia-the Journal of Natural Products* **37**, 112-113.
- Croteau R, Kutchan TM, Lewis NG.** 2000. *Natural products (Secondary metabolites)*. Rochville: American society of plant physiologist.
- Daolio C, Schneider B.** 2012. Coupling liquid chromatography and other separation techniques to nuclear magnetic resonance spectroscopy. In: Shalliker RA, ed. *Hyphenated and alternative methods of detection in chromatography*. London: Taylor & Francis – CRC Press, 61-98.
- Day A, Ruel K, Neutelings G, Crônier D, David H, Hawkins S, Chabbert B.** 2005a. Lignification in the flax stem: evidence for an unusual lignin in bast fibers. *Planta* **222**, 234-245.
- Day RC, Grossniklaus U, Macknight RC.** 2005b. Be more specific! Laser-assisted microdissection of plant cells. *Trends in Plant Science* **10**, 397-406.
- De Tullio P, Chiap P, Francotte P, Van Heugen JC, Florence X, Frederich M, Gillotin F, Kremers P, Lebrun P, Pirotte B.** 2008. In vitro metabolism study of several 3-alkylamino-4H-1,2,4-benzo-thiadiazine 1,1-dioxides as ATP-sensitive potassium channel openers: combined use of LC-Q-TOF MS/MS and LC-SPE-NMR. *Fundamental & Clinical Pharmacology* **22**, 225-225.
- DellaGreca M, Previtiera L, Zarrelli A.** 2008. Revised structures of phenylphenalene derivatives from *Eichhornia crassipes*. *Tetrahedron Letters* **49**, 3268-3272.
- Dias DA, Goble DJ, Silva CA, Urban S.** 2009. Phenylphenalenones from the Australian plant *Haemodorum simplex*. *Journal of Natural Products* **72**, 1075-1080.
- Dixon RA, Achnine L, Kota P, Liu CJ, Reddy MSS, Wang LJ.** 2002. The phenylpropanoid pathway and plant defence - a genomics perspective. *Molecular Plant Pathology* **3**, 371-390.
- Dora G, Edwards JM, Campbell W.** 1990. Thyrsiflorin: A novel phenalenone pigment from *Wachendorfia thyrsiflora*. *Planta Medica* **56**, 569.
- Edwards JM.** 1974. Phenylphenalenones from *Wachendorfia* species. *Phytochemistry* **13**, 290-291.
- Edwards JM, Mangion M, Anderson JB, Rapposch M, Hite G.** 1979. Lachnanthospirone, a dimeric 9-phenylphenalenone from the seeds of *Lachnanthes tinctoria* Ell. *Tetrahedron Letters*, 4453-4456.
- Edwards JM, Weiss U.** 1972. Quinone methides derived from 5-oxa and 5-aza-9-phenyl-1-phenalenone in flowers of *Lachnanthes tinctoria* (Haemodoraceae). *Tetrahedron Letters*, 1631-1634.
- Edwards JM, Weiss U.** 1974. Phenalenone pigments of the root system of *Lachnanthes tinctoria*. *Phytochemistry* **13**, 1597-1602.
- Eeckhaut E, Struijs K, Possemiers S, Vincken JP, De Keukeleire D, Verstraete W.** 2008. Metabolism of the lignan macromolecule into enterolignans in the gastrointestinal lumen as determined in the simulator of the human intestinal microbial ecosystem. *Journal of Agricultural and Food Chemistry* **56**, 4806-4812.
- El-Din Saad El-Beltagi H, Amin Mohamed A.** 2010. Variations in fatty acid composition, glucosinolate profile and some phytochemical contents in selected oil seed rape (*Brassica napus* L.) cultivars. *Grasas Y Aceites* **61**, 143-150.
- Eliasson C, Kamal-Eldin A, Andersson R, Åman P.** 2003. High-performance liquid chromatographic analysis of secoisolariciresinol diglucoside and hydroxycinnamic acid glucosides in flaxseed by alkaline extraction. *Journal of Chromatography A* **1012**, 151-159.
- Ernst RR, Anderson WA.** 1966. Application of Fourier transform spectroscopy to magnetic resonance. *Review of Scientific Instruments* **37**, 93-102.
- Ettre LS, Sakodynskii KI.** 1993a. M. S. Tswett and the discovery of chromatography I: Early work (1899-1903). *Chromatographia* **35**, 223-231.
- Ettre LS, Sakodynskii KI.** 1993b. M. S. Tswett and the discovery of chromatography II: Completion of the development of chromatography (1903-1910). *Chromatographia* **35**, 329-338.
- Exarchou V, Krucker M, van Beek TA, Vervoort J, Gerotheranassis IP, Albert K.** 2005. LC-NMR coupling technology: recent advancements and applications in natural products analysis. *Magnetic Resonance in Chemistry* **43**, 681-687.
- Fang JJ, Kai M, Schneider B.** 2012. Phytochemical profile of aerial parts and roots of *Wachendorfia thyrsiflora* L. studied by LC-DAD-SPE-NMR. *Phytochemistry* **81**, 144-152.
- Fang JJ, Paetz C, Hölischer D, Munde T, Schneider B.** 2011. Phenylphenalenones and related natural products from *Wachendorfia thyrsiflora* L. *Phytochemistry Letters* **4**, 203-208.
- Fenwick GR.** 1982. The assessment of a new protein source - Rapeseed. *Proceedings of the Nutrition Society* **41**, 277-288.

- Ford JD, Huang KS, Wang HB, Davin LB, Lewis NG. 2001. Biosynthetic pathway to the cancer chemopreventive secoisolariciresinol diglucoside-hydroxymethyl glutaryl ester-linked lignan oligomers in flax (*Linum usitatissimum*) seed. *Journal of Natural Products* **64**, 1388-1397.
- Freudiger CW, Min W, Saar BG, Lu S, Holtom GR, He CW, Tsai JC, Kang JX, Xie XS. 2008. Label-free biomedical imaging with high sensitivity by stimulated Raman scattering microscopy. *Science* **322**, 1857-1861.
- Fukuyama Y, Mizuta K, Nakagawa K, Wenjuan Q, Xiue W. 1986. A new neo-lignan, a prostaglandin I-2 inducer from the leaves of *Zizyphus jujuba*. *Planta Medica*, 501-502.
- Gafner S, Wolfender JL, Mavi S, Hostettmann K. 1996. Antifungal and antibacterial chalcones from *Myrica serrata*. *Planta Medica* **62**, 67-69.
- Gang DR, Kasahara H, Xia ZQ, Vander Mijnsbrugge K, Bauw G, Boerjan W, Van Montagu M, Davin LB, Lewis NG. 1999. Evolution of plant defense mechanisms - Relationships of phenylcoumaran benzylic ether reductases to pinoresinol-lariciresinol and isoflavone reductases. *Journal of Biological Chemistry* **274**, 7516-7527.
- Gates M, Tschudi G. 1952. The synthesis of morphine. *Journal of the American Chemical Society* **74**, 1109-1110.
- Gates M, Tschudi G. 1956. The synthesis of morphine. *Journal of the American Chemical Society* **78**, 1380-1393.
- Gillotin F, Chiap P, Frederich M, Van Heugen J-C, Francotte P, Lebrun P, Pirotte B, de Tullio P. 2010. Coupling of Liquid Chromatography/Tandem Mass Spectrometry and Liquid Chromatography/Solid-Phase Extraction/NMR Techniques for the Structural Identification of Metabolites following In Vitro Biotransformation of SUR1-Selective ATP-Sensitive Potassium Channel Openers. *Drug Metabolism and Disposition* **38**, 232-240.
- Godejohann M, Heintz L, Daolio C, Berset J-D, Muff D. 2009. Comprehensive Non-Targeted Analysis of Contaminated Groundwater of a Former Ammunition Destruction Site using 1H-NMR and HPLC-SPE-NMR/TOF-MS. *Environmental Science & Technology* **43**, 7055-7061.
- Godejohann M, Tseng LH, Braumann U, Fuchser J, Spraul M. 2004. Characterization of a paracetamol metabolite using on-line LC-SPE-NMR-MS and a cryogenic NMR probe. *Journal of Chromatography A* **1058**, 191-196.
- Gottlieb HE, Kotlyar V, Nudelman A. 1997. NMR chemical shifts of common laboratory solvents as trace impurities. *Journal of Organic Chemistry* **62**, 7512-7515.
- Graser G, Oldham NJ, Brown PD, Temp U, Gershenzon J. 2001. The biosynthesis of benzoic acid glucosinolate esters in *Arabidopsis thaliana*. *Phytochemistry* **57**, 23-32.
- Griffiths J. 2008. A brief history of mass spectrometry. *Analytical Chemistry* **80**, 5678-5683.
- Gulland JM, Robinson R. 1923. The morphine group. Part I. A discussion of the constitutional problem. *Journal of the Chemical Society* **123**, 980-998.
- Gutierrez L, Conejero G, Castelain M, Guénin S, Verdeil JL, Thomasset B, Van Wuytswinkel O. 2006. Identification of new gene expression regulators specifically expressed during plant seed maturation. *Journal of Experimental Botany* **57**, 1919-1932.
- Gutierrez L, Van Wuytswinkel O, Castelain M, Bellini C. 2007. Combined networks regulating seed maturation. *Trends in Plant Science* **12**, 294-300.
- Gutowsky HS, Mccall DW, Slichter CP. 1951. Coupling among nuclear magnetic dipoles in molecules. *Physical Review* **84**, 589-590.
- Hölscher D, Bringmann G, Reichert M, Görls H, Ohlenschläger O, Schneider B. 2006. Monolaterol, the first configurationally assigned phenylphenalenone derivative with a stereogenic center at C-9, from *Monochoria elata*. *Journal of Natural Products* **69**, 1614-1617.
- Hölscher D, Schneider B. 1995. A diarylheptanoid intermediate in the biosynthesis of phenylphenalenones in *Anigozanthos preissii*. *Journal of the Chemical Society-Chemical Communications*, 525-526.
- Hölscher D, Schneider B. 1997. Phenylphenalenones from root cultures of *Anigozanthos preissii*. *Phytochemistry* **45**, 87-91.
- Hölscher D, Schneider B. 1999. HPLC-NMR analysis of phenylphenalenones and a stilbene from *Anigozanthos flavidus*. *Phytochemistry* **50**, 155-161.
- Hölscher D, Schneider B. 2000. Phenalenones from *Strelitzia reginae*. *Journal of Natural Products* **63**, 1027-1028.
- Hölscher D, Schneider B. 2005. The biosynthesis of 8-phenylphenalenones from *Eichhornia crassipes* involves a putative aryl migration step. *Phytochemistry* **66**, 59-64.
- Hölscher D, Schneider B. 2007. Laser microdissection and cryogenic nuclear magnetic resonance spectroscopy: an alliance for cell type-specific metabolite profiling. *Planta* **225**, 763-770.
- Hölscher D, Schneider B. 2008. Application of laser-assisted microdissection for tissue and cell-specific analysis of RNA, proteins, and metabolites. In: Lüttge UE, Beyschlag W, Murata J, eds. *Progress in Botany*, Vol. 69. Berlin, Heidelberg: Springer, 141-167.
- Hölscher D, Shroff R, Knop K, Gottschaldt M, Crecelius A, Schneider B, Heckel DG, Schubert US, Svatoš A. 2009. Matrix-free UV-laser desorption/ionization (LDI) mass spectrometric imaging at the single-cell level: distribution of secondary metabolites of *Arabidopsis thaliana* and *Hypericum* species. *Plant Journal* **60**, 907-918.

- Hänsch R, Koprek T, Mendel RR, Schulze J. 1995. An Improved Protocol for Eliminating Endogenous Beta-Glucuronidase Background in Barley. *Plant Science* **105**, 63-69.
- Halász I, Horváth C. 1963. Open tube columns with impregnated thin layer support for gas chromatography. *Analytical Chemistry* **35**, 499-505.
- Halkier BA, Gershenzon J. 2006. Biology and biochemistry of glucosinolates. *Annual Review of Plant Biology* **57**, 303-333.
- Hano C, Martin I, Fliniaux O, Legrand B, Gutierrez L, Arroo RRJ, Mesnard F, Lamblin F, Lainé E. 2006. Pinoresinol-lariciresinol reductase gene expression and secoisolariciresinol diglucoside accumulation in developing flax (*Linum usitatissimum*) seeds. *Planta* **224**, 1291-1301.
- Harborne JB. 1967. *Comparative Biochemistry of the Flavonoids*. New York: Academic Press.
- Harborne JB, Williams CA. 2000. Advances in flavonoid research since 1992. *Phytochemistry* **55**, 481-504.
- Hartmann T. 2007. From waste products to ecochemicals: Fifty years research of plant secondary metabolism. *Phytochemistry* **68**, 2831-2846.
- Hawkins, S., Pilate, G., Duverger, E., Boudet, A.M., Grima-Pettenati, J. 2002. The use of *GUS* histochemistry to visualise lignification gene expression during wood formation. In: Chaffey, N., Ed. *Wood formation in trees – Cell and molecular biology techniques*. London: Taylor & Francis Inc. 271-295.
- Heller HG, Swinney B. 1967. Stereochemistry and isomerisation of α -benzyl- α' -benzylidenesuccinic acid and related compounds. *Journal of the Chemical Society C-Organic*, 2452-2456.
- Helm RF, Ralph J. 1992. Lignin-hydroxycinnamyl model compounds related to forage cell-wall structure. 1. Ether-linked structures. *Journal of Agricultural and Food Chemistry* **40**, 2167-2175.
- Helme N, Linder HP. 1992. Morphology, evolution and taxonomy of *Wachendorfia* (Haemodoraceae). *Bothalia* **22**, 59-75.
- Hemmati S, von Heimendahl CBI, Klaes M, Alfermann AW, Schmidt TJ, Fuss E. 2010. Pinoresinol-lariciresinol reductases with opposite enantiospecificity determine the enantiomeric composition of lignans in the different organs of *Linum usitatissimum* L. *Planta Medica* **76**, 928-934.
- Hu C, Yuan YV, Kitts DD. 2007. Antioxidant activities of the flaxseed lignan secoisolariciresinol diglucoside, its aglycone secoisolariciresinol and the mammalian lignans enterodiol and enterolactone *in vitro*. *Food and Chemical Toxicology* **45**, 2219-2227.
- Hu CY, Chee PP, Chesney RH, Zhou JH, Miller PD, O'Brien WT. 1990. Intrinsic *GUS*-like activities in seed plants. *Plant Cell Reports* **9**, 1-5.
- Hufford CD, Oguntimein BO. 1980. Dihydrochalcones from *Uvaria angolensis*. *Phytochemistry* **19**, 2036-2038.
- Jaroszewski JW. 2005a. Hyphenated NMR methods in natural products research, Part 1: Direct hyphenation. *Planta Medica* **71**, 691-700.
- Jaroszewski JW. 2005b. Hyphenated NMR methods in natural products research, Part 2: HPLC-SPE-NMR and other new trends in NMR hyphenation. *Planta Medica* **71**, 795-802.
- Jefferson RA, Kavanagh TA, Bevan MW. 1987. Gus fusions: β -glucuronidase as a sensitive and versatile gene fusion marker in higher plants. *Embo Journal* **6**, 3901-3907.
- Jitsaeng K, Schneider B. 2010. Metabolic profiling of *Musa acuminata* challenged with *Sporobolomyces salmonicolor*. *Phytochemistry Letters* **3**, 84-87.
- Johnsson P, Kamal-Eldin A, Lundgren LN, Åman P. 2000. HPLC method for analysis of secoisolariciresinol diglucoside in flaxseeds. *Journal of Agricultural and Food Chemistry* **48**, 5216-5219.
- Jung HA, Woo JJ, Jung MJ, Hwang GS, Choi JS. 2009. Kaempferol glycosides with antioxidant activity from *Brassica juncea*. *Archives of Pharmacal Research* **32**, 1379-1384.
- Kaiser H, Richter U, Keiner R, Brabant A, Hause B, Dräger B. 2006. Immunolocalisation of two tropinone reductases in potato (*Solanum tuberosum* L.) root, stolon, and tuber sprouts. *Planta* **225**, 127-137.
- Kamal-Eldin A, Peerlkamp N, Johnsson P, Andersson R, Andersson RE, Lundgren LN, Åman P. 2001. An oligomer from flaxseed composed of secoisolariciresinoldiglucoside and 3-hydroxy-3-methyl glutaric acid residues. *Phytochemistry* **58**, 587-590.
- Kammerer B, Scheible H, Zurek G, Godejohann M, Zeller KP, Gleiter CH, Albrecht W, Laufer S. 2007. In vitro metabolite identification of ML3403, a 4-pyridinylimidazole-type p38 MAP kinase inhibitor by LC-Qq-TOF-MS and LC-SPE-cryo-NMR/MS. *Xenobiotica* **37**, 280-297.
- Kamo T, Hirai N, Iwami K, Fujioka D, Ohigashi H. 2001. New phenylphenalenones from banana fruit. *Tetrahedron* **57**, 7649-7656.
- Kamo T, Hirai N, Tsuda M, Fujioka D, Ohigashi H. 2000. Changes in the content and biosynthesis of phytoalexins in banana fruit. *Bioscience Biotechnology and Biochemistry* **64**, 2089-2098.
- Kamo T, Kato N, Hirai N, Tsuda M, Fujioka D, Ohigashi H. 1998. Phenylphenalenone-type phytoalexins from unripe Buñgulan banana fruit. *Bioscience Biotechnology and Biochemistry* **62**, 95-101.
- Karr C, Childers EE, Warner WC. 1963. Analysis of aromatic hydrocarbon samples by liquid chromatography with operating conditions analogous to those of gas chromatography. *Analytical Chemistry* **35**, 1290-1291.
- Kashina AA, Tulaikin AI, Yakovlev GP. 2008. Phenolcarbonic acids in *Myrica gale* (Myricaceae) above-ground part. *Rastitel'nye Resursy* **44**, 95-99.

- Kaur H, Heinzel N, Schöttner M, Baldwin IT, Gális I.** 2010. R2R3-NaMYB8 regulates the accumulation of phenylpropanoid-polyamine conjugates, which are essential for local and systemic defense against insect herbivores in *Nicotiana attenuata*. *Plant Physiology* **152**, 1731-1747.
- Kehr J.** 2001. High resolution spatial analysis of plant systems. *Current Opinion in Plant Biology* **4**, 197-201.
- Kehr J.** 2003. Single cell technology. *Current Opinion in Plant Biology* **6**, 617-621.
- Kim JE, Jung MJ, Jung HA, Woo JJ, Cheigh HS, Chung HY, Choi JS.** 2002. A new kaempferol 7-O-triglucoside from the leaves of *Brassica juncea* L. *Arch Pharm Res* **25**, 621-624.
- Klosterman HJ, Smith F.** 1954. The isolation of β -hydroxy- β -methylglutaric acid from the seed of flax (*Linum usitatissimum*). *Journal of the American Chemical Society* **76**, 1229-1230.
- Kosugi S, Ohashi Y, Nakajima K, Arai Y.** 1990. An improved assay for β -glucuronidase in transformed cells: methanol almost completely suppresses a putative endogenous β -glucuronidase activity. *Plant Science* **70**, 133-140.
- Kusano T, Berberich T, Tateda C, Takahashi Y.** 2008. Polyamines: essential factors for growth and survival. *Planta* **228**, 367-381.
- Kwon M, Davin LB, Lewis NG.** 2001. In situ hybridization and immunolocalization of lignan reductases in woody tissues: implications for heartwood formation and other forms of vascular tissue preservation. *Phytochemistry* **57**, 899-914.
- Landry LG, Chapple CCS, Last RL.** 1995. Arabidopsis mutants lacking phenolic sunscreens exhibit enhanced ultraviolet-B injury and oxidative damage. *Plant Physiology* **109**, 1159-1166.
- Lapierre C, Monties B, Rolando C.** 1986. Preparative thioacidolysis of spruce lignin - Isolation and identification of main monomeric products. *Holzforschung* **40**, 47-50.
- Larsen J, Staerk D, Cornett C, Hansen SH, Jaroszewski JW.** 2009. Identification of reaction products between drug substances and excipients by HPLC-SPE-NMR: Ester and amide formation between citric acid and 5-aminosalicylic acid. *Journal of Pharmaceutical and Biomedical Analysis* **49**, 839-842.
- Lazzaro A, Corominas M, Marti C, Flors C, Izquierdo LR, Grillo TA, Luis JG, Nonell S.** 2004. Light- and singlet oxygen-mediated antifungal activity of phenylphenalenone phytoalexins. *Photochemical & Photobiological Sciences* **3**, 706-710.
- Lepiniec L, Debeaujon I, Routaboul JM, Baudry A, Pourcel L, Nesi N, Caboche M.** 2006. Genetics and biochemistry of seed flavonoids. *Annual Review of Plant Biology* **57**, 405-430.
- Lewis DA, Fields WN, Shaw GP.** 1999. A natural flavonoid present in unripe plantain banana pulp (*Musa sapientum* L. var. paradisiaca) protects the gastric mucosa from aspirin-induced erosions. *Journal of Ethnopharmacology* **65**, 283-288.
- Li JY, Ou-Lee TM, Raba R, Amundson RG, Last RL.** 1993. Arabidopsis flavonoid mutants are hypersensitive to UV-B irradiation. *Plant Cell* **5**, 171-179.
- Li SH, Schneider B, Gershenzon J.** 2007. Microchemical analysis of laser-microdissected stone cells of Norway spruce by cryogenic nuclear magnetic resonance spectroscopy. *Planta* **225**, 771-779.
- Li X, Bergelson J, Chapple C.** 2010. The *ARABIDOPSIS* accession Pna-10 is a naturally occurring *sng1* deletion mutant. *Molecular Plant* **3**, 91-100.
- Li X, Yuan JP, Xu SP, Wang JH, Liu X.** 2008. Separation and determination of secoisolariciresinol diglucoside oligomers and their hydrolysates in the flaxseed extract by high-performance liquid chromatography. *Journal of Chromatography A* **1185**, 223-232.
- Liu Q, Wu L, Pu HM, Li CY, Hu QH.** 2012. Profile and distribution of soluble and insoluble phenolics in Chinese rapeseed (*Brassica napus*). *Food Chemistry* **135**, 616-622.
- Luis JG, Echeverri F, Quiñones W, Brito I, López M, Torres F, Cardona G, Aguiar Z, Pelaez C, Rojas M.** 1993. Irenolone and emenolone - Two new types of phytoalexin from *Musa paradisiaca*. *Journal of Organic Chemistry* **58**, 4306-4308.
- Luo J, Fuell C, Parr A, Hill L, Bailey P, Elliott K, Fairhurst SA, Martin C, Michael AJ.** 2009. A novel polyamine acyltransferase responsible for the accumulation of spermidine conjugates in *Arabidopsis* seed. *Plant Cell* **21**, 318-333.
- Luque-Ortega JR, Martinez S, Saugar JM, Izquierdo LR, Abad T, Luis JG, Pinero J, Valladares B, Rivas L.** 2004. Fungus-elicited metabolites from plants as an enriched source for new leishmanicidal agents: Antifungal phenyl-phenalenone phytoalexins from the banana plant (*Musa acuminata*) target mitochondria of *Leishmania donovani* promastigotes. *Antimicrobial Agents and Chemotherapy* **48**, 1534-1540.
- Maas PJM, Maas-van de Kamer H.** 1993. Haemodoraceae. *Flora Neotropica* **61**, 1-44.
- Madhusudhan B, Wiesenborn D, Schwarz J, Tostenson K, Gillespie J.** 2000. A dry mechanical method for concentrating the lignan secoisolariciresinol diglucoside in flaxseed. *Lwt-Food Science and Technology* **33**, 268-275.
- Malterud KE.** 1992. C-Methylated dihydrochalcones from *Myrica gale* fruit exudate. *Acta Pharmaceutica Nordica* **4**, 65-68.
- Malterud KE, Anthonson T, Hjortas J.** 1976. 14-Oxa-[7.1]-metapara-cyclophanes from *Myrica gale* L., a new class of natural products. *Tetrahedron Letters* **17**, 3069-3072.
- Malterud KE, Anthonson T, Lorentzen GB.** 1977. Two new C-methylated flavonoids from *Myrica gale*. *Phytochemistry* **16**, 1805-1809.

- Malterud KE, Diep OH, Sund RB.** 1996. C-methylated dihydrochalcones from *Myrica gale* L: Effects as antioxidants and as scavengers of 1,1-diphenyl-2-picrylhydrazyl. *Pharmacology & Toxicology* **78**, 111-116.
- Malterud KE, Faegri A.** 1982. Bacteriostatic and fungistatic activity of C-methylated dihydrochalcones from the fruits of *Myrica gale* L. *Acta Pharmaceutica Suecica* **19**, 43-46.
- Martin AJP, Synge RLM.** 1941. A new form of chromatogram employing two liquid phases 1. A theory of chromatography 2. Application to the micro-determination of the higher monoamino-acids in proteins. *Biochemical Journal* **35**, 1358-1368.
- Matas AJ, Yeats TH, Buda GJ, Zheng Y, Chatterjee S, Tohge T, Ponnala L, Adato A, Aharoni A, Stark R, Fernie AR, Fei ZJ, Giovannoni JJ, Rose JKC.** 2011. Tissue- and cell-type specific transcriptome profiling of expanding tomato fruit provides insights into metabolic and regulatory specialization and cuticle formation. *Plant Cell* **23**, 3893-3910.
- Mathiesen L, Malterud KE, Sund RB.** 1995. Antioxidant activity of fruit exudate and C-methylated dihydrochalcones from *Myrica gale*. *Planta Medica* **61**, 515-518.
- Mathiesen L, Malterud KE, Sund RB.** 1996. Uncoupling of respiration and inhibition of ATP synthesis in mitochondria by C-methylated flavonoids from *Myrica gale* L. *European Journal of Pharmaceutical Sciences* **4**, 373-379.
- Mazumder A, Kumar A, Purohit AK, Dubey DK.** 2010. Application of high performance liquid chromatography coupled to on-line solid-phase extraction-nuclear magnetic resonance spectroscopy for the analysis of degradation products of V-class nerve agents and nitrogen mustard. *Journal of Chromatography A* **1217**, 2887-2894.
- Merh PS, Daniel M, Sabnis SD.** 1986. Chemistry and taxonomy of some members of the Zingiberales. *Current Science* **55**, 835-839.
- Milkowski C, Strack D.** 2010. Sinapate esters in brassicaceous plants: biochemistry, molecular biology, evolution and metabolic engineering. *Planta* **232**, 19-35.
- Moco S, Schneider B, Vervoort J.** 2009. Plant micrometabolomics: The analysis of endogenous metabolites present in a plant cell or tissue. *Journal of Proteome Research* **8**, 1694-1703.
- Morihara M, Sakurai N, Inoue T, Kawai KI, Nagai M.** 1997. Two novel diarylheptanoid glucosides from *Myrica gale* var. *tomentosa* and absolute structure of plane-chiral galeon. *Chemical & Pharmaceutical Bulletin* **45**, 820-823.
- Morreel K, Ralph J, Kim H, Lu FC, Goeminne G, Ralph S, Messens E, Boerjan W.** 2004. Profiling of oligolignols reveals monolignol coupling conditions in lignifying poplar xylem. *Plant Physiology* **136**, 3537-3549.
- Moss GP.** 2000. Nomenclature of lignans and neolignans (IUPAC Recommendations 2000). *Pure and Applied Chemistry* **72**, 1493-1523.
- Muir AD.** 2006. Flax Lignans - Analytical methods and how they influence our understanding of biological activity. *Journal of Aoac International* **89**, 1147-1157.
- Mukker JK, Kotlyarova V, Singh RSP, Alcorn J.** 2010. HPLC method with fluorescence detection for the quantitative determination of flaxseed lignans. *Journal of Chromatography B-Analytical Technologies in the Biomedical and Life Sciences* **878**, 3076-3082.
- Munde T, Brand S, Hidalgo W, Maddula RK, Svatoš A, Schneider B.** 2012. Biosynthesis of tetraoxygenated phenylphenalenones in *Wachendorfia thyrsiflora*. *Phytochemistry*, doi:10.1016/j.phytochem.2012.02.020.
- Munde T, Maddula RK, Svatoš A, Schneider B.** 2011. The biosynthetic origin of oxygen functions in phenylphenalenones of *Anigozanthos preissii* inferred from NMR- and HRMS-based isotopologue analysis. *Phytochemistry* **72**, 49-58.
- Murashige T, Skoog F.** 1962. A revised medium for rapid growth and bio assays with tobacco tissue cultures. *Physiologia Plantarum* **15**, 473-497.
- Naczki M, Amarowicz R, Sullivan A, Shahidi F.** 1998. Current research developments on polyphenolics of rapeseed/canola: a review. *Food Chemistry* **62**, 489-502.
- Nag S, Saha K, Choudhuri MA.** 2001. Role of auxin and polyamines in adventitious root formation in relation to changes in compounds involved in rooting. *Journal of Plant Growth Regulation* **20**, 182-194.
- Nagai M, Dohi J, Morihara M, Sakurai N.** 1995. Diarylheptanoids from *Myrica gale* var *tomentosa* and revised structure of porson. *Chemical & Pharmaceutical Bulletin* **43**, 1674-1677.
- Nakajima K, Hashimoto T.** 1999. Two tropinone reductases, that catalyze oppositesterespecific reductions in tropane alkaloid biosynthesis, are localized in plant root with different cell-specific patterns. *Plant Cell Physiology* **40**, 1099-1107.
- Nakashima J, Chen F, Jackson L, Shadle G, Dixon RA.** 2008. Multi-site genetic modification of monolignol biosynthesis in alfalfa (*Medicago sativa*): effects on lignin composition in specific cell types. *New Phytologist* **179**, 738-750.
- Naran R, Chen GB, Carpita NC.** 2008. Novel rhamnogalacturonan I and arabinoxylan polysaccharides of flax seed mucilage. *Plant Physiology* **148**, 132-141.
- Nelson T, Gandotra N, Tausta SL.** 2008. Plant cell types: reporting and sampling with new technologies. *Current Opinion in Plant Biology* **11**, 567-573.

- Nelson T, Tausta SL, Gandotra N, Liu T. 2006. Laser microdissection of plant tissue: What you see is what you get. *Annual Review of Plant Biology* **57**, 181-201.
- Nesi N, Delourme R, Brégeon M, Falentin C, Renard M. 2008. Genetic and molecular approaches to improve nutritional value of *Brassica napus* L. seed. *Comptes Rendus Biologies* **331**, 763-771.
- Newman DJ, Cragg GM. 2007. Natural products as sources of new drugs over the last 25 years. *Journal of Natural Products* **70**, 461-477.
- Newman DJ, Cragg GM. 2012. Natural products as sources of new drugs over the 30 years from 1981 to 2010. *Journal of Natural Products* **75**, 311-335.
- Newman DJ, Cragg GM, Snader KM. 2000. The influence of natural products upon drug discovery. *Natural product reports* **17**, 215-234.
- Newman DJ, Cragg GM, Snader KM. 2003. Natural products as sources of new drugs over the period 1981-2002. *Journal of Natural Products* **66**, 1022-1037.
- Obel N, Erben V, Schwarz T, Kuhnel S, Fodor A, Pauly M. 2009. Microanalysis of plant cell wall polysaccharides. *Molecular Plant* **2**, 922-932.
- Olofsson L, Lundgren A, Brodelius PE. 2012. Trichome isolation with and without fixation using laser microdissection and pressure catapulting followed by RNA amplification: Expression of genes of terpene metabolism in apical and sub-apical trichome cells of *Artemisia annua* L. *Plant Science* **183**, 9-13.
- Oomah BD. 2001. Flaxseed as a functional food source. *Journal of the Science of Food and Agriculture* **81**, 889-894.
- Opitz S, Hölscher D, Oldham NJ, Bartram S, Schneider B. 2002a. Phenylphenalenone-related compounds: chemotaxonomic markers of the Haemodoraceae from *Xiphidium caeruleum*. *Journal of Natural Products* **65**, 1122-1130.
- Opitz S, Otálvaro F, Echeverri F, Quiñones W, Schneider B. 2002b. Isomeric oxabenzochrysenones from *Musa Acuminata* and *Wachendorfia thyrsiflora*. *Natural Product Letters* **16**, 335-338.
- Opitz S, Schneider B. 2002. Organ-specific analysis of phenylphenalenone-related compounds in *Xiphidium caeruleum*. *Phytochemistry* **61**, 819-825.
- Opitz S, Schneider B. 2003. Oxidative biosynthesis of phenylbenzoisochromenones from phenylphenalenones. *Phytochemistry* **62**, 307-312.
- Opitz S, Schnitzler JP, Hause B, Schneider B. 2003. Histochemical analysis of phenylphenalenone-related compounds in *Xiphidium caeruleum* (Haemodoraceae). *Planta* **216**, 881-889.
- Opitz S. 2002. Phenylphenalenones and related phenolic pigments of the Haemodoraceae: structure, biosynthesis and accumulation patterns in *Xiphidium caeruleum* and *Wachendorfia thyrsiflora*, Friedrich Schiller University, Jena, Germany.
- Oracz K, Voegelé A, Tarkowská D, Jacquemoud D, Turečková V, Urbanová T, Strnad M, Sliwinski E, Leubner-Metzger G. 2012. Myriganone A inhibits *Lepidium sativum* seed germination by interference with gibberellin metabolism and apoplastic superoxide production required for embryo extension growth and endosperm rupture. *Plant and Cell Physiology* **53**, 81-95.
- Otálvaro F, Görls H, Hölscher D, Schmitt B, Echeverri F, Quiñones W, Schneider B. 2002. Dimeric phenylphenalenones from *Musa acuminata* and various Haemodoraceae species. Crystal structure of anigorootin. *Phytochemistry* **60**, 61-66.
- Otálvaro F, Jitsaeng K, Munde T, Echeverri F, Quiñones W, Schneider B. 2010. O-Methylation of phenylphenalenone phytoalexins in *Musa acuminata* and *Wachendorfia thyrsiflora*. *Phytochemistry* **71**, 206-213.
- Otálvaro F, Nanclares J, Vásquez LE, Quiñones W, Echeverri F, Arango R, Schneider B. 2007. Phenalenone-type compounds from *Musa acuminata* var. "Yangambi km 5" (AAA) and their activity against *Mycosphaerella fijiensis*. *Journal of Natural Products* **70**, 887-890.
- Oyama KI, Kondo T. 2004. Total synthesis of apigenin 7,4'-di-O- β -glucopyranoside, a component of blue flower pigment of *Salvia patens*, and seven chiral analogues. *Tetrahedron* **60**, 2025-2034.
- Pan CK, Liu F, Ji Q, Wang W, Drinkwater D, Vivilecchia R. 2006. The use of LC/MS, GC/MS, and LC/NMR hyphenated techniques to identify a drug degradation product in pharmaceutical development. *Journal of Pharmaceutical and Biomedical Analysis* **40**, 581-590.
- Pascual-Villalobos MJ, Rodríguez B. 2007. Constituents of *Musa balbisiana* seeds and their activity against *Cryptolestes pusillus*. *Biochemical Systematics and Ecology* **35**, 11-16.
- Pavan FR, Leite CQF, Coelho RG, Coutinho ID, Honda NK, Cardoso CAL, Vilegas W, Leite SRD, Sato DN. 2009. Evaluation of anti-*Mycobacterium tuberculosis* activity of *Campomanesia adamantium* (myrtaceae). *Quimica Nova* **32**, 1222-1226.
- Perkin AG. 1900. Yellow colouring principles contained in various tannin matters. Part VII. *Arctostaphylos uvaursi*, *Hoematoxylon campeachianum*, *Rhus metopium*, *Myrica gale*, *Coriaria myrtifolia*, and *Robinia pseudacacia*. *Journal of the Chemical Society* **77**, 423-432.
- Popova IE, Hall C, Kubátová A. 2009. Determination of lignans in flaxseed using liquid chromatography with time-of-flight mass spectrometry. *Journal of Chromatography A* **1216**, 217-229.
- Popovici J, Bertrand C, Bagnarol E, Fernandez MP, Comte G. 2008. Chemical composition of essential oil and headspace-solid microextracts from fruits of *Myrica gale* L. and antifungal activity. *Natural Product Research* **22**, 1024-1032.

- Popovici J, Bertrand C, Jacquemoud D, Bellvert F, Fernandez MP, Comte G, Piola F.** 2011. An allelochemical from *Myrica gale* with strong phytotoxic activity against highly invasive *Fallopia x bohemica* taxa. *Molecules* **16**, 2323-2333.
- Popovici J, Comte G, Bagnarol E, Alloisio N, Fournier P, Bellvert F, Bertrand C, Fernandez MP.** 2010. Differential effects of rare specific flavonoids on compatible and incompatible strains in the *Myrica gale*-*Frankia* actinorhizal symbiosis. *Applied and Environmental Microbiology* **76**, 2451-2460.
- Pourcel L, Routaboul JM, Cheynier V, Lepiniec L, Debeaujon I.** 2007. Flavonoid oxidation in plants: from biochemical properties to physiological functions. *Trends in Plant Science* **12**, 29-36.
- Proctor WG, Yu FC.** 1950. The dependence of a nuclear magnetic resonance frequency upon chemical compound. *Physical Review* **77**, 717-717.
- Rabi II, Zacharias JR, Millman S, Kusch P.** 1938. A new method of measuring nuclear magnetic moment. *Physical Review* **53**, 318-318.
- Rabkin YM.** 1987. Technological innovation in science: The adoption of infrared spectroscopy by chemists. *Isis* **78**, 31-54.
- Rajhi I, Yamauchi T, Takahashi H, Nishiuchi S, Shiono K, Watanabe R, Mliki A, Nagamura Y, Tsutsumi N, Nishizawa NK, Nakazono M.** 2011. Identification of genes expressed in maize root cortical cells during lysigenous aerenchyma formation using laser microdissection and microarray analyses. *New Phytologist* **190**, 351-368.
- Renouard S, Corbin C, Lopez T, Montguillon J, Gutierrez L, Lamblin F, Lainé E, Hano C.** 2012. Abscisic acid regulates pinoresinol-lariciresinol reductase gene expression and secoisolariciresinol accumulation in developing flax (*Linum usitatissimum* L.) seeds. *Planta* **235**, 85-98.
- Renouard S, Hano C, Corbin C, Fliniaux O, Lopez T, Montguillon J, Barakzoy E, Mesnard F, Lamblin F, Lainé E.** 2010. Cellulase-assisted release of secoisolariciresinol from extracts of flax (*Linum usitatissimum*) hulls and whole seeds. *Food Chemistry* **122**, 679-687.
- Sakurai N, Hosono Y, Morihara M, Ishida J, Kawai KI, Inoue T, Nagai M.** 1997. A new triterpenoid myricalactone and others from *Myrica gale* var. *tomentosa*. *Yakugaku Zasshi-Journal of the Pharmaceutical Society of Japan* **117**, 211-219.
- Sakushima A, Coskun M, Maoka T.** 1995. Sinapinyl but-3-enylglucosinolate from *Boreava orientalis*. *Phytochemistry* **40**, 483-485.
- Salum ML, Robles CJ, Erra-Balsells R.** 2010. Photoisomerization of ionic liquid ammonium cinnamates: One-pot synthesis-isolation of Z-cinnamic acids. *Organic Letters* **12**, 4808-4811.
- Santos SC, Waterman PG.** 2000. Condensed tannins from *Myrica gale*. *Fitoterapia* **71**, 610-612.
- Schantz MV, Kapetani I.** 1971. Qualitative and quantitative study on essential oil of *Myrica gele* L. (Myricaceae). *Pharmaceutica Acta Helveticae* **46**, 649-&.
- Schiebold S, Tschiersch H, Borisjuk L, Heinzl N, Radchuk R, Rolletschek H.** 2011. A novel procedure for the quantitative analysis of metabolites, storage products and transcripts of laser microdissected seed tissues of *Brassica napus*. *Plant Methods* **7**, 19.
- Schad M, Mungur R, Fiehn O, Kehr J.** 2005. Metabolic profiling of laser microdissected vascular bundles of *Arabidopsis thaliana*. *Plant Methods* **1**, 2.
- Schmitt B, Schneider B.** 1999. Dihydrocinnamic acids are involved in the biosynthesis of phenylphenalenones in *Anigozanthos preissii*. *Phytochemistry* **52**, 45-53.
- Schneider B, Paetz C, Hölischer D, Opitz S.** 2005. HPLC-NMR for tissue-specific analysis of phenylphenalenone-related compounds in *Xiphidium caeruleum* (Haemodoraceae). *Magnetic Resonance in Chemistry* **43**, 724-728.
- Seger C, Godejohann M, Spraul M, Stuppner H, Hadacek F.** 2006. Reaction product analysis by high-performance liquid chromatography-solid-phase extraction-nuclear magnetic resonance - Application to the absolute configuration determination of naturally occurring polyene alcohols. *Journal of Chromatography A* **1136**, 82-88.
- Simpson AJ, Brown SA.** 2005. Purge NMR: Effective and easy solvent suppression. *Journal of Magnetic Resonance* **175**, 340-346.
- Simpson MJA, MacIntosh DF, Cloughley JB, Stuart AE.** 1996. Past, present and future utilisation of *Myrica gale* (Myricaceae). *Economic Botany* **50**, 122-129.
- Singh KK, Mridula D, Rehal J, Barnwal P.** 2011. Flaxseed: A potential source of food, feed and fiber. *Critical Reviews in Food Science and Nutrition* **51**, 210-222.
- Skene KR, Sprent JI, Raven JA, Herdman L.** 2000. *Myrica gale* L. *Journal of Ecology* **88**, 1079-1094.
- Sokolova M, Orav A, Koel M, Kailas T, Muurisepp M.** 2005. Composition of the oil and supercritical fluid CO₂ extract of sweet gale (*Myrica gale* L.) fruits. *Journal of Essential Oil Research* **17**, 188-191.
- Someya S, Yoshiki Y, Okubo K.** 2002. Antioxidant compounds from bananas (*Musa Cavendish*). *Food Chemistry* **79**, 351-354.
- Strack D.** 1981. Sinapine as a supply of choline for the biosynthesis of phosphatidylcholine in *Raphanus sativus* seedlings. *Zeitschrift Fur Naturforschung C-a Journal of Biosciences* **36**, 215-221.
- Strack D, Vogt T, Schliemann W.** 2003. Recent advances in betalain research. *Phytochemistry* **62**, 247-269.

- Struijs K, Vincken JP, Doeswijk TG, Voragen AGJ, Gruppen H.** 2009. The chain length of lignan macromolecule from flaxseed hulls is determined by the incorporation of coumaric acid glucosides and ferulic acid glucosides. *Phytochemistry* **70**, 262-269.
- Svatoš A.** 2011. Single-cell metabolomics comes of age: new developments in mass spectrometry profiling and imaging. *Analytical Chemistry* **83**, 5037-5044.
- Švehlíková V, Bennett RN, Mellon FA, Needs PW, Piacente S, Kroon PA, Bao YP.** 2004. Isolation, identification and stability of acylated derivatives of apigenin 7-O-glucoside from chamomile (*Chamomilla recutita* [L.] Rauschert). *Phytochemistry* **65**, 2323-2332.
- Takahata Y, Ohnishi-Kameyama M, Furuta S, Takahashi M, Suda I.** 2001. Highly polymerized procyanidins in brown soybean seed coat with a high radical-scavenging activity. *Journal of Agricultural and Food Chemistry* **49**, 5843-5847.
- Tanaka Y, Sasaki N, Ohmiya A.** 2008. Biosynthesis of plant pigments: anthocyanins, betalains and carotenoids. *Plant Journal* **54**, 733-749.
- Tanrisever N, Fronczek FR, Fischer NH, Williamson GB.** 1987. Ceratiolin and other flavonoids from *Ceratiola ericoides*. *Phytochemistry* **26**, 175-179.
- Thiel J, Mueller M, Weschke W, Weber H.** 2009. Amino acid metabolism at the maternal-filial boundary of young barley seeds: a microdissection-based study. *Planta* **230**, 205-213.
- Thompson LU, Robb P, Serraino M, Cheung F.** 1991. Mammalian lignan production from various foods. *Nutrition and Cancer-an International Journal* **16**, 43-52.
- Toki K, Saito N, Iimura K, Suzuki T, Honda T.** 1994. (Delphinidin 3-gentiobiosyl) (apigenin 7-glucosyl) malonate from the flowers of *Eichhornia crassipes*. *Phytochemistry* **36**, 1181-1183.
- Tokunaga N, Sakakibara N, Umezawa T, Ito Y, Fukuda H, Sato Y.** 2005. Involvement of extracellular dilignols in lignification during tracheary element differentiation of isolated *Zinnia* mesophyll cells. *Plant and Cell Physiology* **46**, 224-232.
- Touchstone JC.** 1993. History of chromatography. *Journal of Liquid Chromatography* **16**, 1647-1665.
- Tseng LH, Braumann U, Godejohann M, Lee SS, Albert K.** 2000. Structure identification of aporphine alkaloids by on-line coupling of HPLC-NMR with loop storage. *Journal of the Chinese Chemical Society* **47**, 1231-1236.
- Tzagoloff A.** 1963. Metabolism of sinapine in mustard plants. I. Degradation of sinapine into sinapic acid and choline. *Plant Physiology* **38**, 202-206.
- Umezawa T, Davin LB, Lewis NG.** 1991. Formation of lignans (-)-secoisolaricresinol and (-)-matairesinol with *Forsythia intermedia* cell-free extracts. *Journal of Biological Chemistry* **266**, 10210-10217.
- Uyar T, Malterud KE, Anthonsen T.** 1978. Two new dihydrochalcones from *Myrica gale*. *Phytochemistry* **17**, 2011-2013.
- Van Loo P, De Bruyn A, Buděšínský M.** 1986. Reinvestigation of the structural assignment of signals in the ¹H and ¹³C NMR-spectra of the flavone apigenin. *Magnetic Resonance in Chemistry* **24**, 879-882.
- Verdcourt B, Polhill R.** 1997. Proposals to conserve the names *Myrica* and *Gale* (Myricaceae) with conserved types. *Taxon* **46**, 347-348.
- Von Schantz M, Kapetani I.** 1971. Qualitative and quantitative study on essential oli of *Myrica gale* L. (Myricaceae). *Pharmaceutica Acta Helveticae* **46**, 649-656.
- Wada H, Tanaka N, Murakami T, Uchida T, Kozawa K, Saiki Y, Chen CM.** 1988. Chemical and chemotaxonomical stuies of filices. LXXVI. An unusual flavanone derivative from *Wagneriopteris japonoca* Loeve et Loeve. *Yakugaku Zasshi* **108**, 740-744.
- Wallis AFA.** 1968. Stereochemistry of cycloligans - a revised structure for thomasic acid. *Tetrahedron Letters* **9**, 5287-5288.
- Wang MZ, Cai XH, Luo XD.** 2011. New phenylphenalene derivatives from water hyacinth (*Eichhornia crassipes*). *Helvetica Chimica Acta* **94**, 61-66.
- Watanabe N, Niki E.** 1978. Direct-coupling of FT-NMR to high performance liquid chromatography. *Proceedings of the Japan Academy Series B-Physical and Biological Sciences* **54**, 194-199.
- Westcott ND, Muir AD.** 2003. Flax seed lignan in disease prevention and health promotion. *Phytochemistry reviews* **2**, 401-417.
- Whetten RW, MacKay JJ, Sederoff RR.** 1998. Recent advances in understanding lignin biosynthesis. *Annual Review of Plant Physiology and Plant Molecular Biology* **49**, 585-609.
- Wiesenborn D, Tostenson K, Kangas N.** 2003. Continuous abrasive method for mechanically fractionating flaxseed. *Journal of the American Oil Chemists Society* **80**, 295-300.
- Willför SM, Ahotupa MO, Hemming JE, Reunanen MHT, Eklund PC, Sjöholm RE, Eckerman CSE, Pohjamo SP, Holmbom MR.** 2003. Antioxidant activity of knotwood extractives and phenolic compounds of selected tree species. *Journal of Agricultural and Food Chemistry* **51**, 7600-7606.
- Wilson KE, Wilson MI, Greenberg BM.** 1998. Identification of the flavonoid glycosides that accumulate in *Brassica napus* L. cv. Topas specifically in response to ultraviolet B radiation. *Photochemistry and Photobiology* **67**, 547-553.

- Wilson MI, Greenberg BM.** 1993. Protection of the D1 photosystem-II reaction center protein from degradation in ultraviolet-radiation following adaptation of *Brassica napus* L. to growth in ultraviolet-B. *Photochemistry and Photobiology* **57**, 556-563.
- Winde I, Wittstock U.** 2011. Insect herbivore counteradaptations to the plant glucosinolate-myrosinase system. *Phytochemistry* **72**, 1566-1575.
- Wink M.** 2003. Evolution of secondary metabolites from an ecological and molecular phylogenetic perspective. *Phytochemistry* **64**, 3-19.
- Wolfram K, Schmidt J, Wray V, Milkowski C, Schliemann W, Strack D.** 2010. Profiling of phenylpropanoids in transgenic low-sinapine oilseed rape (*Brassica napus*). *Phytochemistry* **71**, 1076-1084.
- Wollenweber E, Dietz VH, Schilling G, Favrebonvin J, Smith DM.** 1985a. Flavonoids from chemotypes of the Goldback Fern, *Pityrogramma triangularis*. *Phytochemistry* **24**, 965-971.
- Wollenweber E, Kohorst G, Mann K, Bell JM.** 1985b. Leaf gland flavonoids in *Comptonia peregrina* and *Myrica pensylvanica* (Myricaceae). *Journal of Plant Physiology* **117**, 423-430.
- Wubshet SG, Johansen KT, Nyberg NT, Jaroszewski JW.** 2012. Direct ¹³C NMR detection in HPLC hyphenation mode: Analysis of *Ganoderma lucidum* terpenoids. *Journal of Natural Products* **75**, 876-882.
- Yao CS, Lin M, Wang L.** 2006. Isolation and biomimetic synthesis of anti-inflammatory stilbenolignans from *Gnetum cleistostachyum*. *Chemical & Pharmaceutical Bulletin* **54**, 1053-1057.
- Yuan JP, Li X, Xu SP, Wang JH, Liu X.** 2008. Hydrolysis kinetics of secoisolariciresinol diglucoside oligomers from flaxseed. *Journal of Agricultural and Food Chemistry* **56**, 10041-10047.
- Zhang DM, Miyase T, Kuroyanagi M, Umehara K, Noguchi H.** 1998. Oligosaccharide polyesters from roots of *Polygala glomerata*. *Phytochemistry* **47**, 45-52.
- Zhang WB, Xu SY, Wang Z, Yang RJ, Lu RR.** 2009. Demucilaging and dehulling flaxseed with a wet process. *Lwt-Food Science and Technology* **42**, 1193-1198.

Supplementary material

Table S1 of 3.4 Co-occurrence of phenylphenalenones and flavonoids in <i>Xiphidium caeruleum</i> Aubl. flowers.	110
Figures S1 and S2 of 4.2 Tissue-specific distribution of secondary metabolites in rapeseed (<i>Brassica napus</i> L.).	111
Figures S1, S2 and S3 of 5.2 Laser microdissection-assisted quantitative cell layer-specific detection of secoisolariciresinol diglucoside in flaxseed coats (Preliminary version).	112

3.4 Co-occurrence of phenylphenalenones and flavonoids in *Xiphidium caeruleum* Aubl. flowers.Table S1. HMBC correlations of compounds **6**, **11**, **17**, **19** and **21** obtained by LC-DAD-SPE-NMR (500 MHz, MeCN-*d*₃).

Position	6			11			17			19			21		
	δ H	HMBC (H \rightarrow C)	δ H	HMBC (H \rightarrow C)	δ H	HMBC (H \rightarrow C)	δ H	HMBC (H \rightarrow C)	δ H	HMBC (H \rightarrow C)	δ H	HMBC (H \rightarrow C)	δ H	HMBC (H \rightarrow C)	
3	7.86	C-1, 4, 9b, 1''	6.31	C-1, 4, 3a, 9b, 1'''	7.90	C-1, 4, 9b, 1''	7.60	C-1, 4, 9b, 1''	7.81	C-1, 4, 9b, 1''	7.81	C-1, 4, 9b, 1''	7.81	C-1, 4, 9b, 1''	
4	6.99	C-3, 5, 6, 9b	7.53	C-3, 5, 6, 9b	7.03	C-3, 5, 6, 9b	6.84	C-3, 5, 6, 9b	7.01	C-3, 5, 6, 9b	7.01	C-3, 5, 6, 9b	7.01	C-3, 5, 6, 9b	
8	7.54	C-6a, 9a, 1'	7.45	C-6a, 9a, 1'	7.55	C-6a, 9a, 1'	7.49	C-6a, 9a, 1'	7.55	C-6a, 9a, 1'	7.55	C-6a, 9a, 1'	7.55	C-6a, 9a, 1'	
9	8.62	C-1, 7, 9b	8.22	C-1, 7, 9b	8.64	C-1, 7, 9b	8.54	C-1, 7, 9b	8.64	C-1, 7, 9b	8.64	C-1, 7, 9b	8.64	C-1, 7, 9b	
2'/6'	7.34	C-7, 4'	7.31	C-7, 4'	7.34	C-7, 4'	7.30	C-7, 4'	7.34	C-7, 4'	7.34	C-7, 4'	7.34	C-7, 4'	
3'/4'/5'	7.41-7.44	C-1', 3', 5'	7.46	C-1'	7.41-7.44	C-1', 3', 5'	7.38-7.42	C-1', 3', 5'	7.41-7.44	C-1', 3', 5'	7.41-7.44	C-1', 3', 5'	7.41-7.44	C-1', 3', 5'	
1''	5.43	C-1, 3, 3'', 4''			5.25	C-1, 3, 2'', 3'', 4'', 5''	5.58	C-1, 3'', 1''	5.60	C-1, 3, 2'', 3'', 6''	5.60	C-1, 3, 2'', 3'', 6''	5.60	C-1, 3, 2'', 3'', 6''	
2''a	3.30	C-1'', 3'', 4''	2.64	C-1'', 3''	2.57	C-1''	3.63	C-1'', 1''', 2''', 6''	2.16	C-1'', 4'', 5'', 6''	2.16	C-1'', 4'', 5'', 6''	2.16	C-1'', 4'', 5'', 6''	
2''b	3.07	C-1'', 3'', 4''					3.45	C-1'', 3'', 1''', 2''', 6''	2.04	C-1'', 4'', 5'', 6''	2.04	C-1'', 4'', 5'', 6''	2.04	C-1'', 4'', 5'', 6''	
3''					1.18	C-1'', 2'', 4''			1.50	C-1''	1.50	C-1''	1.50	C-1''	
4''					0.88	C-1'', 2'', 3''			0.96	C-2'', 5''	0.96	C-2'', 5''	0.96	C-2'', 5''	
5''									0.94	C-2'', 4''	0.94	C-2'', 4''	0.94	C-2'', 4''	
2'''/6'''							7.18	C-2'', 4''			7.18	C-2'', 4''			
3'''/5'''							7.18	C-1''			7.18	C-1''			
4'''							7.15	C-2''', 6'''			7.15	C-2''', 6'''			

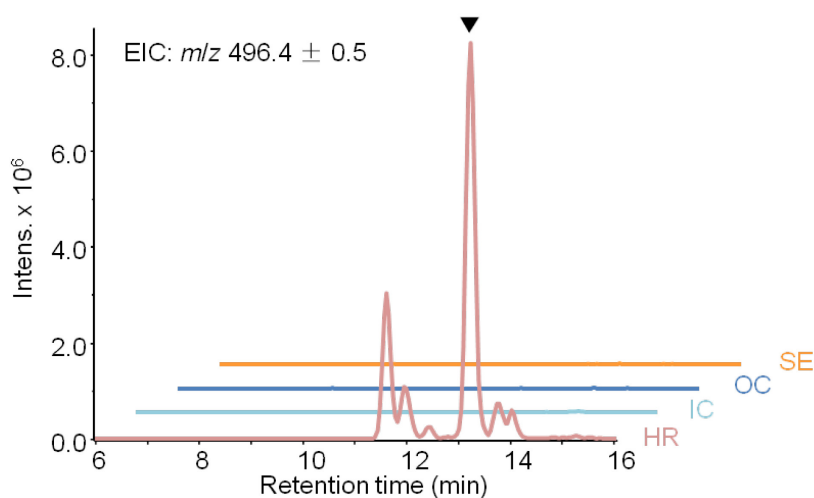
4.2 Tissue-specific distribution of secondary metabolites in rapeseed (*Brassica napus* L.).

Figure S1. Extracted ion chromatograms for the cyclic spermidine in different rapeseed tissues. Extracted ion chromatograms (EIC) for ions at m/z 496.4 ± 0.5 measured in positive ionization mode of samples from different laser-microdissected rapeseed tissues. **13**: Major cyclic spermidine conjugate (for structure, see Figure 4A). ▼ major cyclic spermidine conjugate (**13**) peak. HR, hypocotyl and radicle; IC, inner cotyledon; OC, outer cotyledon; and SE, seed coat and endosperm.

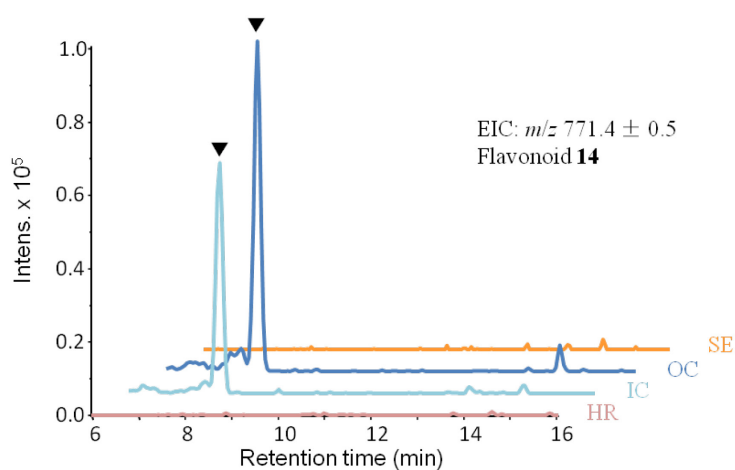
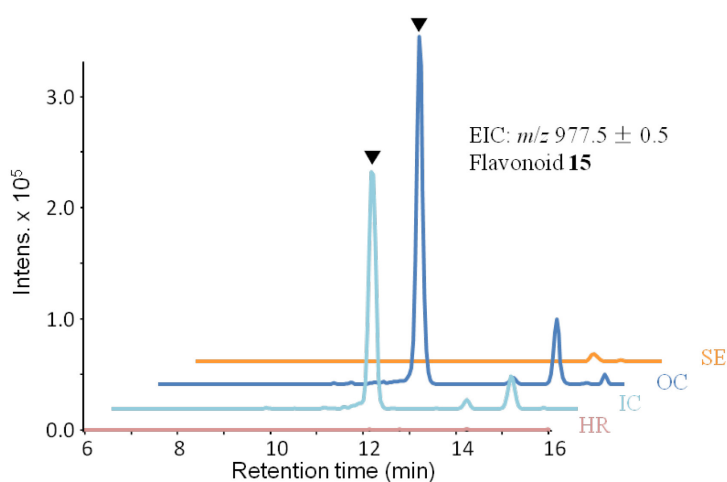


Figure S2. Extracted ion chromatograms for the two major flavonoids in different rapeseed tissues. Extracted ion chromatograms (EIC) of samples from different rapeseed tissues measure in negative ionization mode for (A) ions at m/z 771.4 ± 0.5 of flavonoid **14**; and (B) ions at m/z 977.5 ± 0.5 of flavonoid **15**. For structures, see Figure 5A. HR, hypocotyl and radicle; IC, inner cotyledon; OC, outer cotyledon; and SE, seed coat and endosperm. ▼ flavonoid **14** peaks in (A) and flavonoid **15** peaks in (B).



B

5.2 Laser microdissection-assisted quantitative cell layer-specific detection of secoisolariciresinol diglucoside in flaxseed coats (Preliminary version).

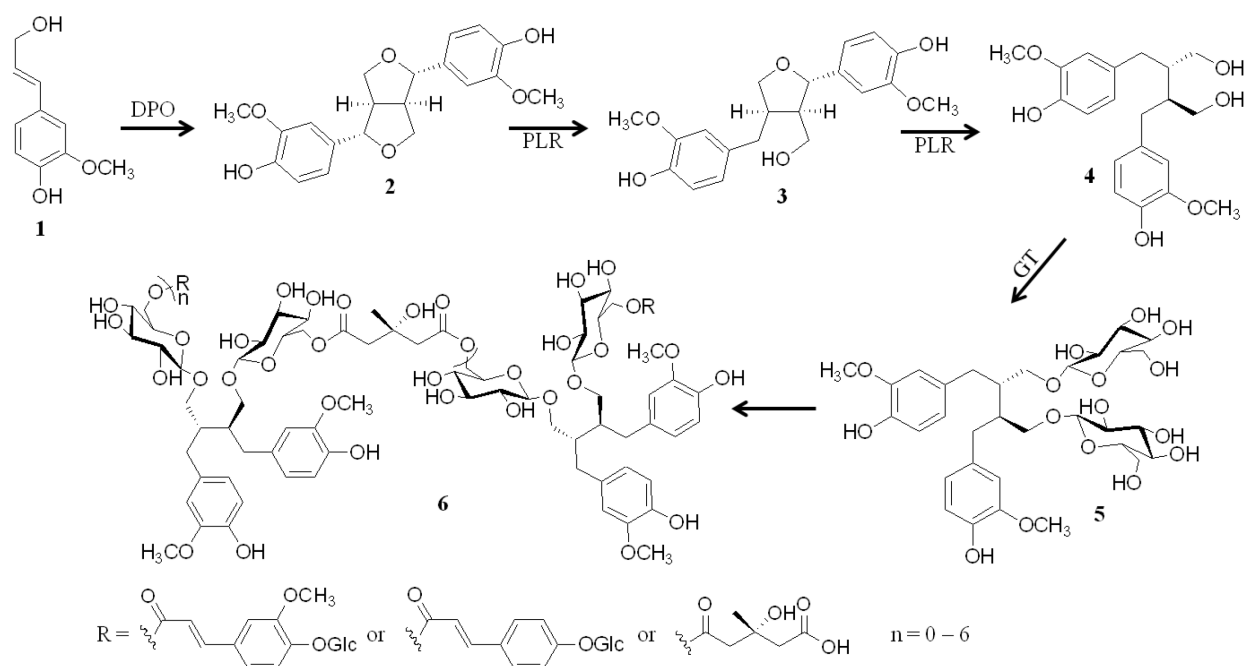


Fig. S1. Proposed biosynthesis pathway of SDG oligomer in flaxseed. DPO, dirigent-protein oxidase; PLR, pinoresinol-lariciresinol reductase; GF, glucosyltransferase. **1**, *E*-coniferyl alcohol; **2**, (-)-pinoresinol; **3** (-)-lariciresinol; **4**, (+)-secoisolariciresinol; **5**, SDG; **6**, SDG-HMG oligomer.

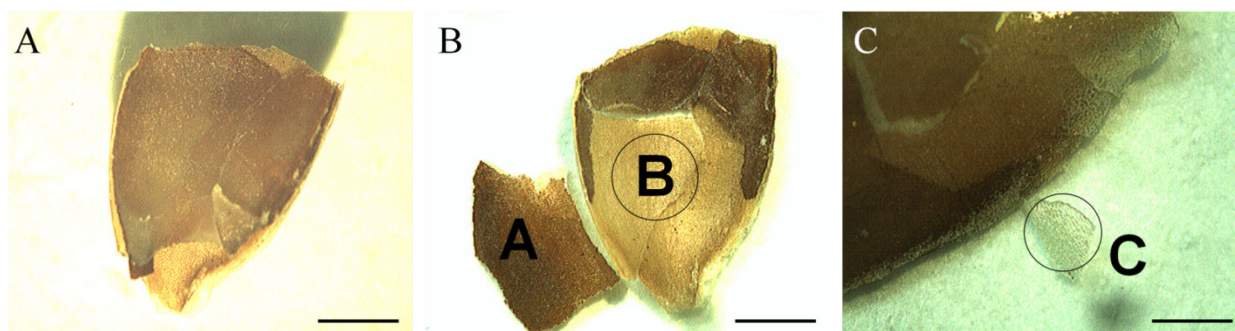


Fig. S2. Mechanical separation of the flaxseed coats. (A) Picture of the flaxseed coats; (B) flaxseed coats separated into two parts **A** and **B**; (C) some mucilaginous cell (MC) material was isolated from seed coats as part **C**. Bars in **A** and **B** represent 1.0 mm, and the bar in **C** represents 0.5 mm.

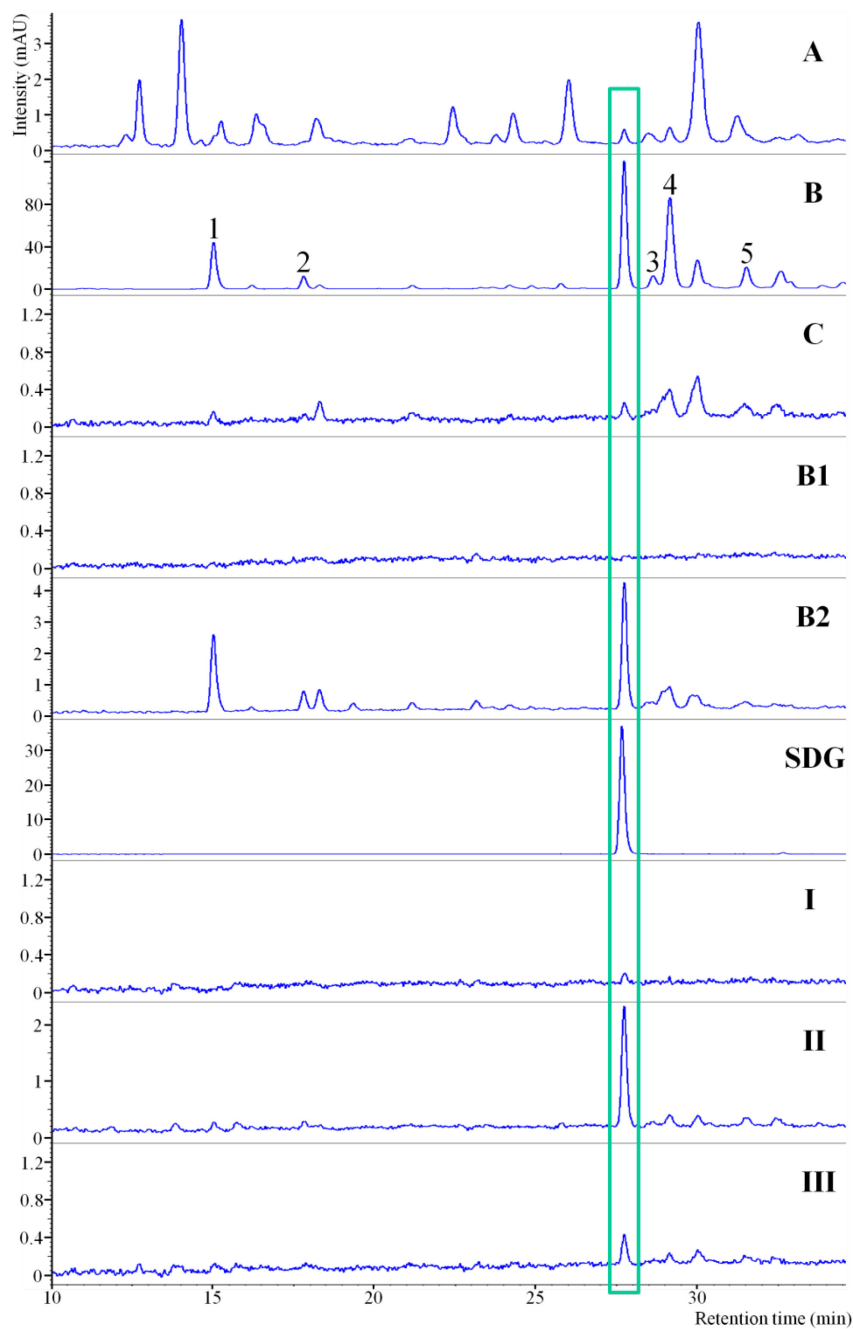


Fig. S3. HPLC chromatograms of alkaline hydrolysis of separated samples. Chromatograms **A**, **B**, **C**, **B1**, and **B2** were obtained from mature seed samples. **SDG**: Chromatogram of secoisolariciresinol diglucoside (SDG). Chromatograms **I**, **II**, and **III** were obtained from 25 DAF seed samples. For details of sample preparation, see Figs. 1 and 2. Framed peaks in different chromatograms represent SDG. Some peaks in chromatogram **B** were identified by comparing with standards as 4-(β -D-glucopyranosyl) coumarate (1), 4-(β -D-glucopyranosyl) ferulate (2), methyl 4-(β -D-glucopyranosyl) caffeate (3), methyl 4-(β -D-glucopyranosyl) coumarate (4), and methyl 4-(β -D-glucopyranosyl) ferulate (5).

Acknowledgements

It could not be possible for me to complete this dissertation without helps from many people, of course, including far more than the names mentioned here.

First of all, I am deeply thankful to my supervisor Dr. Bernd Schneider for giving me the opportunity to work in his group, introducing me into NMR research and guiding my PhD research.

I am grateful to two other co-supervisors, Prof. Hans Peter Saluz from HKI and Dr Christian Paetz, for their detailed suggestions about my PhD project.

I would like to thank all the colleagues in the NMR group, Christian Paetz, who is also one of my co-supervisors, for helping me a lot in learning everything in the lab and with fruitful discussion; Dirk Hölscher and Renate Ellinger for teaching me to use the laser microdissection and HPLC-SPE-NMR, respectively, with which I completed most of my PhD work; other current and former colleagues, Sara Agnolet, Silke Brand, Claudia Cervellati, Felix Feistel, Kati Grüner, William Hidalgo, Kusuma Jitsaeng, Kayla A. Hamersky Kaiser, Tobias Munde, Tri R. Nuringtyas, Sonja Rosenlöcher, Dávid Szamosvari, Kamel H. Shaker, Evangelos Tatsis, Anne-Christin Warskulat for helping me with all kinds of problems from academy to daily life and having much pleasant time together in the office and lab. I really appreciate the assistance you offered me, although I can't enumerate all of them.

Many thanks to all the coworkers for making this institute a perfect place for scientific research. I would like to thank MS group, especially to Dr. Ravi Kumar Maddula and Dr. Macro Kai for recording MS data for many compounds. I am thankful to Dr. Michael Reichelt from Biochemistry department for a lot of quantification work in rapeseed project. I really appreciate greenhouse team for their hard work to take care my plants, and the administration staffs for their every efficient help. Many thanks to Dr. Karin Groten for her help in all the IMPRS stuffs.

I want to express my gratitude to all the coauthors of the manuscripts I involved in for sharing their scientific experience with me, and to Emily Wheeler for her editorial assistance with all manuscripts.

Thanks to all the friends including the Chinese friends and the football friends I met in Jena for making my outside-lab life wonderful.

Thank my grandparents, parents and younger sister for their constant support.

I truly thank my girlfriend Fei for her love and everything she did for our future.

I would like to thank IMPRS for offering me a PhD scholarship and Max Planck Society for financial support.

Curriculum Vitae

Personal data

First name: Jingjing

Family name: Fang

Date of birth: 18.10.1982

Place of birth: Anhui, China

Nationality: Chinese

Education

02.2009-present: PhD student in Max Planck Institute for Chemical Ecology, Jena, Germany.

09.2004-06.2007: MS student in Shanghai Institute of Materia Medica, Chinese Academy of Sciences, Shanghai, China.

09.2000-06.2004: BS student in Anhui Agricultural University, Hefei, Anhui, China.

Working experience

07.2007-12.2008: Application engineer in Tegent Scientific Ltd., Shanghai, China.

Publications

1. Guan Ye, **Jing-jing Fang**, Ming-song Fan, Cheng-gang Huang. Structure elucidation and complete NMR spectral assignments of a novel sesquiterpene glycoside from *Ixeris sonchifolia*. *Magnetic Resonance in Chemistry* 2007, (45): 362-363.
2. **Jing-Jing Fang**, Guan Ye, Wen-Liang Chen, Wei-Min Zhao. Antibacterial phenolic components from *Eriocaulon buergerianum*. *Phytochemistry* 2008, (69): 1279-1286.
3. **Jing-Jing Fang**, Guan Ye. Flavonoids and xanthenes from *Tripterospermum chinense*. *Chemistry of Natural Compounds* 2008, (44): 514-515.
4. **Jingjing Fang**, Christian Paetz, Bernd Schneider. Phytochemical study of the seed shell of the *Myrica gale* by HPLC-SPE-NMR. *Planta Medica* 2010, (76): 1243-1243. (Conference paper)
5. **Jingjing Fang**, Christian Paetz, Bernd Schneider. C-methylated flavanones and dihydrochalcones from *Myrica gale* seeds. *Biochemical Systematics and Ecology* 2011, (39): 68-70.
6. **Jingjing Fang**, Christian Paetz, Dirk Hölscher, Tobias Munde, Bernd Schneider.

- Phenylphenalenones and related natural products from *Wachendorfia thyrsiflora* L. *Phytochemistry Letters* 2011, (4): 203-208.
7. **Jingjing Fang**, Marco Kai, Bernd Schneider. Phytochemical profile of aerial parts and roots of *Wachendorfia thyrsiflora* L. studied by LC-DAD-SPE-NMR. *Phytochemistry* 2012, (81): 144-152.
 8. **Jingjing Fang**, Dirk Hölscher, Bernd Schneider. Co-occurrence of phenylphenalenones and flavonoids in *Xiphidium caeruleum* Aubl. Flowers. *Phytochemistry* 2012, (82) : 143-148.
 9. **Jingjing Fang**, Aina Ramsay, Christian Paetz, Evangelos C. Tatsis, Sullivan Renouard, Christophe Hano, Eric Grand, Ophélie Fliniaux, Albrecht Roscher, Francois Mesnard, Bernd Schneider. Concentrations kinetics of secoisolariciresinol diglucoside and its biosynthetic precursor coniferin in developing flaxseed. *Phytochemical analysis* 2012, DOI: 10.1002/pca.2377.
 10. **Jingjing Fang**, Michael Reichelt, Marco Kai, Bernd Schneider. Metabolic profiling of lignans and other secondary metabolites from rapeseed (*Brassica napus* L.). *Journal of Agricultural and Food Chemistry* 2012, under revision.
 11. **Jingjing Fang**, Michael Reichelt, William Hidalgo, Sara Agnolet, Bernd Schneider. Uneven distribution of minor secondary metabolites in rapeseed (*Brassica napus*). *Plos One* 2012, under revision.
 12. **Jingjing Fang**, Aina Ramsay, Sullivan Renouard, Christophe Hano, Frédéric Lamblin, Brigitte Chabbert, François Mesnard, Bernd Schneider. Laser microdissection-assisted quantitative cell layer-specific detection of secoisolariciresinol diglucoside in flaxseed coats. In preparation.
 13. Maria Heinrich, Christian Hettenhausen, Theo Lange, Hendrik Wünsche, **Jingjing Fang**, Ian T. Baldwin, Jianqiang Wu. Jasmonic acid suppresses transcript accumulations of *GA20ox* and the biosynthesis of gibberellins in the stems of *irCDPK4/5* plants. *Plant Journal* 2012, under review.

Oral presentations

1. **Jingjing Fang**, Aina Ramsay, Francois Mesnard, Bernd Schneider. Cell-specific detection of secoisolariciresinol diglucoside in flax (*Linum usitatissimum*) seeds. *Trends in Natural Products Research: A PSE Young Scientists' Meeting*, Kolymvari-Crete, Greece, 14.06.2010.
2. **Jingjing Fang**, Aina Ramsay, Francois Mesnard, Bernd Schneider. Cell-specific detection of secoisolariciresinol diglucoside in flaxseed (*Linum usitatissimum*). *11th International*

Max Planck Research School Symposium, Dornburg, Germany, 22.02.2012.

Poster presentations

1. **Jingjing Fang**, Bernd Schneider. Laser microdissection combined with LC-SPE-NMR for organ and cell-specific analysis of natural products. *JSMC Workshop on Method & Concept Transfer*, Jena, Germany, 04.06.2009.
2. **Jingjing Fang**, Bernd Schneider. The phenylphenalenone profile of *Xiphidium caeruleum* flowers. *MPI-CE Symposium (2009)*, Jena, Germany, 22-23.06.2009.
3. **Jingjing Fang**, Bernd Schneider. Study of the secondary metabolites of *Wachendorfia thyrsiflora* seeds by HPLC-SPE-NMR. *9th International Max Planck Research School Symposium*, Dornburg, Germany, 15-16.02.2010.
4. **Jingjing Fang**, Christian Paetz, Bernd Schneider. Phytochemical study of the seed shell of the *Myrica gale* by HPLC-SPE-NMR. *The 58th International Congress and Annual Meeting of the Society for Medicinal Plant and Natural Product Research / The 7th Tannin Conference*, Berlin, Germany, 28.08-2.09.2010.
5. **Jingjing Fang**, Bernd Schneider. HPLC-SPE-NMR and the conventional methods to elucidate the structures of the triacylglycerols from linseed oil. *5th Shanghai International Symposium on Analytical Chemistry (AnalyticaChina 2010)*, Shanghai, China, 15-17.09.2010.
6. **Jingjing Fang**, Bernd Schneider. Localization of secoisolariciresinol diglucoside in flax (*Linum usitatissimum*) seed. *The Meeting of the Scientific Advisory Aboard of MPG-CE*, Jena, Germany, 25-27.10.2010.
7. **Jingjing Fang**, Aina Ramsay, Francois Mesnard, Bernd Schneider. Cell-specific detection of secoisolariciresinol diglucoside in flax (*Linum usitatissimum*) seeds. *2nd International Conference on Plant Metabolism*, Qingdao, China, 30.06-03.07.2011.
8. **Jingjing Fang**, Aina Ramsay, Francois Mesnard, Bernd Schneider. Cell-specific detection of secoisolariciresinol diglucoside in flax (*Linum usitatissimum*) seeds. *MPI-CE Symposium (2011)*, Jena, Germany, 22-23.09.2011.

Declaration of independence

I declare in accordance with the regulations of the conferral of the doctor degree from the Faculty of Biology and Pharmacy of Friedrich Schiller University Jena that I have written this dissertation independently only with the assistance and literature cited in the text. People who contributed in the experiments, data analysis and writing manuscripts are listed as coauthors of respective manuscripts. The dissertation has not been previously submitted whether to Friedrich Schiller University Jena or to any other university.

Jena, 20.08.2012

Jingjing Fang